Automotive spark-ignited direct-injection gasoline engines

F. Zhao, M. –C. Lai, D.L. Harrington

PERGAMON

PROGRESS IN ENERGY AND COMBUSTION SCIENCE

An International Review Journal

Automotive spark-ignited direct-injection gasoline engines

Editors

F. ZHAO, M.-C. LAI, D.L. HARRINGTON

PERGAMON

Published originally as a special issue (Volume 25:5) of the international journal *Progress in Energy and Combustion Science* and also available in hard-bound edition (ISBN: 0 08 0436765)

ELSEVIER SCIENCE Ltd
The Boulevard, Langford Lane
Kidlington, Oxford OX5 1GB, UK

Reprinted from: *Progress in Energy and Combustion Science* - ISSN: 0360-1285

Library of Congress Cataloging in Publication Data
A catalog record from the Library of Congress has been applied for.

British Library Cataloguing in Publication Data
A catalogue record from the British Library has been applied for.

ISBN: 0-08 043676-5

♾ The paper used in this publication meets the requirements of ANSI/NISO Z39.48-1992 (Permanence of Paper).
Printed in Great Britain by Polestar Wheatons Ltd, Exeter

PERGAMON

Progress in Energy and Combustion Science 25 (1999) 437–562

PROGRESS IN ENERGY AND COMBUSTION SCIENCE

www.elsevier.com/locate/pecs

Automotive spark-ignited direct-injection gasoline engines

F. Zhao[a,*], M.-C. Lai[a], D.L. Harrington[b]

[a]*Department of Mechanical Engineering, Wayne State University, 5050 Anthony Wayne Dr., Detroit, MI 48202, USA*
[b]*Thermal and Energy Systems Laboratory, General Motors Research and Development Center, 30500 Mound Road, Warren, MI 48090, USA*

Abstract

The development of four-stroke, spark-ignition engines that are designed to inject gasoline directly into the combustion chamber is an important worldwide initiative of the automotive industry. The thermodynamic potential of such engines for significantly enhanced fuel economy, transient response and cold-start hydrocarbon emission levels has led to a large number of research and development projects that have the goal of understanding, developing and optimizing gasoline direct-injection (GDI) combustion systems. The processes of fuel injection, spray atomization and vaporization, charge cooling, mixture preparation and the control of in-cylinder air motion are all being actively researched, and this work is reviewed in detail and analyzed. The new technologies such as high-pressure, common-rail, gasoline injection systems and swirl-atomizing gasoline fuel injectors are discussed in detail, as these technologies, along with computer control capabilities, have enabled the current new examination of an old objective; the direct-injection, stratified-charge (DISC), gasoline engine. The prior work on DISC engines that is relevant to current GDI engine development is also reviewed and discussed.

The fuel economy and emission data for actual engine configurations are of significant importance to engine researchers and developers. These data have been obtained and assembled for all of the available GDI literature, and are reviewed and discussed in detail. The types of GDI engines are arranged in four classifications of decreasing complexity, and the advantages and disadvantages of each class are noted and explained. Emphasis is placed upon consensus trends and conclusions that are evident when taken as a whole. Thus the GDI researcher is informed regarding the degree to which engine volumetric efficiency and compression ratio can be increased under optimized conditions, and as to the extent to which unburned hydrocarbon (UBHC), NO_x and particulate emissions can be minimized for specific combustion strategies. The critical area of GDI fuel injector deposits and the associated effect on spray geometry and engine performance degradation are reviewed, and important system guidelines for minimizing deposition rates and deposit effects are presented. The capabilities and limitations of emission control techniques and aftertreatment hardware are reviewed in depth, and areas of consensus on attaining European, Japanese and North American emission standards are compiled and discussed.

All known research, prototype and production GDI engines worldwide are reviewed as to performance, emissions and fuel economy advantages, and for areas requiring further development. The engine schematics, control diagrams and specifications are compiled, and the emission control strategies are illustrated and discussed. The influence of lean-NO_x catalysts on the development of late-injection, stratified-charge GDI engines is reviewed, and the relative merits of lean-burn, homogeneous, direct-injection engines as an option requiring less control complexity are analyzed. All current information in the literature is used as the basis for discussing the future development of automotive GDI engines.

Keywords: Automotive; Four stroke; Gasoline; Direct injection; Spark ignition; Engine

* Corresponding author. Currently with Liberty and Technical Affairs, DaimlerChrysler Corporation, CIMS 482-01-19, 800 Chrysler Dr. E, Auburn Hills, MI 48326, USA.

0360-1285/99/$ - see front matter
PII: S0360-1285(99)00004-0

Contents

Nomenclature 439
1. Introduction 440
   1.1. Overview 440
   1.2. Key potential benefits: GDI engine versus PFI engine 441
2. Direct-injection gasoline fuel system 444
   2.1. Fuel system requirements 444
   2.2. Fuel injector considerations 446
   2.3. Fuel spray characteristics 452
      2.3.1. Atomization requirements 452
      2.3.2. Single-fluid high-pressure swirl injector 455
      2.3.3. Effect of injector sac volume 462
      2.3.4. Air-assisted injection 464
      2.3.5. Best practice performance of current GDI injectors 467
      2.3.6. Future requirements of GDI fuel sprays 468
3. Combustion chamber geometry and in-cylinder mixture dynamics 470
   3.1. Flow structure 470
   3.2. Fuel–air mixing 476
4. Combustion process and control strategies 485
   4.1. Combustion chamber geometry 485
   4.2. In-cylinder charge cooling 494
   4.3. Engine operating modes and fuel injection strategies 495
   4.4. Combustion characteristics 501
   4.5. Injector deposit issues 507
5. Fuel economy and emissions 512
   5.1. Fuel economy potential 512
   5.2. Emissions versus fuel economy compromise 516
      5.2.1. UBHC emissions 518
      5.2.2. NO_x emissions 524
      5.2.3. Particulate emissions 529
6. Specific combustion systems and control strategies 532
   6.1. Early research engines 532
   6.2. Mitsubishi combustion system 536
   6.3. Toyota combustion system 539
   6.4. Nissan combustion system 541
   6.5. Ford combustion system 543
   6.6. Isuzu combustion system 543
   6.7. Mercedes-Benz combustion system 544
   6.8. Mazda combustion system 544
   6.9. Audi combustion system 545
   6.10. Honda combustion system 545
   6.11. Subaru combustion system 546
   6.12. Fiat combustion system 546
   6.13. Renault combustion system 547
   6.14. Ricardo combustion system 548
   6.15. AVL combustion system 548
   6.16. FEV combustion system 550
   6.17. Orbital combustion system 552
7. Conclusion 552
References 552

Nomenclature

ATDC	after top dead center
BDC	bottom dead center
BMEP	brake mean effective pressure
BSFC	brake specific fuel consumption
BSU	Bosch smoke unit
BTDC	before top dead center
CAFE	corporate average fuel economy
CC	close-coupled
CCD	charge-coupled device
CFD	computational fluid dynamics
CIDI	compression-ignition direct-injection
CO	carbon monoxide
COV	coefficient of variation
CVCC	compound vortex combustion chamber
CVT	continuously variable transmission
D32	Sauter mean diameter of a fuel spray
DI	direct-injection
DISC	direct-injection stratified-charge
DISI	direct-injection spark-ignited
DMI	direct mixture injection
DOHC	dual overhead cam
DV10	spray droplet size for which 10% of the fuel volume is in smaller droplets
DV90	spray droplet size for which 90% of the fuel volume is in smaller droplets
EFI	electronic fuel injection
EGT	exhaust gas temperature
EGR	exhaust gas recirculation
EOI	end of injection
FID	flame ionization detector
GDI	gasoline direct injection
HC	hydrocarbon
IDI	indirect injection
IMEP	indicated mean effective pressure
IPTV	incidents per thousand vehicles
ISFC	indicated specific fuel consumption
kPa	kilopascal
LDA	laser Doppler anemometry
LDV	laser Doppler velocimetry
LEV	low-emission-vehicle emission standard
LIF	laser-induced fluorescence
MAP	manifold absolute pressure
MBT	maximum brake torque
MCP	Mitsubishi combustion process
MPa	megapascal
MPI	multi-point port injection
NO	nitrous oxide
NO_x	nitric oxides
OEM	original equipment manufacturer
PDA	phase Doppler anemometry
PFI	port fuel injected
PIV	particle imaging velocimetry
PLIF	planar laser-induced fluorescence
PROCO	Ford programmed combustion control system
SCRC	stratified charge rotary combustion

SCV	swirl control valve
SI	spark ignition
SIDI	spark-ignited direct-injection
SMD	Sauter mean diameter of a fuel spray
SOHC	single overhead cam
SOI	start of injection
SULEV	super ULEV
TCCS	Texaco controlled combustion system
TDC	top dead center
TWC	three-way catalyst
UBHC	unburned hydrocarbons
ULEV	ultra-low-emission-vehicle emission standard
VVT	variable valve timing
VVT-i	variable valve timing—intelligent (Toyota)
WOT	wide open throttle.

Various acronyms for gasoline direct injection technology that are encountered in the worldwide literature

DGI	direct gasoline injection
DIG	direct injection gasoline
DI-G	direct injection gasoline
DISI	direct-injection spark-ignited
GDI	gasoline direct injection
G-DI	gasoline direct injection
SIDI	spark-ignited direct-injection

1. Introduction

1.1. Overview

With the increasing emphasis on achieving substantial improvements in automotive fuel economy, automotive engineers are striving to develop engines having enhanced brake-specific fuel consumption (BSFC), and which can also comply with future stringent emission requirements. The BSFC, and hence the fuel economy, of the compression-ignition, direct-injection (CIDI), diesel engine is superior to that of the port-fuel-injected (PFI) spark-ignition engine, mainly due to the use of a significantly higher compression ratio, coupled with unthrottled operation. The diesel engine, however, generally exhibits a higher noise level, a more limited speed range, diminished startability, and higher particulate and NO_x emissions than the spark ignition (SI) engine. Over the past two decades, attempts have been made to develop an internal combustion engine for automotive applications that combines the best features of the SI and the diesel engines. The objective has been to combine the specific power of the gasoline engine with the efficiency of the diesel engine at part load. Such an engine would exhibit a BSFC approaching that of the diesel engine, while maintaining the operating characteristics and specific power output of the SI engine.

Research has indicated that a promising candidate for achieving this goal is a direct-injection, four-stroke, spark-ignition engine that does not throttle the inlet mixture to control the load. In this engine, a fuel spray plume is injected directly into the cylinder, generating a fuel–air mixture with an ignitable composition at the spark gap at the time of ignition. This class of engine is designated as a direct-injection, stratified-charge (DISC) engine. This engine type generally exhibits an improved tolerance for fuels of lower octane number and driveability index, and a significant segment of the early work on prototype DISC engines focused on the inherent multi-fuel capability [1–3]. In a manner similar to that of the diesel, the power output of this engine is controlled by varying the amount of fuel that is injected into the cylinder. The induction air is not significantly throttled, thus minimizing the negative work of the pumping loop of the cycle. By using a spark plug to ignite the fuel as it mixes with air, the engine is provided with direct ignition, thus avoiding many of the requirements of autoignition quality that are inherent in fuels for the diesel engine. Furthermore, by means of the relative alignment of the spark plug and the fuel injector, overall ultra-lean-operation may be achieved, thus yielding an enhanced BSFC [4–8].

From a historical perspective, interest in these significant benefits has promoted a number of important investigations of the potential of DISC engines. Several detailed combustion strategies were proposed and implemented, including the Texaco Controlled Combustion System (TCCS) [9], MAN-FM of Maschinenfabrik Auguburg-Nurnberg [10–12], and the Ford programmed combustion (PROCO) system [13,14]. These earlier systems were based upon

engines having two valves per cylinder, with a bowl-in-piston combustion chamber. Late injection was achieved by utilizing a mechanical pump-line-nozzle fuel injection system from a diesel engine application. Unthrottled operation was obtained throughout most of the load range, with a BSFC that was competitive with an indirect-injection (IDI) diesel engine. A major drawback was that late injection timing was maintained even at full load due to the limitations of the mechanical fuel injection system. This provided smoke-limited combustion for air–fuel ratios richer than 20:1. The necessity of using diesel fuel injection equipment, coupled with the need for a turbocharger to provide adequate power output culminated in an engine that had cost and performance characteristics that were similar to those of a diesel engine, but which had poor part-load unburned hydrocarbon (UBHC) emissions. The combination of relatively poor air utilization and the use of fuel injection equipment that was limited in speed range meant that the engine specific power output was quite low. A discussion of the geometric configuration of these early systems is given in Section 6.1.

Many of the basic limitations that were encountered in the earlier work on DISC engines can now be circumvented. This is particularly true for the significant control limitations that existed for the direct-injection (DI) injectors of 15 years ago. New technologies and computer-control strategies are currently being invoked by a number of automotive companies to reexamine the extent to which the potential benefits of the gasoline direct injection (GDI) engine can be realized in production engines [15–37,276–288,303,306, 318]. These engines and combustion strategies are discussed in detail in Sections 6.2–6.17.

The information in this document will provide the reader with a comprehensive review of the mixture dynamics and combustion control strategies that may be utilized in four-stroke, spark-ignited, direct-injection, gasoline engines. The current state of knowledge, as exhibited in more than 370 key publications, many of which remain untranslated into English, is discussed in detail, and the critical research and development needs for the near future are identified.

1.2. Key potential benefits: GDI engine versus PFI engine

The major difference between the PFI engine and the GDI engine is in the mixture preparation strategies, which are illustrated schematically in Fig. 1. In the PFI engine, fuel is injected into the intake port of each cylinder, and there is an associated time lag between the injection event and the induction of the fuel and air into the cylinder. The vast majority of current automotive PFI engines utilize timed fuel injection onto the back of the intake valve when the intake valve is closed. During cranking and cold starting, a transient film, or puddle, of liquid fuel forms in the intake valve area of the port. This causes a fuel delivery delay and an associated inherent metering error due to partial vaporization, making it necessary to supply amounts of fuel that

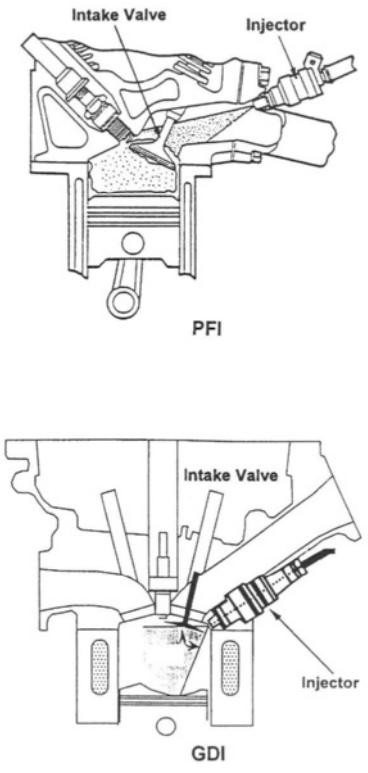

Fig. 1. Comparison of the PFI [375] and GDI [42] mixture preparation systems.

significantly exceed that required for the ideal stoichiometric ratio. This puddling and time lag may cause the engine to either misfire or experience a partial burn on the first 4–10 cycles, with an associated significant increase in the UBHC emissions. Alternatively, injecting fuel directly into the engine cylinder totally avoids the problems associated with fuel wall wetting in the port, while providing enhanced control of the metered fuel for each combustion event, as well as a reduction in the fuel transport time. The actual mass of fuel entering the cylinder on a given cycle can thus be more accurately controlled with direct injection than with PFI. The GDI engine offers the potential for leaner combustion, less cylinder-to-cylinder variation in the air–fuel ratio and lower operating BSFC values. The UBHC emissions during a cold start are also potentially lower with direct injection, and the engine transient response can be enhanced. As a result of the higher operating fuel pressure of the GDI system, the fuel entering the cylinder is much better atomized than that of the PFI system, particularly under cold operating conditions, thus yielding much higher rates of fuel vaporization. The mean drop size is typically 16 microns SMD as compared to 120 microns SMD with the PFI system. It is important to note, however, that injection of fuel directly into the cylinder is not a guarantee that fuel film problems are not present. The wetting of piston crowns or other combustion chamber surfaces,

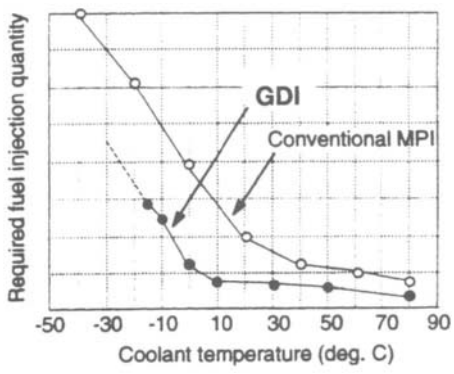

Fig. 2. Comparison of the fuel quantity required to start GDI and PFI engines at different ambient temperatures [41].

whether intentional or unintentional, does introduce the important variable of transient wall film formation and evaporation.

The GDI concept does indeed offer many opportunities for circumventing the basic limitations of the PFI engine, particularly those associated with port wall wetting. The fuel film in the intake port of a PFI engine acts as an integrating capacitor, and the engine actually operates on fuel inaccurately metered from the pool in the film, not from the current fuel being accurately metered by the injector [38]. During a cold start, the fuel from more than 10 cycles must be injected to achieve a steady, oscillatory film of liquid fuel in the intake port. This means that the cold PFI engine does not fire or start on the first few cycles, even though fuel is being repetitively injected into the film pool. Control algorithms must be used to provide significant over-fueling if acceptable PFI start times are to be achieved, even though the catalyst temperature is below the light-off threshold at this condition and UBHC emissions will be increased. Thus it is not unusual for PFI systems to generate 90% of the total UBHC emissions in the US FTP emission test within the first 90 s [39].

The direct injection of gasoline into the cylinder of a four-stroke, gasoline, spark-ignition engine eliminates the integrating fuel film in the intake port. It is well established that the direct injection of gasoline with little or no cold enrichment can provide starts on the second cranking cycle [40], and can exhibit significant reductions in UBHC spikes during load transients. An excellent example of the comparison of the fuel quantity required to start GDI and PFI engines is provided in Fig. 2 [41]. It is quite evident that the GDI engine requires much less fuel to start the engine, and that this difference in the minimum fuel requirement becomes larger as the ambient temperature decreases.

Another limitation of the PFI engine is the requirement of throttling for basic load control. Even though throttling is a well-established and reliable mechanism of load control in the PFI engine, the thermodynamic loss associated with throttling is substantial. Any system that utilizes throttling to adjust load levels will experience the thermodynamic loss that is associated with this pumping loop, and will exhibit thermal efficiency degradation at low levels of engine load. Current advanced PFI engines still utilize, and will continue to require, throttling for basic load control. They also have, and will continue to have, an operating film of liquid fuel in the intake port. These two basic PFI operating requirements represent major impediments to achieving significant breakthroughs in PFI fuel economy or emissions. Continuous incremental improvements in the older PFI technology will be made, but it is unlikely that the long-range fuel economy and emission objectives can be simultaneously achieved. The GDI engine, in theory, has neither of these two significant limitations, nor the performance boundaries that are associated with them. The theoretical advantages of the GDI engine over the contemporary PFI engine are summarized as follows, along with the enabling mechanism:

- Improved fuel economy (up to 25% potential improvement, depending on test cycle resulting from:
  - less pumping loss (unthrottled, stratified mode);
  - less heat losses (unthrottled, stratified mode);
  - higher compression ratio (charge cooling with injection during induction);
  - lower octane requirement (charge cooling with injection during induction);
  - increased volumetric efficiency (charge cooling with injection during induction);
  - fuel cutoff during vehicle deceleration (no manifold film).

- Improved transient response.
  - less acceleration-enrichment required (no manifold film).

- More precise air–fuel ratio control.
  - more rapid starting;
  - less cold-start over-fueling required.

- Extended EGR tolerance limit (to minimize the use of throttling).
- Selective emissions advantages.
  - reduced cold-start UBHC emissions;
  - reduced CO_2 emissions.

- Enhanced potential for system optimization.

The significantly higher injection pressures used in common-rail GDI injection systems as compared to PFI fuel systems increase both the degree of fuel atomization and the fuel vaporization rate, and, as a result, it is possible to achieve stable combustion from the first or second injection cycle without supplying excess fuel. Therefore, GDI engines have the potential of achieving cold-start UBHC emissions that can approach the level observed for steady

running conditions. Takagi [23] reported that the cold-start UBHC emissions obtained with the Nissan prototype GDI engine are approximately 30% lower than that of an optimized PFI engine under comparable conditions. Another potential advantage of the GDI engine is the option of using fuel cutoff on deceleration. If implemented successfully, fuel cutoff can provide additional incremental improvements in both fuel economy and engine-out UBHC emission levels. For the PFI engine, which operates from an established film of fuel in the intake port, the cutoff of fuel during vehicle deceleration is not a viable option, as it causes a reduction or elimination of the liquid fuel film in the port. This generates very lean mixtures in the combustion chamber for a few cycles following the restoration of the load, generally resulting in an engine misfire.

It should be noted that design engineers, managers and researchers who must evaluate and prioritize the published information on the advantages of GDI engines over PFI engines should be aware of one area of data comparison and reporting that is disconcerting. In many papers the GDI performance is compared to PFI baselines that are not well defined, thus making it very difficult for the reader to make a direct engineering comparison between GDI and PFI performance. One extreme example is the comparison of GDI and PFI fuel economy data that was obtained using two different vehicles with two different inertial weights. An example of a more subtle difference is the evaluation of the BSFC reduction resulting from the complete elimination of throttling in a GDI engine, but not noting or subtracting the parasitic loss of a vacuum pump that would have to be added for braking and other functions. A number of published comparisons lie between these two extremes. The readers are cautioned to review all claims of comparative GDI/PFI data carefully as to the precise test conditions for each, and the degree to which the systems were tested under different conditions or constraints.

PFI engines do have some limited advantages over GDI engines due to the fact that the intake system acts as a prevaporizing chamber. When fuel is injected directly into the engine cylinder, the time available for mixture preparation is reduced significantly. As a result, the atomization of the fuel spray must be fine enough to permit fuel evaporation in the limited time available between injection and ignition. Fuel droplets that are not evaporated are very likely to participate in diffusion burning, or to exit the engine as UBHC emissions. Also, directly injecting fuel into the engine cylinder can result in unintended fuel impingement on the piston or the cylinder wall. These factors, if present in the design, can contribute to levels of UBHC and/or particulate emissions, and to cylinder bore wear that can easily exceed that of an optimized PFI engine. Some other advantages of PFI engines such as low-pressure fuel system hardware, higher power density at part load and the feasibility of using three-way catalysis and higher exhaust temperatures for improved catalyst efficiency present an evolving challenge to the GDI engine.

Although the GDI engine provides important potential advantages, it does have a number of inherent problems that are similar to those of the early DISC engines. The replacement of the PFI engine by the GDI engine as the primary production automotive powerplant is constrained by the following areas of concern:

- difficulty in controlling the stratified charge combustion over the required operating range;
- complexity of the control and injection technologies required for seamless load changes;
- relatively high rate of formation of injector deposits and/or ignition fouling;
- relatively high light-load UBHC emissions;
- relatively high high-load NO_x emissions;
- high local NO_x production under part-load, stratified-charge operation;
- soot formation for high-load operation;
- increased particulate emissions;
- three-way catalysis cannot be utilized to full advantage;
- increased fuel system component wear due to the combination of high-pressure and low fuel lubricity;
- increased rates of cylinder bore wear;
- increased electrical power and voltage requirements of the injectors and drivers;
- elevated fuel system pressure and fuel pump parasitic loss.

The above concerns must be addressed and alleviated in any specific design if the GDI engine is to supplant the current PFI engine. If future emission regulations such as the ultra-low-emission-vehicle (ULEV), the super ultra-low-emission-vehicle (SULEV), and corporate average fuel economy (CAFE) requirements can be achieved using PFI engines without the requirement of complex new hardware, the market penetration rate for GDI engines will be reduced, as there will most assuredly be a GDI requirement for sophisticated fuel injection hardware, a high-pressure fuel pump and a more complex engine control system. An important constraint on GDI engine designs has been relatively high UBHC and NO_x emissions, and the fact that three-way catalysts could not be effectively utilized. Operating the engine under overall lean conditions does reduce the engine-out NO_x emissions, but this generally cannot achieve the minimum 90% reduction level that can be attained using a three-way catalyst. Much work is underway worldwide to develop lean-NO_x catalysts, but at this time the attainable conversion efficiency is still much less than that of three-way catalysts. The excessive UBHC emissions at light-load also represent a significant research problem to be solved. In spite of these concerns and difficulties, the GDI engine offers an expanded new horizon for future applications as compared to the well-developed PFI engine.

In summary, the potential advantages of the GDI concept are too significant to receive other than priority status. The concept offers many opportunities for achieving significant improvements in engine fuel consumption, while simultaneously realizing large reductions in engine-out UBHC

emissions. The current high-tech PFI engine, although highly evolved, has nearly reached the limit of the potential of a system that is based upon throttling and a port fuel film; however, the technical challenge of competing with, and displacing, a proven, evolved performer such as the PFI engine is not to be underestimated. Since the late 1970s, when a significant portion of the DISC engine work was conducted, the SI engine has continued to evolve monotonically as an ever-improving baseline. The fuel system has also evolved continuously from carburetor to throttle-body injection, then to simultaneous-fire PFI, and more recently to phased-sequential-fire PFI. The result is that today the spark-ignited PFI engine remains the benchmark standard for automobile powerplants [38]. In order to displace this standard, the practical development targets for future GDI engines, as compared to current best-practice PFI engines, are as follows [42]:

- 15–20% reduction in BSFC over an integrated cycle;
- compliance with stringent future emissions regulations;
- specific power output that is comparable to PFI;
- driveability during cold starts, warm-up and load transients that is comparable to PFI.

In addition to the above, reliable and efficient hardware and control strategies for gasoline direct injection technology will have to be developed and verified under field conditions. For the same reasons that port fuel injection gradually replaced carburetor and throttle-body injection, a GDI combustion configuration that will be an enhancement of one of the concepts outlined in this paper will emerge as the predominate engine system, and will gradually displace the sequential PFI applications.

2. Direct-injection gasoline fuel system

Unthrottled operation with the load controlled by the fuel quantity has been shown to be a very efficient operating mode for the internal combustion engine, as the volumetric efficiency is increased and the pumping loss is significantly reduced. This strategic approach is very successful in the diesel engine, as ignition occurs spontaneously at points within the combustion chamber where the mixture is well prepared for autoignition. The fixed location of the ignition source in the SI engine, however, makes it quite difficult to operate in the unthrottled mode for other than full load. This imposes a critical additional requirement on the mixture formation process of this type of engine in that the mixture cloud that results from fuel vaporization and mixing must be controlled both spatially and temporally in order to obtain stable combustion. Preparing a desired mixture inside the combustion chamber over the full range of engine operating conditions is quite difficult, as the fuel–air mixing process is influenced by many time-dependent variables. The development of a successful combustion system depends upon the optimized design of the fuel injection system and the proper matching of the system components to control the in-cylinder flow field and burn rate.

The fuel injection systems of early DISC engines were derived from the basic diesel injection system. For example, the Texaco TCCS engine [9] utilized a diesel-type injector that produced a spray with relatively poor atomization and fuel–air mixing quality, and with high penetration rates relative to sprays from current pressure-swirl atomizers. The Ford PROCO engine [14] used an outwardly opening pintle atomizer with vibration to enhance the fuel atomization; however, the poppet opening pressure was on the order of 2.0 MPa, which is quite low. (Note: all the pressures used in this document refer to gauge pressure.) Gasoline injection using single-hole or multi-hole narrow-angle sprays from diesel injection systems nearly always result in substantial UBHC emissions due to the compactness of the spray and the high penetration velocity. In order to avoid this problem, combustion systems using direct wall impingement and fuel film formation such as the MAN-FM [11] were developed. For early DISC engine experiments using multi-hole injectors, the singularity of the ignition source proved to be a definite problem, as compared to a diesel combustion system where multiple ignition sites occur simultaneously. Another severe problem for the diesel-based DISC injection system is the lack of variability of injection characteristics between part load and full load. For full-power DISC engine operation, injection of maximum fuel quantities early in the intake stroke resulted in significant wall impingement of the fuel, mainly due to the high penetration rate of the fuel sprays.

2.1. Fuel system requirements

In recent years, significant progress has been made in the development of advanced computer-controlled fuel injection systems, which has had much to do with the research and development activities related to GDI engines being expanded. In this section, the key components that are utilized in the fuel system and their important roles in the mixture preparation and combustion processes are described in detail.

The fuel injection system in a GDI engine is a key component that must be carefully matched with the specific in-cylinder flow field to provide the desired mixture cloud over the entire operating range of the engine. A well-atomized fuel spray must be produced for all operating conditions. For the efficient combustion of a stratified mixture, a stable and compact spray geometry is necessary [20]. A GDI fuel system needs to provide for at least two, and possibly three or more distinct operating modes. For unthrottled, part-load operation, the injection system should provide the capability for rapid injection late in the compression stroke into an ambient pressure of up to 1.0 MPa, which requires a relatively high fuel injection pressure. The fuel injection pressure has been determined to be very important for obtaining both effective spray atomization and the required level of spray penetration. A higher fuel injection

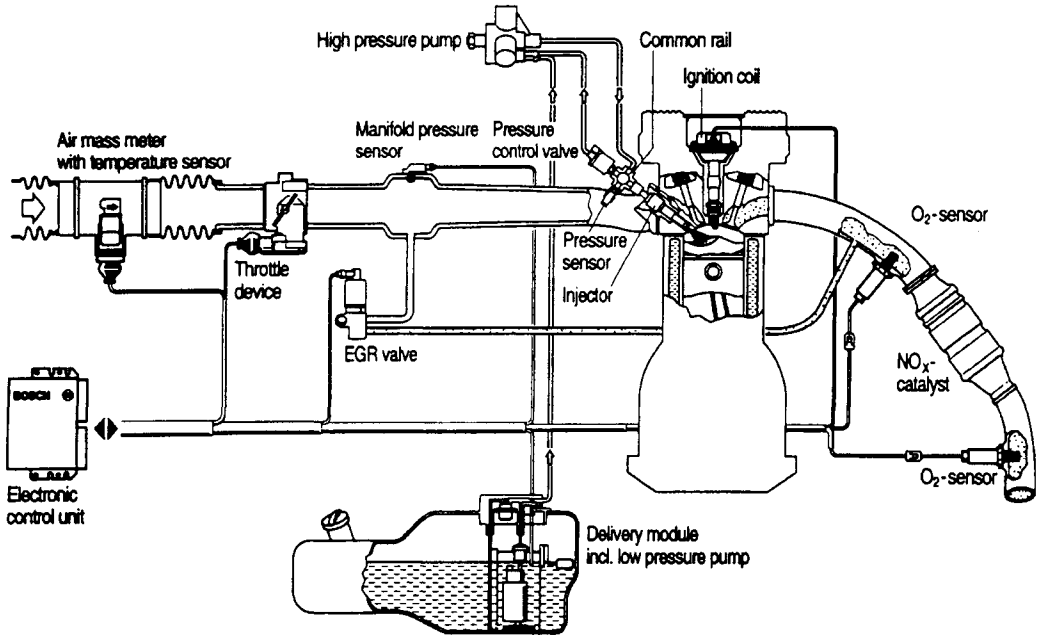

Fig. 3. Typical GDI engine system layout [95].

pressure reduces the mean diameter of the spray approximately as the inverse square root of the pressure differential ($P_{inj} - P_{cyl}$), whereas the use of a lower pressure generally reduces the pump parasitic load, system priming time and injector noise, which generally increases the operating life of the fuel pump system. The use of a very high fuel injection pressure, such as 20 MPa, will enhance the atomization but will most likely generate an overpenetrating spray, resulting in fuel wall wetting. The fuel pressures that have been selected for most of the current prototype and production GDI engines range from 4 to 13 MPa, which are quite low when compared with diesel injection system pressures of 50–160 MPa, but are relatively high in comparison with typical PFI injection pressures of 0.25–0.45 MPa. It should be noted that the level of noise emitted from GDI injectors and fuel pumps is of concern, and noise abatement research must continue. A constant fuel injection supply line pressure is utilized in a common-rail configuration for most of the current GDI applications; however, a strategy using a variable fuel injection pressure does offer an alternative method of obtaining the required flow range while reducing the linear-dynamic-range requirements of the injector itself [64], and for meeting different fuel-spray requirements corresponding to a range of engine loads [44]. This is an important consideration that must be evaluated for each GDI application.

Fuel injection systems for full-feature GDI engines must have the capability of providing both late injection for stratified-charge combustion at part load, as well as injection during the intake stroke for homogeneous-charge combustion at full load. At part load a well-atomized compact spray or mixture plume is desirable to achieve rapid mixture formation and controlled stratification. At full load, a well-dispersed fuel spray or mixture plume is desirable to ensure a homogeneous charge for even the largest fuel quantities. This is generally achieved by early injection at low cylinder pressure, similar to the mode of open-valve fuel injection in the PFI engine. In total, these fuel system requirements are more comprehensive than those of either the diesel or the PFI injection systems. Based on recent experimental investigations, it has been concluded that common-rail injection systems with electromagnetically activated injectors can meet these exacting requirements [28,45–48]. The typical components of the common-rail fuel system of a GDI engine are illustrated in Fig. 3. In principle, this common-rail fuel system is comparable to those utilized in current PFI and advanced diesel engines, with the GDI application having an intermediate fuel pressure level.

The capabilities of current control systems permit complex strategies for mixture formation and control. For example, in the Toyota GDI D-4 combustion system [43], a two-stage injection strategy is utilized to improve the transition between part-load and full-load operations. Similar two-stage injection strategies have also been proposed to avoid engine knock, thus increasing engine torque, by injecting the fuel partially during the intake stroke and partially during the compression stroke [17,48]. A late injection strategy during the expansion stroke has been employed in the Mitsubishi production GDI engine of the European market to increase the exhaust temperature for quicker catalyst light-off during the cold start [17,18,49]. It has been observed that for such a two-stage injection the split fraction is very critical.

During the engine cold crank and start, the high-pressure fuel pump generally cannot deliver fuel at the full design pressure due to the short time available and the low engine cranking speed. To solve this priming-time problem, the Mitsubishi GDI engine uses an in-tank fuel feed pump that is similar to that used in PFI engines. A bypass valve is used to allow the fuel to bypass the high-pressure regulator for engine crank and start. As a result, the electric feed pump supplies the fuel directly to the fuel rail. As the engine speed and fuel line pressure increase, the bypass valve is closed and the high-pressure regulator begins to regulate the fuel pressure to 5.0 MPa. As a result, it is reported that this engine can be started within 1.5 s for both cold and hot restart conditions [50,51]. Shelby et al. [52] visualized the spray structure of two Zexel GDI injectors with cone angles of 20° and 60° when operating at a cranking fuel pressure of 0.3 MPa. It was found that both injectors are still able to develop the hollow cone structure under such a low fuel injection pressure, however the atomization is noticeably degraded. It was reported that the injection duration required for a stoichiometric mixture is approximately four times as long as when operating from the main fuel pump, as the injection duration required is proportional to the square root of the fuel injection pressure.

Based upon a review of the literature, the key points of information related to GDI fuel systems are:

- 4.0–13.0 MPa have been utilized as fuel rail design pressures;
- a fuel rail pressure of from 5.0 to 7.5 MPa is most common in current GDI systems;
- 7.0–10.0 MPa is the most likely design rail pressure range for future systems;
- pump life, noise and system priming rate are important concerns, particularly at pressures above 8.5 MPa;
- variable injection pressure is a viable system strategy.

A wide range of gasoline, having variable alcohol content, sulfur content and driveability indices are available in the field. This quality range makes it a necessity that a robust fuel system be developed and proven for GDI production engines [296]. To avoid dilution of the engine oil, most GDI fuel pumps are lubricated with gasoline [373]. However, gasoline has a lower lubricity, viscosity, and a higher volatility than diesel fuel, generally resulting in higher friction and a greater potential for wear and leakage as compared to diesel fuel pumps. It should be noted, however, that hydrodynamic lubrication may be used at high fuel pressures to compensate for the low viscosity.

2.2. *Fuel injector considerations*

The fuel injector is considered to be the most critical element in the GDI fuel system, and it should have the following attributes. Many of the required characteristics of the GDI injector are equivalent to those of the port fuel injector, which are [38]:

- accurate fuel metering (generally a ±2% band over the linear flow range);
- desirable fuel mass distribution pattern for the application;
- minimal spray skew for both sac and main sprays;
- good spray axisymmetry over the operating range;
- minimal drippage and zero fuel leakage, particularly for cold operation;
- small sac volume;
- good low-end linearity between the dynamic flow and the fuel pulse width;
- small pulse-to-pulse variation in fuel quantity and spray characteristics;
- minimal variation in the above parameters from unit to unit.

In certain critical areas the specification tolerances of a GDI injector design are more stringent than that of the port-fuel injector, or there are requirements that are not present for PFI applications. These areas are:

- significantly enhanced atomization level; a smaller value of spray mean drop size;
- expanded dynamic range;
- combustion sealing capability;
- avoidance of needle bounce that creates unwanted secondary injections;
- reduced bandwidth tolerance for static flow and flow linearity specifications;
- more emphasis on spray penetration control;
- more emphasis on the control of the sac volume spray;
- enhanced resistance to deposit formation;
- smaller flow variability under larger thermal gradients;
- ability to operate at higher injector body and tip temperatures;
- leakage resistance at elevated fuel and cylinder pressures;
- zero leakage at cold temperature;
- more emphasis on packaging constraints;
- flexibility in producing off-axis sprays in various inclined axes to meet different combustion system requirements.

The GDI injector should be designed to deliver a precisely metered fuel quantity with a symmetric and highly repeatable spray geometry, and must provide a highly atomized fuel spray having a Sauter mean diameter (SMD) of generally less than 25 μm, and with a droplet diameter corresponding to the cumulative 90% volume point (DV90) not exceeding 45 μm [53–55]. The SMD is sometimes denoted more formally in the spray literature as D32. The DV90 statistic is a quantitative statistical measure of the largest droplets in the total distribution of all droplet sizes. Smaller values than these are even more beneficial, provided sufficient spray penetration is maintained for good air utilization. The fuel pressure required is at least 4.0 MPa for a single-fluid injector, with 5.0–7.0 MPa being more desirable if the late-injection stratified mode is to be invoked. Even if successful levels of atomization could be achieved at fuel pressures lower than 4.0 MPa, significant metering errors could result from the variation of

metering pressure differential ($P_{inj} - P_{cyl}$) with cylinder pressure, although this could be corrected by the engine control system (ECS) if cylinder pressures were monitored.

The sac volume within the injector tip is basically the volume of fuel, resulting from the previous injection, which is not at the fuel line pressure; therefore it retards the acceleration of the injected fuel and generally degrades both the fuel atomization and the resulting combustion. There is a consensus that the sac spray influences the air entrainment and the resulting spray cone angle, particularly at elevated ambient densities. In general, the smaller the sac volume, the fewer large peripheral drops that will be generated when the injector opens. Needle bounce on closure is to be avoided, as a secondary injection generally results in uncontrolled atomization consisting of larger droplets of lower velocity or possible unatomized fuel ligaments. Needle bounce on closure also degrades the fuel metering accuracy and contributes to increases in the UBHC and particulate emissions. Needle bounce on opening is not nearly as important as that on closure, but should be controlled. The result of a needle bounce on opening is a small modulation in the injection rate.

The ability to provide a high rate of injection, which is equivalent to delivering the required fuel with a short fuel pulse, is much more important for the GDI engine than for the PFI engine, particularly for light-load stratified-charge operation. Therefore, much more significance is attached to the low-pulse-width region of the GDI injector, effectively increasing the importance of the injector dynamic range requirement. Standard measures of injector capabilities are the dynamic (linear) range, the shortest operating pulse width on the linear flow curve and the lowest stable fuel pulse width. Fuel pulse widths that are shorter than the linear range limit can be used in the calibration by means of a lookup table of pulse width if the fuel mass delivery is stable at that operating point. The optimal design of the injector to resist coking is also one of the important requirements of the GDI injector, as is discussed in detail in the section on injector deposits. Sometimes overlooked are the voltage and power requirements of the injector solenoids and drivers. A number of current prototype GDI injectors have power requirements that would be considered unacceptable for a production application. It is also worth noting that it is advantageous to injector packaging to have the body as small as possible. This provides more flexibility in optimizing the injector location and in sizing and locating the engine ports and valves.

In spite of decades of continuous development on diesel multi-hole injectors, it has been demonstrated that these nozzle-type injectors are generally poor choices for GDI applications. A multi-hole VCO nozzle used in a GDI engine application results in an unstable flame kernel when ignited by a single fixed spark plug. The rich mixture zones are close to the lean mixture zones; thus the flame front does not propagate uniformly through the combustion chamber. With the multi-hole nozzle, the orientation of the

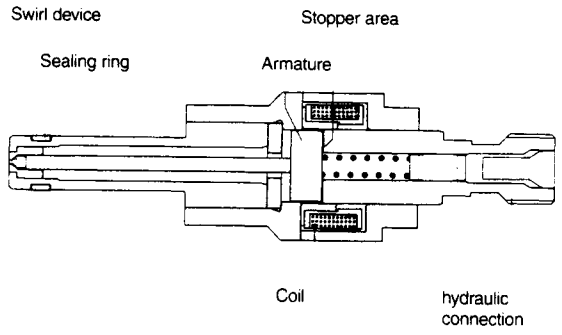

Fig. 4. Schematic of the inwardly opening, single-fluid, high-pressure, swirl injector [272].

nozzle hole is an important factor in determining engine combustion performance. It has been found that the hole distribution that is effective in ensuring good spray dispersion and reliable flame propagation between the spray plumes generally provides good engine performance. The effect of the cone angle of individual spray plumes on GDI engine performance was studied by Fujieda et al. [56]. A multi-hole GDI injector similar to that used in diesel engines was designed and tested. It was found that with an increase in the spray cone angle the lean limit is extended, due to the improvement in air utilization. It was also determined that reducing the nozzle flow area and/or increasing the number of holes can achieve the same purpose.

Currently, the most widely utilized GDI injector is the single-fluid, swirl-type unit that utilizes an inwardly opening needle, a single exit orifice and a fuel pressure in the range from 5.0 to 10 MPa. A schematic of this type of injector is illustrated in Fig. 4. This general configuration can be regarded conceptually as a multi-hole nozzle with an infinite number of holes, with a uniform distribution of the fuel around the cone circumference being obtained. As a consequence, wall impingement at full load can be minimized for an appropriate injector position and spray cone angle [57]. The needle-type, swirl-spray injector is designed to apply a strong rotational momentum to the fuel in the injector nozzle that adds vectorially to the axial momentum. In a number of nozzle designs, liquid flows through a series of tangential holes or slots into a swirl chamber. The liquid emerges from the single discharge orifice as an annular sheet that spreads radially outward to form an initially hollow-cone spray. The initial spray cone angle may range from a design minimum of 25° to almost 180°, depending on the requirements of the application, with a delivered spray SMD ranging from 14 to 25 μm. In the swirl-type injector, the pressure energy is effectively transformed into rotational momentum, which enhances atomization. Moreover, the spray mass distribution of a swirl-type injector is generally more axisymmetric than that obtained without swirl [58,59]. Fig. 5 shows a comparison of the spray characteristics of hole-type and swirl-type nozzles. The reported spray atomization characteristics were obtained by means of laser

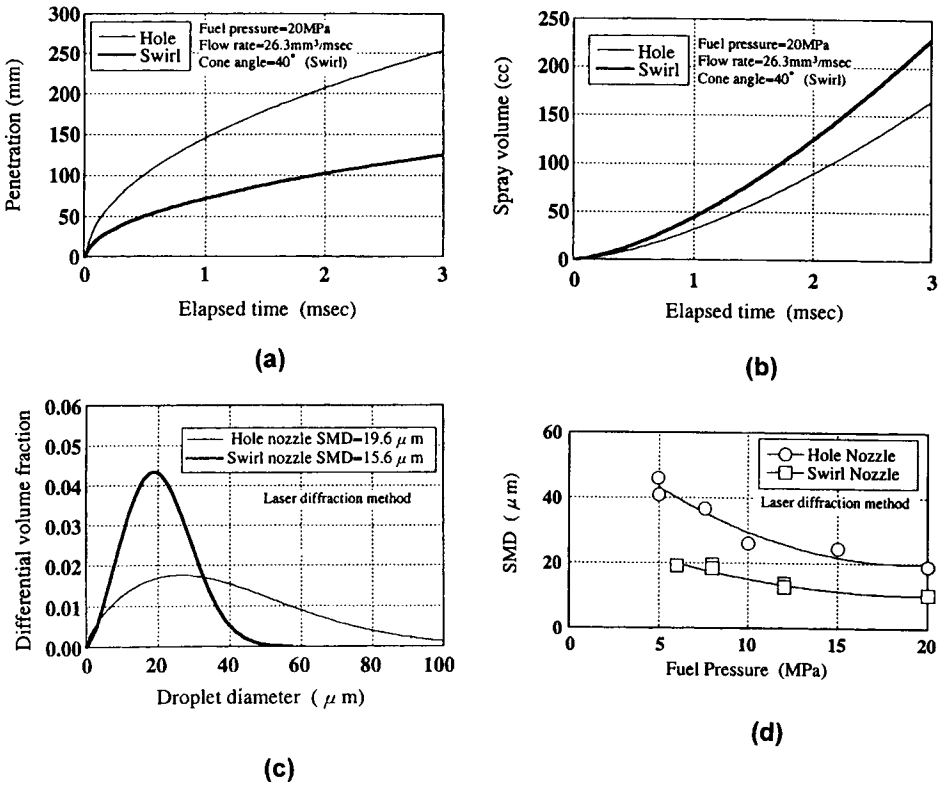

Fig. 5. Comparison of the spray characteristics of hole-type and swirl-type high-pressure injectors for an injection pressure of 20 MPa [60].

diffraction, and the spray penetration and spray volume represent the calculated results from empirical equations.

The swirl nozzle generally produces a spray having a narrower distribution of drop sizes (DV90–DV10) than is obtained with the standard hole-type nozzle, with the best atomization occurring at high delivery pressures and wide spray angles. An additional advantage is that the injector designer can customize the spray penetration curve by altering the swirl ratio with only small changes in the atomization level, thus providing the necessary variability of spray configuration in order to meet different stratification requirements. However, increased surface roughness of the orifice wall in swirl injectors tends to exacerbate the formation of streams or fingers of fuel in the fuel sheet exiting the nozzle, resulting in the formation of pockets of locally rich air–fuel mixture. In order to minimize such mixture inhomogeneity, precise control of the swirl channel surface finish and nozzle tip quality is required [60]. The spray formation mechanism of the swirl-type injector and three typical designs of the swirler nozzle are illustrated in Fig. 6 [61]. The three types of swirler tips in Fig. 6(b) generate similar spray characteristics when the swirl Reynolds number is maintained. The tangential-slot-type swirler was selected for the Mitsubishi GDI engine. The effect of swirl Reynolds number on the spray cone angle and spray tip penetration of this injector for injection into an ambient pressure of 0.5 MPa is shown in Fig. 7 [50,51]. The strong dependence of spray characteristics such as mean droplet size, spray cone angle, and penetration on the swirl intensity makes the customized tailoring of each individual spray parameter difficult.

The pressure-swirl injector concept was successfully applied to meet the production requirements of their GDI engine by engineers at Mitsubishi. In their design, the fuel swirl is generated by a swirler tip located upstream of the injector hole. The effect of the fuel swirl level on the droplet size and spray structure was studied extensively by Kume et al. [20] and by Iwamoto et al. [50,51], and the results are summarized in Figs. 8 and 9. It was found that when the swirl level is increased, a comparatively lower fuel pressure suffices for achieving an acceptable level of atomization. Increasing the fuel swirl level also promotes air entrainment, with the toroidal vortex ring that is initially generated near the injector tip growing to a larger scale vortex during the latter portions of the injection event. Droplet velocity measurements using a phase Doppler analyzer (PDA) showed that the axial velocity component decreases with distance from the injector tip, whereas the swirl-component remains fairly constant. The decrease in the axial velocity is caused by drag on the fuel droplets that are moving relative to the ambient air. In contrast, the swirl component drag is not significant because the ambient air rotates with the fuel droplets. As illustrated in Fig. 10, for the case of reduced

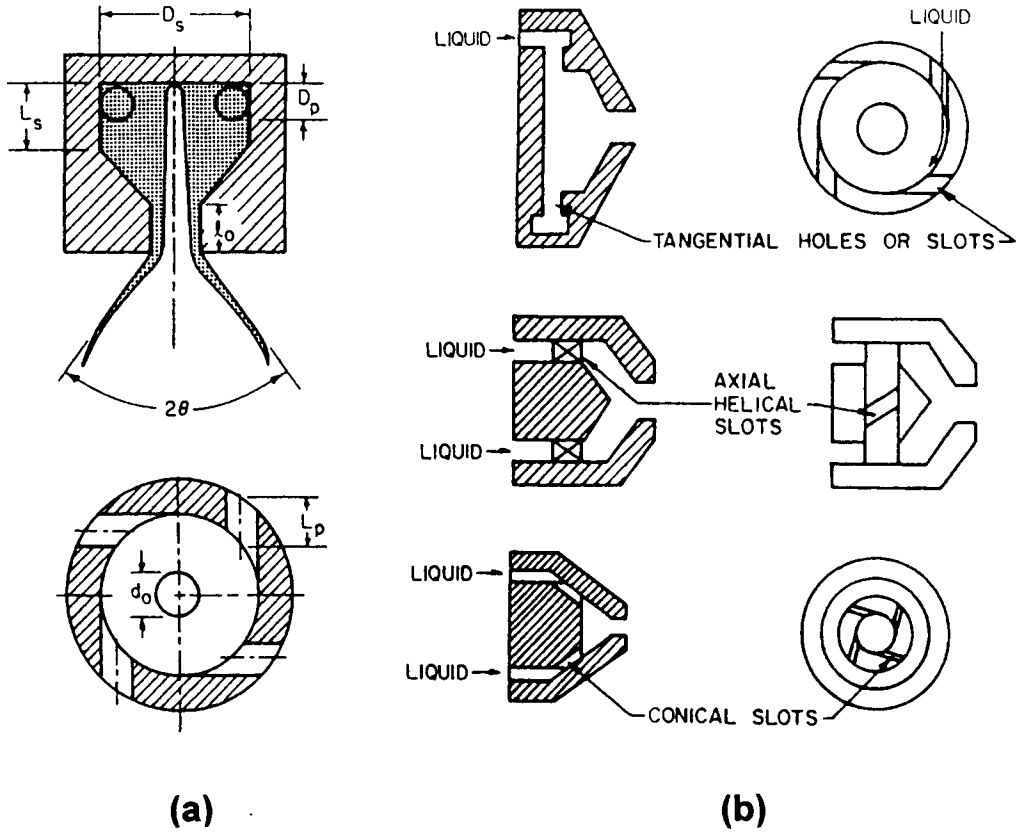

Fig. 6. Spray formation mechanism of the swirl-type injector and three typical designs of the swirler nozzle [61].

ambient pressure during early injection, the fuel spray has a wide, hollow-cone structure. In the case of higher ambient pressure, the higher drag force changes the spray into a narrower, solid-cone shape. Ader et al. [35] modeled and predicted the air velocity distribution inside a spray. It was found that the spray-induced airflow is much higher for the high-ambient-pressure condition, which was theorized to lead to a strong deflection of droplets to the center of the spray, thus causing the spray cone to collapse as depicted in Fig. 11.

Most current GDI injectors are inwardly opening; however, work on developing an outwardly opening injector for automotive GDI applications was reported by engineers at Delphi [58,62,63]. A schematic of this single-fluid, outwardly opening, swirl injector is shown in Fig. 12. It was claimed that an outwardly opening pintle design has some advantages that should be considered. For example, the outwardly opening pintle injector is able to avoid the initial sac spray generated by the sac volume of most inwardly opening GDI injectors. Moreover, the initial liquid sheet thickness is directly controlled by the pintle stroke rather than by the angular velocity of the swirling fuel in an inwardly opening nozzle. As a result, the outwardly opening injector has a design flexibility that allows the spray angle, penetration and droplet size to be controlled with less coupling. Swirling flow may also be used in the outwardly opening pintle design for reducing the spray penetration, and for increasing the spray cone angle. In addition, the initial sheet thickness provided by the outwardly opening pintle was claimed to be smaller during the valve opening and closing events due to the reduced pressure drop at the swirler. As a result, it is claimed that the atomization level obtained during opening and closing is even better than is obtained during the main spray portion,

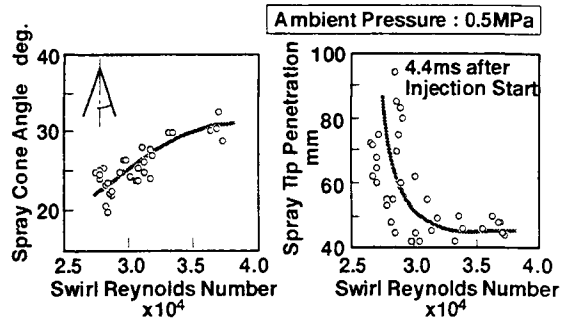

Fig. 7. Effect of the swirl Reynolds number on the spray cone angle and the spray tip penetration of a high-pressure swirl injector for injection into an ambient pressure of 0.5 MPa [50,51].

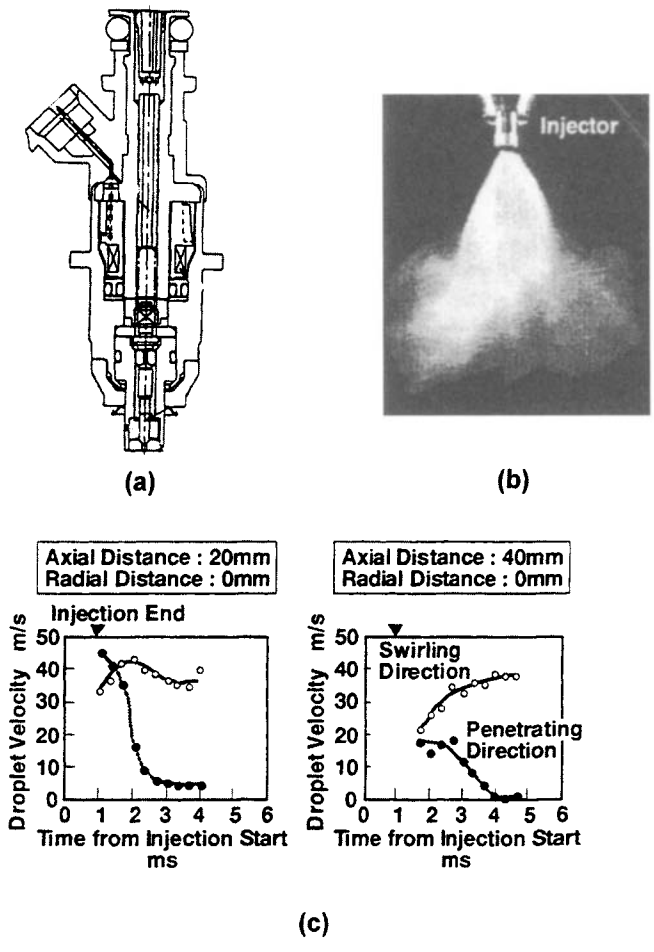

Fig. 8. Spray characteristics of the Mitsubishi GDI injector [20,50,51]: (a) injector design; (b) spray outlook; and (c) spray characteristics.

which is the opposite of what is generally obtained using inwardly opening pintles. Since no nozzle holes are directly exposed to the combustion chamber environment, this outwardly opening design may prove to be more robust to combustion product deposition. More development and evaluation experience is required on this issue. According to Xu and Markle [58], the outwardly opening injector is able to produce a spray with an SMD of less than 15 μm as measured by laser diffraction at 30 mm downstream from the nozzle, a DV90 of less than 40 μm, and a maximum limiting penetration of 70 mm into one atmosphere. With regards to the relative advantages of inwardly opening versus outwardly opening needles, the inwardly opening needle generally provides better pulse-to-pulse repeatability of the spray cone geometry, especially when a flow guide bushing is present at the needle tip, and does provide enhanced design flexibility in achieving angled sprays. The outwardly opening geometry is, however, acknowledged to have enhanced leakage resistance [64,65] due to the fact that the combustion gas pressure assists in sealing the injector positively. A comparison of the aforementioned three typical GDI injector designs for four key criteria is provided in Fig. 13. As may be noted, the inwardly opening design has some significant advantages and has consequently been widely utilized in GDI development.

In some applications having significant packaging constraints, the GDI injector is required to deliver a spray that is angled, or offset, from that of the injector axis. Both the Toyota and Nissan production GDI engines use an offset-spray injector [21,66]. This requirement makes the GDI injector design much more complicated, as some of the techniques for producing a symmetric and well-atomized spray may no longer be as effective. For example, swirling flow, as an effective technique to enhance the atomization of a symmetric spray, may be significantly less effective in an injector design having an offset spray. As a result, a higher injection pressure may be required to achieve the same degree of spray atomization for an on-axis spray design. Also, achieving an offset-spray may not be possible with an outwardly opening pintle.

Even with a symmetric fuel distribution, the conventional cone-shaped spray tends to coat the piston surface

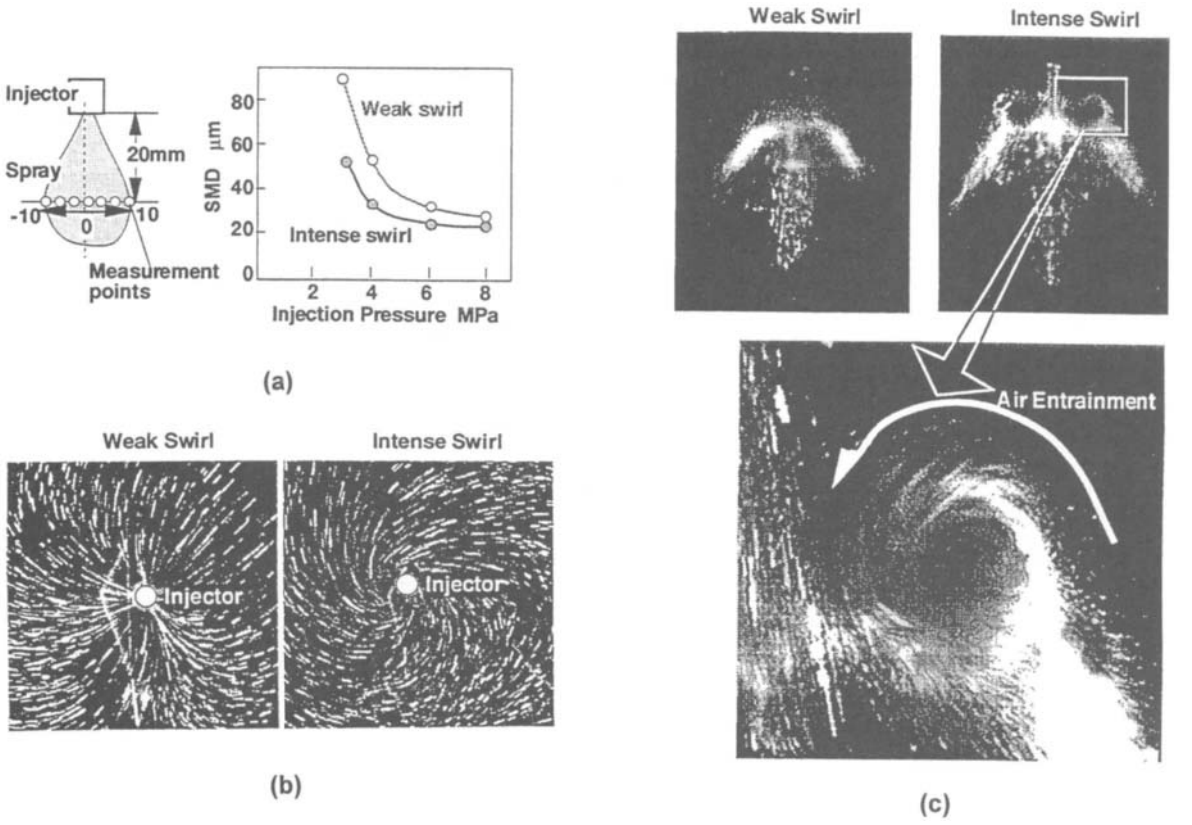

Fig. 9. Effect of the nozzle swirl on the spray characteristics of the Mitsubishi GDI injector [20,50,51]: (a) effect of the nozzle swirl intensity on droplet size; (b) spray-induced air motion at different nozzle swirl intensities; and (c) spray structure at different nozzle swirl intensities.

nonuniformly when the injector is installed with the injector axis inclined to the piston surface, which is common in many combustion chamber applications. Consequently, the region of the piston closer to the injector tends to have a larger fraction of impinging fuel, as shown in Fig. 14(a). This may result in a thicker film of fuel being formed at that location, causing increased UBHCs and particulate emissions. To avoid this problem, engineers at Nissan [66,263] developed the CASTING NET injector that provides an angled spray with a uniform fuel distribution on the piston crown, as depicted in Fig. 14(b). As illustrated in Fig. 14(c), the offset angle of the spray axis from that of the injector axis, β, which is denoted as the deflected angle, and the spray short-side and long-side lengths $L2$ and $L1$ are key parameters to be optimized. It was reported that both $L1/L2$ and the deflected angle β have marked impacts on engine combustion stability, torque and smoke emissions. The injection-timing window was claimed to be about 45 crank angle degrees wider with the CASTING NET injector than that with the conventional injector. With early injection timing, liquid film formation on the piston crown is avoided by weakening the vertical component of spray velocity with this injector. With late injection timing, improved mixture homogeneity is claimed due to strengthened horizontal component of the spray. In both cases, smoke generation was found to be reduced to an acceptable level due to improved mixture formation.

Some other injector concepts such as the two-step injection nozzle [65] for meeting different load requirements and the PZT nozzle [22] for flexible injection timing control and rapid opening and closing response have also been proposed

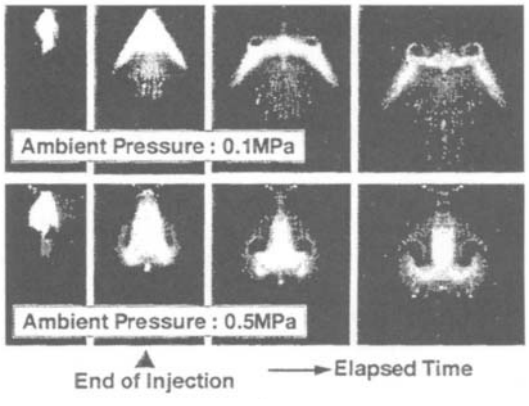

Fig. 10. Effect of the ambient pressure on the spray characteristics of the Mitsubishi GDI injector [50,51].

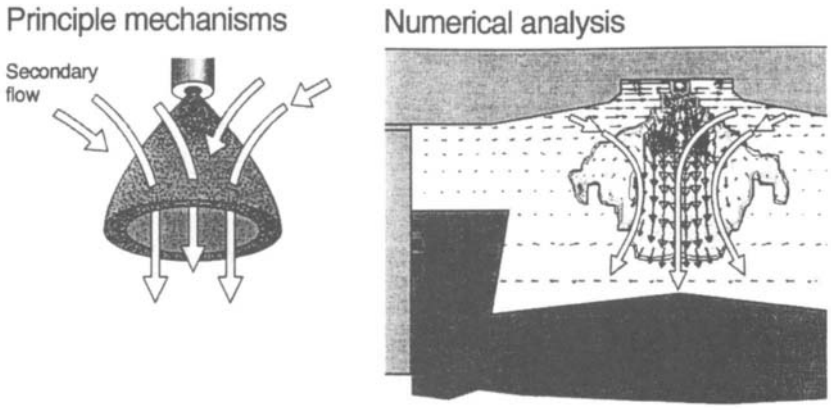

Fig. 11. Mechanisms of air entrainment and spray contraction at elevated ambient pressure [95].

and investigated. A schematic representation of these two injector concepts is shown in Fig. 15.

2.3. Fuel spray characteristics

As is the case for diesel combustion, the fuel spray characteristics are of significant importance to direct-injection gasoline combustion systems. Parameters such as the spray cone angle, mean drop size, spray penetration, and fuel delivery rate are known to be critical, and the optimum matching of these parameters to the airflow field, piston bowl geometry and spark location usually constitute the essence of a GDI combustion system development project. In contrast, the primary fuel spray characteristics of a port fuel injector generally have much less influence on the subsequent combustion event, mainly due to the integrating fuel effects of the residence time on the closed valve, and due to the secondary atomization that occurs as the induction air flows through the valve opening. For direct injection in both GDI and diesel engines, however, the mixture preparation time is significantly less than is available for port fuel injection, and there is much more dependence on the primary spray characteristics to prepare and distribute the fuel to the optimum locations. It is well established that a port-injected gasoline engine can operate quite acceptably using a spray of 200 μm SMD, whereas a GDI engine will generally require atomization that is an order of magnitude finer. Most GDI applications will require a fuel spray having an SMD of less than 25 μm, and may require as low as 15 μm, in order to achieve acceptable levels of UBHC emissions and coefficient of variation (COV) of indicated mean effective pressure (IMEP). The diesel engine, of course, generally requires a fuel spray having an SMD that is less than 10 μm, as the fuel is less volatile than gasoline.

Even though a relatively complete correlation database has been established for diesel sprays [67,68], the bulk of these correlations unfortunately cannot be applied to predict the characteristics of DI gasoline sprays. This is the result of significant differences in fuel properties, injection pressure levels, droplet velocities and size ranges, ambient pressure and temperature levels, and droplet drag regimes. It may thus be seen that the correlation and predictive characterization of the fuel sprays from GDI injectors represent a new and important research area. Until such time as a comprehensive and proven correlation database is available, the spray parameters for individual injector designs will have to be measured in order to provide data for CFD model initiation and design comparisons.

2.3.1. Atomization requirements

An important operating criterion of a well-designed GDI engine is that the fuel must be vaporized before the spark event occurs in order to limit UBHC emissions to an acceptable level. Moreover, the complete evaporation of the fuel can make the ignition process more robust. For a gasoline droplet with a diameter of 80 μm, vaporization under typical compression conditions takes tens of milliseconds, corresponding to more than a hundred crank angle degrees at an engine speed of 1500 rpm. By contrast, the vaporization of a 25 μm droplet requires only several milliseconds,

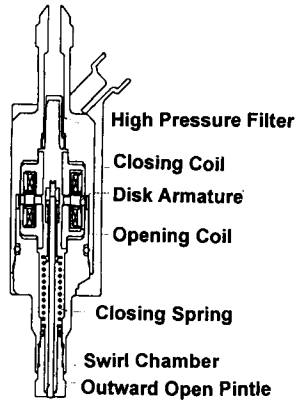

Fig. 12. Schematic of the outwardly opening, single-fluid, high-pressure, swirl injector [63].

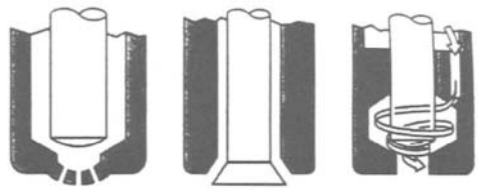

Criteria	Multi hole concept	Outward opening concept	Inward opening concept
Flexibility of spray pattern	++	+	+
Potential for inclined spray axis	+	–	++
Atomization quality at system pressure = 10 MPa	–	0	++
Robustness against fouling	–	++	+

Fig. 13. Concept evaluation of three typical GDI injector designs [95].

corresponding to tens of crank angle degrees. This is the essence of the degradation of GDI engine combustion characteristics for sprays in which the droplet mean diameter exceeds 25 μm. The rapid vaporization of very small droplets helps to make the direct gasoline injection concept feasible [40,69]. Therefore, many techniques have been proposed for enhancing the spray atomization of GDI injectors. The most common technique for GDI combustion systems is to use an elevated fuel pressure in combination with a swirl nozzle [20,44,59,69]. The required fuel rail pressure level is generally on the order of 5.0 MPa, or in some cases up to 13 MPa [21], in order to atomize the fuel to the acceptable range of 15–25 μm SMD or less. The pulse-pressurized, air-assisted injector has also been applied to direct-injection gasoline engines [70–74] and certainly provides a spray with an SMD of less than 20 μm; however, numerous considerations such as fuel retention in the mixing cavity (fuel hang-up), the requirement of a high-pressure, secondary air compressor and the additional complexity of two solenoids per cylinder have thus far limited its wide application to GDI combustion systems [57].

The required spray characteristics and the minimum thresholds change significantly with the GDI engine operating conditions. In the case of fuel injection during the induction event, a widely dispersed fuel spray is generally required in order to achieve good air utilization for the homogeneous mixture. The impingement of the fuel spray on the cylinder wall should be avoided. For injection that occurs during the compression stroke, a compact spray with a reduced penetration rate is preferred in order to achieve a stratified mixture distribution. At the same time, the spray should be very well atomized since the fuel must vaporize in a very short time [20], even though fuel impingement on the bowl surface of a hot piston may promote vaporization. It may be seen that a suitable control of spray cone angle and penetration over the engine-operating map is advantageous, but is very difficult to achieve in practice.

The in-cylinder droplet evaporation process was evaluated by Dodge [54,55] using a spray model, and it was recommended that a mean droplet size of 15 μm SMD or smaller be utilized for GDI combustion systems. Based on calculation, a differential fuel pressure of at least 4.9 MPa is required for a pressure-swirl atomizer to achieve the required degree of fuel atomization. It was noted from the calculations that the additional time available with early injection does not significantly advance the crank angle positions at which complete droplet vaporization is achieved. This is because the high compression temperatures are very influential in vaporizing the droplets, and these temperatures occur near the end of the compression stroke. It was also noted that the atomization level that is utilized in some widely studied GDI engines may not be sufficient to avoid some excessive UBHC emissions due to reduced fuel evaporation rates that are associated with fuel impingement on solid surfaces.

The SMD may not, in fact, be the single best indicator of the spray quality required for the GDI engine, as a very small percentage of large droplets is enough to degrade the engine UBHC emissions even though the SMD may be quite small. Each 50 μm fuel droplet in a spray having a SMD of 25 μm not only has eight times the fuel mass of the mean droplet, but will remain as liquid long after the 25 μm drop has evaporated. In fact, when all of the 25 μm droplets are evaporated, the original 50 μm droplets will still have a diameter of 47 μm. An injector that delivers a well-atomized spray, but which has a wide spread in the drop-size distribution may require an even smaller SMD than quoted above to operate satisfactorily in a GDI engine combustion system. This spread may be quantified by the parameter of DV90-DV10. It is conjectured by the authors that DV90 may be a parameter that is superior to SMD (D32) in correlating the UBHC emissions of different fuel sprays in GDI combustion systems. When examining the result in Fig. 5(c) which shows a comparison of the droplet

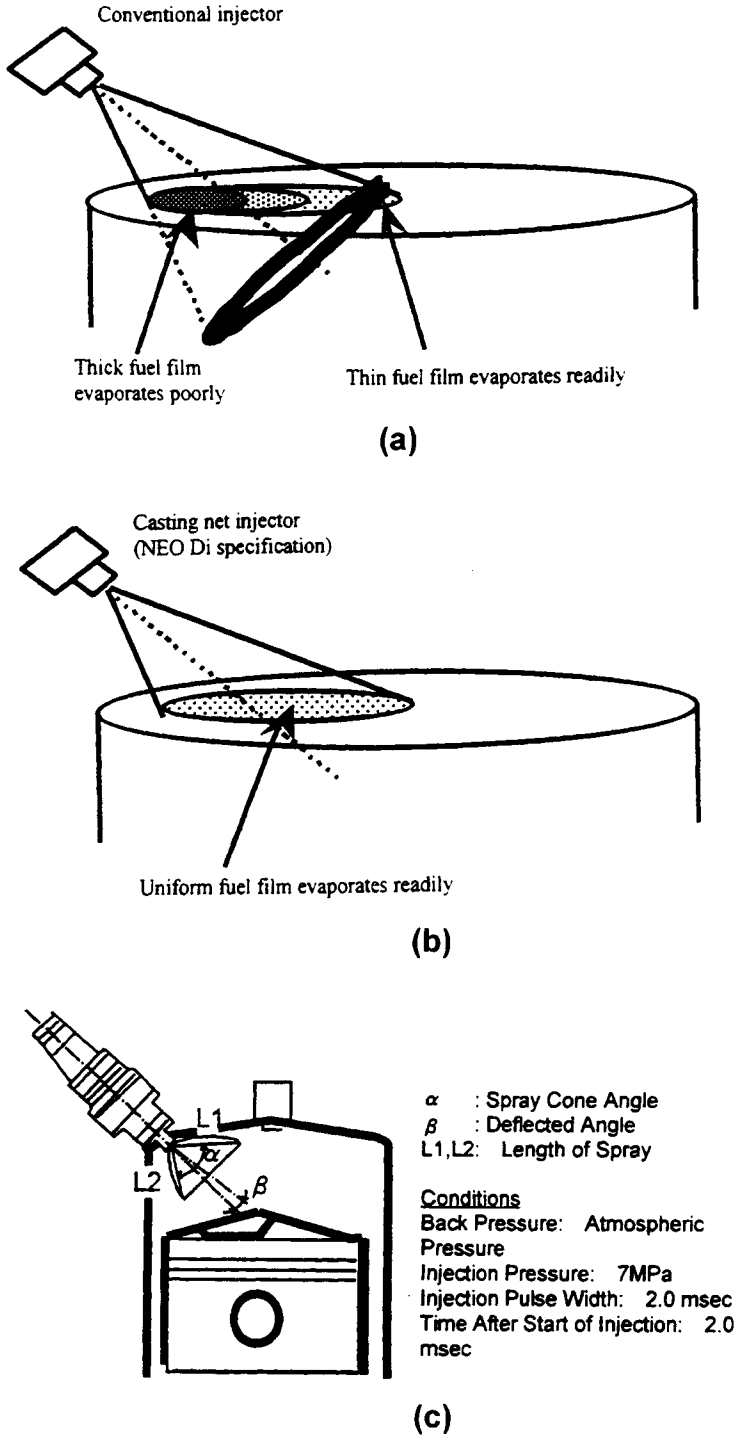

Fig. 14. Comparison of the spray structure between the conventional and CASTING NET injectors [66]: (a) spray structure from a conventional injector; (b) spray structure from a CASTING NET injector; and (c) key parameters controlling the spray structure of the CASTING NET injector.

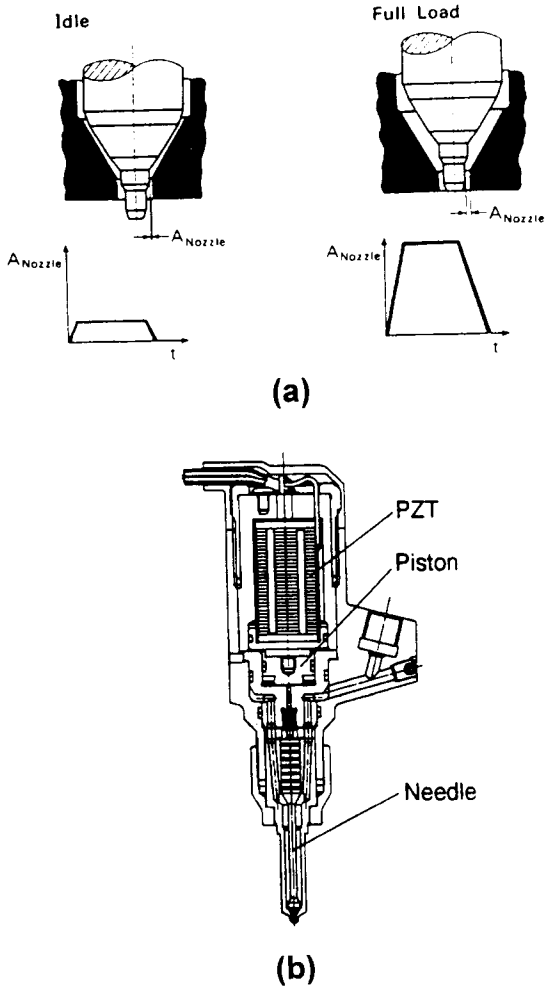

Fig. 15. Schematic of other GDI injector concepts: (a) two-step nozzle [65]; and (b) PZT nozzle [22].

size distributions between swirl-type and hole-type high-pressure fuel injectors [60], it is clear that even though the difference in the mean droplet size (SMD) between the sprays from these two injectors is only 4 μm, the hole-type nozzle produces a wider droplet-size distribution having many larger droplets that are theorized to be responsible for the observed increase in the UBHC emissions. It should be noted that the use of finer atomization may or may not reduce the UBHC emissions, depending upon the in-cylinder turbulence level, due to small pockets of very lean fuel–air mixtures [75–77,348]. A strong turbulence level in the combustion chamber is required to enhance the fuel–air mixing process by eliminating small pockets of very lean mixture. An important point to consider is that the increased droplet drag that is associated with finer atomization reduces the spray penetration, which can degrade air utilization.

Even though a design fuel rail pressure of 5.0 MPa seems

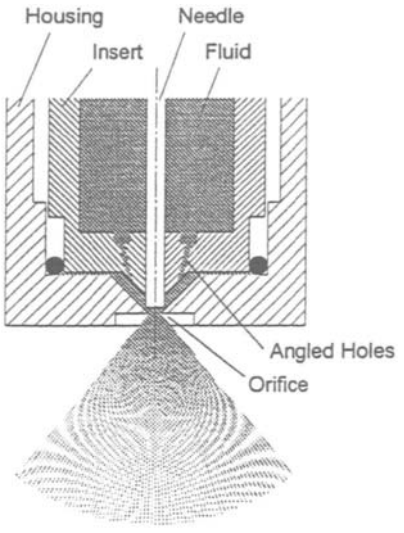

Fig. 16. Schematic of the AlliedSignal high-pressure swirl injector [83].

to be high enough for producing an acceptable GDI spray, Xu and Markle [58] recommended a higher fuel pressure for some of the reasons listed below. From their measurements, the SMD of the Delphi outwardly opening GDI injector is reduced from 15.4 to 13.6 μm as the fuel pressure is increased from 5.0 to 10 MPa. Such a small SMD reduction does not seem to be significant, but the total surface area for an injected quantity of 14 mg of fuel is increased 13%, which should lead to a direct improvement in the fuel vaporization rate. More importantly, an elevated high injection pressure may be required to reduce the key statistic for the maximum droplet size of the spray, namely the DV90. It was reported that the DV90 of the Delphi GDI injector spray at 30 mm downstream from the injector tip is reduced from 40 to 28 μm when the fuel injection pressure is increased from 5.0 to 10 MPa. In addition to its effect on spray characteristics, an elevated fuel rail pressure may also reduce the injector flow rate sensitivity to injector stroke variations.

2.3.2. Single-fluid high-pressure swirl injector

The development of the spray from a GDI injector may be divided into discrete stages. The first is the initial atomization process that occurs at or near the injector exit. This is mainly dependent on the injector design factors such as nozzle geometry, opening characteristics, and the fuel pressure [275,289]. The second stage of spray development is the atomization that occurs during the spray penetration process, which is dominated by the interaction of the fuel droplets with the surrounding airflow field. The spray cone angle is an important parameter that is nominally determined by the injector design; however, in the actual application the spray cone angle of a swirl injector also varies with the in-cylinder air density and, to a lesser degree, with the fuel injection pressure [78–81]. With the pressure-swirl

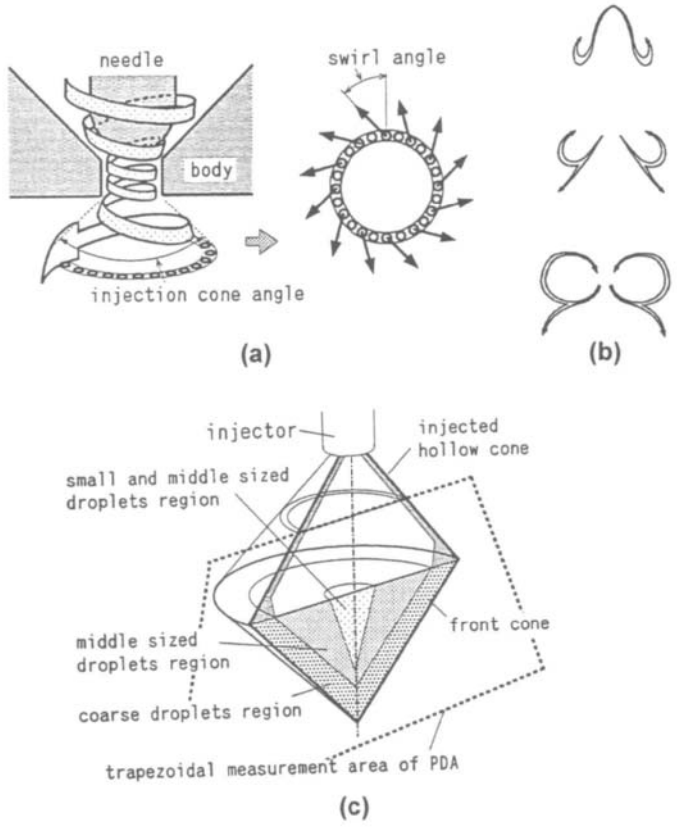

Fig. 17. Schematic and spray characteristics of a high-pressure, swirl injector [86]: (a) nozzle geometry; (b) schematic representation of a hollow-cone spray structure at three stages; and (c) schematic of the droplet size distribution inside a hollow-cone spray at 0.9 ms after the start of injection.

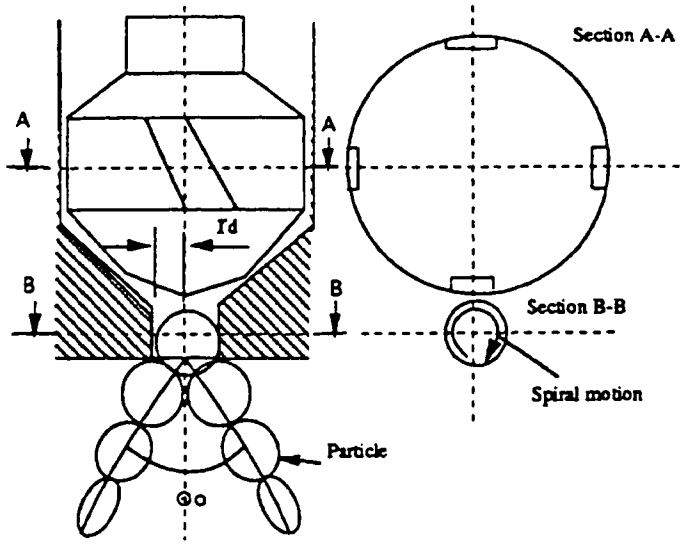

Fig. 18. Nozzle configuration of the Zexel high-pressure swirl injector [88].

injector, the spray cone angle generally decreases with an increase in ambient gas density until a minimum angle is reached. The ambient gas density also has a strong influence on the minimum atomization level produced by pressure-swirl atomizers. Fraidl et al. [82] reported measurements verifying that ambient pressure has a greater effect on the spray cone angle than does the fuel injection pressure. With nonswirl atomizers, however, an increase in ambient gas density generally yields a wider spray cone angle. This results from an increased aerodynamic drag on the droplets, which produces a greater deceleration in the axial direction than in the radial direction. Under conditions of higher in-cylinder air density, corresponding to late injection at part load, a more compact droplet plume is required for a higher degree of stratification. This would imply that the high-pressure swirl injector might be more applicable to GDI late-injection applications.

The spray structure of an AlliedSignal high-pressure swirl injector which utilizes a fuel injection pressure of 6.9 MPa was characterized by Evers [83]. This injector design is shown schematically in Fig. 16. Four regions denoted as leading-edge, cone, trailing-edge, and vortex-cloud, were identified for the hollow-cone spray that is produced. The leading-edge region was found to show the largest droplet size due to the low fuel velocity at the beginning of the fuel injection pulse. After the pintle is opened fully, the fuel attains a steady velocity and a conical region of small droplets is formed. The trailing-edge region is produced as the pintle closes, whereas the vortex-cloud region is formed by the circulating air that carries small droplets from the spray. As the injection pulse ends, the vortex-cloud region continues to grow. An increase in the ambient pressure results in an increase in the droplet size within the spray region, and an increase in the level of swirl of the fuel leaving the fuel injector yields an increase in the mean droplet size in the leading-edge and cone regions of the spray. The droplet size of the vortex-cloud region is not significantly influenced by the fuel swirl number. This was theorized to result from the fact that the size of the droplets entrained into the vortex cloud is determined by the ambient air properties. As the ambient air density is increased, the droplet size in the vortex cloud region also increases due to changes in the entrainment characteristics of the ambient air. The droplet size in the vortex cloud is not changed when the fuel injection pressure is increased, as the ambient air properties are not altered.

The detailed structure of sprays from Siemens high-pressure fuel injectors was studied by Zhao et al. [84,85] using laser-light sheet photography and phase Doppler techniques. A toroidal vortex was observed late in the injection event at reduced injection pressures or short injection durations. The circumferential distribution of the spray was found to be fairly irregular. The spray tip penetration and the spray cone angle were found to decrease monotonically with an increase in the ambient pressure.

The characteristics of hollow-cone sprays generated by a high-pressure swirl injector with an exit-angle of 70°C were predicted using the generalized tank-and-tube (GTT) code with an included spray model, and were validated using PDA measurements by Yamauchi and Wakisaka [86] and Yamauchi et al. [87]. The schematic representation of the injector nozzle geometry is illustrated in Fig. 17(a). The predictions were for a swirl angle of 40° and an initial droplet velocity of 60 m/s to simulate a spray injected at 7.0 MPa into air at 1 atm. The schematic representation of the hollow-cone spray structure derived from the calculation is shown in Fig. 17(b). The transient spray development was classified into three time regimes. During the first stage of spray formation, the droplets form a hollow cone. In the second stage, the spray structure changes as the later-injected droplets move towards the previously injected droplets, which are slowed due to drag. A toroidal vortex is formed around the lower part of the cone and appears as two counter-rotating vortices in the vertical cross section. In the third and final stage, the spray structure attains a steady-state condition, and the entire spray grows and moves away from the injector tip. The interaction between the droplets and the gas flow were found to vary with the detailed spray structure, and was found to be more pronounced for smaller droplets. It is interesting to note that for the case corresponding to a monodisperse spray of 40 μm droplets, the droplets do not form a torus. For the sprays with different droplet size distributions but the same fuel flow rates, the spray structures are considerably different. It was also found that the fuel swirl component plays an important role in the spray development. The spray shapes at the transition between cone growth and torus formation are quite different with and without fuel swirl. The spray cone-angle for the case with swirl was found to be significantly larger than that for the nonswirl case [330]. However, the spray-penetration characteristics for the swirl and nonswirl cases were found to be similar, which is somewhat surprising. As expected, the mean droplet size at the spray tip was found to increase with an increase in the ambient gas pressure due to the influence of the coalescence.

As is schematically illustrated in Fig. 17(c), droplets in the mid-size range are found inside the coarse droplet region while droplets smaller than 10 μm do not form a hollow cone and are observed to concentrate towards the injector axis. At 0.4 ms after the start of injection, all droplets near the injector tip were found to concentrate in a small region near the injector axis, verifying that the cone angle at the start of fuel injection is very small. At 0.6 ms after the initiation of injection, it was found that droplets near the injector tip are concentrated in an angular ring, indicating a wider cone angle. The instantaneous spray cone angle was found to increase from nearly zero to the steady value in proportion to the needle opening time. The measured droplet number density after the end of fuel injection confirmed that apparent vortex formation occurs only for droplets in the range of 10–25 μm, not for other droplet diameter ranges. Moreover, the total number of droplets in the diameter range

of 10–25 μm was found to be larger than those in the other ranges. It was predicted that the mean size of droplets forming the toroidal vortex is about 20 μm, and the droplets that move directly down the cone have a diameter of the order of 50 μm.

The spray atomization process of a Zexel high-pressure swirl injector was analyzed by Naitoh and Takagi [88] using the synthesized-spheroid-particle (SSP) method developed at Nissan Motor Co. The configuration of this nozzle is shown in Fig. 18 where sections A–A and B–B are the cross sections of the needle guide and nozzle hole. It was found that both the initial spray cone angle and the spray penetration decrease with an increase in the ambient pressure. The mean droplet size in the spray cross section 50 mm from the injector tip also increases with the ambient pressure. The SMD of drops at a cross section 50 mm from the injector tip is larger than the total spray-averaged SMD during the injection event, indicating that the smallest droplets do not penetrate 50 mm.

Shelby et al. [52] investigated the spray structure of three GDI injectors during early injection using the PLIF technique. Four distinct phases were identified during the spray development process, which were categorized as the delay phase, liquid jet phase, wide-spray-cone phase and fully developed phase. It was found that the delay phase, which is the period of time when the signal to inject is sent to the injector driver and fuel is first detected with the PLIF system varies significantly with injector design. It was also observed that once a conical spray structure has developed, entrainment of the ambient air causes a low-pressure zone to develop in the spray center, resulting in a cone contraction for the fully developed spray [360,366].

The structure of an evaporating hollow-cone spray from a high-pressure swirl-type injector was predicted by Han et al. [89,307,308] using the KIVA code for the conditions of 500 K initial air temperature, 4.76 MPa fuel injection pressure and 1 atm ambient pressure. The air temperature used is somewhat higher than occurs in the actual engine. It was predicted that the liquid phase maintains the hollow-cone spray structure although it is deformed due to the air entrainment. However, the recirculating airflow carries the vapor fuel to the center region of the spray and the vapor phase is distributed in a solid cone.

Lippert et al. [90] modeled the effects of fuel components on the structure of a spray from a high-pressure swirl injector using the KIVA-II code. Nearly all of the CFD analyses of GDI spray mixing in the literature have used a single component fuel to predict the fuel–air mixing process. For a fuel with a multi-component blend, there will be regions of lighter components and other regions where the composition is dominated by heavier components. This implies that the local equivalence ratio is not only a function of the fuel vapor concentration, but also of the local composition. The prediction conditions are 0.5 MPa and 500 K, corresponding approximately to the condition in an engine when injection is initiated at 60° BTDC during the compression stroke. The volume of fuel injected is 19 mm^3, the injection duration is 1.32 ms, and the initial injection delay is 0.2 ms. It was found that the initial vaporization of the multi-component spray is only slightly higher than for the single component case, and that the rate decreases more rapidly toward the end. This was due to the more volatile components vaporizing slightly more rapidly at first, while at later stages the heavier components take longer to vaporize. However, the two cases show almost identical predictions of the spray penetration in the axial and radial directions. As the tip penetration of the spray is dominated by the trajectories of the largest droplets, and as the diameters of the largest droplets are similar, the close agreement between the two cases is not unexpected. The predictions for a single component also show a predominantly hollow-cone liquid spray, with very few liquid droplets present near the spray centerline. This does not hold true for the multi-component case, in which many smaller droplets are predicted near the spray center. For a multi-component fuel, more rich-mixture areas are observed during the initial stages of spray development. A decrease in the area of maximum equivalence ratio is predicted for the multi-component case as compared with the single-component case. It was also found that the lighter components are present toward the tip and center of the spray, and that the overall composition exhibits an increase in molecular weight as the heavier (less volatile) species in the liquid phase are vaporized.

In order to quantify certain spray characteristics that are not obtainable by other means, Hoffman et al. [91] measured the spray mass flux distributions using a timed-sampling spray patternator [312]. Stoddard solvent at 6.9 MPa was used instead of gasoline, with an injected quantity of 90 mm^3 in an injection duration of 5 ms. The experimental visualization of the spray structure of a swirl GDI injector shows that the core region of the spray is initially skewed from the injector axis. Near the end of the injection event, there is no longer an observable central core vortex. Furthermore, the penetration of the core spray region results in the formation of a toroidal vortex. Fig. 19(a) shows the average liquid volume per injection that passed through each of the 23 measurement points equally spaced on a line 30 mm from the nozzle exit. The measurement results are plotted for four different times after the initiation of the injection. It is evident that the distribution of the liquid mass within the spray is that of a hollow-cone, with over 99% of the liquid mass located in an angular ring with an inner radius of 5 mm and an outer radius exceeding 20 mm. The highest liquid flux was observed at a radius of about 15 mm. The substantial changes in the spray geometry with time can be easily observed from the figure. The thickness of the spray cone walls was found to increase with time, while the outer boundary of the spray, which would typically be used to identify the spray cone angle, does not change at all. Fig. 19(b) shows the estimates of the average liquid mass flux passing through various points below the injector. The designation of "infinite" after BOI indicates the measurement

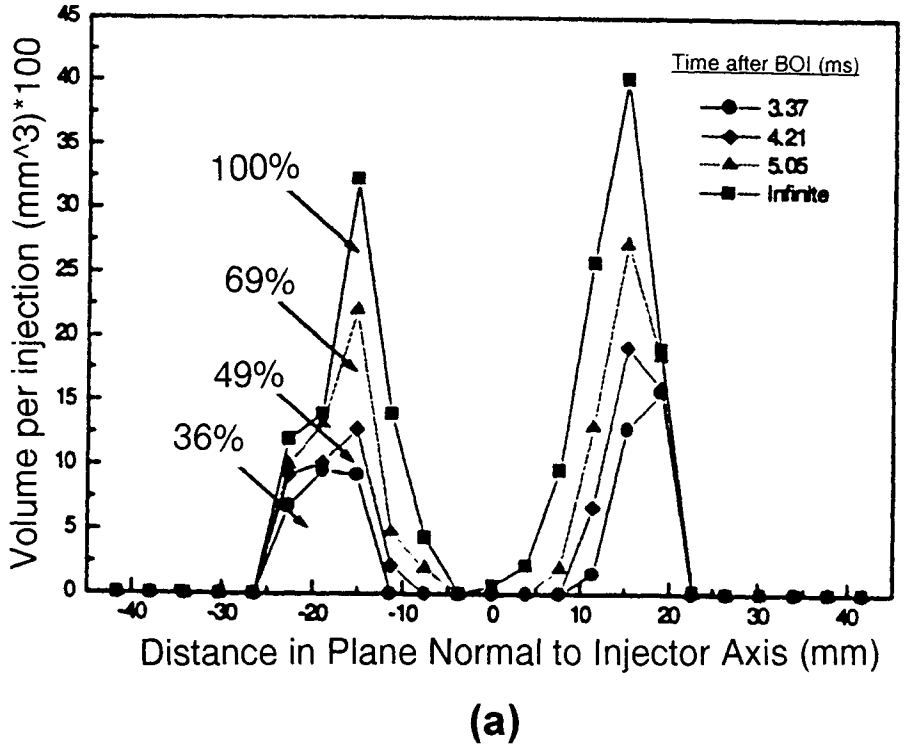

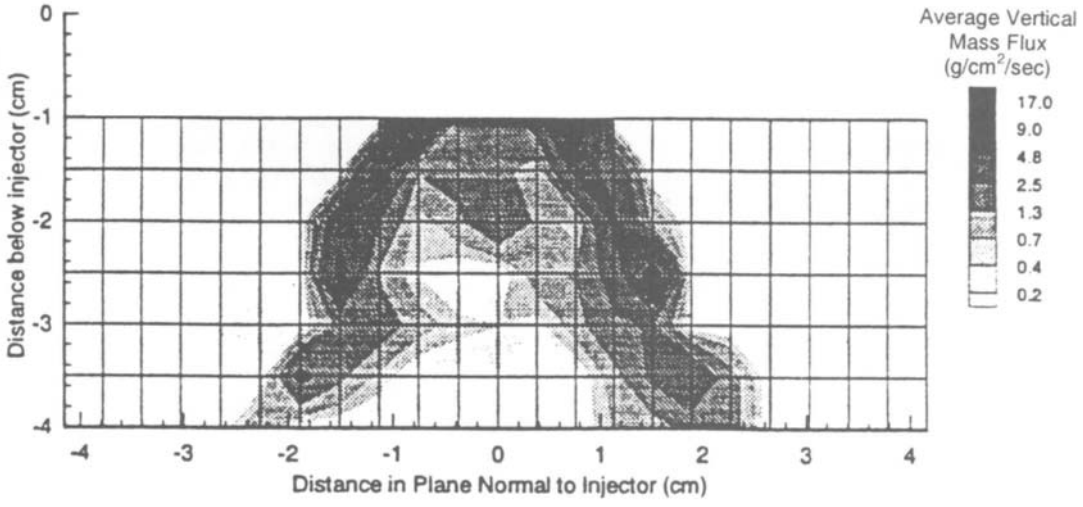

Fig. 19. Liquid fuel distributions inside a hollow-cone spray [91]: (a) averaged liquid fuel volume per injection passing through each of the 23 sample points at a plane of 30 mm below the nozzle tip; and (b) averaged liquid mass flux contours for the moments of 3.3 and 4.21 ms after the start of injection.

is for steady injection. The spray structure shown is similar to that visualized by the pulsed-laser-light-sheet method.

Pontoppidan et al. [64] conducted a basic study of the effect of the nozzle-tip design on the resulting spray characteristics. The three different nozzle configurations that were tested are shown in Fig. 20. Type I is a simple needle-type nozzle having a single cylindrical metering hole, which produces a single jet solid-cone spray. The

Type II nozzle has a swirl channel upstream of the needle, which is designed to have a 45° main axis intersection between the flow vector and the nozzle axis, and generates a hollow-cone spray. Type III has a single cylindrical metering hole in which the fuel is injected into a sac volume having three nonmetering outlet holes. This produces three individual atomized streams, each forming a solid cone. Variation in the circular symmetry of the spray from the Type I nozzle was observed, and it was reported that the spray quality was directly related to the surface quality of the needle and its attachment to the needle. One, or occasionally two, secondary injections were observed following the programmed needle closure due to needle bounce. In this study, it was found to be difficult to completely avoid after-injection at a fuel injection pressure level of 8.0 MPa, but it was possible to reduce it through an appropriate matching of the active needle cross section and the needle spring characteristics. The conclusion is that the Type I nozzle requires a high degree of precision in surface finish and needle-axis alignment in comparison to the other two nozzle types in order to produce a symmetric spray. The Type I nozzle was also found to generate a spray with a larger penetration, which may increase the possibility of fuel impingement on the piston crown and cylinder wall. The high spray momentum produced by the Type I nozzle will make the spray less affected by the in-cylinder airflow field. Hence, it is generally more difficult to achieve a highly stratified mixture using this type of nozzle. It is suitable for pre-chamber designs or for the centrally mounted position in a GDI engine using the early injection mode. It was claimed by Pontoppidan et al. that a GDI combustion system using this type of nozzle is more injector-dependent. In comparison, the Type II nozzle has a reduced spray penetration and improved mixture dispersion characteristics, and is more sensitive to the in-cylinder airflow. The Type III nozzle produces a three-jet spray, which has a low spray-tip penetration. It was emphasized that such a low-momentum spray requires an optimum airflow field inside the cylinder to achieve adequate mixture preparation. As a result, the fuel–air mixing characteristics of this type of nozzle are more dependent upon the particular combustion-chamber-design. Also, the inherent sac volume may generate an initial spray with larger droplets. The Type III nozzle should, however, be less sensitive to injector deposits, as the metering function is performed upstream of the outlet holes. This director-plate design has been utilized for more than a decade in PFI injectors to enhance the deposit resistance and also improve spray atomization.

By means of a computational analysis of the flow field inside a high-pressure swirl injector, Ren and coworkers [92–94,293] conclude that increases in the swirl inlet port area and/or decreases in exit orifice diameter lead to an increase in swirl port discharge coefficient. The resultant spray cone angle widens with a decrease in swirl inlet port area and with an increase in orifice diameter. The discharge coefficient and the spray cone angle were found to be

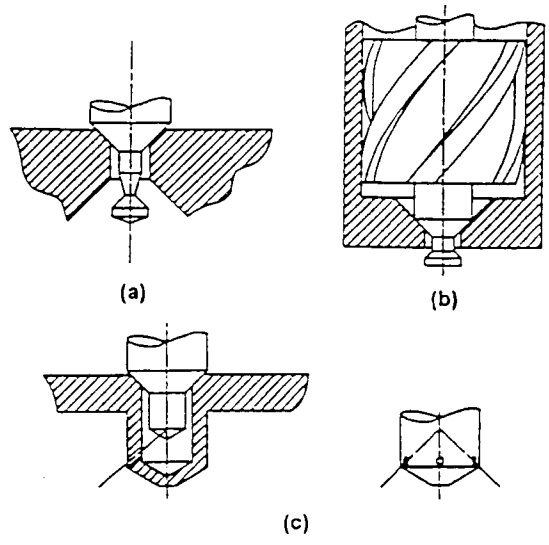

Fig. 20. Schematic of three test nozzles [64]: (a) Type I (pintle-type); (b) Type II (swirl-type); and (c) Type III (hole-type).

relatively insensitive to the injection pressure differential over the range of 3.5–10 MPa. The existence of an air core at the needle tip was also confirmed, which was considered to obstruct the central portion of the exit orifice. As the orifice diameter decreases, the size of the air core decreases significantly, which increases the discharge coefficient.

Preussner et al. [95] conducted a detailed measurement of the spray characteristics of a GDI swirl injector using premium unleaded gasoline. Fig. 21 shows droplet measurement results using PDA technique under various ambient and fuel injection pressures. It was found that mean droplet size increases as the ambient pressure increases, but decreases as the spray cone angle and fuel injection pressure increase. Wider spray cone angle increases spray dispersion, which can reduce the probability of droplet coalescence and as a result, the mean diameter of the droplet is reduced. The spray penetrations as a function of fuel injection duration and injection pressure are shown in Fig. 22. The maximum penetrations of both the initial sac spray and the main spray increase linearly as the injection duration increases. For injection corresponding to the idle operation, the axial penetration of the initial sac spray is larger than that of the main spray, with both exhibiting less dependence on the injection pressure as compared to sprays at higher engine loads.

The Toyota GDI combustion system uses a design fuel rail pressure that is higher than nearly all other production or prototype GDI engines. A fuel rail pressure of 5.0–7.0 MPa is quite common; however, the Toyota GDI fuel system uses a variable fuel pressure of up to 13 MPa [21]. The high-pressure swirl injector that is used in this application is illustrated in Fig. 23(a), and the resulting spray and atomization characteristics are shown in Fig. 23(b). It is evident that the spray is well atomized, but it is not widely dispersed from the spray axis. As expected, the mean diameter of the

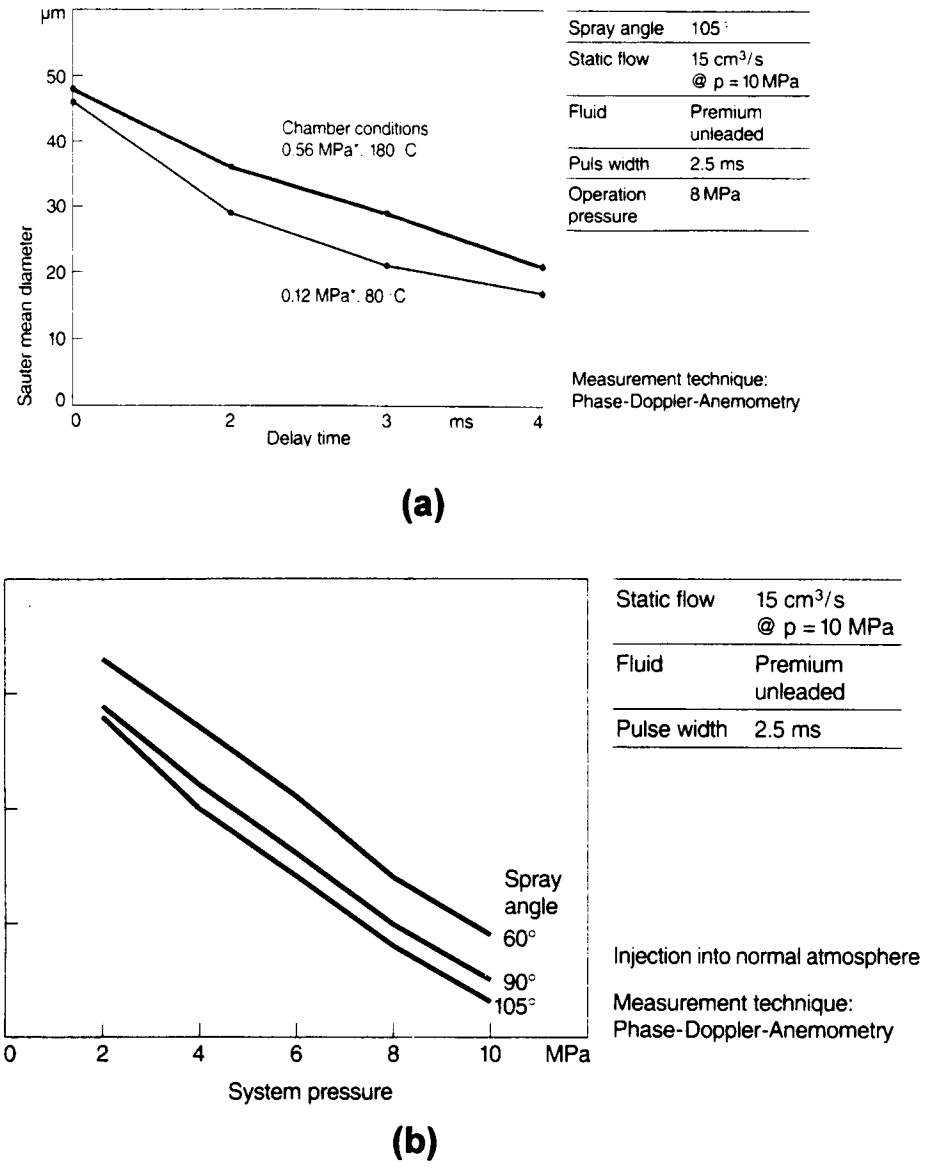

Fig. 21. Effects of ambient pressure, spray cone angle and fuel-rail pressure on droplet size measured at 30 mm downstream from the injector tip [95]: (a) temporal development of the droplet size over two ambient pressures; and (b) droplet size as a function of the fuel injection pressure for three spray cone angles.

droplets decreases as the injection pressure is increased. The effect of increased fuel rail pressure on the resultant fuel economy is shown in Fig. 24. It was found that for engine speeds in the range from 1600 to 2400 rpm the fuel economy continually improves as the fuel injection pressure is increased, while at the lower engine speeds from 800 to 1200 rpm the best fuel economy is obtained at 8.0 MPa. This may be an injection rate effect rather than a mean-drop-size effect, as a lower fuel injection pressure yields comparatively longer fuel injection duration, thus providing more time for fuel evaporation and dispersion. At higher engine speeds, a higher fuel injection pressure combined with a shorter fuel injection duration is reported to be effective in avoiding over-dispersion of the fuel, which degrades stratification [43]. It is claimed that for part-load operation at higher engine speeds the injection duration must be as short, and the fuel pressure as high, as the dynamic range of the injector and the fuel pump design will allow.

It is well known that the entraining airflow interacts with the spray droplets and directly influences the spray cone development. Iwamoto et al. [50,51] conducted a detailed investigation of the interaction between a transient fuel spray and the ambient air by injecting the fuel into a

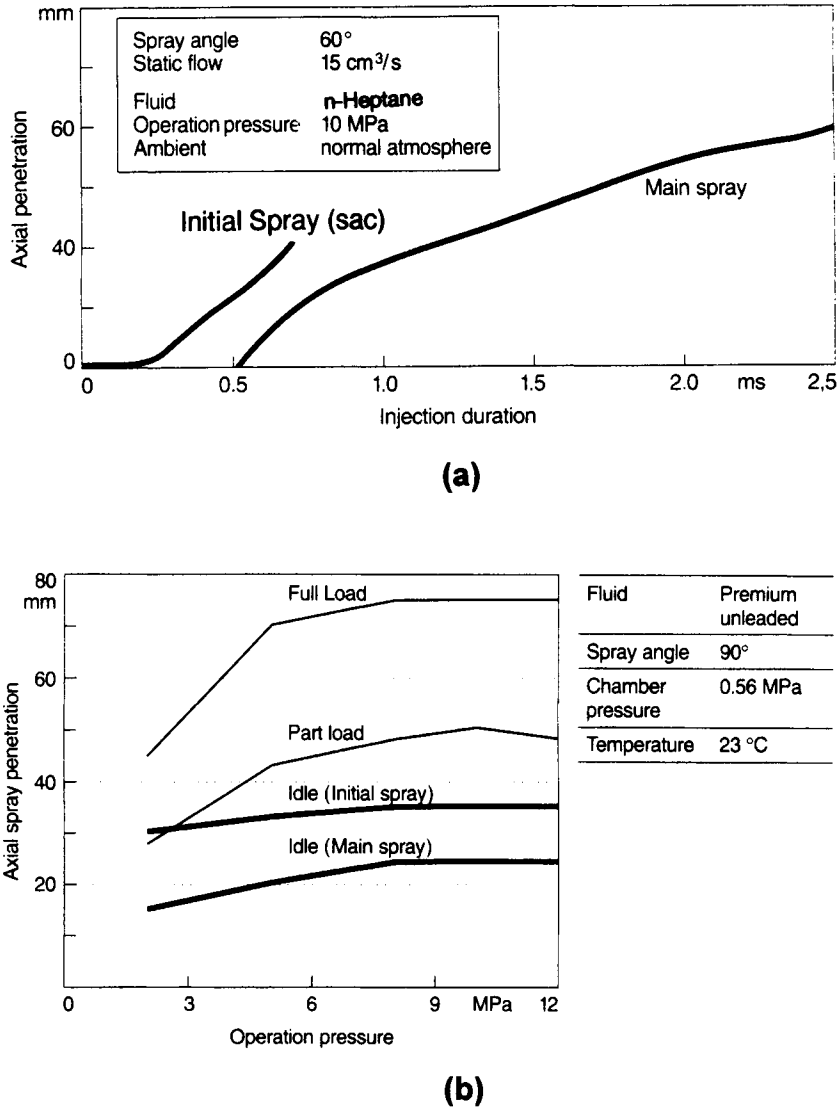

Fig. 22. Spray-tip penetration as a function of the injection duration and fuel-rail pressure [95]: (a) spray-tip penetrations of the initial and main sprays as a function of injection duration; and (b) effect of the fuel rail pressures on spray-tip penetration for different loads.

chamber filled with tracer particles of polymer microballoons. The airflow structure was mapped by the trajectories of the tracer particles, which are shown in Fig. 25. It was found that an intense, turbulent airflow field is generated at the center of the hollow cone due to the movement of the fuel spray.

2.3.3. Effect of injector sac volume

The sac volume within the injector tip between the pintle sealing surface and the tip discharge orifice plays an important role in the transient spray formation process because it contributes to the formation of large droplets at the initiation of fuel injection and can influence the spray cone dynamics. The sac volume in any particular injector design is the geometric space within the injector tip that contains fuel which is not at the fuel line pressure. Fuel remaining from the previous injection resides in this space, and as it is downstream from the pintle sealing line, this stagnant fuel is not at the rail pressure. When the pintle is first lifted, this portion of liquid fuel does not have enough tangential velocity to form a hollow cone spray, and thus is generally injected directly along the injector axis as poorly atomized droplets having relatively high velocities. This is denoted as the sac spray, but descriptive terms such as sling spray, core spray and center spike may also be encountered in the literature. Thus, the sac and main sprays in most GDI injectors are actually two distinct sprays, each having its own drop size distribution. Therefore, a large sac volume can significantly

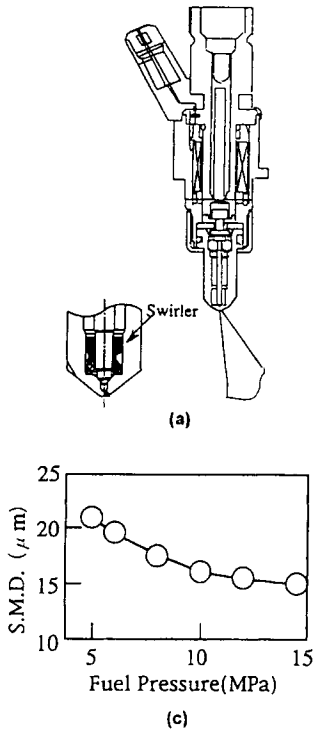

Fig. 23. Schematic and spray characteristics of the Toyota GDI injector [21]: (a) nozzle geometry; and (b) spray atomization characteristics.

degrade the mixture formation process and can contribute to an increase in UBHC emissions, especially for light-load, stratified-charge operation in which the sac volume may constitute a major fraction of the fuel required.

Parrish and Farrell [96] characterized the spray structure of a high-pressure GDI injector for an ambient pressure of 1 atm using laser diffraction and backlighting techniques. In addition to particle size measurements, obscuration measurements were performed. These measurements determined the ratio of unscattered laser light intensity with and without a spray sample, with large values of obscuration indicating optically dense sprays. From the spray visualization, a clear leading mass, or slug, was observed along the center line of the spray. It is generally accepted that this initial slug is comprised of fuel that was in the sac volume. For the fuel pressure range of 3.45–6.21 MPa, the initial axial velocity of the leading mass near the injector tip was in the range of 68–86 m/s, which is higher than the velocity of 45–58 m/s for the main body of the spray. Both the leading-mass and main-spray velocities decrease rapidly with time. Fig. 26(a) shows the SMD measurements with two measurement time scales. The shorter time scale is used to show the initial spray characteristics while the longer time scale is useful to indicate the entire development process of the transient spray. The droplet size measurements in Fig. 26(a) show that the SMD initially rises rapidly as the leading

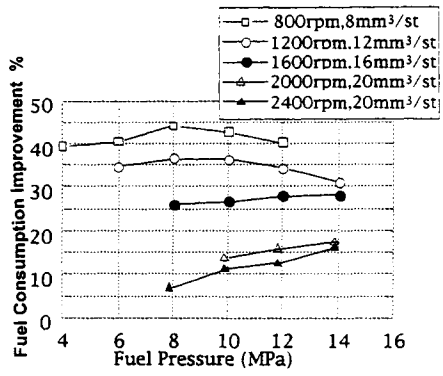

Fig. 24. Effect of the fuel rail pressure on the fuel economy improvement of the Toyota GDI D-4 engine [21].

mass of fuel first enters the measurement location of 38.75 mm from the injector tip along the center line of the spray. A peak SMD value is recorded for this initial sac-volume slug before the instantaneous mean droplet size decreases rapidly for the main spray body. This can also be observed from the obscuration characteristics as a function of time in Fig. 26(b). The result from the transient patternator measurements of the spray volume flux is shown in Fig. 26(c). It is clear that as the closing time is retarded, more fuel is collected. Part of the leading mass is captured in the 1.5 ms closing time curve. At a closing time of 2 ms, the outer regions of the spray begin to be collected, and for a 4 ms closing time the mass collected off-axis is larger than that collected on-axis. It was also found that short injection duration concentrates more fuel mass in the center than is achieved for longer durations.

Wirth et al. [97] measured the droplet size distributions during the entire spray development process. Fig. 27 shows the typical droplet size distributions for a swirl-type GDI injector at ambient conditions, corresponding to a medium-load injection quantity. It was reported that, in the first phase of the injection process, a narrow cone jet associated with the sac volume penetrates with high velocity but poor atomization. The initial quantity of fuel is injected with very low swirl, resulting in larger droplets [35]. It was found that the acceleration of the swirl inside the injector swirl cavity leads to the transient evolution of the initially hollow spray cone. The sac volume quantity affects the spray plume geometry even in the later phases of the injection process when a stable cone is established at the injector nozzle. The intermediate phase of spray development clearly shows the turbulent spray cone breakup in a distance of approximately 25 mm from the nozzle exit. After the end of injection, a well-distributed plume with a low penetration is present with slightly increasing droplet sizes due to slightly degraded atomization at pintle closure and possible droplet coalescence within the spray plume.

The initial fuel slug or sac spray associated with the sac volume of a high-pressure swirl injector was also observed

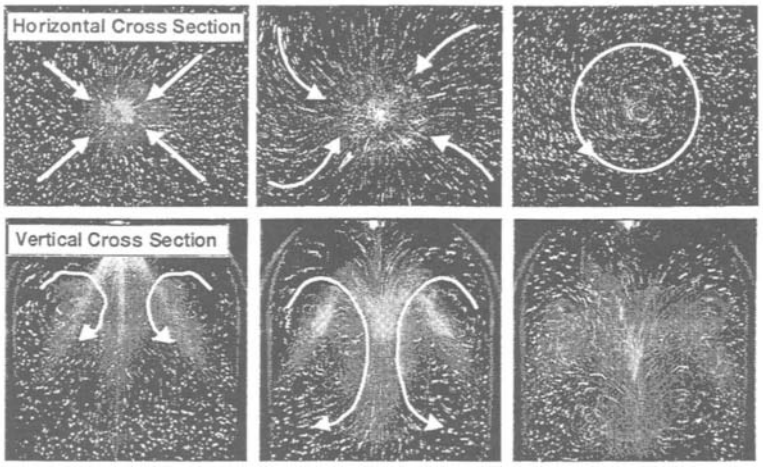

Fig. 25. Schematic of the air entrainment into the spray at an ambient pressure of 0.1 MPa [50,51].

by Salters et al. [98] inside a firing engine having a four-valve pentroof head and a centrally mounted injector. It was found that this slug, consisting of relatively larger droplets with high velocity, penetrates tens of millimeters prior to the formation of the main spray cone, and impacts directly on the piston crown for early injection. An important point is that observations for an injection timing of 80° ATDC on the intake stroke confirmed that there is no major impingement of the fuel spray upon the piston except for this initial slug of fuel from the sac volume. For earlier injection timings, however, a large portion of the main spray directly impacts the piston crown.

It is well established that different GDI operating modes require different spray characteristics for optimum performance. For homogeneous operation, a spray with a wide cone angle is generally optimum; whereas a narrower-cone spray may be effective in creating a highly stratified charge. However, these general guidelines may be less applicable for complex GDI combustion systems. The compromise between spray penetration and cone angle needs to be considered in optimizing air utilization. Engineers at Nissan [27,99,100] and at Hitachi [101] utilized the initial sac volume spray to meet these two conflicting cone angle requirements. The spray tends to collapse to a narrower cone when injected into elevated ambient air densities corresponding to late injection. It was noted that this tendency becomes more pronounced as the fuel quantity in the sac spray is increased, resulting in a further reduction in cone angle. Fig. 28(a) shows the difference of the collected mass for two sprays with different sac volumes. The initial center spray was defined on the basis of the amount of fuel collected within an angle of 20° from the spray center by a 37-ring patternator. The 5% COV limit map between ignition timing and injection end timing is illustrated in Fig. 28(b). It is claimed that increasing the quantity of fuel in the initial sac spray improves engine combustion stability and that the region of stable combustion becomes wider. For those reasons, an injector with a relatively large cone angle (70°) and an appropriate quantity of initial center spray was developed in order to accommodate the requirements of both homogeneous and stratified operations. However, the possible increase in overall mean droplet size and engine UBHC emissions with increasing sac volume must be carefully evaluated for a particular application before invoking this strategy.

2.3.4. Air-assisted injection

A significant number of references exist for the application of air-assisted injectors to gasoline direct-injection in *two-stroke* engines [102–120,317] and PFI engines [38,82,121–124,374]. Unfortunately, the number dealing with four-stroke DI gasoline engines is much more limited [71,72,125–129], although it is important to note that a large portion of the basic information is applicable to both types of engines. The majority of air-assisted GDI injectors utilize outwardly opening poppet valves, whereas the majority of single-fluid swirl injectors are inwardly opening. The air-assisted injectors also use two solenoids per injector, although it should be noted that there is an increasing use of two solenoids on single-fluid swirl injectors to enhance opening and closing characteristics. A further point of information is that injector designs that rely on a poppet cracking pressure tend to exhibit some injection rate variations due to lift oscillations, and tend to exhibit poppet bounce on closure. Each injector design should be evaluated for these tendencies. Air-assisted fuel injection systems provide an interesting alternative for future GDI applications and this option is receiving increased attention among four-stroke GDI developers [72,73]. Air-assisted GDI injectors are being evaluated for several four-stroke GDI applications, and a schematic of the performance of an Orbital GDI injector is illustrated in Fig. 29. As shown, for injection

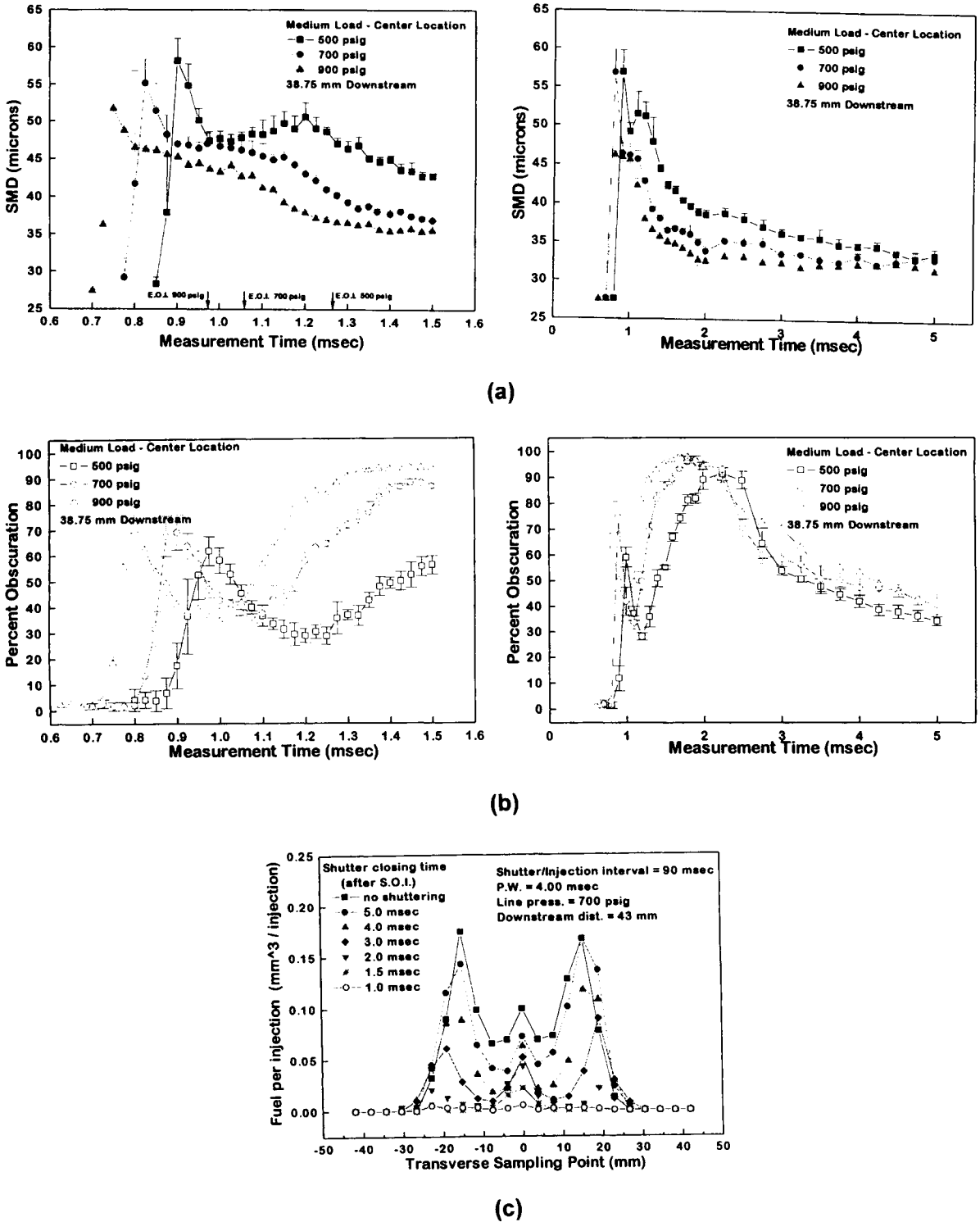

Fig. 26. Spray characteristics of a high-pressure swirl injector at an injection duration of 1.06 ms and an injection pressure of 4.83 MPa [96]: (a) SMD at different time scales; (b) obscuration characteristics of the spray at different time scales; and (c) transient characteristics of the spray volume flux.

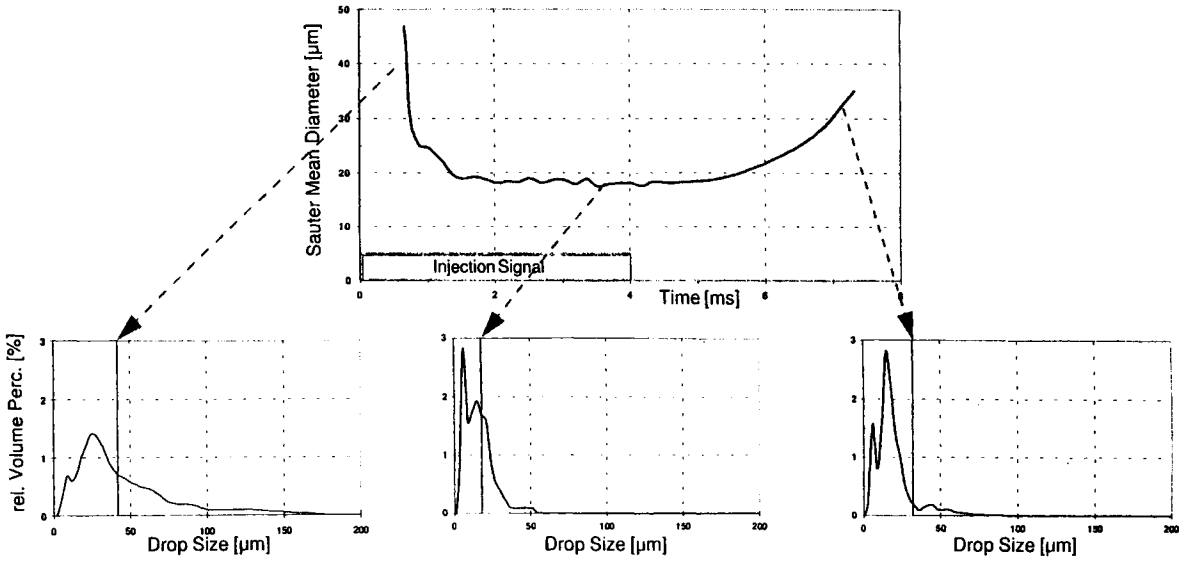

Fig. 27. Transient spray characteristics of a swirl-type GDI injector at the atmospheric condition for a medium-load injection quantity [97].

corresponding to low load, the injected air mass/injected fuel mass ratio is in the range of 1:1–2:1, and exhibits a gradual decrease to 0.2:1 at full load. It was reported that further fine-tuning of the quantity of injected air can also be made independent of the metered fuel by adjusting either the opening duration or the supply air pressure. The air-assisted injection system is able to provide a mean droplet size of less than 17 µm with only a moderate pressure differential. This results from utilizing shear between the air and the fuel components rather than high-pressure fuel alone, therefore enabling the system to maintain good charge preparation even at very late injection timings (or low differential pressure). The fuel pump requirements for such injections are less demanding than that for high-pressure, single-fluid injectors; however, an on-board air compressor and storage plenum must be supplied. A comparison of spray characteristics between air-assisted and single-fluid, high-pressure swirl injectors is shown in Fig. 30.

The spray structure of an air-assisted injector that was developed for a four-stroke GDI application was analyzed by Miyamoto et al. [71]. The injector geometry that was used is illustrated in Fig. 31(a). As shown in Fig. 31(b), three main regions were identified for the spray structure. These were denoted in this investigation as the unsteady, steady and stagnant-flow regions, respectively. In the unsteady region, the flow can be characterized by a starting vortex moving downstream. In the steady region, a fixed vortex is formed below the poppet valve and air is entrained from outside the spray cone. In the steady region, small droplets form a solid-cone structure, due to the fact that the trajectories of small droplets are significantly influenced by the airflow field. The large droplets, in contrast, tend to maintain their trajectories due to a decreased drag relative to their larger inertia, yielding a hollow cone structure. Thus, the mean droplet size was found to be larger at the spray tip and near the surface of the spray cone, and smaller within the cone. For this particular study, a decrease in the spray cone angle was found to be associated with a slight improvement in the level of atomization. This is counter to what is generally observed for single-fluid swirl injectors.

The injection characteristics obtained using both pressure atomization and air-assisted atomization were compared by Hoffman et al. [130] by means of mass flux measurements using a spray patternator. The air-assisted atomizer utilized an outwardly opening poppet, with the injection cycle starting with the opening of a fuel solenoid and charging the mixing cavity with fuel. Pressurized air then further charges the cavity and elevates the chamber pressure until the poppet is forced to open at a pre-set cracking pressure. Due to the counteracting forces of spring tension and pressure, the poppet was observed to oscillate during the entire fuel injection process. Fig. 32 shows the poppet lift and injection volume of this air-assisted injector. This air-assisted system operating with a quantity of 69 mm^3 was found to deliver 83% of the fuel within a 2.5 ms period even though the poppet was observed to oscillate for a total of 7.25 ms. This suggests that fuel delivery occurs during the first three poppet cycles, with the first poppet bounce delivering the highest fuel volume flux. This particular air-assisted system also exhibits a wide hollow cone spray structure. A comparison of the injection rates between the pressure atomizer and the air-assisted injector is illustrated in Fig. 33. The high-pressure atomizer generates a solid-cone spray at the beginning of injection, which then develops into a hollow-cone structure that eventually contracts or collapses to a smaller spray cone. The mass flux measurement results suggest that the interaction of the spray with the entrainment vortex contribute to the spray sheet dispersion and the final

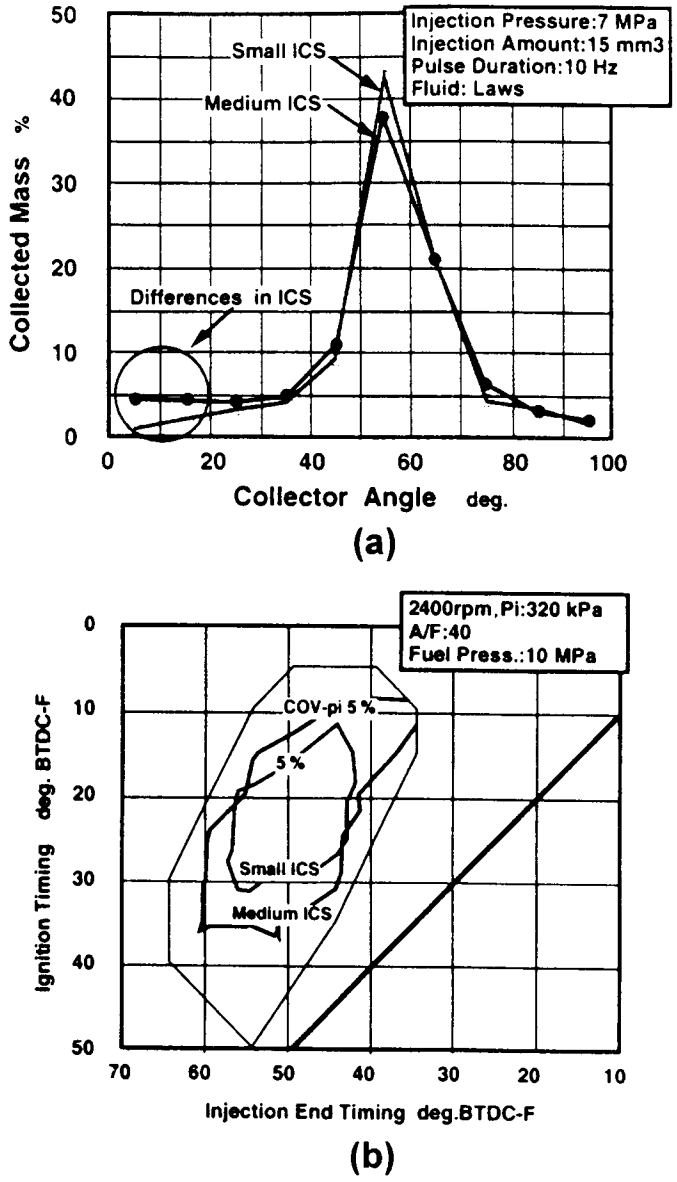

Fig. 28. Effect of the initial center spray on combustion stability [27]: (a) fuel mass distribution measured by a 37-ring parameter in sprays having different initial center sprays; and (b) effect of the initial center spray on the stability map.

cone angle after collapse. The pressure atomizer was found to provide a constant fuel delivery rate over the main portion of the injection pulse, with the flow rate decaying only during the very last portion of the pulse due to the pintle closing.

2.3.5. Best practice performance of current GDI injectors

The area of GDI injector design is currently one of rapid changes. These developments may be classified as those occurring in the basic atomization type, those occurring in injector packaging, and the most extensive area of change, which is continuous improvement in delivered injector performance. The types of GDI injectors now being developed include the pulse-pressurized, air-assisted unit and the outwardly opening, high-pressure, single-fluid injector. These designs complement the more common high-pressure, single-fluid, inwardly opening, swirl-channel injector. Pulse-pressurized air-assisted injectors utilize significantly reduced fuel pressure of less than one megapascal, but require two separate solenoids and a source of compressed air. The design generally employs an outwardly opening poppet. The outwardly opening designs, whether air-assisted or single-fluid, have no sac-volume spray in the classic sense, which tends to yield a slightly improved

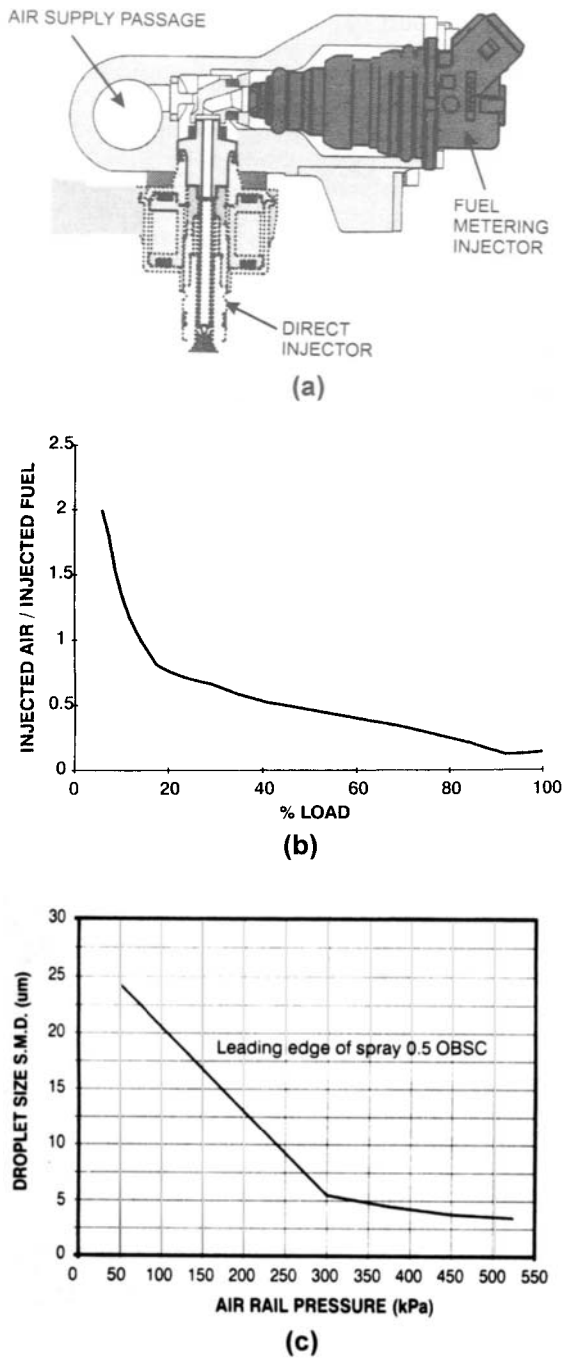

Fig. 29. Schematic and spray characteristics of the air-assisted injector [72]: (a) schematic of the injector design; (b) injected air-to-fuel ratio as a function of the engine load; and (c) effect of the air rail pressure on droplet size.

overall mean drop size. However, it is generally agreed that it is more difficult to develop a portfolio of off-axis, angled sprays with this constraint. The off-axis spray is one of the developments that address the packaging of injection systems. Component packaging in GDI design is a primary constraint, and the movement from a 12 mm to a 10 mm to an 8 mm injector mounting diameter is being driven by the need to enhance packaging options. The availability of injectors that deliver fuel sprays that are directed 10°, 20° or 30° from the injector mounting axis can offer significant flexibility in the original design configuration of a GDI combustion chamber.

The high-pressure, single-fluid, swirl-channel injector using an inwardly opening pintle is by far the most common GDI injector type, and there are intense programs by injector manufacturers to continue to improve injector and spray performance. The non-spray performance parameters of the injector include the opening time, closing time, pintle bounce, durability, dynamic range, noise level, power consumption, leakage and operating pressure range. The spray performance parameters include the mean diameters of the delivered main spray and the sac spray, as well as the corresponding values for DV90. Other key spray parameters include the cone angles of the spray (both the initial angle and the final collapsed spray angle), the spray-deviation (skew) angles of the main and sac-volume sprays, the sac and main tip penetration rates and velocities, the drippage, after-injections or ligament formation upon injector closure and the fuel mass distribution within the spray. Additional measures of performance, both spray and nonspray, are related to injection-to-injection and unit-to-unit variability in all of the above parameters.

With such rapid development occurring in GDI injector design and performance, it is obvious that a compilation of best performance values for each of the above parameters, which constitutes a table of best practice performance, is a living document. The injector performance envelope is continually being pushed as new and improved injectors are designed, built and tested. Table 1 contains a tabulation of current best practice for a number of key injector performance parameters. As injectors have a range of design fuel rail pressures, four categories are listed, with each category having current best-practice values for the performance metrics. All of the droplet size statistics presented in the table were obtained by a two-component, phase Doppler, real-time-system analyzer for a very wide range of injector hardwares. All injectors were measured for indolene fuel at 20°C using a standard test protocol.

2.3.6. Future requirements of GDI fuel sprays

Research by a number of workers in Japan, Europe and the United States indicates that a working design goal for current GDI fuel injection systems should be to achieve a symmetric fuel spray having a SMD of less than 20 μm, with 90% of the injected fuel volume (DV90) in drops smaller than 40 μm, while requiring fuel pressures that are on the order of 5.0–7.5 MPa. This fuel pressure range will generally provide a longer pump life than is obtained using 8.0–13 MPa, with less pump noise and a pressure rise to a greater percentage of

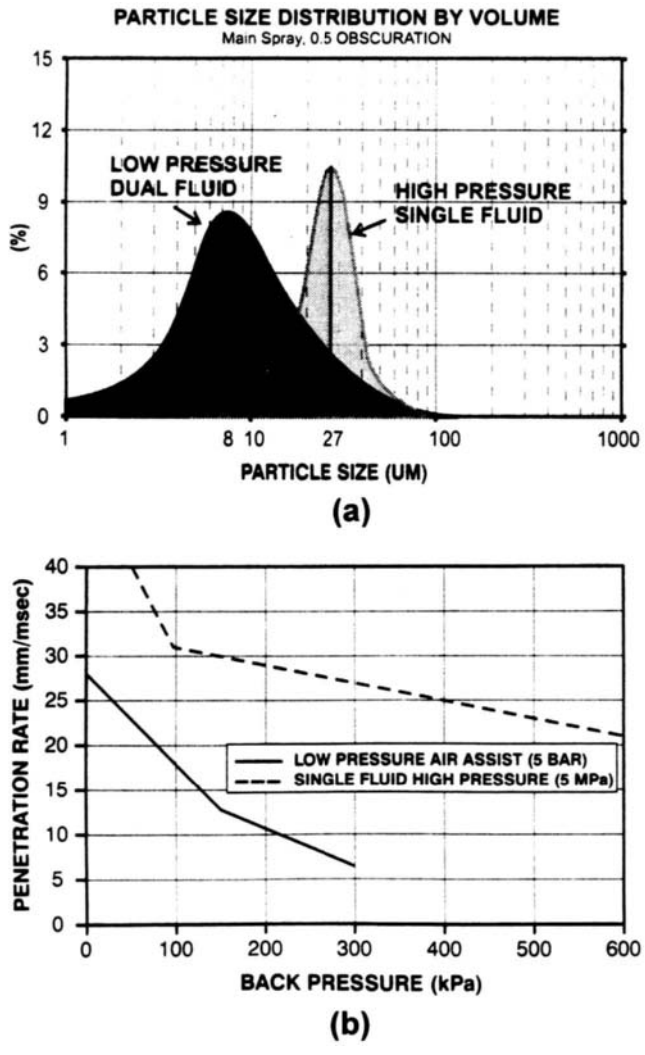

Fig. 30. Comparison of the spray characteristics of air-assisted and single-fluid swirl injectors [72]: (a) droplet size distribution; and (b) spray-tip penetration rate.

the design rail pressure during crank and start. It may also permit a fuel system without an accumulator to be used. The spray cone angle should ideally become smaller as the required engine air utilization is reduced. This can be achieved mechanically or electrically, or may occur due to the inherent collapse of a swirling cone of droplets that are injected into elevated air densities.

For the more stringent emissions and performance requirements of future (2002–2008) GDI vehicles, the fuel spray requirements of future GDI engines set threshold performance limits for the fuel injectors and for the fuel system as a whole. Some of the key requirements for the next generation of injectors (2002–2008) are as follows.

- SMD: 16 μm or less (main spray);
- SMD: 21 μm or less (sac spray);
- DV90: 30 μm or less (main spray);
- DV90: 34 μm or less (sac spray);
- sac volume of less than 6% of idle fuel delivery;
- sufficient spray symmetry to permit injector rotation or rail mounting tolerance without combustion degradation;
- narrower spray footprint (cone collapse) for injection into higher ambient density;
- a design fuel pressure of 5.0–9.0 MPa;
- stable injection at 0.75 ms pulse width;
- 0.25 ms or less opening time;
- 0.40 ms or less closing time;
- no after injection;
- reduced power consumption;
- reduced noise level.

Table 1
Best practice performance of current GDI injectors for key parameters (spray cone angle for single-fluid injectors: 55–75°; air and fuel pressures for air-assisted injectors: 0.5–1.0 MPa; amount of fuel per injection: 15 mg; indolene fuel at 20°C; injection into 1 atm)

GDI injector class	Single-fluid			Air-assisted
Fuel rail pressure (MPa)	5.0	7.5	10.0	Pulse-pressurized
SMD main spray (μm)[a]	16.8	15.6	14.3	17.1
DV90 main spray (μm)[a]	32.7	29.5	25.2	31.3
SMD sac spray (μm)[b]	22.4	20.4	18.7	19.6
DV90 sac spray (μm)[b]	36.0	31.2	29.4	33.4
SMD closing spray (μm)[c]	19.5	17.8	16.6	17.5
DV90 closing spray (μm)[c]	34.6	30.5	27.9	32.8
After injections	None	None	None	One small
Main spray skew (°)	0.0	< 1.0	< 1.5	< 1.0
Sac spray skew (°)	< 1.0	< 2.0	< 2.5	< 1.0
Opening time (ms), 12 V design	0.29	0.31	0.33	0.26
Opening time (ms), 24–70 V design	0.18	0.20	0.22	–
Closing time (ms)	0.38	0.37	0.36	0.41

[a] Fuel-volume-flux weighted PDA across entire spray at 50 mm from injector tip.
[b] PDA at 50 mm from injector tip on sac spray centerline over sac arrival time.
[c] PDA at 20 mm from injector tip on injector axis for 3 ms following actual closure.

3. Combustion chamber geometry and in-cylinder mixture dynamics

3.1. Flow structure

The transient in-cylinder flow field that is present during the intake and compression strokes of a GDI engine is one of the key factors in determining the operational feasibility of the system. The magnitude of the mean components of motion, as well as their resultant variations throughout the cycle, are of importance that is comparable to that of the fuel injection system. On a microscopic scale, a high level of turbulence is essential for enhancing the fuel–air mixing process; but additionally, a controlled mean or bulk flow is generally required for the stabilization of a stratified mixture plume. For SI engines it is known that the turbulence velocity fluctuations near top dead center (TDC) on compression can attain the same order of magnitude as the mean velocity, and that the turbulent diffusive transport and convective transport can be of equal influence in determining the initial state of the combustion process [97,131–133]. The integral scale of the mixture concentration fluctuation inside the combustion chamber can be as large as that of the velocity fluctuation [75]. This results in strong concentration fluctuations at a fixed position, such as the spark gap location, which can lead to difficulties in obtaining a stable flame kernel.

There are four key controlling features of the in-cylinder flow field; the mean flow components, the stability of the mean flow, the temporal turbulence evolution during the

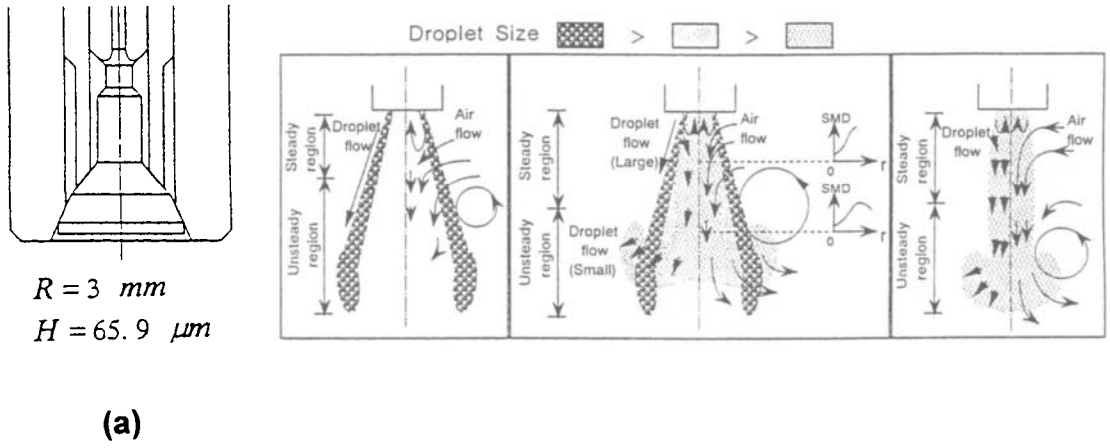

Fig. 31. Spray structure of an air-assisted injector [71]: (a) schematic of the air-assisted injector; and (b) schematic representation of the hollow-cone spray structure.

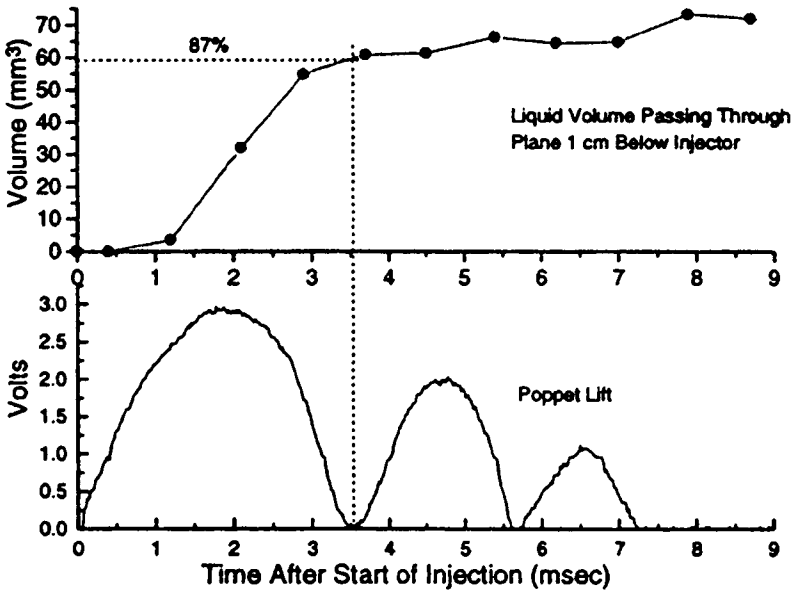

Fig. 32. Poppet lift and injection volume of a poppet-type, air-assisted injector [130].

compression stroke, and the mean velocity near the spark gap at the time of ignition. For homogeneous combustion in the SI engine, the combination of high turbulence intensity and low mean velocity at the spark gap is desirable. This is generally achieved for PFI engines, and also for GDI engines that operate exclusively in the early injection mode. Therefore, a flow structure that can transform the mean-flow kinetic energy into turbulence kinetic energy late in the compression stroke is considered desirable for the homogeneous combustion case. The GDI engine using late injection, however, operates best with a flow field having an elevated mean velocity and a reduced turbulence level, which aids in obtaining a more stable stratification of the mixture. This indicates that the optimum flow field depends upon the injection strategy that is being used, which is a difficult compromise for full-feature GDI engines that operate with both strategies. For the GDI combustion system, control of the mixing rate by means of the bulk flow seems to have more potential than the scheduling of turbulence generation. This is not to imply that turbulence is not important to the combustion process. In fact, turbulence is known to be an important factor in entraining the EGR into the local combustion area [134].

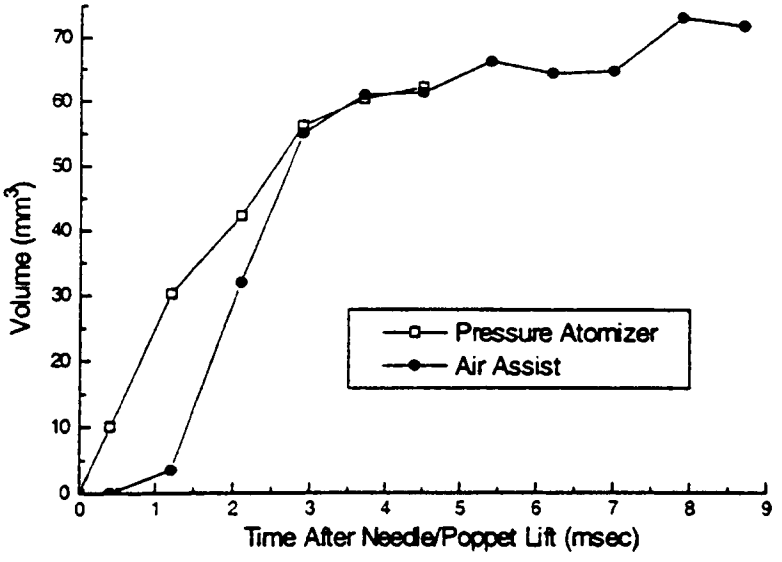

Fig. 33. Comparison of the injection characteristics between the pressure atomizer and the air-assisted injector [130].

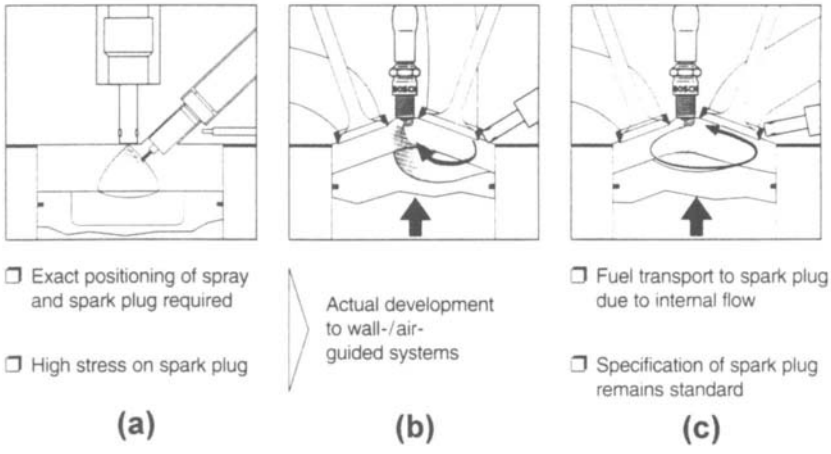

Fig. 34. Classification of GDI combustion systems [376]: (a) spray-guided system; (b) wall-guided system; and (c) flow-guided system.

In general, a rotating flow structure exists within the cylinder and the combustion chamber, and this coherent structure has an instantaneous angle of inclination between the cylinder axis and the principal axis of rotation. The rotational component having an axis that is parallel to the axis of the cylinder is denoted as swirl, and the component having an axis that is perpendicular to the axis of the cylinder is denoted as tumble. The magnitudes of both the swirl and tumble components are very dependent on the particulars of the intake port design, intake valve geometry, bore/stroke ratio, and the shape of the combustion chamber. Both swirl-dominated [43] and tumble-dominated [20] flow structures are used to achieve stratified combustion in GDI engines. For the tumble case, the fuel plume is deflected from a shaped cavity in the piston, and the vapor and liquid fuel are then transported to the spark plug. For the swirl-dominated flow field, the mixture cloud is concentrated at the periphery of the piston cavity [294]. Another air motion that must be evaluated in detail in GDI combustion system development is squish. This flow is generated in the radial direction inside the piston-to-head clearance when the piston is close to the compression TDC. Some of the features of swirl, tumble and squish and their roles in GDI combustion system are summarized as follows.

- Swirl:
  - yields less viscous dissipation and is preserved longer into the compression stroke;
  - good for maintaining stratification;
  - intensified when combined with squish;
  - engine speed dependent, thus yields a limited operation zone for adequate fuel–air mixing.
- Tumble:
  - transformed into turbulence near TDC by tumble deformation and the associated velocity gradients;
  - only totally transformed into turbulence with a flat pancake chamber;
  - incomplete transformation into turbulence may lead to an elevated mean flow;
  - effective in creating high levels of near-wall flow velocities for promoting wall film evaporation;
  - effective in enhancing mixing by turbulence generation;
  - yields larger cycle-to-cycle variations than does swirl;
  - tends to decay into a large-scale secondary flow structure, making stratification more difficult.
- Squish:
  - not pronounced until piston is near TDC;
  - only changes the bulk flow, intensifying the swirl or tumble;
  - increases tendency to autoignition due to extended crevice regions;
  - may require a reduction of compression ratio;
  - effect of reverse squish must be evaluated.

Owing to the more favorable geometry, the swirl component of the in-cylinder motion generally experiences less viscous dissipation than the tumble component, therefore it is preserved longer into the compression stroke and is of greater utility for maintaining mixture stratification. The swirl flow is usually combined with a squish flow that imparts a radial component to the air motion as the piston approaches TDC on compression. A shaped cavity in the piston may also be utilized to obtain the required turbulence production late in the compression stroke. The combined effects of squish and swirl lead to intensified swirl and augmented turbulence intensity during the early portion of the combustion period. It should be noted that the concept of using swirl to promote the fuel–air mixing is considered to have a limited zone of

operation. This is because the momentum of the swirling air increases in proportion to the engine speed, whereas the momentum of the fuel spray is independent of the engine speed. As a result, the engine speed range in which the adequate fuel–air mixing can be realized may be limited [51].

The tumble component of the flow field is transformed into turbulence near TDC by tumble deformation and the associated large velocity gradients, and can only be totally transformed if the combustion chamber geometry is sufficiently flat. Otherwise, an incomplete transformation of tumble kinetic energy will occur, which generally results in an elevated mean flow velocity at the spark gap. Also, tumble-dominated flow fields in GDI engines generally yield larger cycle-to-cycle variations in the mean flow than those obtained for swirl-dominated flows [135,304]. These variations influence both the centroid and the shape of the initial flame kernel following ignition, but do not produce significant changes in the combustion period or flame speed [23]. Further, the tumble component of the motion tends to decay into large-scale secondary flow structures due to the effect of the curved cylinder wall, which makes maintaining a stable mixture stratification more difficult. With respect to turbulence generation, the presence of a significant tumble component is effective in enhancing the turbulence intensity at the end of the compression stroke, which is essential to compensate for the reduced flame speed of a lean stratified mixture. The tumble motion that is present early in the compression stroke rapidly decays into multiple vortices that have a size on the order of the turbulence length scale. This rapid transformation of kinetic energy into turbulence is not generally observed for swirl-dominated flow fields. The swirl flow continues to rotate relative to a center point that generally precedes in a complex, precessing path around the vertical cylinder axis for the entire time period from the beginning of the compression stroke to the end of TDC. The cylindrical geometry of the chamber is obviously quite favorable for maintaining a swirling flow with little viscous dissipation [294]. It should be noted, however, that high-swirl-ratio flows may centrifuge the largest droplets from the fuel spray onto the cylinder wall, causing an increase in fuel wall wetting.

Numerous varied approaches to GDI combustion systems have been proposed with a wide range of combinations of in-cylinder charge motion (swirl, tumble, squish), combustion chamber shape, piston geometry, and spark plug and injector locations. A number of these systems will be discussed in detail in Section 6. Each of the GDI combustion systems in the literature can be assigned to one of these major classifications: spray-guided, wall-guided and flow-guided (or air-guided), on the basis of strategies for realizing stratified charge operation during part load. A schematic presentation of these concepts is shown in Fig. 34. This specific class assignment depends upon whether the spray dynamics, the spray impingement on a piston surface or the mixture flow field is primarily utilized to achieve

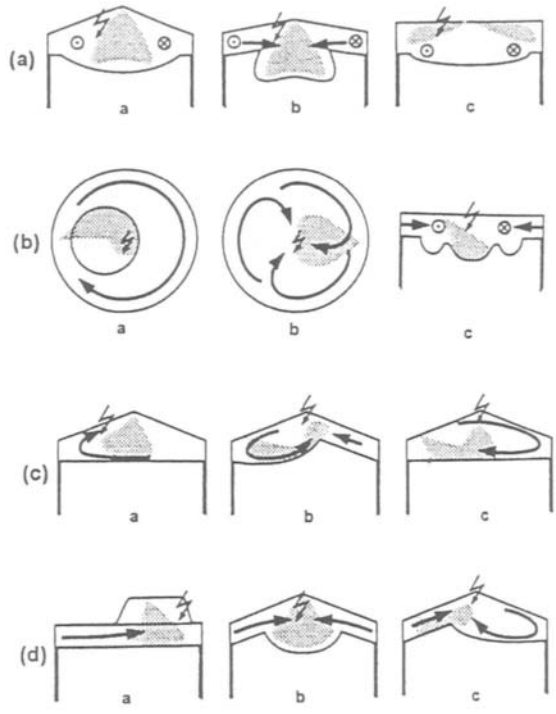

Fig. 35. Mixture preparation strategies for GDI combustion systems [57]: (a) swirl-based systems with centrally mounted injector; (b) swirl-based systems with centrally mounted spark plug; (c) tumble-based systems; and (d) squish-based systems.

stratification. It should be noted that regardless of the classification, the stratification is generally achieved by some combination of these three mechanisms, in which the relative contribution of each individual process varies. The majority of GDI combustion systems that have been developed and reported to date, including the classic DISC engine concepts, utilize in-cylinder air swirl as the primary in-cylinder air motion. The swirl-dominated, in-cylinder flow is generally combined with either a simple, open combustion chamber or a cylindrical or reentrant bowl in the piston. Some key examples of GDI combustion systems, as summarized by Fraidl et al. [57], are illustrated in Fig. 35(a). All of these systems use a swirling in-cylinder flow to stabilize the mixture stratification. Ignition stability is maintained in the majority of these systems by positioning the spark gap at the periphery of the fuel spray. This arrangement generally requires spark plugs with extended electrodes, which has led to some plug durability problems at higher engine loads. Some special designs using a central spark plug and a noncentral injector position are shown in Fig. 35(b). The concept of an off-axis piston bowl, fuel injection onto the bowl wall, and a central spark gap in the main cylinder is depicted in Fig. 35(b)-a. An adaptation of the flow-collision concept to the GDI engine is shown in Fig. 35(b)-b. This concept invokes the flow-to-flow collision at the center of the combustion chamber

where the ignition occurs. An open chamber designed to generate a quasi-divided chamber near TDC is illustrated in Fig. 35(b)-c. This quasi-divided chamber limits and controls the air quantity that mixes with the late-injected fuel [131].

As a result of its inherent rotational acceleration during compression, the tumble motion can be effective in creating high levels of near-wall flow velocities even relatively late in the compression stroke. This can promote the evaporation of a wall film that is formed by an impinging fuel spray. The transport of fuel vapor to the point of ignition may also be enhanced by this flow structure. In recent years, the tumble-dominated flow field is being intensively applied to GDI combustion systems. Engineers at Mitsubishi [20] and Ricardo [136,137] first proposed the reverse tumble concept in conjunction with a specially designed piston cavity which creates a stratified charge near the spark gap. The cavity is designed to control the spray impingement and flame propagation by enhancing the reverse tumble flow throughout the compression stroke, with the squish flow from the exhaust to the intake side of the chamber increasing the flame speed inside the piston cavity. Reverse tumble as the dominant in-cylinder air motion may be effective for designs in which the spark plug is centrally located and the injector is positioned below the intake valve. In such designs, the reverse tumble can be effective in moving the vapor and liquid fuel toward the spark gap after spray impingement on the walls of the piston cavity. The reverse tumble of the Mitsubishi GDI engine is achieved by a straight, vertical intake port. This design is also effective in providing additional space in the cylinder head to accommodate the injector. Three examples of GDI combustion systems using tumble, as summarized by Fraidl et al. [57], are shown in Fig. 35(c).

A comparison of the engine performance of a GDI engine that operates using both the swirl and reverse-tumble concepts show that these two types of flow fields provide similar light-load engine performance for the air–fuel ratio range of 35–40. However, for the high-load region in the air–fuel ratio range of 20–30, problems of combustion stability and smoke emissions are encountered for the swirl-dominated engines. Also, the required engine control system for this type of engine is more complex in order to accommodate engine load transients [138]. Based upon experience gained in developing lean-burn engines, Yamada [139] proposed a GDI engine concept using an "inclined swirl". This in-cylinder flow contains both swirl and tumble in a design that ostensibly combines the best features of these two flow structures. As reported by Furuno et al. [140], an inclined swirl at an angle of 45° significantly enhances the turbulence intensity and provides a reduction in the COV of IMEP.

Yamashita et al. [141] investigated the effects of in-cylinder airflow pattern (tumble vs. swirl) on the Mazda prototype GDI combustion characteristics for stratified-charge operation. It was found that when the engine is operated at light load, the swirl flow exhibits an improved ISFC, whereas a tumble flow results in a marked combustion instability that requires additional intake throttling. In-cylinder hydrocarbon (HC) measurements obtained near the spark plug by fast FID indicate that for the reference swirl case a stable combustible mixture is formed near the spark plug gap at the time of ignition, yielding low UBHC fluctuations. For tumble flow the air–fuel ratio was found to be about 24 and the associated in-cylinder UBHC fluctuation is much larger. It should be noted that this combustion system was most likely optimized for swirl flow. It was also found that an increase in the swirl ratio can further reduce the ISFC, which is attributed to improved fuel transport, more rapid evaporation of fuel in the film on the piston-bowl surface and the reduced fuel dispersion.

Fraidl et al. [142,143] and Wirth et al. [144] reported that the stratified-operation requirements of GDI combustion systems can be achieved with either swirl or tumble air motion concepts. Usually the performance differences between swirl and tumble systems are smaller than is obtained between different methods of establishing the stratified charge, such as the spray-guided versus the wall-guided techniques. With a flat combustion chamber, the intake-generated charge motion required, even beyond TDC, can be achieved quite effectively by a swirl port that introduces a swirling intake flow. With a pentroof-shaped combustion chamber, however, tumble flow is generally found to be more efficient. The tumble-flow concept is recommended for a four-valve engine having a valve angle that exceeds 40°, whereas the swirl-flow concept is recommended for four- and three-valve engines having valve angles of less than 30°. With valve angles from 30 to 40°, either charge-motion strategies can be applied effectively. Variable charge motion is recommended to achieve good performance at both part and full load. This requirement favors swirl-flow, as variable swirl by means of port throttling or deactivation can be achieved with less complexity than variable tumble. For a four-valve GDI system, the valve cross sections necessary for achieving competitive full load characteristics leave little design flexibility in the pentroof geometry. In general, tumble-based combustion systems require relatively deep piston bowls with medium or smaller valve angles. However, the use of deep bowls is found to degrade homogeneous combustion significantly. Comparatively, swirl flow can be preserved more efficiently due to reduced momentum dissipation through transformation into small-scale flow. Therefore, the use of swirl flow can provide good results even with relatively shallow piston bowls. In such a case, the combustion chamber height can be reduced to accommodate designs having a small valve angle.

Some systems that employ squish as the dominant motion for charge stratification are illustrated in Fig. 35(d) [57]. The principle is to use the squish to generate turbulence in order to enhance the evaporation of fuel on the combustion chamber walls and improve mixture preparation. The squish area needs to be carefully determined for these systems in order to limit autoignition under full-load homogeneous

operation. It is important to design a system that can minimize fuel encroachment into the squish area. Jackson et al. [145] calculated the nondimensional squish velocities for combustion chambers with two different clearance heights, basing the calculation solely on volume changes during compression. The combustion characteristics and engine performance with these two different clearance heights were also compared in an engine test by simply raising the cylinder head and liner relative to the crankcase, which had the effect of reducing the engine compression ratio from 12.7 to 10.4. It was concluded that the effect of the squish flow on the mixture preparation and combustion is quite limited. It was also found that NO_x levels are similar, which suggests that there is little or no change in the air–fuel ratio in the vicinity of the spark plug. The similarity in the response of UBHCs to combustion phasing further suggests little change in the transport time. It was also reported that the observed change in fuel consumption is less than would be expected for the decrease in the compression ratio. This was assumed to be due to the reduction in friction resulting from the lower cylinder pressures.

Another important issue that should be noted in GDI combustion system design is that the spray-induced flow field can exert a significant influence on the in-cylinder airflow field [145,146,343,368,372]. The secondary flows induced by the spray itself may lead to spray contraction depending on the droplet size and the in-cylinder ambient conditions [290,295,373]. Han et al. [147] used the KIVA code to predict the effect of a spray-induced flow field on the flow structure inside the combustion chamber of a GDI engine having a center-mounted injector. For the early injection case, it was found that the momentum generated by the injected stream of liquid droplets is partially transferred to the surrounding gases, which increases the kinetic energy of the charge soon after the fuel is injected. This spray-induced flow enhances the in-cylinder air–fuel mixing; however, the increased kinetic energy rapidly decays as the piston moves up during the compression stroke, and the increase in the TDC kinetic energy over the noninjection case was found to be relatively insignificant. The spray-induced motion does affect the large-scale, in-cylinder flow structures. In particular, it increases the mean velocities of the gases in the spray region, and significantly suppresses the intake-generated bulk flow for all of the injection timings considered in the study. For injection later than 150° ATDC on intake, the turbulence intensity as enhanced by fuel injection is substantially higher than that of the noninjection case. About 10% extra turbulence intensity is generated by the typical GDI spray when the initiation of fuel injection occurs later than 150° ATDC on intake. It was concluded that for operation in the early injection, homogeneous mode, the later the start of the injection, the higher the turbulence intensity at TDC on compression.

Lake et al. [148] predicted the variation of the turbulence intensity of a GDI engine for injection timings corresponding to both homogeneous and stratified operation, using the Ricardo VECTIS CFD code. These predictions are shown in Fig. 36. A marked difference in the turbulence level was found between the early injection and late injection strategies. Early injection contributes to the generation of turbulence with intensity twice that of late fuel injection, which exhibits the typical turbulence history of a typical four-valve PFI engine. The turbulence generated directly by the spray during the intake stroke was found to be sustained well into the compression stroke. The subsequent decay of the mean flow at a higher initial level of turbulence results in a correspondingly greater peak turbulence level near TDC on compression. It was also noticed that the peak of the turbulence intensity for the case of charge stratification with late injection is slightly higher than that obtained from the conventional PFI engine. This is considered to be directly attributable to the turbulence induced by the injection event. Stanglmaier et al. [149], Hall et al. [150] and Alger et al. [151] experimentally studied the spray–air and spray–piston interaction process during the early injection mode. It was found that there was a slight decrease in the tumble intensity caused by the injection event. However, this reduced tumble appears to persist longer into the compression stroke than was observed for the no-injection case. It was also observed that a decrease in the spray–piston impingement occurred with increasing engine speed.

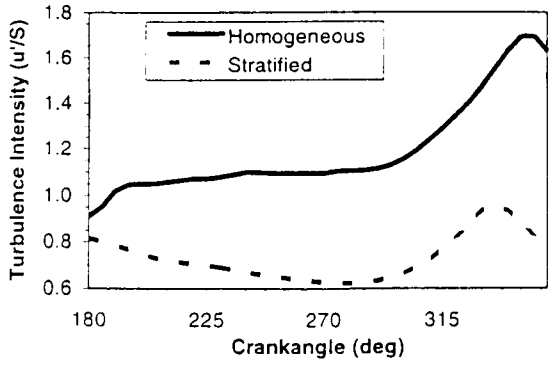

Fig. 36. Effect of the spray-induced flow field on the variation of turbulence intensity for both homogeneous-and stratified-charge operations [148].

Moriyoshi et al. [132,152–154,333–336] proposed a swirl stratification concept for maintaining a rich mixture pocket near the spark plug gap. The concept is to create a high swirl during the latter stages of the intake stroke by an electronically controlled, swirl-control-valve (SCV). The swirl ratio in the top portion of the cylinder would be higher than that near the piston crown with this technique. This swirl difference is conjectured to result in a pressure difference along the cylinder axis that will yield a net flow from the piston crown to the spark plug, suppressing the mixture diffusion in the cylinder axial direction. Engineers at Nissan [88,100] observed this type of air motion in their GDI combustion system. This particular air motion was designated as the Liftup Swirl, and has been confirmed by both

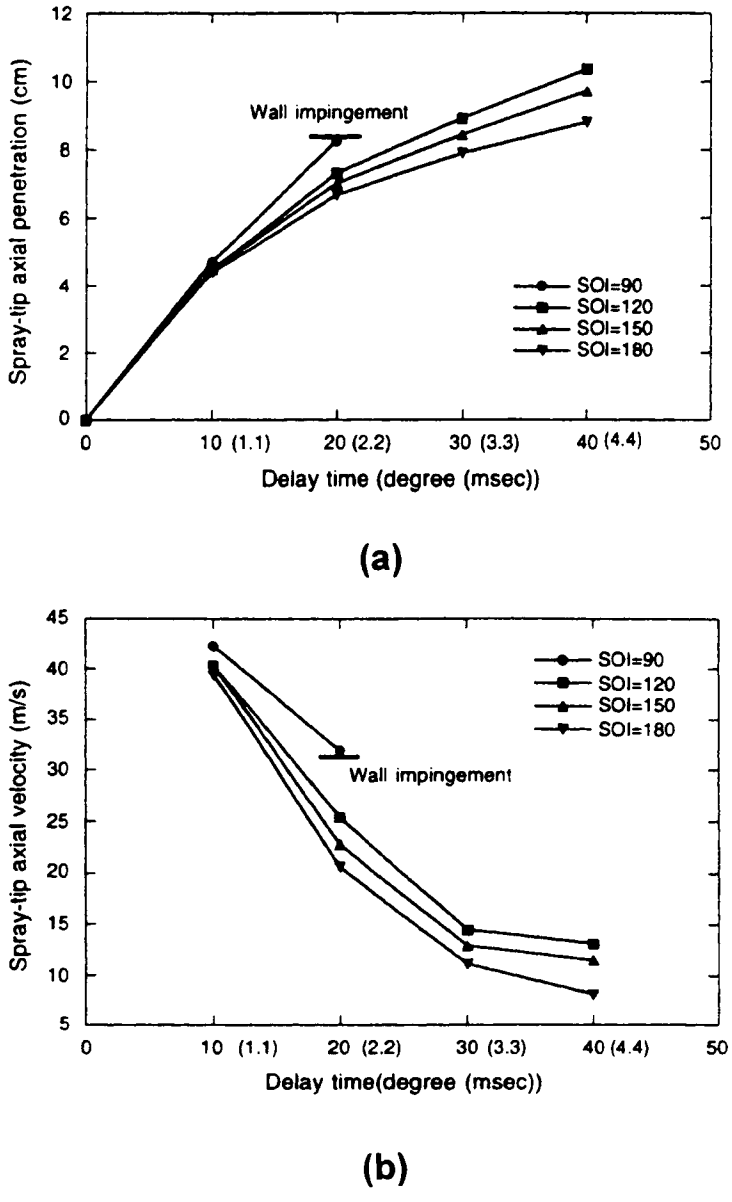

Fig. 37. Computed spray-tip penetration characteristics [147]: (a) spray-tip axial penetration; and (b) spray-tip axial velocity.

CFD calculation and LIF measurement. Two types of swirl are identifiable in a bowl-in-piston chamber: one is the main-chamber swirl and the other is the bowl swirl. The two swirl ratios can be significantly different when one of the two intake valves is closed to induce swirl. In general, the pressure at the swirl center is lower than that at the periphery. As a result, a pressure gradient exists from the bowl to the spark plug and an upward flow is generated from the edge of the bowl to the center of the chamber. CFD calculations show that the presence of horizontal swirl in the compression stroke generates a strong vertical flow inside the piston bowl, which enhances the transport of the mixture plume from inside the bowl to the spark plug.

3.2. Fuel–air mixing

The conditions inside the engine cylinder, such as the temperature, pressure and the airflow field exert a very substantial effect on the spray atomization and dispersion, the air entrainment in the spray plume, and upon the subsequent fuel–air mixing process. The complex and time-dependent spray–airflow-interaction process will determine the rate of fuel–air mixing and the degree of mixture

stratification. The mixture preparation process is strongly dependent on the spray geometry, the in-cylinder flow structure, and the fuel injection strategy [155]. Han et al. [156] examined the effect of the mean flow components of swirl and tumble on the in-cylinder fuel–air mixing process of a GDI engine using a modified version of the KIVA-3 code to simulate early fuel injection. The configuration analyzed was a center-mounted injector that injects fuel axially into the cylinder during the intake stroke. The injected hollow-cone sprays were found to be significantly deflected by the intake flow, with the droplets tending to follow the airflow stream lines. The spray-tip penetration for the tumble-dominated flow field was found to be greater than that for either the swirl-dominated or the quiescent flow fields. Spray–wall impingement was found to occur by bottom dead center (BDC) on intake, after which some of the liquid fuel was predicted to remain as a wall film while other droplets were entrained by the airflow. A rich-vapor region was predicted to remain near the piston surface during the compression stroke in the relative quiescent, nontumble flow field. For both the tumble-flow and swirl-flow cases, the rich-vapor region was found to move with the main flow stream and disperse. However, some pockets of rich mixture do remain near the piston surface. According to Spiegel and Spicher [157] who evaluated the combustion characteristics of a GDI engine utilizing both hollow-cone sprays and sprays from multi-hole (diesel-type) injection nozzles, the hollow-cone spray is easily deflected by a strong swirl and, as a result, it is difficult to maintain a stable stratified mixture. For the multi-hole nozzle, however, a strong swirl was found to be effective in achieving a stable stratified mixture-cloud. Conflicts related to the suitability of multi-hole nozzles for stratified-charge operation exist in the literature.

Han et al. [147,158] extended an earlier investigation to a detailed prediction of the effect of the in-cylinder flow field on the spray dispersion process inside the combustion chamber of a GDI engine. It was found that the hollow-cone spray structure that occurs for bench tests in a quiescent environment is also obtained in the engine when injection occurs during the intake stroke. However, the intake-generated flow field does influence the trajectory of the injected spray, with the spray being deflected and the spray-tip axial penetration being increased. Due to the combined effect of deflection and increased penetration, spray impingement on the cylinder liner occurs when fuel is injected between 90 and 120° ATDC on intake, even though the spray is injected axially. The computed spray-tip penetrations of the main spray in the cylinder axial direction versus the delay time after the start of injection are shown in Fig. 37(a). The spray-tip axial velocities for different injection timings are plotted in Fig. 37(b). These velocities were deduced from the spray-tip penetration data. The intake flow was found to have the largest influence on the spray for injection timings that are earlier than 90° ATDC in the intake stroke. The details of the spray–wall impingement depend not only on the injection timing, and upon the phasing between the spray and piston velocities, but also on the details of the instantaneous flow field. Fig. 38 shows the time histories of the liquid fuel fraction on various combustion chamber surfaces. As computed for this configuration, the amount of liquid fuel that impacts all wall surfaces is as high as 18% of the total fuel injected, leading to the formation of relatively rich vapor regions near the piston surface late in the compression stroke. The fraction of injected fuel vaporized is shown in Fig. 39 for an injection timing of 120° ATDC. It is predicted that almost 90% of the fuel will be vaporized at a crank angle of 330° ATDC on intake. Other prediction results show that the distributions of the mixture in the three different equivalence ratio ranges ($\phi > 1.5$, $1.5 > \phi > 0.5$, $\phi < 0.5$) are not significantly different for an injection timing later than 90° ATDC on intake. This was considered to be due to the fact that the remaining liquid in these cases, which is about 3% of the total fuel injected, is located near the piston surface, and the rich mixture in this region is less affected by the in-cylinder flow field. Although variations in injection timing result in differing levels of charge stratification, the general trend with respect to the locations of rich and lean regions is not modified. It was concluded that the gross features of the charge distribution are primarily determined by the injection and flow-field orientations. For the early-injection cases considered, the mixture ratio was found to be generally leaner in the main-chamber region and richer in the squish region, with the air–fuel ratio ranging from 8 to 24.

Yamauchi et al. [86] divided the mixture formation process of a centrally mounted injector into three stages. Stage I is called the free-spray stage during which fuel droplets form a hollow cone and generate a toroidal vortex. The tumble component of the in-cylinder flow was found to have a slight effect on both the spray trajectory and the fuel vapor distribution. The tumble flow considerably alters the effect of the fuel injection event on the gas motion. Stage II begins with spray impingement on the piston crown. During this stage the piston cavity shape controls the outline of the spatial distribution of air–fuel mixture. After the completion of spray impingement on the piston cavity, the diffusion and convection of the air–fuel mixture is denoted as stage III. In this stage, the number of fuel droplets significantly decreases due to evaporation resulting from a steep rise in the ambient gas temperature at the end of compression. The rich mixture region rapidly diminishes in extent and the air–fuel distribution becomes more uniform. Throughout these three stages the interaction between the spray and the in-cylinder flow field is primarily determined by the relative amounts of momentum of the in-cylinder flow and the free and impinged sprays. The spray geometry can be significantly influenced by this interaction. Further, the impinged spray trajectory is greatly influenced by the angle of impingement and the cavity shape. The final distribution of fuel vapor concentration at the time of ignition is primarily determined by this interaction and the cavity shape. Hall et al. [150] reported that for a centrally mounted swirl GDI injector, the toroidal vortex formed near the head of the spray and its upward transport is inhibited on the intake

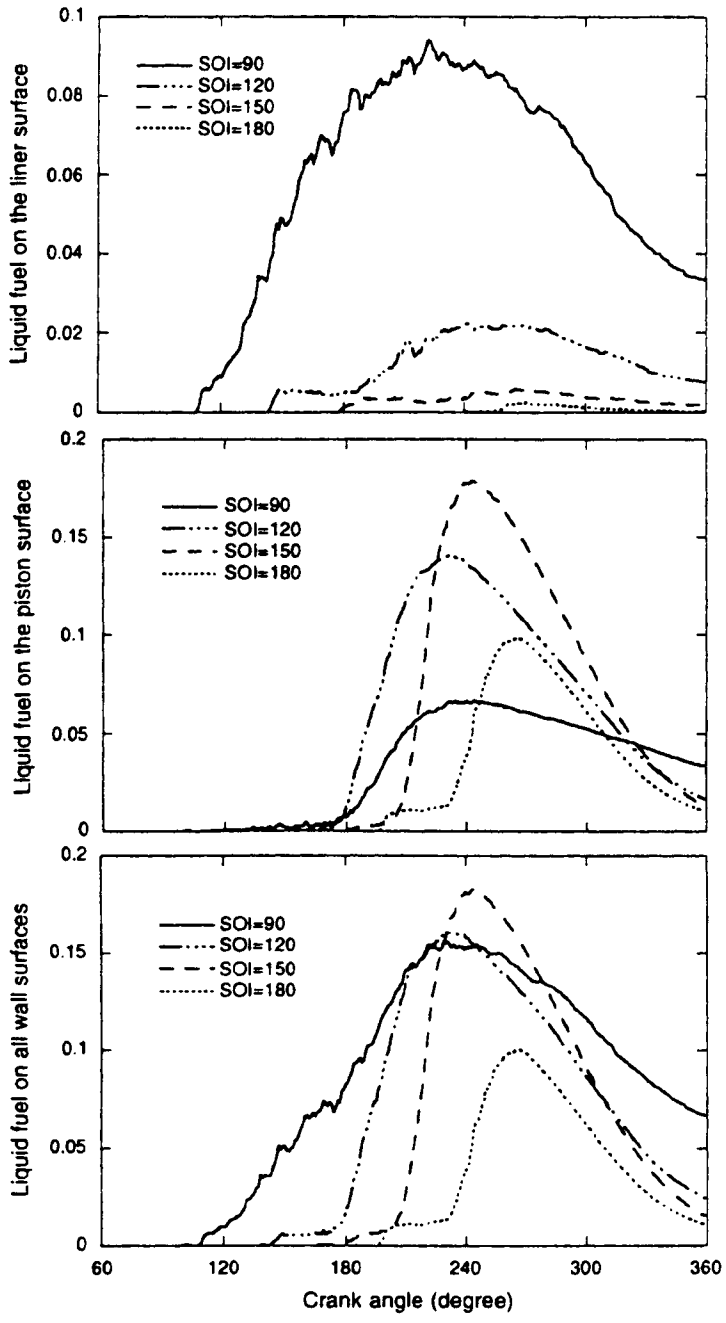

Fig. 38. Computed histories of the liquid fuel fraction of the totally injected fuel on the cylinder wall, the piston crown and the sum of the two cases [147].

side of the cylinder. The greatest fuel droplet density is observed along the axis of the spray even though the spray is ostensibly a hollow cone. The recirculation of small droplets induced by the toroidal vortex may be largely responsible for this. The tumble momentum is reduced by the fuel entrained in the flow, while a downward airflow component is induced by the spray. This momentum difference is detectable well into the compression stroke.

Ohsuga et al. [159] studied the mixture formation process inside the combustion chamber using a centrally mounted fuel injector. Airflow fields of variable swirl and tumble components were created inside the intake port by an air jet passage and an external control valve. It was reported

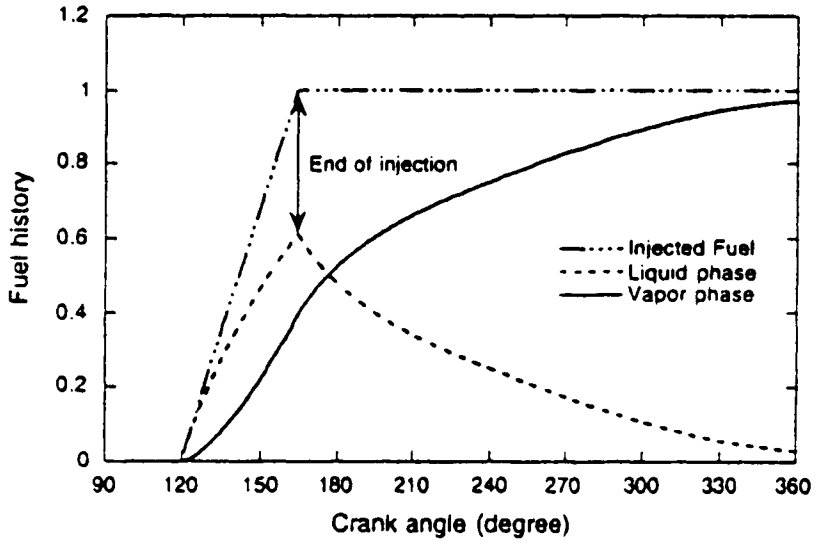

Fig. 39. Computed vaporization history of the injected fuel normalized by the total amount of fuel injected for an injection timing of 120° ATDC [158].

that a tumble flow field is likely to deflect the spray towards the cylinder wall for the centrally mounted injector position, and it was noted that a swirl flow concentrated the spray plume at the center of the cylinder and is effective in reducing cylinder wall wetting. The effects of the spray cone angle and spray-tip velocity on the lean limit were also investigated. It was found that the lean limit could be extended markedly when the spray-tip velocity is reduced and the spray cone angle becomes narrower. For a solid-cone spray with a spray angle of 45°, the test engine could be operated at an overall air–fuel ratio of 40.

Optimizing the spray cone angle and tip penetration is one of the most important steps in minimizing fuel impingement for GDI systems other than wall-guided. With substantial fuel impingement on the combustion chamber surfaces, improved fuel atomization can only partially enhance the mixture preparation. Pool-burning of the wall film will occur, along with the associated negative effects of increased heat loss and UBHC emissions. Dodge [54,55] calculated the fuel wall impingement that is associated with droplet penetration in GDI engines by computing the drag coefficients of the droplets. This penetration distance for impact was 20 mm for late injection versus 80 mm for early injection. For the case of early injection of a spray having a SMD of 15 μm, it was found that most of the droplets decelerate to a very low air velocity prior to reaching the piston crown. Similar results were also found for late injection, in spite of the significantly reduced penetration distance that is available before the spray impacts the piston. The rapid droplet deceleration is due mainly to the higher air densities that are encountered for the late injection condition, which results in increased droplet drag and enhanced vaporization rates. The worst case that was analyzed was for a spray from a pressure-swirl atomizer with a cone angle of 52°, which was found to maximize the penetration distance while preserving spray impact on the piston crown and cylinder wall.

The general relationship between the initial spray-tip velocity and the spray SMD is shown in Fig. 40 for GDI injectors and fuel pressure levels tested by Fraidl et al. [57]. It is evident from the figure that there is a limitation on the spray-atomization benefit that can be obtained by increasing the spray tip velocity. Any further increase in the initial spray-tip velocity may aggravate the problem of excessive spray penetration, but may not significantly enhance atomization. Currently, most fuel systems for GDI engines utilize fuel pressures in the range of 5.0–7.5 MPa, although there are some systems that use fuel pressures of 10–13 MPa. The curve shows that optimum atomization is associated with initial spray-tip velocities that are in the range of 40–50 m/s, which is approximately twice the typical peak flow velocity of the in-cylinder flow field. Depending upon the orientation of the spray axis relative to the in-cylinder flow field, the momentum of the fuel spray can be a substantial addition to the momentum of the flow field. As the clearance height is generally quite small in GDI engines, the spray of swirl injectors could result in some degree of wall impingement even though the initial spray-tip velocity is significantly less than is obtained with a diesel system.

Lake et al. [148] obtained numerical predictions of the details of fuel–air mixing inside the cylinder of a GDI engine with a side-mounted injector. For early injection, fuel was introduced into the cylinder between 170 and 190° ATDC on intake, whereas the corresponding values for late injection were 20–40° BTDC on compression. It

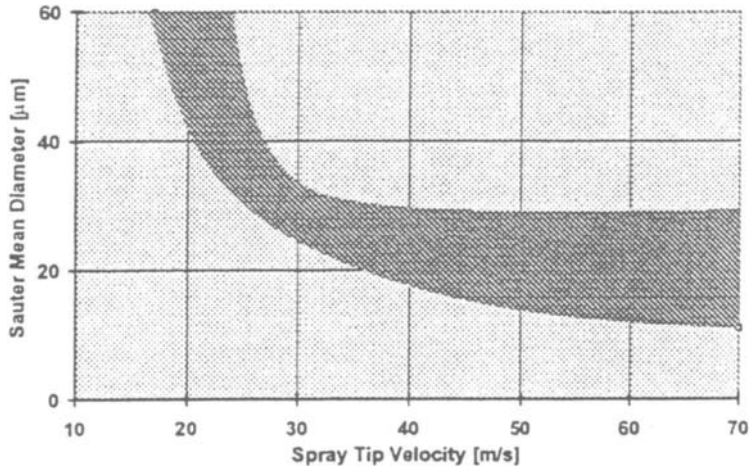

Fig. 40. Effect of the spray-tip velocity on the mean droplet size for a wide range of injectors and fuel rail pressures [57].

was reported that for early injection the initial development of the spray is largely unaffected by the air motion due to the high spray momentum. Spray impingement on the cylinder wall was predicted to occur at 185° ATDC on intake, causing a rich mixture to remain near the piston crown throughout most of the compression stroke. At a crank angle of 25° BTDC on compression, the bulk tumble motion begins to decay rapidly and a fairly homogeneous stoichiometric mixture is produced. It was predicted that over 90% of the injected fuel is vaporized by 20° BTDC on compression. For the case of late injection, with the injection event initiated at 40° BTDC on compression, fuel impinges directly on the piston crown. It was found that only 50% of the injected fuel is vaporized by 20° BTDC on compression. This indicates that the particular geometric configuration that was analyzed would not be able to operate in the stratified-charge mode.

Duclos et al. [160] studied the fuel–air mixing process of the Mitsubishi GDI engine using CFD. The computational results show that, for early injection operation, the homogeneity of the mixture is degraded by increasing the average equivalence ratio. For overall lean homogeneous operation the mixture is nearly homogeneous, while a rich region exists above the center of the piston for overall stoichiometric operation. The analysis for stratified operation shows that the fuel initially ignited by the spark plug comes directly from the injector and is not guided by the piston bowl. The main function of the bowl geometry would appear to be the confining of the fuel during the flame propagation process. It was noted that some improvements of the description of the interaction between hot surfaces and the spray (the wall-film sub-model) are required even for the early injection timing, as the fuel distribution in the cylinder directly affects flame propagation. Interactions between impinging liquid droplets and the piston are also an important consideration for stratified charge operation.

The interaction of the fuel spray with the in-cylinder airflow was investigated by Kono et al. [161]. Fig. 41(a) shows the combustion chamber geometry that was used, and illustrates the locations of the injector nozzle and spark plug. A single-hole nozzle was used to inject fuel into the piston bowl of the engine. Three spark plug locations were selected, all having the same distance from the nozzle tip. As a result, three injection directions were used to direct the fuel towards the spark plug, including one with swirl, which is denoted as the forward direction, one radial, denoted as the central injection, and one against the swirl, denoted as the reverse direction. The measured engine performance and emissions obtained using these three different injection directions with different quantities of injected fuel are shown in Fig. 41(b). The KIVA calculations of the spray-dispersion characteristics inside the piston bowl indicate that significant bowl wall wetting occurs for injection in the forward direction. A rich fuel zone appears in the vicinity of the cavity wall and the spark gap. The fuel is dispersed by the swirl, and a lean mixture zone is formed downstream of the injector. As a result, the measured fuel consumption and UBHC emissions were found to be higher for the forward direction than for the other injection directions. Large fluctuations in IMEP were noted, indicating that ignition and combustion are not stable for this injection direction. For the case of reverse injection direction, the tip of the spray is rapidly decelerated, and the mixture cloud is formed in the vicinity of the spark gap. As a consequence, good fuel economy and stable combustion are obtained. For the central injection direction, the spray development and penetration are not significantly influenced by the swirl, and the tip of the spray penetrates across the cylinder bowl and impinges on the far wall. Therefore, a combustible mixture is not formed around the spark gap. Interestingly, the UBHC emissions for central injection were found to be equal to that for the reverse injection direction for all of the fuel amounts that were evaluated. This work demonstrates the important relationship between the airflow field and the spray orientation.

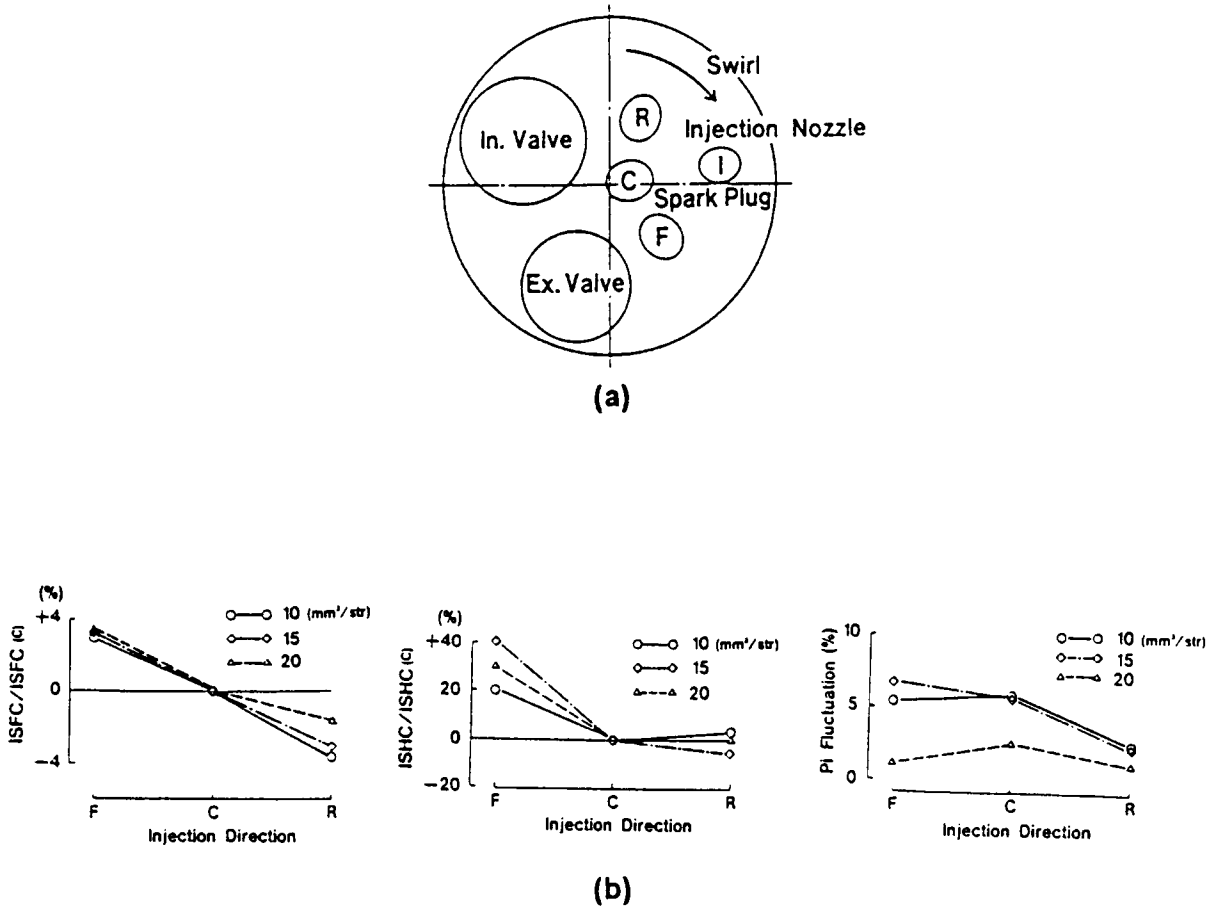

Fig. 41. Effect of fuel injection direction on engine performance and emissions [161]: (a) configuration of the cylinder head; and (b) measured engine performance and emissions (F: forward; R: reverse; C: central).

The amount of fuel–wall impingement is known to vary significantly with the injection timing and engine speed, thus the injection timing must be optimized in order to avoid spray over-penetration and wall-wetting [20,40,161, 326]. There is a general consensus that the timing for early injection should be adjusted so that the spray-tip chases the receding piston without significantly impacting it. Fig. 42 shows an example comparison of the phasing of spray-tip penetration and the piston crown trajectory at 1000 rpm for various injection timings [20]. The injection timing is critical to avoiding spray impingement for both early and late injection. To enhance the fuel evaporation and the fuel–air mixing process, it is necessary to set a minimum time interval between the end of fuel injection and the occurrence of the spark in order to avoid an over-rich mixture near the spark plug. As a result, the injection timing should be advanced as the engine speed increases. According to Matsushita et al. [43], the fuel injection timing must occur between the intake TDC and 160° BTDC on compression in order to provide enough time for the fuel to completely vaporize. For the avoidance of spray impingement, start-of-injection (SOI) timing is the most meaningful and for mixture preparation, end-of-injection (EOI) timing is the most applicable injection timing parameter. Both should be recorded during GDI engine development programs.

Iiyama et al. [99,100] investigated the effect of injection

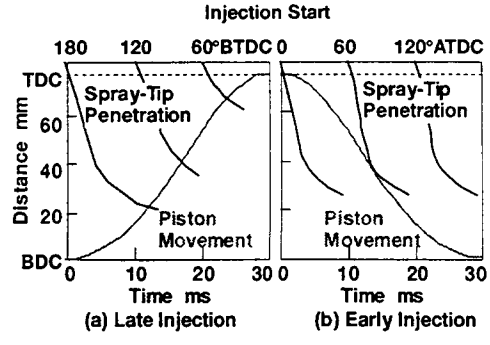

Fig. 42. Spray-tip penetration and piston trajectory for an engine speed of 1000 rpm [20].

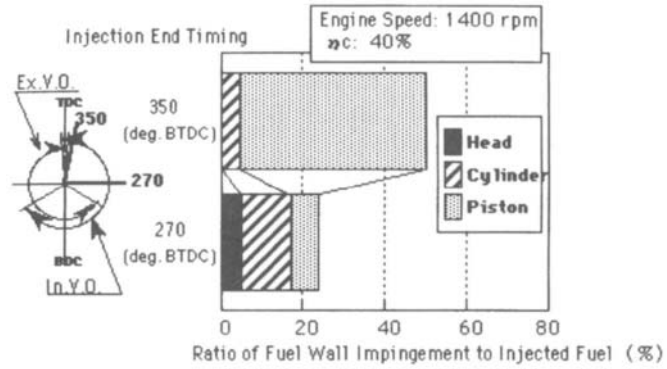

Fig. 43. Effect of the injection timing on fuel wall wetting of the Nissan GDI engine [100].

timing on fuel wall wetting of the Nissan GDI combustion system. Fig. 43 shows the calculation results for an engine speed of 1400 rpm. It was found that when injection occurs during the early intake stroke, namely 350° BTDC on compression, serious fuel wetting of the piston crown occurs, little or no fuel wetting of the cylinder head was obtained. With a later injection timing, the extent of fuel wall wetting decreases markedly. At an injection timing of 270° BTDC on compression, the wetting of the piston crown is diminished significantly, whereas the wetting of the cylinder wall is nearly doubled as compared with that obtained for an injection timing of 350° BTDC on compression. Fig. 44 shows the effect of fuel impingement and fuel film thickness on smoke emissions. The smoke emission level was obtained in engine tests conducted for a range of injection timings and injected fuel quantities. The amount of fuel wall wetting and wall film thickness were calculated by CFD code for each test. It is shown that the smoke is more dependent on the wall film thickness and less dependent on the total fuel amount on the piston surface. A thick wall film does not evaporate completely before ignition occurs and the remaining fuel film causes a diffusion flame that produces smoke. This indicates that even a small amount of fuel that impinges on the piston crown would produce a considerable amount of smoke if the wall film were thick. With a wall-guided concept, fuel impingement on a special piston cavity is utilized to create a stable stratified charge at light load. For all other GDI combustion system types, fuel wall wetting should be avoided to the greatest extent.

The effects of the in-cylinder swirl ratio and nozzle type on the resulting penetrations of gasoline, direct-injection fuel sprays were reported by Harrington [163]. Six nozzle types of one-, two- and three-hole configurations were used to obtain spray penetration data for three swirl ratios and four in-cylinder pressure levels. It was found that the spray-tip penetration and trajectory was strongly dependent on both swirl ratio and the nozzle geometry. Variations in the spray-tip velocity with distance and time for in-cylinder injection of gasoline were measured by Harrington [164]. It was found that time histories of spray penetration predicted from individual droplet drag correlations were not accurate, as the spray tip is not comprised of a single collection of droplets during the injection event and does not experience the same drag force history as any one individual

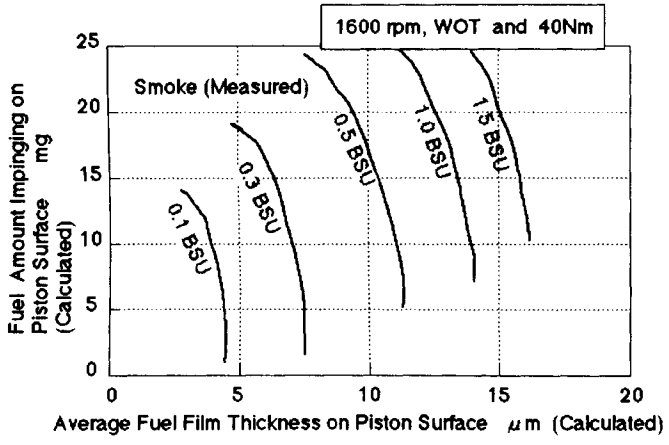

Fig. 44. Effect of the amount of fuel impinging on the piston crown and the thickness of fuel film on smoke emissions [100].

droplet. A three-regime method of penetration and velocity correlation was found to be necessary for accurate predictions; an early time regime that is determined by the injector opening characteristics, a middle-time region that is controlled by spray-tip drag, and a late-time region that is dominated by the in-cylinder flow field.

In achieving a stable stratified mixture, the important considerations are the combustion chamber geometry, the airflow field, and the shortening of the interval between injection and ignition. Tomoda et al. [60] investigated the possibility of creating a stable stratified charge using two high-flow-rate fuel injectors; a hole-type nozzle and a swirl nozzle, each with a piezoelectric actuator with the capability of rapidly opening and closing the needle valve at fuel pressure levels exceeding 15 MPa. The concept of this limiting case is to control the degree of fuel vaporization from the liquid film on the piston by means of the hole nozzle, and to control the fraction of fuel vaporization in the airflow field by means of the swirl nozzle. The injectors selected had the capability of injecting fuel at very high pressures (>20 MPa) in a short duration (>0.25 ms) to permit the flow rates to be set independently. It was found that the hole nozzle produces a spray with a narrow cone and a high penetration, thus it is suitable to achieving a stratified mixture around the spark plug at light load. As the fuel vaporization rate achieved using the hole nozzle depends chiefly upon heat transfer from the piston, the delivered droplet size distribution was found to be of less importance than that of the swirl nozzle. Visualization of the spray development shows that vaporization of the fuel spray from the swirl nozzle starts before any wall impingement occurs. For this nozzle it was found that the vaporization rate does not substantially depend on heat transfer from the heated wall. For the hole nozzle, the vaporization rate is suddenly enhanced as the fuel spray impacts the wall. Therefore, an effective utilization of the thermal energy of the piston is very important if a hole nozzle is to be used to achieve a stratified mixture. For the low-load, low-speed condition, the two nozzle types exhibit opposite trends of BSFC variation with the fuel injection pressure. For the hole nozzle the BSFC was found to increase with a decreased fuel pressure, whereas the swirl nozzle was found to yield an improvement in BSFC as the fuel pressure is reduced. This trend continued up to a limiting value of 8 MPa. For the medium-load, high-speed condition, both nozzles require a high fuel injection pressure to maintain low BSFC. It may be assumed that if the injection-to-ignition interval is decreased, the fuel pressure must be elevated in order to shorten the injection duration. In general, since the fuel spray of the hole nozzle has less entrainment and dispersion than that of the swirl nozzle, a suitable stratified mixture can be more readily achieved at light load. At higher loads, a suitable stratified mixture could be achieved most readily with a swirl nozzle, due to its higher rate of spray dispersion. A study on the effect of the mean swirl ratio on the BSFC indicates that, at light load, the BSFC is enhanced as the swirl ratio increases.

Witaker et al. [165] studied the effect of fuel spray characteristics on engine emissions. It was reported that spray characteristics are of particular importance for homogeneous operation. A comparison of the effects of spray characteristics on engine UBHC emissions during early injection was made between a solid-cone spray (A) and a hollow-cone spray (B). The measured spray characteristics and the resultant UBHC emissions for these two injectors are tabulated in Fig. 45. It was found that the use of a hollow-cone spray yields a decrease in UBHC emissions as the injection timing is varied from 20° ATDC to 150° ATDC on intake. At a timing of 20° ATDC, the measured UBHC difference between the solid-cone and hollow-cone injectors is quite small, but becomes significant at later injection timings. For the solid-cone spray, the UBHC emissions increase linearly as the injection timing occurs later during the intake stroke. For the hollow-cone injector, however, the UBHC decreases as the injection timing is retarded within the experimental range. The results were derived from the same engine setup, with only the injector changed.

The effect of fuel volatility on spray characteristics was investigated in detail by VanDerWege and coworkers [166–168]. It was found that the cylinder head temperature significantly affects the resulting spray structure. The spray changed from hollow to solid cone when the head temperature was increased from 30 to 90°C. Three types of fuel were tested under different in-cylinder pressures. It was found that at high temperature and low pressure, an acetone-doped isooctane spray experienced flash boiling which caused the spray to change from the hollow-cone structure observed under cold conditions to a solid-cone distribution. The transition in apparent structure takes place around 70°C. As the ambient pressure increases, the transition into a solid cone is less pronounced; at 0.6 bar, an intermediate change was observed. This change was not observed at higher pressures, under which flash boiling was considered not likely to occur, or without the low-boiling-point acetone dopant. Experiments with indolene showed results similar to that of the acetone-doped isooctane. This indicates that the light components in the indolene vaporize in the high-temperature, low-pressure case. The observed solid-cone structure was explained by fast evaporation and flash boiling of the volatile species, followed by entrainment of the smaller droplets into the center of the jet, along with the induced airflow. It is interesting to notice the marked effect of head temperature on the spray characteristics. It is well known that an elevated head operating temperature tends to promote injector deposits. The amount of fuel delivered by the injector will, in general, also vary with the increased injector body temperature. Thus, the standard test specification for the thermal flow shift of an injector must also be considered. Koike et al. [169,324] reported that a high fuel injection pressure is effective in enhancing the fuel evaporation at low ambient temperature and pressure, and is also

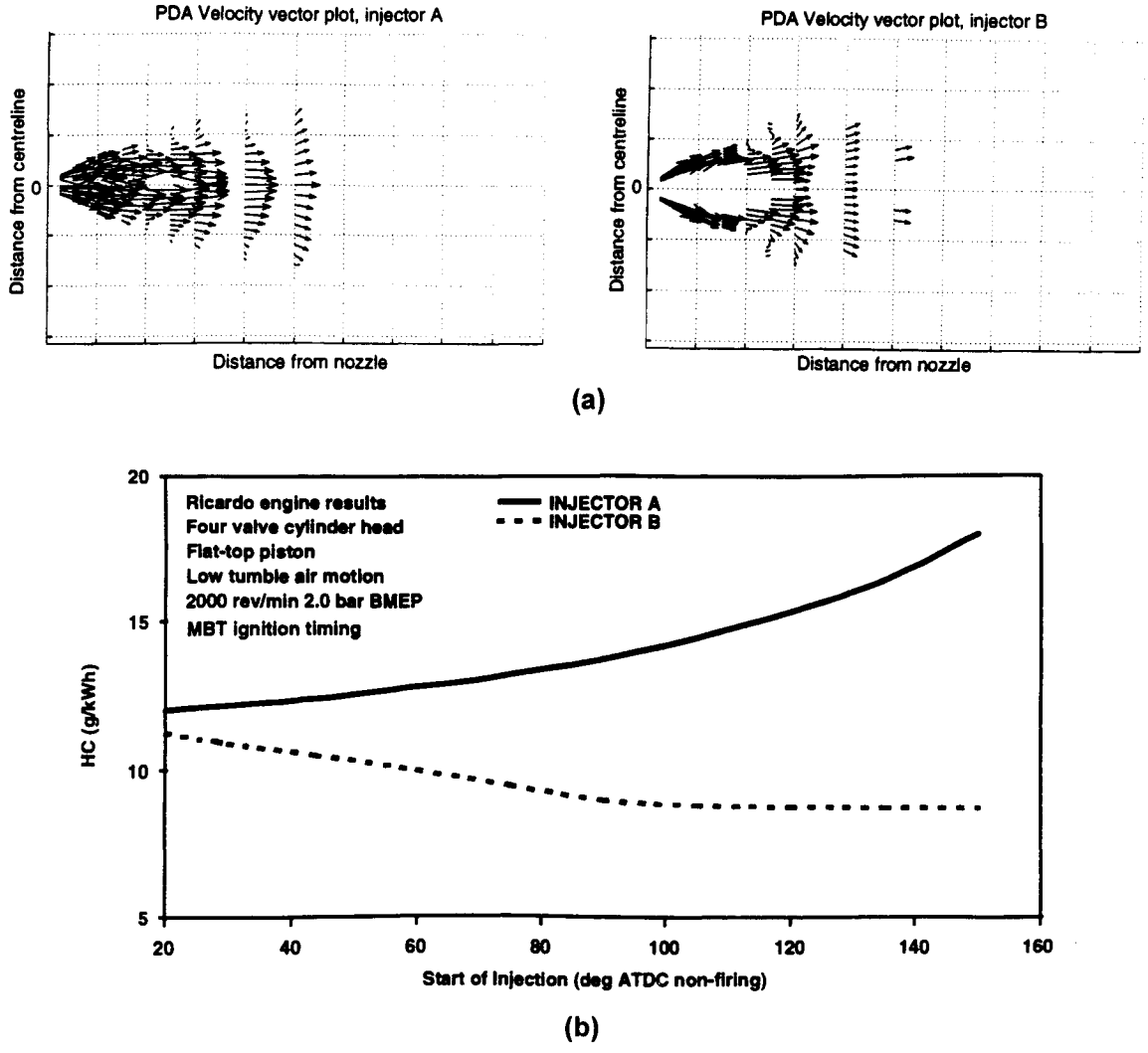

Fig. 45. Effect of the spray characteristics on UBHC emissions for early injection [165]: (a) PDA velocity vector plots of two injectors; and (b) effect of spray characteristics on early-injection UBHC emissions.

effective in increasing the mixing rate at high ambient temperature and pressure. This effect can only be observed when the injection pressure is higher than 10 MPa. When the in-cylinder pressure is higher than the fuel saturation pressure and the in-cylinder temperature is high, which is the stratified charge case, no significant difference in the evaporation rate can be expected for fuels with different saturation vapor pressures.

Unintended fuel impingement on the combustion chamber surfaces, either the cylinder wall or the piston crown or both, is often observed in current GDI engines. Nonoptimal fuel injection strategies may lead to fuel wetting of the cylinder wall, leading to the occurrence of gasoline being scraped off by the moving piston, and transported into the oil pan [170–172]. This can degrade the oil very quickly. Oil dilution resulting from the gasoline impingement on the cylinder wall is one of the factors to be investigated during GDI development. The key factors that affect the amount of fuel impacting the cylinder wall are:

- spray-tip penetration curves for sac and main sprays;
- injector spray characteristics (cone angle, mean drop size, sac volume);
- mounting location and orientation of spray axis;
- combustion chamber geometry (piston bowl, dam or baffle);
- in-cylinder charge motion, especially during injection;
- engine operating conditions (in-cylinder air density and temperature);
- fuel injection strategies (injection timing, injection pressure).

Engineers at Toyota [170] investigated the extent of oil

dilution in the GDI D-4 engine for a range of engine operating conditions. The experimental results from this study are summarized in Fig. 46. As shown in Fig. 46(a), a significant oil dilution was measured in the GDI D-4 engine at high load, but was not observed in a conventional PFI engine. For late injection corresponding to stratified charge operation, a similar degree of oil dilution was observed in both the PFI and GDI engines. For this operating point, fuel is trapped inside the piston bowl and fuel wetting of the cylinder wall is effectively avoided. For a similar reason, earlier injection timing seems to be effective in limiting the oil dilution, as shown in Fig. 46(c). It was also found that the oil temperature, coolant temperature and engine operating time are important parameters in minimizing the oil dilution. Closing the SCV valve was found to be another effective way of reducing the oil dilution, due to the fact that the particular air–fuel pattern introduced by the SCV affects the amount of liquid fuel that impinges on the cylinder wall. The use of a solid-cone spray was also reported to be useful in reducing the oil dilution. This was attributed to the low fuel mass fraction at the periphery of the spray as compared to that of a hollow-cone spray. In general, the Toyota GDI combustion system with a side-mounted injector and the spray penetration associated with a very high injection pressure (up to 13 MPa) was expected to experience more cylinder wall fuel wetting, especially for early injection. However, vehicle test results indicate that the overall level of oil dilution in the field is similar to that observed for PFI vehicles. This is quite different from what has been observed in the dynamometer tests. The rapid rise in the engine oil and the coolant temperatures in the vehicle were considered to be the reason.

In summary, the preparation of the fuel–air mixture is one of the most important processes in ensuring a successful GDI combustion system. The spray–air–wall interaction and the spray-induced air motion all must be well examined in order to optimize the mixture formation process. Some of the guidelines for an optimal mixture preparation strategy are summarized as follows.

- Spray characteristics:
  - appropriate cone angle to insure good air utilization for early injection;
  - appropriate fuel mass distribution within the cone to avoid fuel wetting of the cylinder wall and the piston crown outside of the bowl;
  - appropriate penetration characteristics to insure good air utilization for early injection while avoiding wall impingement;
  - small sac volume and no after-injection.
- Optimized spray-axis angle to achieve a combustible mixture at the spark plug gap while avoiding wall impingement.
- Injection timing for the early injection, homogeneous operating mode should be advanced to take full advantage of in-cylinder charge cooling.
- Spray should "chase" the piston to minimize spray/piston-crown impingement during early injection.
- Injection timing for the stratified-charge operating mode:
  - timing as retarded as possible to minimize excessive fuel diffusion;
  - timing advanced enough to enable reliable ignition;
  - sufficient injection rate and low-pulse-width stability to reliably inject small fuel quantities.
- Optimized combustion chamber geometry.
- Optimized combination of the above parameters.

4. Combustion process and control strategies

4.1. Combustion chamber geometry

The location and orientation of the fuel injector relative to the ignition source are critical geometric parameters in the design and optimization of a GDI combustion system. During high-load operation, the selected injector spray axis orientation and cone angle must promote good fuel–air mixing with the induction air in order to maximize the air utilization. For late injection, the spark plug and injector locations should ideally provide an ignitable mixture cloud at the spark gap at an ignition timing that will yield the maximum work from the cycle for a range of engine speeds. In general, no single set of positions is optimum for all speed-load combinations; thus the positioning of the injector and spark plug is nearly always a compromise.

In extending the time-honored considerations for designing PFI engine combustion chambers to the design of GDI combustion chambers, a number of additional requirements must be satisfied. To minimize the flame travel distance, and to increase the knock-limited power for a specified octane requirement, a single spark plug is generally positioned in a near-central location. As with PFI systems, this location usually provides the lowest heat losses during combustion. As pointed out by Jackson et al. [173], spark plug eccentricity should be less than 12% of the bore diameter for achieving a low octane requirement. For a majority of the concepts, the only constant factor in the variety seems to be the central position of the spark plug in the cylinder head [174]. The use of two spark plugs may also be a possible choice for increasing the probability of effective ignition, however, two ignition sources contribute to already difficult packaging problems. The main reasons for a near-centrally-mounted spark plug are to obtain a symmetric flame propagation, to maximize the burn rate and specific power, and to decrease the heat losses and autoignition tendency.

Once a near-central location has been specified for the spark plug, numerous factors must be taken into account in positioning and orienting the fuel injector. The location selection process can be aided by laser diagnostics

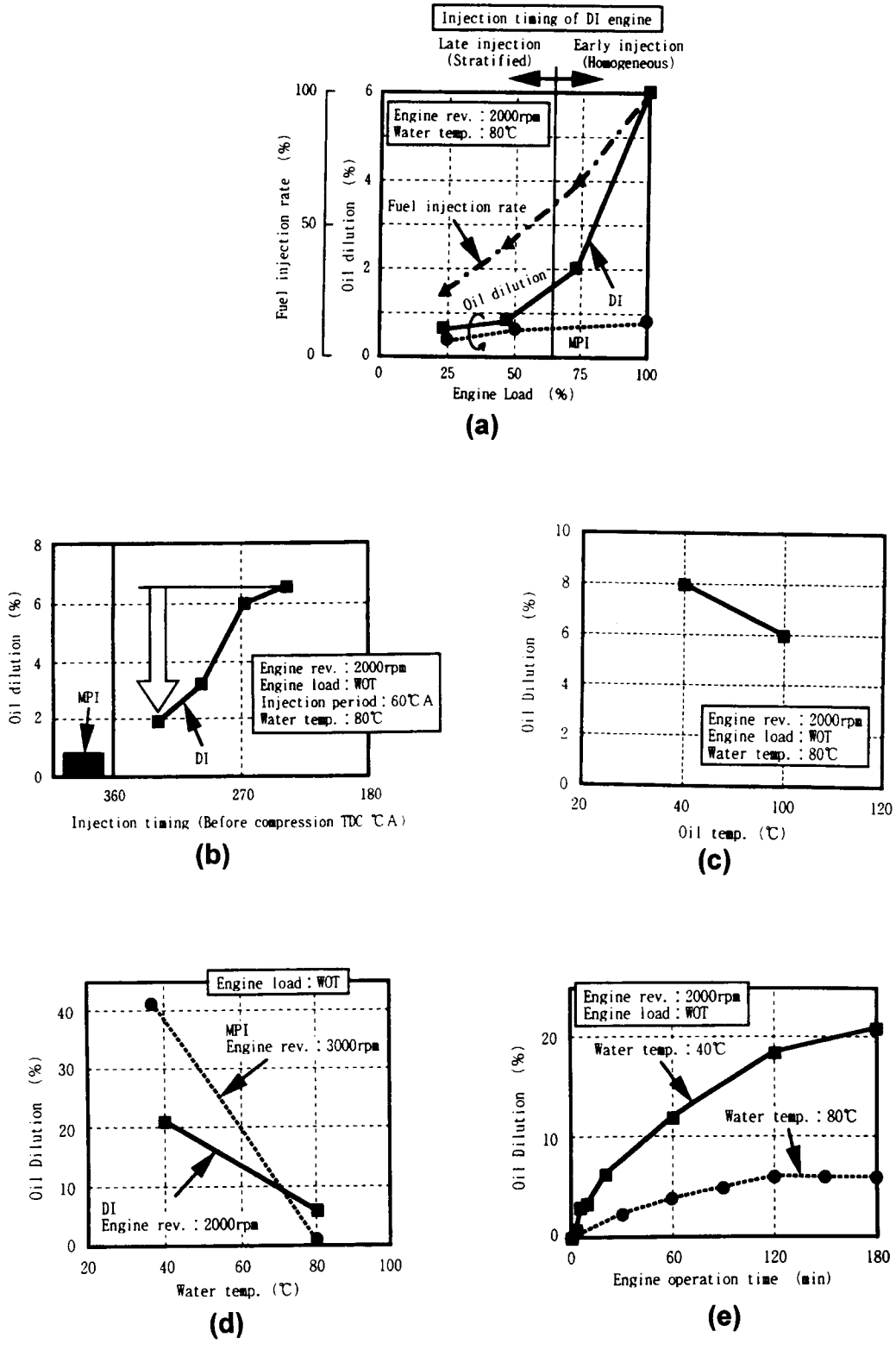

Fig. 46. Oil dilution results from the Toyota GDI D-4 engine [170]: (a) effect of engine load; (b) effect of fuel injection timing; (c) effect of oil temperature; (d) effect of coolant temperature; and (e) effect of engine operation time.

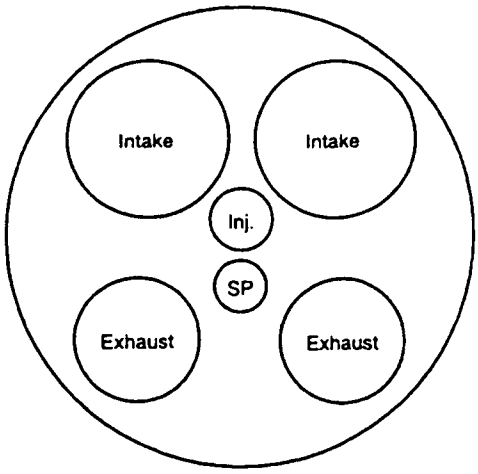

Fig. 47. Configuration of the Ford prototype GDI engine head [69].

[175,176,300,302,315,320,322,325,329] and CFD analyses [177–180,297–299,301,347,349,357] that include spray and combustion models; however, laser-based optical diagnostics requires a large modification of the engine combustion chamber, and GDI spray models and wall-film submodels are considered to still be in the development stage. This means that, although CFD can be used to screen some possible locations, much of the verification work on injector spray-axis positioning will consist of prototype hardware evaluation on an engine dynamometer. The basic considerations are that the injector should be located in a position that can provide a stable stratified charge at light load, a homogeneous mixture with good air utilization at high load, and avoid the impingement of fuel on the cylinder wall and on the piston crown outside of the bowl. Other important factors include the injector tip temperature and the fouling tendencies of the spark plug and injector, the compromise between intake valve size and injector location, and the design constraints of injector access and service. The effective area available for the intake valves is noted because most proposed injector locations generally reduce the space available for the engine valves, forcing smaller valve flow areas to be used. There are seven important parameters that will influence the final selected location of the injector and spark plug. These are:

- head, port and valve packaging constraints;
- injector spray characteristics;
- structure and strength of the in-cylinder flow field;
- combustion chamber geometry;
- piston crown and bowl geometry;
- injector body and tip temperature limits;
- spark plug design and allowable extent of electrode extension.

In general, the GDI injector should not be located on the exhaust side of the chamber, as injector tip temperatures of more than 175°C may result, causing injector deposits and durability problems as discussed in more detail in the injector deposit section. In tests of the Isuzu GDI engine [181,182], the Ford GDI engine [40,69], and the Honda GDI engine [183], the fuel injector was positioned near the center of the chamber with the spark plug being located near the spray cone as shown in Fig. 47. This location is preferable in many chamber designs as it virtually assures the presence of a rich mixture near the spark gap at the time of ignition. In addition, the vertical, centrally mounted injector location has the advantages of distributing the atomized fuel symmetrically in the cylindrical geometry, thus promoting good air utilization. For late injection, however, the centrally mounted, vertical location directs the fuel spray at the piston and is likely to yield higher UBHC emissions than an optimally inclined orientation. Also, it should be noted that the combustion stability of a GDI engine that uses a centrally mounted, vertical injector for stratified-mode operation is known to be quite sensitive to variations in the fuel spray characteristics. For example, variations in spray symmetry, skew or cone angle due to production variations or injector deposits can result in excessive values of COV of IMEP. For significant distortions of the expected baseline spray geometry, misfires and partial burns can occur. Thus, for GDI engine designs that incorporate a centrally mounted, vertical fuel injector, maintaining the designed spray geometry and quality is critical. The requirement for very close spacing of the injector and spark plug in some designs results in an additional reduction of valve sizes. It also introduces considerations of ignition fouling from the impingement of the spray periphery on the electrodes. Additionally, the use of higher ignition energy to make these systems less susceptible to fouling places greater demands on the durability of the spark plug [331]. The rate of formation of injector deposits is always a concern, but placing the injector tip closer to the ignition source could increase this rate.

The maximum intake valve size that can be utilized in conjunction with a head-mounted injector is shown in Fig. 48 [57]. Fig. 48(a) and (b) shows the possible layouts where the injector and spark plug are close to each other, which is often designated as the narrow-spacing design. Fig. 48(c) shows several possible locations for a widely-spaced spark plug and injector, which is designated as the wide-spacing design [184]. The significant design constraint is evident, and necessitates the use of auxiliary methods for improving the volumetric efficiency, such as optimizing the intake port design. According to Iwamoto et al. [50,51], the centrally mounted injector location also increases the possibility of smoke emissions. Some cases of spark-plug fouling have been noted for spark gaps positioned within the periphery of a fuel spray from a centrally mounted injector.

For a combustion chamber layout with a centrally mounted injector and spark plug, Whitaker et al. [165] and Lake et al. [185] recommended that the injector be located on the exhaust side, with the spark plug on the intake side, which allows conventional tumble in the correct direction to carry the fuel cloud to the spark plug during the compression stroke. This is schematically shown in Fig. 49. In addition,

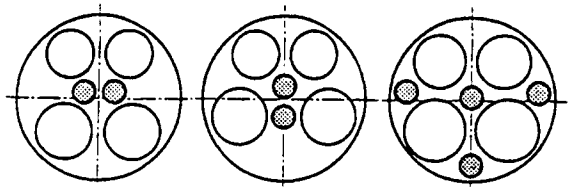

Fig. 48. Valve size limitation for optional injector and spark plug locations [57].

this configuration avoids spark plug wetting during early injection by taking advantage of the intake charge motion. However, there was no mention as to how the higher thermal loading on the exhaust side could negatively affect the injector deposit buildup. Another configuration was investigated that had the injector and spark plug mounted longitudinally, namely in line with the crankshaft in order to avoid the adverse effect of air motion on transporting the fuel to the spark plug in a wall-guided system. An air-guided system was also discussed for this geometry, which was reported to require an injector location that was offset towards the exhaust side. A central piston bowl was used for optimizing the wall-guided system, whereas a piston bowl offset toward the exhaust side was used for optimizing the air-guided system. It was reported that the central injector engine, in a wall-guided configuration, produces the highest UBHC emissions among all the concepts evaluated; and that the MBT combustion phasing is far more advanced. Lake et al. [185] reported that the central spark plug and injector configuration is not common, but that it does provide a long spray path before wall impingement. It was found to yield excellent homogeneous operation with good EGR tolerance at part load and good air utilization at full load. It was claimed that this configuration can be successfully packaged

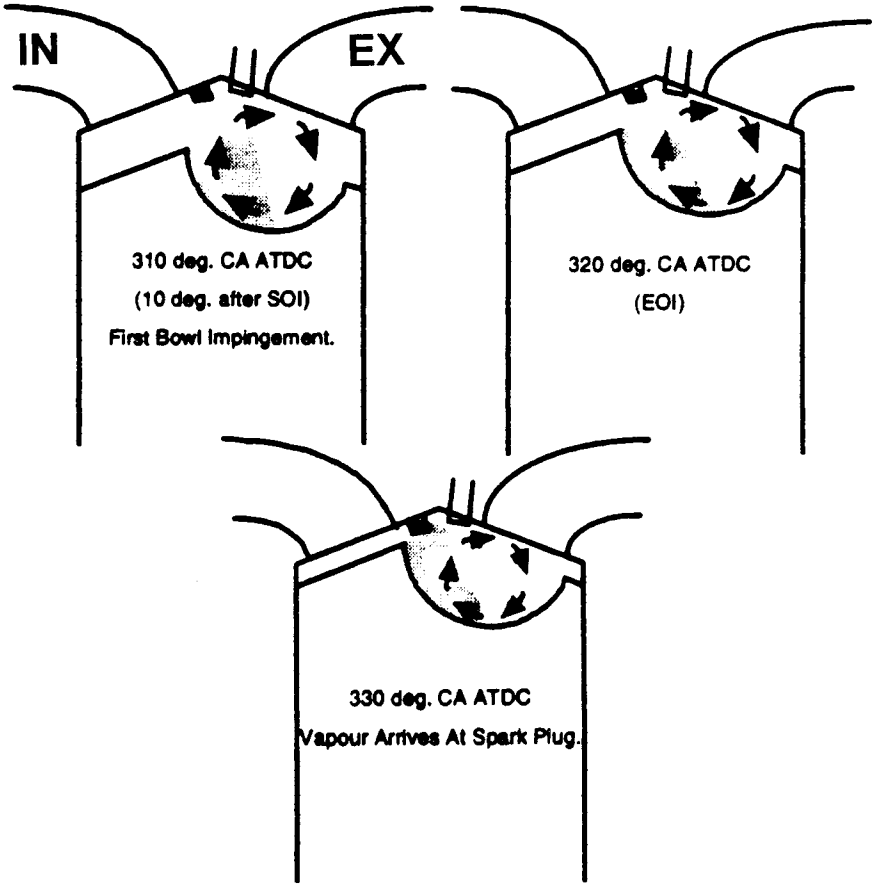

Fig. 49. Combustion chamber layout of the close-spaced fuel injector and spark plug with a conventional tumble flow for creating a stratified charge [185].

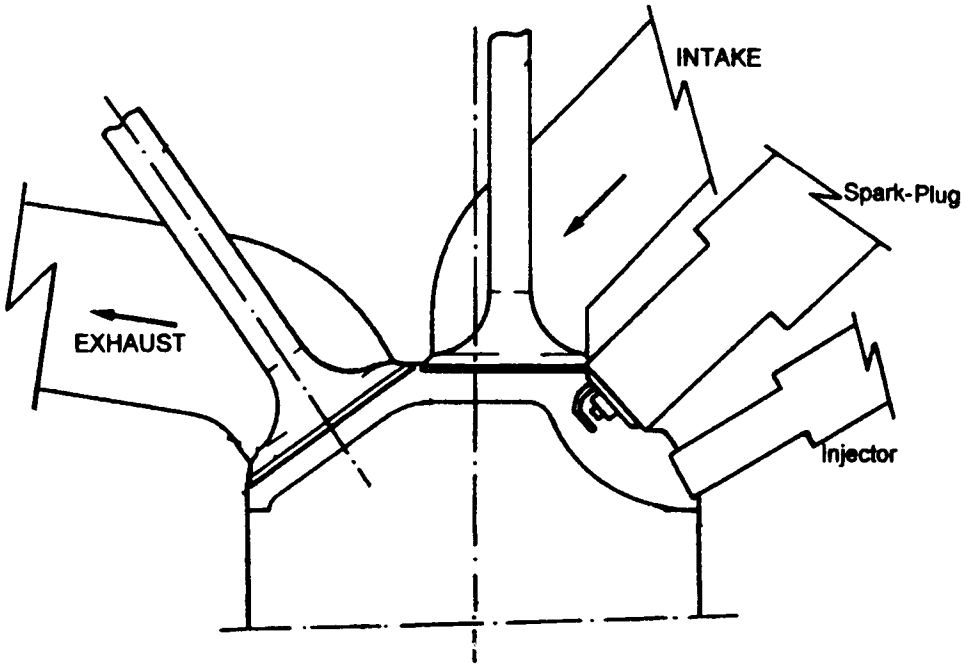

Fig. 50. Schematic of a close-spaced, three-valve, GDI combustion chamber for a small-bore engine [186].

in a bore size as smaller as 82 mm. Compared to other GDI layouts, this configuration requires the fewest changes from a conventional PFI design. A swirl-flow configuration using a side-mounted injector was reported to provide the best unthrottled stratified results in the tests; however, it was noted that more development efforts to achieve satisfactory WOT operation were required.

To relieve the packaging difficulty associated with applying GDI technology to small-bore engines, Leduc et al. [186] recommended that the narrow-spacing concept is more suitable. For GDI engines with a bore diameter of less than 75 mm, a three-valve per cylinder layout with the spark plug close to the injector and a piston cavity that confines the fuel spray to the vicinity of the spark gas was proposed. Fig. 50 shows a schematic of this proposed combustion chamber. To allow a large intake valve diameter, the intake valve stems are vertical. The exhaust valve is located in the pentroof of the combustion chamber. This single exhaust valve was also considered an advantage in providing a more rapid catalyst light-off than is achieved with a two-valve combustion chamber. An eccentric location of the spark plug was chosen for packaging considerations. It was reported that due to the smaller bore size, such a location did not result in a large degradation regarding heat loss and knock resistance. The confinement of the fuel spray in the vicinity of the spark plug was made possible by a well-optimized bowl in the piston. The inclination angle of the injector and the spray characteristics of cone angle and penetration were considered to be the key parameters that must be optimized to minimize any possible fuel impingement on the cylinder wall and piston crown.

Two important ways to achieve a stable stratified mixture are to decrease the time interval between injection and ignition and to decrease the distance between the injector tip and the spark gap [60]. However, decreasing the distance between the injector and the spark gap also decreases the time available for mixture preparation, which generally has a negative effect on UBHC emissions and soot formation. Improved fuel–air mixture formation can be obtained with the loss of some combustion stability by increasing the separation between the spark gap and the injector tip, or by increasing the time delay between the fuel injection and ignition. For open chamber designs in which the stratification is supported mainly by charge motion, a stable stratification can be obtained with directed spray impingement on the piston crown or bowl cavity, with subsequent transport of the fuel vapor towards the spark plug by the charge motion [15]. With the use of a specially contoured piston and an optimized balance of tumble and swirl, the transport of the fuel that impinges on the piston can be controlled to obtain stratified combustion. For the current, widely used, four-valve, PFI engine, the possible injector locations for increasing the separation between the spark gap and the injector tip are illustrated in Fig. 51. One is to locate the injector on the intake valve side of the combustion chamber, and the other is to locate the injector at the cylinder periphery between the intake and exhaust valves. Miok et al. [177] analyzed the mixture formation process that is associated with an injector located at the periphery of the cylinder between the intake and exhaust valves. For this study, the spray was directed towards the center of the combustion

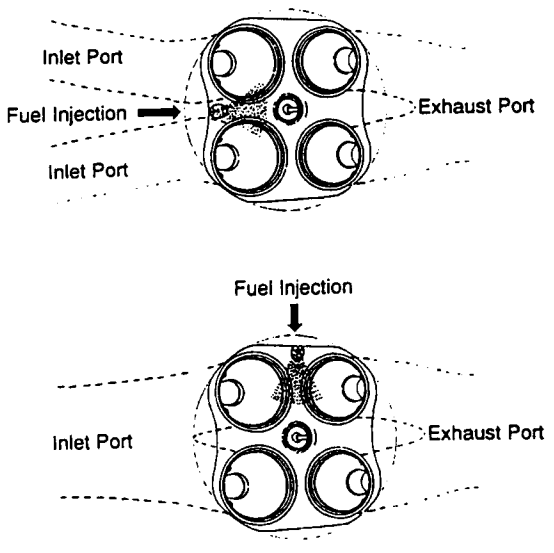

Fig. 51. Two possible locations for the side-mounted GDI injectors [187].

chamber at an angle of 70° down from the horizontal plane. It was found that this injector location and orientation produced a poor mixture distribution near the spark plug when used with a flat piston; however, this may be improved by modifying the piston crown geometry. Lake et al. [148] also verified that an optimized piston-bowl position is very important in directing the fuel spray towards the spark plug when using an injector mounted at the periphery of the cylinder.

The concept of locating the fuel injector underneath the intake port and between the two intake valves, and in positioning the spark plug at the center of the cylinder, has been invoked by a number of groups [20,22–24,27,99,100]. This geometric configuration is considered to be a key element of a compact design for a multi-cylinder GDI engine, particularly for smaller bore diameters [144]. It provides an improved entrainment of the induction air into the fuel spray, as well as enhanced cooling of the injector tip [187]. Systems using spray impingement on solid surfaces to create a stratified mixture generally exhibit a reduced sensitivity to variations in spray characteristics. Hence, these systems tend to be more robust regarding the effects of spray degradation from deposits, pulse-to-pulse variability or part-to-part production variances in the spray envelope. However, Shimotani et al. [181] reported that locating an injector at the periphery of the cylinder on an Isuzu single-cylinder GDI engine produced higher UBHC emissions and fuel consumption than was obtained with the same injector located at the center of the combustion chamber. This was theorized to be due to fuel penetrating to the cylinder wall on the exhaust valve side [42], with an increased absorption of liquid fuel and desorption of fuel vapor by the lubricating oil film. The direct impingement of fuel on the cylinder wall or the piston crown forms a film of liquid fuel on the solid surface, which can result in some pool-burning and an increase in UBHC emissions [162,188]. The use of a side-mounted injector could also result in an increased oil dilution, especially at high-load conditions [170]. An additional consideration in using a spray-impingement system is the necessary compromise that must be made in shaping the piston crown in order to obtain part-load stratification. This compromise will most likely be somewhat detrimental to the air utilization at the high-load conditions for which a homogeneous mixture is required. The piston curvature may even increase the heat losses from the combustion gases.

Andriesse et al. [189,190] compared the homogeneous GDI performance of a side-mounted injector configuration and a centrally mounted injector configuration. It was found that charge homogeneity is the best for a centrally mounted injector, resulting in lower CO_2 and smoke emissions, as well as a higher attainable engine torque. At the same mid-range engine speed, the side injector exhibits a 4.5% BMEP advantage while the central injector provides a 6% BMEP advantage over the PFI baseline. The side injector yields the highest volumetric efficiency, as this configuration permitted larger intake valve dimensions. Results for part-load show a slight advantage in UBHC emissions for the central injector configuration. The overall comparison of the two systems indicates that the performance differences between the two systems are incremental, and only a slight advantage exists for the central injector geometry. It was concluded that the choice of the configuration for production is therefore governed mainly by manufacturability considerations, rather than by the performance increment. It should be noted that the combustion system configurations that were used in this study may not have been optimized for either of the injector orientations. This should be considered in evaluating the conclusions.

The alignment of the injector relative to the intake port is another design challenge for implementing a side-mounted injector. The use of an intake port configuration largely identical to a PFI port design leads to a very shallow injector elevation angle above the horizontal plane [142]. Such a configuration does provide an intake port with known, good flow characteristics, but the spray may impact the intake valves for early injection, possibly causing deposit formation. This can be partially overcome by using either an angled spray or a steeper injector inclination angle. With a steeper injector inclination angle, the interaction between the spray and the target piston cavity is less dependent on the engine crank angle. This leads to a wider speed range for stratified operation. Based on this fact, Mitsubishi [17] updated its GDI combustion system for the European market by installing the injector more vertically to extend the range of stratified operation to higher engine speeds, as shown in Fig. 52. It is claimed that this also improved the combustion stability under high EGR operation. As a result, a significant engine-out NO_x reduction could be achieved.

Engineers at Nissan [99,100,191,192] investigated the

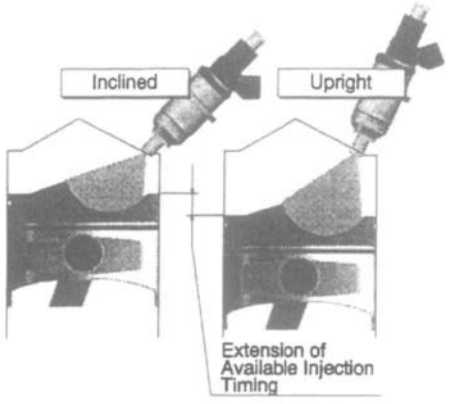

Fig. 52. Comparison of spray targeting for two injector inclination angles in the Mistubishi GDI engine [17].

effect of injector inclination angle on fuel wall wetting, engine performance and exhaust emissions. Fig. 53 shows the fuel amounts, as computed by CFD, on various surfaces of the Nissan GDI combustion system for three injector inclination angles. The injection timing was fixed at 270° BTDC on compression for all three cases. It was found that by increasing the injector inclination angle, namely mounting the injector more vertically, the amount of fuel impinging on the cylinder wall decreases only slightly. The amount of fuel wetting the head surface is reduced significantly and the amount of fuel impinging on the piston crown exhibits a marked increase. With a more vertical injector mounting, the total amount of fuel wetting the solid surfaces decreases during early injection, implying that a more vertical injector mounting is advantageous. However, a more vertical spray axis degrades the Nissan engine performance at WOT, as shown in Fig. 54, due to poor mixture quality.

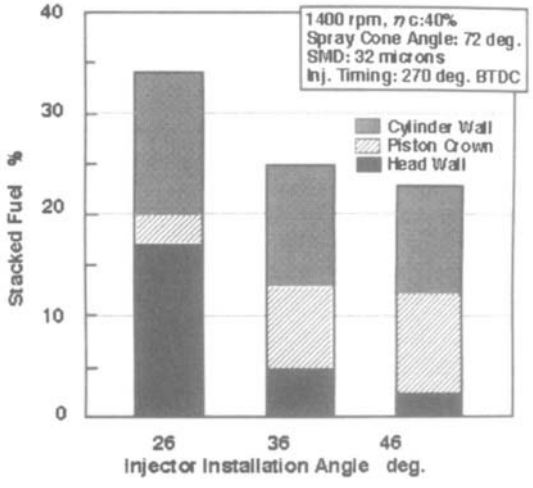

Fig. 53. Effect of the injector inclination angle on the amounts of fuel impinging on the cylinder head, piston crown and cylinder wall for the Nissan GDI engine [100].

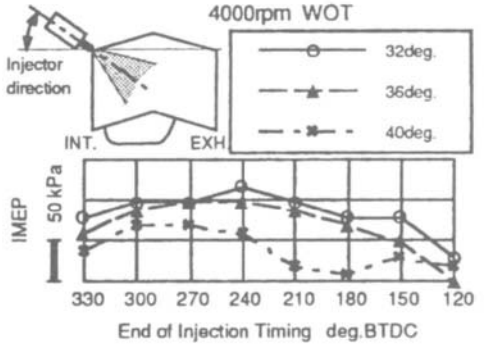

Fig. 54. Effect of the injector inclination angle on the Nissan GDI WOT performance at an engine speed of 4000 rpm [192].

Fig. 55 shows the effect of injector inclination angle on measured engine fuel consumption, emissions and oil dilution for two operating conditions. It was found that increasing the injector inclination angle, or more correctly, the spray-axis inclination angle tends to degrade the fuel–air mixing process in this engine, which increases the smoke emissions and the engine BSFC. Mounting the injector more vertically was also found to increase the oil dilution. There is indeed a consensus in the literature that the spray-axis inclination angle is an important parameter in developing and optimizing a GDI combustion system.

Some additional combinations of fuel injector and spark plug locations proposed by Fraidl et al. [57] are illustrated in Fig. 35. Some of these proposals have been evaluated and found to be lacking in one or more key areas. For example, predictions of the equivalence ratio at the spark gap showed that the mixture at the spark gap is too lean for a flat-top piston at the time of ignition with late injection timings [145,173]. This was for a four-valve configuration with a central spark plug and the injector positioned at the bore edge between the intake valves.

Noda et al. [192] investigated the effect of fuel–air mixing on the Nissan GDI wide-open-throttle (WOT) performance. This GDI engine has a side-mounted injector between the intake valves and underneath the intake port. For early injection, homogeneous-charge operation, it was found that the piston bowl designed for promoting stratified charge operation has a negative impact on the mixture formation process when compared to a flat piston. The extended torque range that is obtained with the flat piston is shown in Fig. 56. Both LIF and CFD results indicate that the use of flat piston promotes a more uniform mixture. It is claimed that the improvement in power output for WOT operation is reduced markedly when a bowl is provided in the piston crown to accomplish the stratified charge combustion. Yamashita et al. [141] investigated the effect of piston-bowl shapes on the Mazda prototype GDI system for stratified-charge operation. The oval shape bowl diameter (large diameter), D, and bowl depth, H, were varied. Three different diameters of $D = 40, 50, 60$ mm and two bowl

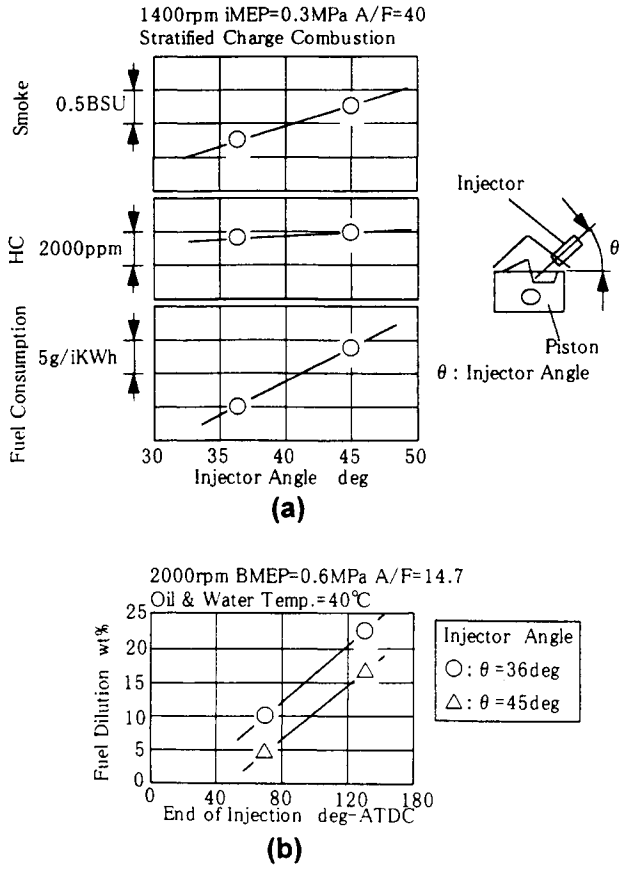

Fig. 55. Effect of the injector inclination angle on the Nissan GDI fuel consumption, emissions and oil dilution [191].

depths were investigated. It was found that the ISFC at light and medium load is higher with the smallest bowl diameter. The FID measurement of UBHC in the vicinity of the spark plug indicates that the mixture at the time of ignition is too rich at this operating condition. A bowl diameter exceeding 50 mm was recommended in order to achieve a wider operating range. With the same bowl diameter, a deeper bowl was found to produce an enhanced ISFC over a wider range of load. Karl et al. [193] investigated the effect of piston-bowl geometry on the engine-out emissions of the Mercedes-Benz prototype GDI combustion system, which has a close-spaced spark plug and fuel injector. As shown in Fig. 57, both the ISFC and the UBHC emissions are reduced by utilizing an open piston-bowl configuration (bowl-shape 2 in the figure), but this also results in an increase in the NO_x emissions.

The spark plug gap must always be positioned in a zone of ignitable and combustible mixture when the spark occurs, and this position is affected by the swirl and tumble ratios, spray cone angle, mean droplet size, and injection and spark timings. Guidelines have been reported on the recommended position of the spark gap for open chamber GDI systems by many researchers, such as by Fraidl et al. [57]

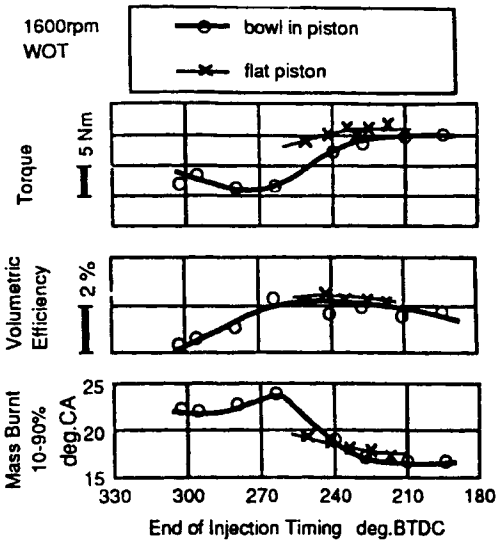

Fig. 56. Effect of the piston bowl configuration on the Nissan GDI WOT performance at an engine speed of 1600 rpm [192].

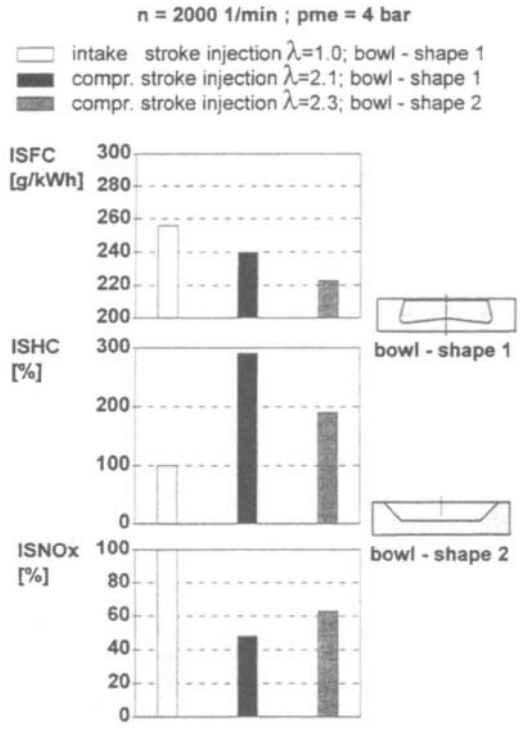

Fig. 57. Effect of the piston bowl configuration on the engine performance and emissions of the Mercedes-Benz GDI engine [193].

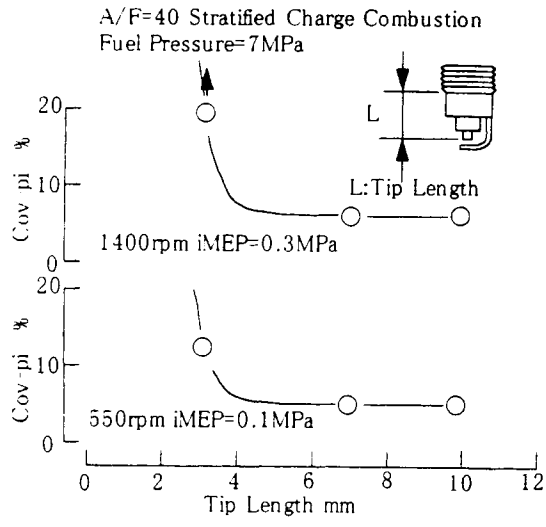

Fig. 58. Effect of the spark plug electrode protrusion on the combustion stability of the Nissan GDI engine [191].

and by Ando [16]. For example, for GDI systems that do not use wall impingement, the spark plug electrodes must generally project into the periphery of the spray cone in order to ignite the combustible mixture, and should also be positioned to shield the gap from being affected by the bulk flow. For low-load operation, it is suggested that the spark gap be near the injector tip; however, close proximity may result in the system being too sensitive to variations in the fuel injection system. Engineers at Mitsubishi [194] incorporated many improvements in the Mitsubishi GDI ignition system, including individual ignition coils for each cylinder, the use of a larger discharge current and a longer discharge time. A platinum electrode with a protrusion of 7 mm was used. Ashizawa et al. [191] investigated the effect of spark plug protrusion on the combustion stability of a Nissan GDI engine for two operating conditions. As shown in Fig. 58, a minimum of 4 mm protrusion is required to achieve a stable stratified charge combustion under tested conditions.

In summary, the spark plug should be located near the center of the combustion chamber to obtain the best engine combustion characteristics. System configurations with close spacing of the injector and spark plug usually have the spark gap located in the periphery of the fuel spray cone. The transport of fuel to the spark plug is mainly achieved by the spray penetration. In-cylinder charge motions and the associated turbulent fluctuations have only a minor influence on the mixture transport. In contrast, ignition occurs in a region with large gradients in the local mixture fraction and is therefore sensitive to cyclic fluctuations of the spray geometry. Any direct impingement of the spray on the spark plug can lead to plug wetting and cold start problems, and spark plug durability must be evaluated. A further disadvantage of narrow spacing is the associated restriction on valve sizes in multi-valve engines [184]. Configurations utilizing a wide spacing of the injector and spark plug have fewer inherent geometric and thermal restrictions for the cylinder head design. The increased time scale for mixture transport from the injector to the ignition location can enhance mixture preparation, but fluctuations in turbulence and related cyclic variability become more critical. Both the narrow-spacing and wide-spacing configurations can be combined with the charge motion concepts of swirl and tumble to achieve viable GDI combustion systems that can operate in the stratified mode. The guidelines for positioning and orienting the GDI fuel injector are listed as follows.

- Centrally mounted GDI injector:
  - higher ignition stability over the engine operating map;
  - high degree of mixture stratification possible but in a narrow time window;
  - good at distributing fuel uniformly;
  - advantageous for homogeneous-charge operating mode;
  - mixture formation relatively independent of piston crown geometry;
  - more difficult installation and removal;

- reduced valve size;
- possible spark plug fouling;
- higher tip temperature and deposit tendency;
- sensitive to variations in fuel spray characteristics;
- higher probability of spray impingement on piston crown;
- special spark plug with extended electrodes may be required.

- Side-mounted GDI injector:
  - larger valve size permitted;
  - increased mixture preparation time available;
  - facilitated injector installation and removal;
  - less effect of variations in fuel spray characteristics;
  - injector tip more readily cooled by intake air;
  - lower tip temperature and deposit tendency;
  - less fuel impingement on spark plug electrodes;
  - standard spark plug possible;
  - more constraints on fuel-rail positioning;
  - low degree of stratification and large-scale fluctuations;
  - higher probability of spray impingement on cylinder wall;
  - increased oil dilution probability.

- Locating the injector on the exhaust-side of the combustion chamber should be avoided.

4.2. In-cylinder charge cooling

For the ideal GDI engine, fuel is injected directly into the cylinder as a very well atomized spray that is vaporized completely by absorbing heat only from the in-cylinder air. This is also a very efficient mechanism for cooling the resident air charge inside the cylinder. The resulting decrease in the charge temperature due to the latent heat of vaporization of the fuel can yield an increased mass of air in the cylinder if injection occurs during the induction process, thus increasing the volumetric efficiency of the engine. The reduced charge temperature at the start of compression also translates into lower compression temperatures, thus enhancing the mechanical octane number of the combustion chamber. As a result of the thermodynamic effects of in-cylinder charge cooling, the ideal GDI engine exhibits the advantages of both higher torque and a higher knock-limited compression ratio as compared to the PFI engine. By way of contrast, fuel droplets of 120–200 μm SMD are injected into the intake port in a typical PFI engine, and a liquid film is formed on the back of the intake valve and on the port wall. This liquid fuel vaporizes under the influence of concentration gradients, port vacuum, and by absorbing heat from the valve and wall surfaces. Therefore, it is difficult to achieve an efficient charge cooling effect in a PFI engine. The cooling of the in-cylinder induction air due to the direct injection of a vaporizing fuel spray during the induction event has been found to provide the following advantages:

- increased volumetric efficiency;
- reduced compression temperature;
- reduced autoignition tendency at the same compression ratio;
- higher knock-limited compression ratio.

The decreased charge temperature that is associated with fuel injection during the induction process was found to provide an increase of 2% in the trapped cylinder mass over the noninjection case; however, as would be expected, the gain in volumetric efficiency disappears when injection is retarded to the end of the intake stroke [147]. At the other extreme, if the injection timing is advanced to the early stages of the intake stroke, fuel impingement on the piston can occur. The increased wall-wetting reduces the effective charge cooling rate, resulting in a smaller temperature decrease and a smaller gain in the trapped mass. Therefore, for injection circumstances that result in significant wall wetting, the benefits of charge cooling will be diminished. The level of atomization does indeed influence the volumetric efficiency gain, as rapid vaporization of fuel droplets in the air stream during induction is the key factor. Droplet sizes must be sufficiently small such that most of the fuel vaporizes during the time available for the induction event. The cooling effect continues as fuel is vaporized, even into the early stages of combustion; however, the volumetric efficiency gain is directly related to the fraction of fuel that is vaporized by the time that induction is completed. The cooling of the intake charge also modifies and improves the engine heat transfer process, particularly for the early injection that is associated with high-load operation. The charge density is increased during the compression stroke, and the charge temperature is elevated to values higher than the wall temperature, with heat being transferred to the walls. It was reported by Han et al. [147] that a maximum reduction in heat losses can be obtained for a GDI injection timing of 120° after top dead center (ATDC) on intake. This heat transfer advantage diminishes rapidly as the injection timing is retarded towards the end of the intake stroke.

Anderson et al. [40] estimated the magnitude of the charge cooling effect on volumetric efficiency for two extreme cases. One case is similar to that of the PFI engine where the fuel is vaporized only by heat transfer from the intake port and valve surfaces. The other case corresponds to the ideal GDI engine where the fuel is vaporized only by absorbing thermal energy from the air. For an assumed initial intake air temperature of 100°C and a fuel temperature of 50°C, it was found that for direct injection the volume of the mixture after vaporization is about 5% smaller than the volume of intake air. Under the same inlet conditions, however, if fuel is vaporized and heated to the intake air temperature by heat transfer from the wall only, the mixture volume will increase by 2% due to the volume of the fuel vapor. Thus, the total difference in the mixture volume of the two extreme cases can be as large as 7%. However, it should be noted that these extreme cases

are not totally descriptive of real GDI and PFI processes, because some vaporization of fuel in air occurs in PFI engines, and some wall film vaporization of fuel occurs in actual GDI engines. Moreover, for the cold-start case, the fuel, air and engine cylinder wall have similar temperatures. As a result, the actual difference in the engine volumetric efficiency between the PFI and GDI engines can be significantly less than that computed from the ideal limiting cases, and is quite dependent on the specific engine design, fuel characteristics and operating conditions. At a constant pressure, the difference in the calculated charge temperature for the two extreme cases can be as large as 30°C, depending on the assumed intake air and fuel temperatures. The charge temperature for the case of injection during intake was found to decrease 15°C by the end of the induction process due to fuel evaporative cooling [40]. This translates into a significant decrease in the gas temperature at the end of the compression stroke. For example, the compression temperature is reduced by 116°C, from 539°C for the noninjection case to 423°C when the fuel is injected at 120° ATDC on intake [147]. Therefore, the GDI engine utilizing a mid-induction injection of fuel will exhibit a lower knocking tendency. This has been verified experimentally, with the advantage being that the knock-limited spark timing may be substantially advanced. Alternatively, the knock-limited compression ratio can be increased by as much as 2 full ratios for 91 RON fuels, thus easily achieving a significant gain in thermal efficiency. Lake et al. [148] and Jackson et al. [145,173,195,196] reported the benefit of the charge cooling resulting from early fuel injection to be an octane number improvement of 4–6, allowing an increase of compression ratio of up to 1.5. Invoking the permitted increase in the compression ratio will directly enhance the power and torque characteristics of the GDI engine, and will result in an immediate and substantial improvement in engine BSFC. Jackson et al. [195] also emphasized that the elimination of fuel vapor in the intake port, which displaces air in the PFI case, is also a contributor to the volumetric efficiency improvement.

Takagi [23] reported that with a stoichiometric air–fuel ratio, charge cooling has the effect of lowering the air temperature at the end of induction by approximately 20°C. As a result, even under wide open throttle (WOT) operation at low engine speed, the GDI test engine exhibited a 6% higher power output as compared to that of a PFI engine. This improvement is attributed in part to the higher intake manifold absolute pressure (MAP) resulting from the improved charging efficiency. Another contributing factor is the ignition timing advance made possible by the reduced knock tendency. The effect of injection timing on the GDI engine volumetric efficiency was compared with that obtained for the baseline PFI engine by Anderson et al. [40,69]. As shown in Fig. 59, the volumetric efficiency improvement was found to be about one-third of the theoretical maximum difference, or about 2.5%, and exhibited a strong dependence on the injection timing.

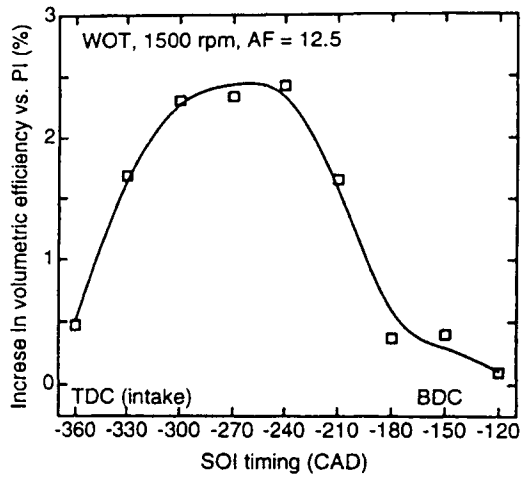

Fig. 59. Increase in volumetric efficiency of the GDI engine over the PFI engine for the early injection mode [69].

In summary, when injection occurs at the beginning of the intake stroke, the piston is relatively close to the injector and is moving away from the injector at a low velocity. For this case, fuel impingement on the piston crown can occur, and the amount of energy supplied by the induction air to vaporize the fuel is reduced. As injection occurs later in the induction stroke, when the piston is more distant from the injector tip and is moving away with a much higher velocity, spray impingement is reduced or eliminated, resulting in an increase in the volumetric efficiency. If injection occurs too close to the time of intake valve closure, the fuel droplets will have insufficient time to vaporize before the intake valve closes. For this timing the charge-cooling effect is significantly reduced. Therefore, the benefit of in-cylinder charge cooling is only fully realizable within a relatively narrow window of injection timing corresponding approximately to mid-induction.

4.3. Engine operating modes and fuel injection strategies

Over the past two decades, a number of concepts have been proposed to exploit the potential benefits of direct gasoline injection for passenger car applications, but until recently none have been incorporated into a production GDI engine. One important reason for this was the lack of controllability in the fuel injection system. Systems that were based upon diesel fuel systems and pressure-activated poppet nozzles experienced significant limitations in regards to performance and control. Although the engines used in the previous attempts were reasonably successful in producing improvements in BSFC, the mechanical pumps that were utilized had limited speed and timing ranges, and the specific power densities obtained with these engines were often much less than that of the diesel engine. The reexamination of the GDI engine over the last seven years has benefited from the application of electronic, common-rail,

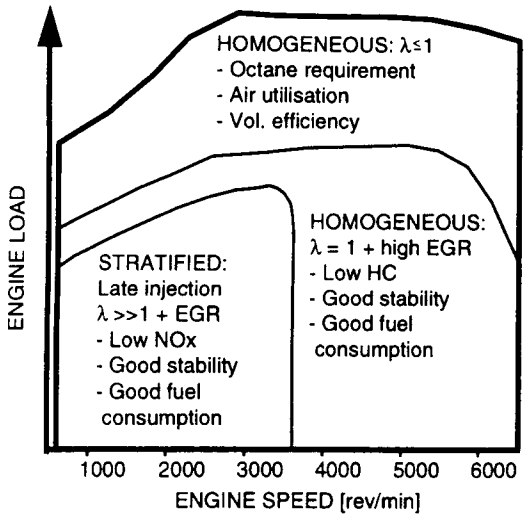

Fig. 60. Typical GDI engine operating map [185].

injection systems to four-stroke GDI engine requirements. It should be noted that this type of injection system, which has long been the production PFI hardware, is currently being applied to diesel engines, and was utilized on two-stroke DI gasoline engines. Such injection systems provide fully flexible timing over the entire speed and load range of current gasoline engines by allowing a strategy of optimum injection timing at all engine-operating points. According to Lake et al. [148], the GDI engine equipped with an electronic common-rail system has the ultimate potential of achieving a significantly improved BSFC while achieving a specific power output that is equivalent to that of a PFI engine. Many of the realized advantages of the GDI combustion system are attributed to the high flexibility of the modern electronic fuel injection system. It may be noted in the typical GDI engine operating map, as shown in Fig. 60, that in order to achieve good medium to full-load performance, even a stratified-charge GDI combustion system must be capable of operating well for early injection, homogeneous-charge conditions. Therefore, all GDI combustion systems, whether stratified or fully homogeneous, must provide good homogeneous combustion characteristics.

In general, the GDI engine operation can be classified into four basic modes starting with the least complex: homogeneous stoichiometric operation for full load with maximum air utilization and optimized cold start; homogeneous lean operation for medium part load for optimized fuel economy and NO_x trade-off; stratified lean operation for idle and low-load operation to achieve maximum fuel economy; and load-transition operation. All modes have been reported and discussed in the literature.

The objective of charge stratification in the GDI engine is to operate the engine unthrottled at part load at an overall air–fuel ratio that is leaner than is possible with the conventional lean-burn or homogeneous mixture. This is achieved by creating and maintaining charge stratification in the cylinder, such that the air–fuel ratio at the spark gap is compatible with stable ignition and flame propagation, whereas areas further from the point of ignition are either very lean or devoid of fuel. In general, air–fuel mixture stratification is realized by injecting the fuel into the cylinder during the compression stroke; however, it may also be possible to achieve stratification with early injection. Some success towards this goal has been obtained with an air-assisted fuel system [197]. The use of charge stratification with an overall lean mixture can provide a significant improvement in engine BSFC [20]. This is obtained primarily by significantly reducing the pumping losses that are associated with throttling, but there are also additional benefits such as reduced heat loss, reduced chemical dissociation from lower cycle temperatures, and an increased specific heat ratio for the cycle.

When the engine operates in the stratified-charge mode, the timing of the end of injection (EOI) is an important parameter, as the last liquid fuel enters the chamber at this time [198,355]. It should be noted that GDI injectors require from 0.35 to 0.70 ms to close, thus fuel will enter the chamber for that time interval after the logic command to close. A retarded EOI timing generally results in a more rapid start of combustion, while an advanced EOI tends to shorten the combustion duration. It was reported that the 50% heat release point occurs before TDC when the EOI timing is advanced from 57° BTDC on compression and occurs after TDC when the EOI timing is retarded [193]. The indicated specific fuel consumption (ISFC) was found to decrease as the EOI timing is retarded; however, the UBHC emissions increase due to degraded mixture quality and an extended combustion duration.

There is a consensus in the literature on GDI that achieving stable, stratified-charge combustion while controlling the engine-out UBHC emissions to a very low level is a difficult task. The interrelationships of injector location, spray characteristics, combustion chamber geometry, EGR rate, injection timing, and spark timing are quite complex, and must be optimized for each system. The GDI engine operating range, in which charge stratification can be effectively utilized to obtain the available thermodynamic benefits, should be chosen to be wide enough to cover the most frequent engine operating conditions [193], otherwise mode transitions will be too frequent. In general, it is exceptionally difficult to achieve full air utilization with a late injection strategy due to incomplete mixing, which may lead to excessive smoke emissions. If the compression ratio is reduced to limit smoke, some of the fuel economy benefit at part load will not be realized. For most prototype GDI combustion systems, obtaining part-load, stratified operation with acceptable values of COV of IMEP has proven to be quite difficult. It should also be noted that no stratified-charge GDI engine has yet demonstrated a sufficiently low level of engine-out NO_x for the attainment of ULEV emissions without a lean-NO_x catalyst.

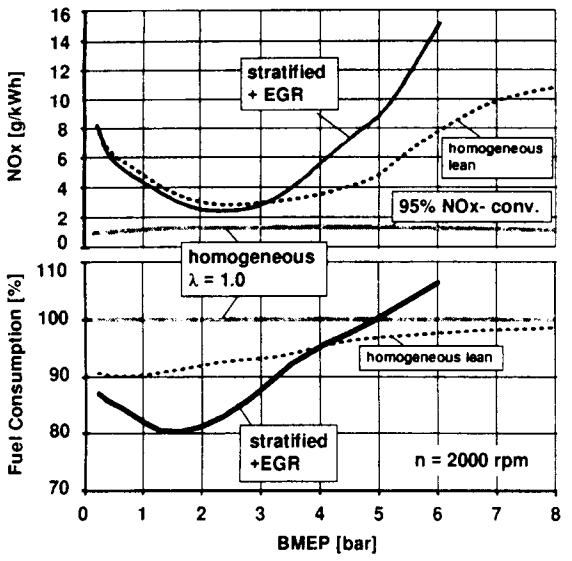

Fig. 61. Comparison of fuel consumption and NO_x emissions under three GDI operating modes [142].

Fig. 61 shows a comparison of engine performance for three GDI operating modes [142]. It is clear that stratified charge operation is only advantageous for low engine loads, even for the optimized charge stratification concepts. If the engine BMEP exceeds 5 bar, an efficient combustion process can be alternatively achieved using the homogeneous lean operation. This has the benefit of comparatively low NO_x emissions. Moreover, if the stratified charge mode is extended to high-load operation, smoke is likely to be produced due to over-rich regions near the spark gap, even though the amount of air is maximized by the fully opened throttle. As the load increases, the injection duration must also increase. This creates a fuel–air mixture cloud that increases in size with load but is constrained by the piston and chamber geometry. The mixture cloud can have locally rich stratification as a consequence of being geometrically constrained and by having a short available mixing time for fuel introduced near the end of injection. When the early part of the fuel cloud is ignited, combustion occurs rapidly because of the locally rich mixture, and may propagate rapidly through the latter portion of the injected fuel that is less than ideally mixed, leading to soot and UBHC emissions. Soot can also be generated by the increased impingement of the fuel spray on the piston crown as the injection duration is increased. The soot formation threshold is considered to be a primary limitation as the load is increased [199]. In this case, the smoke problem can be alleviated by operating the engine in the homogeneous-charge mode using early injection. The injection timing has been found to be an influential parameter in suppressing the formation of soot. A carefully designed transition between the low-load stratified and high-load homogeneous mixture formation is important for realizing particulate-free combustion [45]. It was reported by Kume et al. [20] that the stratified-charge mode using late injection can be extended to 50% of full load without an apparent increase in soot for the Mitsubishi GDI engine. It was theorized that sufficient excess air exists in the cylinder for the soot to oxidize rapidly. When the load exceeds 50%, however, soot particulates begin to be emitted. For the DI diesel engine the amount of fuel that can be injected into the engine cylinder must be restricted so as to limit the soot emissions to permissible levels, resulting in lower performance. In the GDI engine, however, this problem can be circumvented over the entire engine operating range without degrading the engine performance by adjusting the fuel injection timing [43].

Fraidl et al. [142] proposed another operating mode for warm-up, called stratified stoichiometric operation, in order to reduce the engine-out emissions by achieving a reduced catalyst light-off time. This operating mode offers an ultra-low emission approach that complements the well-known lean-burn concepts. This is based on the fact that the use of a stoichiometric or near-stoichiometric stratified charge only retards the initial combustion phase marginally, while the main combustion will be noticeably retarded. Even with very lean overall air–fuel ratios, the nearly stoichiometric mixture in the initial combustion area, combined with high charge turbulence, results in a rapid initial combustion phase. Depending on the degree of charge stratification, combustion chamber geometry, EGR rate, charge motion, and fuel vaporization rate, the burn rate decreases more rapidly than is observed for homogeneous-charge operation. Thus, the use of relatively late combustion is possible even with constant ignition timing. As a result, UBHC and NO_x emissions can be lowered and exhaust gas temperatures can be elevated. Such a stratification measure could be an alternative to conventional catalyst light-off strategies. It must be noted that the additional energy content of the exhaust gas is associated with an increase in fuel consumption; however, this is only effective until the catalyst threshold temperature is achieved, therefore it only marginally influences the overall fuel consumption.

It has been demonstrated that the strategy of early injection in the GDI engine can meet the requirements for higher engine loads. When used in combination with a complementary in-cylinder charge motion, this strategy has the potential of providing full-load performance that is comparable to that of conventional PFI engines [69]. Early injection also makes it possible for the engine to operate at a slightly higher compression ratio, which can provide an additional incremental improvement in fuel economy. An early injection strategy with an essentially homogeneous charge can also achieve a number of benefits in the areas of cold-start and transient emissions. The stoichiometric GDI is able to offer high performance due to increased volumetric efficiency and low tailpipe emissions, mainly due to the permissible use of a three-way catalyst. The strategy also provides rapid engine starting, less cold enrichment, elevated exhaust

temperature and a faster catalyst light-off [186]. The attainable advantages with the early-injection, stoichiometric GDI engine that will be discussed in detail in the following sections are:

- more rapid cold-start;
- less cold-start enrichment required;
- less acceleration-enrichment required;
- quicker catalyst light-off;
- reduced cold-start UBHCs;
- more precise air–fuel ratio control;
- improved transient response;
- reduced heat loss during compression stroke;
- improved combustion stability;
- better EGR tolerance;
- up to 5% improvement in volumetric efficiency;
- up to 2 ratios increase in autoignition-limited compression ratio;
- ability to invoke fuel cutoff on deceleration;
- 6% gain in integrated fuel economy;
- up to 10% increase in peak torque and power;
- possible enabler of some other technologies such as VVT and CVT;
- less control complexity as compared to the stratified-charge GDI engine;
- three-way catalysis can be fully utilized.

The GDI engine combustion characteristics for very early injection are basically the same as those of premixed PFI engines. Shimotani et al. [181] conducted an extensive study on the combustion characteristics of a GDI engine using early injection for a range of injection timings during the intake event. With a center-mounted injector the emissions and engine performance were found to be quite similar to that of a baseline PFI engine when the fuel is injected early in the intake stroke (0–60° ATDC on intake). This indicates that the use of an early injection timing achieves a homogeneous mixture because of the longer time available for mixture preparation. It was found that retarding the injection timing produces higher CO, because the mixture becomes less homogeneous and the combustion becomes less stable. The UBHC emissions were found to be minimized with injection at BDC on intake due to the decrease of the fuel impingement on the piston crown and other quenching areas. High-speed videos of combustion reveal that early fuel injection generates a blue flame that is similar to that observed in the PFI engine; however, a yellow flame that is indicative of stratified combustion is observed when the injection timing is retarded to the end of the intake stroke.

For injection during induction, a later injection timing improves the start of the combustion and advances the 50% heat release point due to the presence of a rich mixture zone around the spark gap. However, changes in injection timing do not significantly change the combustion duration. For the late-injection, stratified-charge mode, an excessively rich mixture near the spark gap must be avoided in order to maintain a stable ignition and minimize smoke. Therefore, it is imperative that a mixture preparation strategy that will accommodate a wide range of engine operating conditions be developed for each specific GDI design [15]. A wide crank-angle window exists for the timing of early injection for homogeneous-charge combustion, but only a narrow operating window is available for the timing of late injection for stratified-charge combustion. At higher loads, the longer injection duration with the accompanying richer mixture results in a decreased sensitivity to injection timing [145,173]. The operating map of the Toyota GDI engine is shown in Fig. 62. Both the early injection mode for homogeneous-charge operation and the late injection mode for stratified-charge operation are widely utilized in current GDI combustion systems; however, misfire or partial burns may occur during the mode transition due to the overall lean mixture. For the mode transition, Matsushita et al. [43] proposed a two-stage, or split-injection strategy that injects portions of the fuel into the cylinder during both the intake and the compression strokes in order to form a weak stratification. As a result, excessively rich or lean mixtures can be avoided and stable combustion can be obtained from an overall lean mixture. It is reported that this two-stage injection facilitates a smooth transition from lean-stratified combustion to full-load, homogeneous combustion. The potential of this two-stage injection for enhancing the engine performance and exhaust emissions can be noted from the data in Fig. 63 [21].

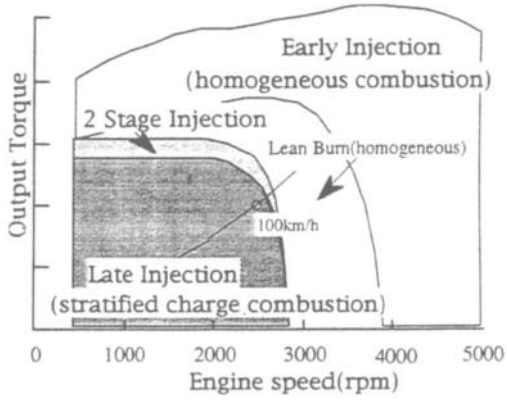

Fig. 62. Toyota GDI control map [43].

Mode transition control is achieved in the Mitsubishi GDI engine by the accurate control of the air flow rate using a conventional throttle valve that is controlled by the accelerator pedal, and by a bypass solenoid value that is electronically actuated using pulse-width modulation [50,51]. Fig. 64 schematically illustrates both the air and air–fuel ratio control during the transition from the stoichiometric operation of early injection to the lean operation of late injection. In order to minimize the torque fluctuation during the transition, the switching should be conducted under the conditions for which the generated torques of both modes at the same

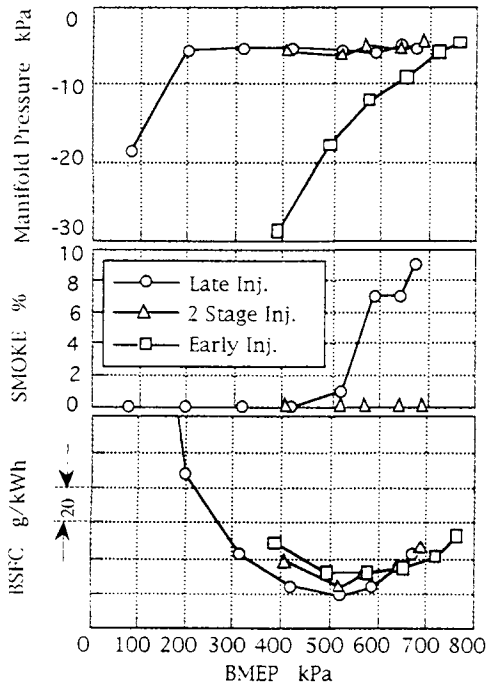

Fig. 63. Effect of the two-stage injection on BSFC and smoke emissions of the Toyota GDI engine during the transition [21].

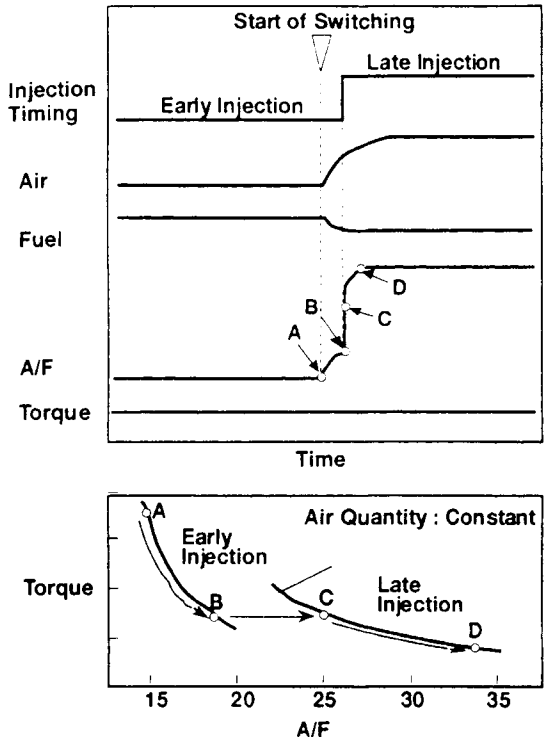

Fig. 64. Air and fuel management during mode-transition operation of the Mitsubishi GDI engine [50,51].

engine airflow rate are identical. As is shown, early injection at an air–fuel ratio of 18, and late injection at an overall air–fuel ratio of 25, generate the same torque at the same airflow while maintaining the injected fuel quantity. The combustion mode is then switched to late injection within one cycle. In the first cycle of the late injection mode, the injected fuel quantity is adjusted to achieve an air–fuel ratio of 25, which is enleaned further to an air–fuel ratio of 35 on subsequent cycles by reducing the injected fuel quantity and increasing the airflow simultaneously. As a consequence, engine operation is managed to minimize the torque differential at any transient conditions.

During the transition between modes, two air–fuel limits were observed in the Bosch GDI control strategy [200]. One applies to stratified operation with a low air–fuel ratio limit of approximately 22 to avoid soot formation. Another applies to homogeneous, lean operation due to combustion instabilities that are associated with air–fuel mixtures that are leaner than 19. A forbidden range of air–fuel ratios (19–22) was found during the transition. This was made possible by a fuel quantity increase that is invoked at the switch-over. The torque is reduced by retarding the spark timing to avoid a torque differential during switch-over. The sequence of the switch-over from homogeneous to stratified operation occurs in the reverse order of that from stratified to homogeneous operation.

Miyamoto et al. [201] and Hattori et al. [202] conducted an extensive study of the potential of two-stage injection. In this injection strategy the main fraction of the fuel is injected into the combustion chamber during the intake stroke in order to form a homogeneous, premixed, lean mixture, then a rich mixture is created near the spark plug by subsequently injecting the remaining fraction of the fuel just prior to the spark in order to provide stable ignition and faster combustion. The lean limit is extended with this technique while the fuel consumption and UBHC emissions attain the same level as that of homogeneous combustion.

Miyamoto et al. [201] evaluated the two-stage injection strategy using a single cylinder engine with a bore of 135 mm and a compression ratio of 9.6:1, which was equipped with a multi-hole nozzle. It was reported that stable combustion could be realized over a wide range of operation without detonation. Although the injection hardware utilized in this study is not representative of current production GDI systems, there are some interesting observations that should be considered. When compared to operation with stoichiometric, homogeneous combustion, significant improvements in fuel consumption and NO_x emissions were achieved. Optimized combinations of spark timing, secondary fuel injection timing, fuel split (between the primary and secondary injections), and the number of nozzle holes were found to be essential for improved ignition and combustion with this strategy. It was noted that both the NO_x and UBHC emissions can be reduced by retarding the ignition timing; however, the BSFC increased due to the reduced degree of constant volume combustion. Retarding the timing of the secondary fuel injection yields similar trends for NO_x and BSFC; however, the

UBHC emissions increase monotonically due to the decrease in the available mixing time. As the split fraction is increased by increasing the fuel quantity in the secondary injection, both UBHC emissions and BSFC are improved, but NO_x increases slightly. As the load is reduced the mixture formed by the first stage injection exhibits a high flame speed and shorter combustion duration, especially at higher levels of excess air. It was found that less volatile fuels and lower octane numbers could be used with this two-stage injection process, and efficient combustion without knock was verified even with a 50/50 blend of gasoline and diesel fuel.

Hattori et al. [202] also reported experiments on GDI engines using a two-stage-injection technique. A water-cooled, four-cylinder engine with a square-shape cavity in the piston, a bore of 102 mm, and a compression ratio of 12:1, was modified to accommodate a spark plug. A lean homogeneous mixture is formed at the end of the compression stroke as a consequence of the early primary injection. This avoids the formation of an ultra-lean mixture that could result in flame extinction, particularly at low engine speeds and light loads. The fuel from the later secondary injection creates a near-stoichiometric mixture near the spark gap, which improves the early development of the flame over a wide range of engine speeds and loads. The optimum fraction of fuel in the secondary injection has to be controlled carefully in order to enhance both the lean limit and the BSFC. This also requires a fuel injector that can accurately and reliably deliver very small quantities of fuel. If the fraction of fuel in the primary injection is too low, the main premixed homogeneous mixture becomes too lean, and the normal flame of the lean homogenous mixture is extinguished. It was found that a spark plug with an extended electrode provides a substantially extended lean limit for a wide range of secondary fuel injection timings.

A similar strategy, designated as two-stage mixing, was invoked by engineers at Mitsubishi to suppress autoignition and improve the GDI engine low-end torque [16,19]. As was the case in the references just discussed, fuel is injected twice during the entire mixture preparation process, with the first injection performed during the early stage of the intake stroke, and the second injection occurring late in the compression stroke. It was reported that this strategy is effective when the majority of the fuel is supplied by the second injection, with the first injection utilized only to create a mixture with an air–fuel ratio of from 30:1 to 80:1. It was reported that significant knock suppression was achieved at low engine speeds. It is theorized that the premixed mixture created by the first injection is too lean to achieve autoignition of the end gas, and that the stratified mixture created by the second injection does not have sufficient reaction time to autoignite. It is also theorized that the second injection may contribute to soot formation when the mixture is rich. According to Ando [17], however, soot emission was not observed when this strategy was utilized except at very low engine speeds, even when the mean air–fuel ratio is 12. It was reported that soot generated during the early stage of the combustion process was later oxidized completely, as depicted in Fig. 65. Further, it was claimed that the presence of soot was effective in extending the flame propagation limits to leaner mixtures. As a result, the low-end torque characteristics of the GDI engine were improved significantly, even when using a higher compression ratio of 12.5.

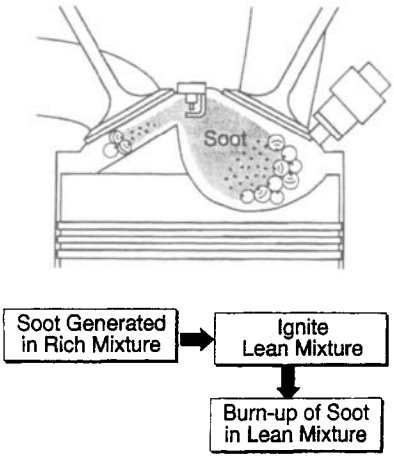

Fig. 65. Schematic of the soot formation and oxidation mechanisms in a stratified-charge mixture [17].

Yang et al. [48] reported a similar strategy to increase full-load torque output. By splitting the total amount of fuel into two separate pulses, both charge cooling and knock suppression can be achieved. It was reported that the timing of the second injection is not necessarily restricted to the latter stages of the compression stroke, but can occur over a wide timing range during the compression stroke. It was pointed out that charge stratification, if formed, may result in soot formation in the over-rich mixture. The combustion stability was reported to be insensitive to the timing of the secondary injection pulse when two-thirds of the fuel is injected in the first fuel phase. The highest IMEP was achieved when the secondary injection occurs at 60° BTDC. By comparison, if half or more of the fuel is delivered by the secondary injection, the start of the secondary injection should be no later than 150° BTDC in order to avoid unstable combustion. In order to improve the combustion robustness, a ratio of 2:1 between the primary and secondary injected fuel quantities was reported to be an optimal choice.

Engineers at Mitsubishi [17,50] also proposed another two-stage injection strategy, designated as two-stage combustion, in order to provide a quick warm-up to an under-floor, three-way catalyst, which is located downstream of a lean NO_x catalyst. With this strategy, the engine is operated lean in the late injection mode under cold-start conditions. A supplementary amount of fuel is injected during the later stage of the expansion stroke, which reacts to increase the exhaust gas temperature.

When the supplementary fuel is injected early in the expansion stroke, a luminous diffusion flame from liquid fuel droplets results. It was found that when the fuel is injected during the mid-portion of the expansion stroke, a slow pre-combustion reaction occurs and ignition is delayed. The later injection timing was selected, and the effect of this strategy on the exhaust gas temperature and the associated UBHC emissions is shown in Fig. 66. This two-stage combustion strategy is only applied for the first 20 s after the initiation of cranking, and this reduced the warm-up time to 100 s from the original 300 s. The expansion-stroke injection strategy did indeed yield a significant reduction in UBHC emissions.

In summary, current GDI combustion systems may be categorized using the following four operating classes. The degree of complexity of the GDI engine operating system progressively increases with the least complex system being the early-injection, homogeneous, stoichiometric GDI engine.

The major GDI operating classifications are

GDI operating class	Description of GDI operating system
1	Late injection: stratified, overall lean, no throttle, swirl/tumble control
2	Late injection: stratified, overall lean, some throttling
3	Early injection: homogeneous, lean
4	Early injection: homogeneous, stoichiometric

The step from a homogeneous GDI system to a stratified-charge system offers a significant fuel economy potential, but there is a consensus that stratified-charge operation is not obtainable without a significant increase in system complexity. The benefit–cost ratio of early injection, homogeneous GDI (Class 3 or 4) could, in some applications, be better than for full-option GDI (Class 1 or 2) due to the more complex hardware and the associated development time required.

The development of advanced GDI engines that meet future stringent emission requirements is likely to penetrate the market in two stages. First, prior to the emergence of a proven lean-NO_x aftertreatment system, the homogeneous-mode GDI (Classes 3 and 4) could be prevalent, with increased engine specific power at high load as a key design goal. These engines will be designed to achieve BSFC values that are slightly superior to current lean-burn engines. The exhaust emissions in the GDI class can be controlled by the combination of three-way catalyst and EGR. A marked reduction in UBHC emissions during the cold start, coupled with improved transient response, will be the major advantages over the conventional PFI engine.

The availability of both an efficient and durable lean-NO_x-catalyst and sufficiently low levels of sulfur in the gasoline supply will enable the second stage of GDI development, and engines incorporating ultra-lean stratified operation for load control will be developed and optimized [313,314]. These engines will most likely be designed to provide both the specific power of the homogeneous mode and a 20% increase in vehicle fuel economy [42].

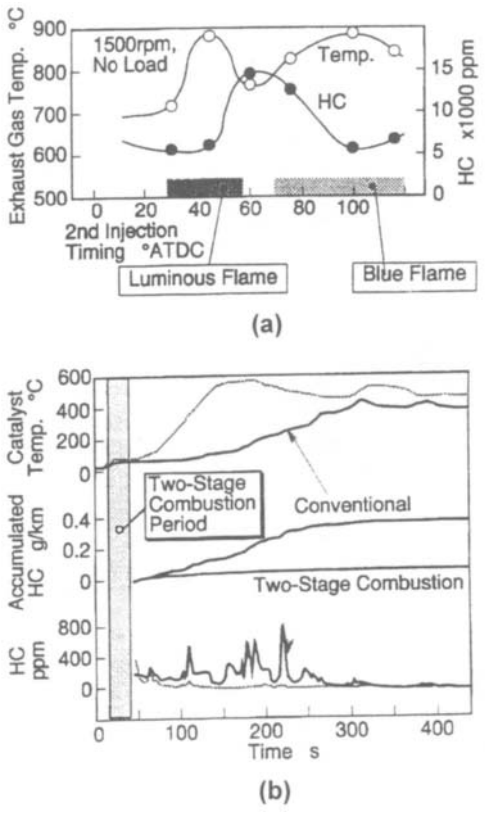

Fig. 66. Effect of the two-stage combustion strategy on catalyst light-off and UBHC emissions [17].

4.4. Combustion characteristics

The combustion characteristics of the GDI engine change significantly with the combustion control strategy that is used. Using flame luminosity analysis, Kume et al. [20] reported that combustion associated with early injection is characterized by flames that are typical of premixed lean or stoichiometric mixtures. The flame luminescence that is observed is attributed to OH and CH chemiluminescence, as well as to CO–O recombination emission. Luminescence at the longer wavelengths normally associated with soot radiation was not observed. For the case of late injection, it was found that the major component of the flame luminosity consists of continuous blackbody radiation emitted from soot particles formed inside the cylinder, which is typical of a stratified-charge combustion process. The soot radiation was found to decrease abruptly after sufficient air

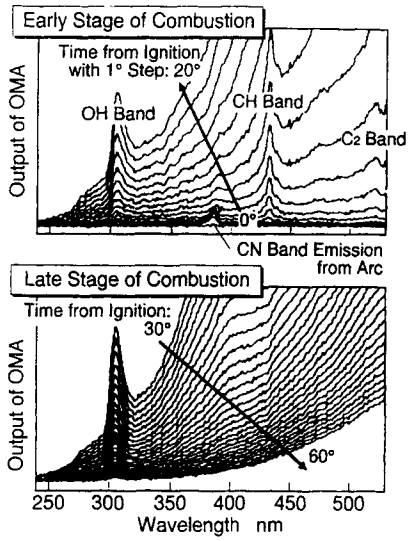

Fig. 67. Spectral characteristics of the flame radiation from the early and late stages of combustion [17].

has been entrained into the reaction zone. Fig. 67 shows the result of the spectral analysis of the flame radiation from both the early and late stages of combustion [17]. For heavy-load operation, soot may be generated for some injection timings as the result of the presence of a liquid film on the piston crown, which can occur for injection early in the intake stroke or for a fuel injector having a large spray droplet size. Another cause of soot generation is an insufficient time for fuel–air mixing, which can occur for high-load injection late in the intake stroke. A number of design parameters such as the piston crown geometry, spray cone angle and penetration, injection timing, and the in-cylinder air motion must be optimized to minimize soot formation.

When the air–fuel mixture is successfully stratified for an idle or low-load condition, the mixture surrounding the spark gap is designed to be slightly rich at the time of the spark. If this is achieved, the reaction rate will be high enough to sustain efficient and stable combustion [316,341]. For the PFI engine operating at the idle condition, the combustion rate is low, and the combustion stability is generally marginal, primarily because of a large amount of residual gas. For the case of the GDI engine at idle, the initial combustion rate was reported to be approximately the same as that for the full-load condition [203]. According to Jackson et al. [136,137], the GDI engine demonstrates a significant advantage in both the ignition delay and the burn duration as compared to a PFI engine of equivalent geometry. The initial flame kernel develops rapidly in the rich mixture region near the spark gap; however, the rate of flame propagation is reduced in the lean outer region of the stratified charge. The significantly reduced combustion rate near the end of the combustion process is one of the causes for the observed increase in UBHC emissions [193]. The overall high flame speed does allow the ignition timing to be retarded more for the GDI engine than for the conventional PFI engine, and the combustion rate and stability are enhanced rather than degraded [203].

The maximum brake torque (MBT) spark timing of stratified-charge GDI engines at part load is generally more advanced than that of the conventional PFI engine. Fraidl et al. [57] reported that the main part of the stratified GDI combustion occurs before TDC on compression for MBT timing, which is quite advanced. For the GDI engine operating in the homogeneous mode at full load, a heat release curve is obtained that is nearly identical to that from the PFI engine. A slightly reduced heat release rate may be observed from some GDI engines at full load, which is indicative of some charge inhomogeniety.

In general, the throttling losses of the PFI spark-ignition engine are relatively small for high-load operation. For this mode, the engine efficiency is determined primarily by the compression ratio and the specific combustion characteristics; however, increases in the compression ratio and advances in the ignition timing for best efficiency are limited by mixture autoignition, which generally occurs in the end gas region. Improvements in combustion-chamber geometry, in piston and charge cooling, and in residual gas control to modify the flame propagation at high load have proven to be effective means for knock reduction in both PFI and GDI engines. Modifications of the charge motion in order to obtain symmetric flame propagation is an effective way to improve the inherent knock resistance of the chamber [204]. In general, the best compromise among UBHC, NO_x, BSFC, and COV of IMEP can be obtained by a combustion process that offers a fast and stable initial phase, a moderate main combustion rate and a locally uniform and symmetric end of combustion to avoid flame quenching.

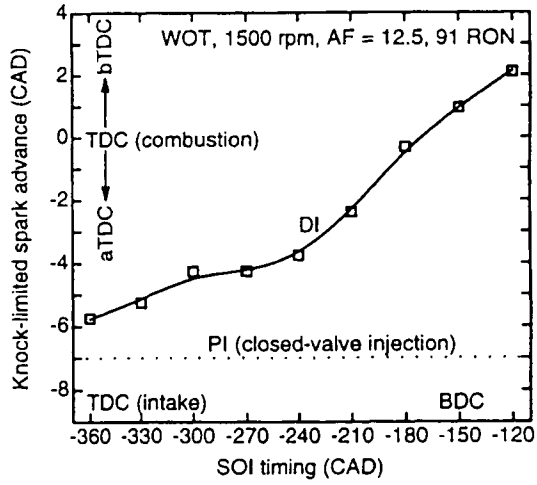

Fig. 68. Comparison of the knock-limited spark advance between GDI and PFI engines [40].

Anderson et al. [40] studied the effect of injection timing on the knock-limited spark advance in a GDI engine and compared the value to that obtained from a PFI engine. As shown in Fig. 68, the knock-limited spark advance continues to increase as the injection timing is retarded for the heavy-load condition. Retarding the injection timing not only reduces wall wetting by the fuel spray but also reduces charge heating by the walls. This results in a lower mixture temperature near TDC on compression and permits more advanced spark timing. However, retarding the injection timing does reduce the time available for mixing, which usually results in a higher cycle-to-cycle variation of IMEP.

It is necessary to carefully phase the ignition timing with the injection timing in order to achieve accurate control of mixture stratification. By using a locally rich mixture near the spark plug, while maintaining a constant overall lean air–fuel ratio, Arcoumanis et al. [205,274] reduced the COV of IMEP by more than 60% in a modified PFI engine. It was reported that 40% of the observed improvement can be attributed to the presence of a rich mixture around the spark gap, with the remaining 60% attributed to the enhancement of mixing due to the injection event.

Jackson et al. [145,173,195,196] reported that the combustion stability of a tumble-dominated, stratified-charge GDI engine can be improved significantly when the ignition is advanced even beyond the MBT timing. However, when ignition is advanced further, the combustion stability deteriorates very rapidly, which is attributed to insufficient time for evaporation and mixing. UBHC emissions were found to decrease with ignition advance while fuel economy initially improves before degrading. NO_x emissions are increased due to the relatively high local gas temperature. It was observed that a reduction in tumble ratio has the beneficial effect of shifting the combustion phasing for minimum UBHC closer to that for the minimum BSFC. With ignition timing set for minimum UBHC emissions, a BSFC improvement of 11% is attained at the same UBHC level; whereas, with BSFC-optimized ignition timing, a reduction in UBHC emissions of 34% is obtained at the same BSFC. One explanation is that the lower tumble ratio modifies the air–fuel ratio history at the spark plug, thereby producing optimum conditions for combustion at a more retarded timing. The reduction in NO_x at all combustion phasings also indicates that the lower tumble ratio has modified the local air–fuel ratio near the spark plug, resulting in a lower peak temperature during combustion. At high load, however, autoignition occurs when operating with a compression ratio higher than 12.0 for gasoline currently available in the field. It was noted that a complex optimization solution could be provided by using a variable compression ratio, with a higher compression ratio utilized at part load.

The combustion characteristics associated with early fuel injection under cold start conditions were investigated in detail by Shimotani et al. [182]. A homogeneous stoichiometric mixture was used for all of the cold start tests. The measured in-cylinder pressures and mass burning rates for injection timings of 30° ATDC on intake, and 110° ATDC on intake at a coolant temperature of 20° are shown in Fig. 69(a). For the early injection timing of 30° ATDC on intake, the heat release rate during the later stage of combustion is quite low due to the slow evaporation of liquid fuel from the piston crown. As a result, the UBHC emissions and BSFC are degraded. The effect of injection timing on the early part of combustion and on the 10–90% burn duration at a coolant temperature of 20°C is shown in Fig. 69(b). Early injection timing delays the initial combustion and extends the main combustion period due to the lean mixture resulting from the slow vaporization of liquid film on piston crown. Visualization of the spray impingement on the piston shows that for an injection timing of 30° ATDC on intake the spray impingement velocity is higher, and the impingement footprint is smaller, than for later timings. Due to the brief time available before spray impingement, the contribution of the in-cylinder airflow field to spray evaporation is limited, resulting in a substantial liquid film being formed on the piston crown. For a later injection timing, with the piston moving away from the injector more rapidly, the impingement velocity of the spray is reduced and the impingement footprint is larger. As a consequence, the fuel film thickness is reduced and the evaporation of fuel droplets in the ambient airflow field is enhanced due to the increased time available prior to impingement. All of these factors contribute directly to a reduction in the amount of fuel on the piston crown. Visualization of the associated combustion indicated that for the case of early injection (30° ATDC on intake), the entire chamber is initially filled with a blue flame, after which a yellow flame is observed at the center of the chamber. This yellow flame persists until the beginning of the exhaust stroke, and is attributed to pool burning of the film of liquid fuel on the piston surface. The presence of a yellow flame is quite limited for an injection timing of 110° ATDC on intake, and it occurs at the periphery of the chamber rather than at the center. It was noted that the yellow flame observed at the periphery of the chamber results from a lower film evaporation rate due to reduced air velocities in this region. If high-velocity air can be directed to the area of spray impingement, the wall film evaporation and fuel transport to the ignition area can be enhanced. Fig. 69(c) shows a comparison of the time histories of the exhaust temperature for GDI and PFI engines during cold start using a coolant temperature of 20°C. The improved A/F control capability of the GDI system results in a more rapid increase in the GDI exhaust temperature than is obtained for the PFI engine.

Matsushita et al. [43] and Harada et al. [21] investigated the combustion characteristics of the Toyota GDI engine for lean, stratified mixtures. Fig. 70 compares the combustion characteristics of the Toyota GDI and the baseline PFI engines. The GDI engine in this study operates at an overall air–fuel ratio of 27 and the PFI operates at 14.7. It was reported that the initial GDI burning rate at light load is

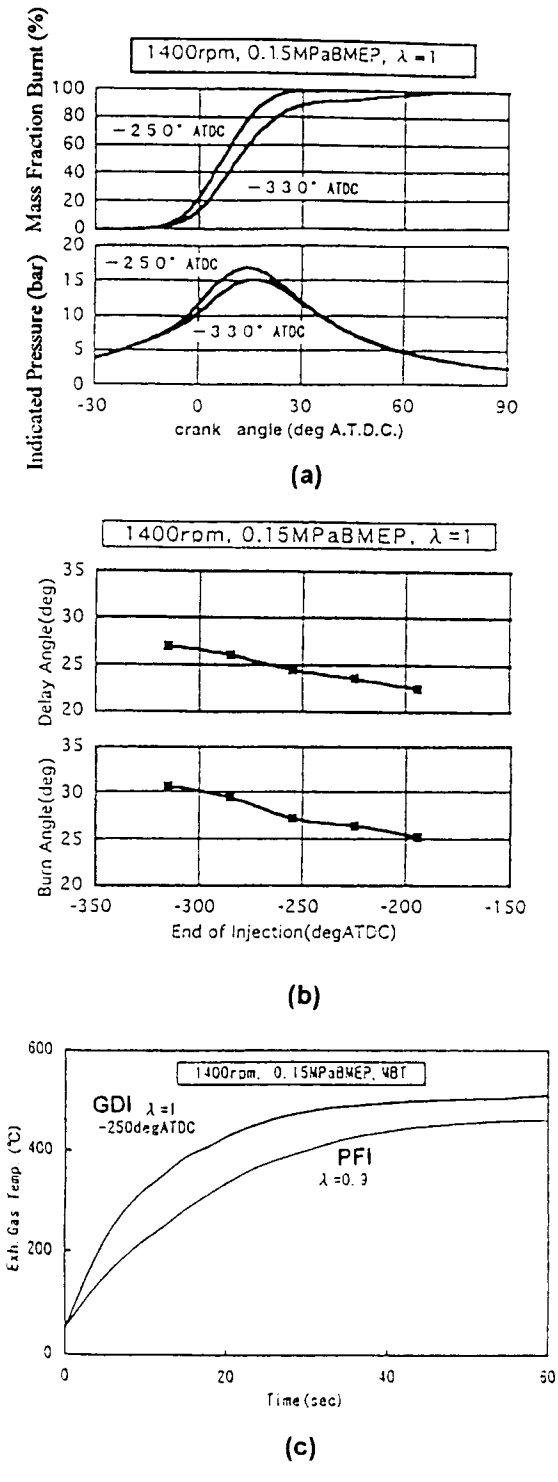

Fig. 69. Effect of injection timing on combustion characteristics [182]: (a) indicated pressure and mass fraction burned; (b) ignition delay angle and combustion duration; and (c) comparison of GDI and PFI exhaust gas temperature histories for a cold-start.

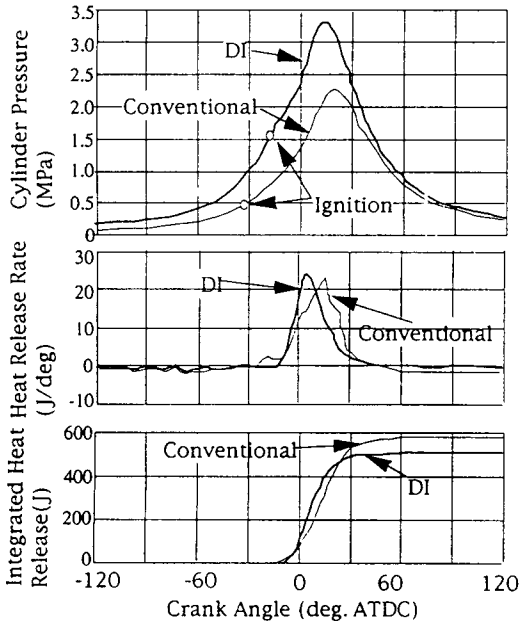

Fig. 70. Comparison of the combustion characteristics of the Toyota GDI and the baseline PFI engines [21].

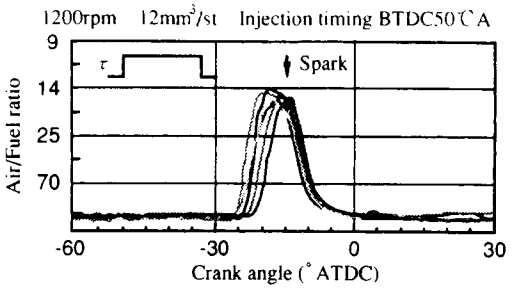

Fig. 71. Time histories of the air–fuel ratio near the spark plug gap of the Toyota GDI engine for an injection timing of 50° BTDC on compression [261].

higher, even though the GDI engine is operated on a mixture that is overall twice as lean as that of the PFI engine. Both the in-cylinder pressure at the beginning of the compression stroke and peak compression pressure are higher as a result of the unthrottled, stratified operation. High-speed photographs of the combustion event indicate that a luminous yellow flame surrounded by a blue flame is formed initially. The blue flame predominates later in the combustion event, but the yellow flame is still visible. Kano et al. [206,261] and Kawamura et al. [321] measured the air–fuel ratio around the spark plug using a spark-plug-type, fast FID probe. Fig. 71 shows the measured time histories of the air–fuel ratio over five cycles. It is interesting to note that the magnitude of the peak air–fuel ratio is quite stable over the measured cycles. However, a large cycle-to-cycle variation of the crank angle position where the peak air–fuel ratio occurs was observed for operation in the stratified charge mode for the Toyota GDI D-4 engine. Visualization of the spray plume also confirmed cycle-to-cycle variations in position and geometry, which also contributes to combustion variation. Kuwahara et al. [207] conducted a detailed study on mixture preparation and flame propagation of the Mitsubishi GDI engine operating in the stratified-charge mode. It was reported that 40° BTDC on compression is the most retarded injection timing that can be achieved if the ignition timing is set at 15° BTDC on compression. The stratified charge in this engine is achieved by fuel reflection after impingement on the piston bowl surface. No significant difference in the combustion duration was observed between optimized injection timing and the earliest possible injection timing. But marked cycle-to-cycle variation was observed for very advanced injection timing due to the over-mixing and dispersion of the fuel spray plume. The flame was found to propagate faster in a stratified charge than in a homogeneous charge. No significant difference in the flame propagation speed was observed among different injection timings. An airflow field that can help confine the fuel spray plume inside the piston cavity was found to be effective in achieving good charge stratification. The use of a luminous flame as an ignition source to burn the lean mixture at the periphery of the chamber was considered promising in the oxidation of UBHCs in the flame-quenching zone.

Jackson et al. [145,173,195,196] investigated the effect of EGR on the combustion characteristics. It was claimed that the rapid flame development associated with stratified combustion, and the higher O_2 and low CO_2 levels in the exhaust gas are the reasons for the enhanced EGR tolerance of the GDI engine. It was reported that the cyclic variability of combustion becomes excessive at an EGR rate of 20% for the baseline PFI engine, whereas excellent stability is possible for stratified operation. The burn duration is significantly increased for the PFI engine as the EGR rate is increased. At an EGR rate of 40%, the GDI engine exhibits improvements of 3% in BSFC, 81% in NO_x and 35% in UBHC emissions as compared to operation without EGR. The improvement in UBHC is theorized to be the result of a richer mixture core, resulting in less bulk quenching. The similar PFI combustion system in the comparative test configuration shows poor EGR tolerance, with an associated increase in fuel consumption. As expected, the GDI engine requires more EGR for the same NO_x reduction when compared to the PFI configuration. Another favorable characteristic of the GDI engine is the improved tolerance to spark retard at higher EGR rates. This is principally due to a lengthening of the early part of combustion, namely the period from the time of ignition to the time at which 10% of the mass is burned, as the burn period from 10 to 90% burned was found to be relatively insensitive to EGR rate. The result for the GDI engine without any EGR shows an

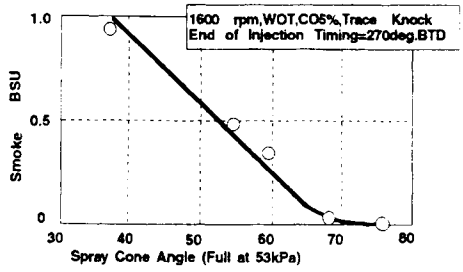

Fig. 72. Effect of the spray cone angle on WOT smoke emissions at an engine speed of 1600 rpm [210].

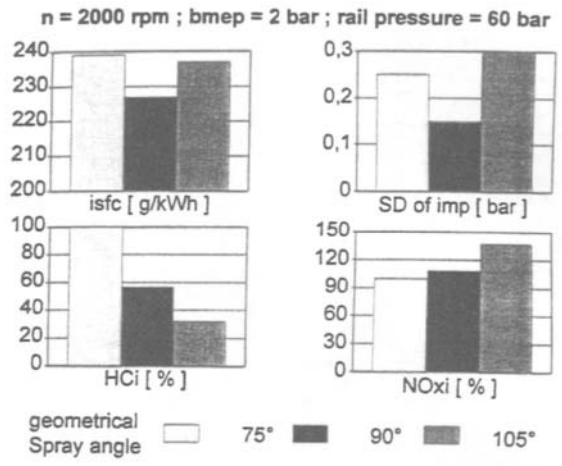

Fig. 73. Effect of the spray cone angle on engine performance and exhaust emissions [193].

early combustion phasing with a higher peak cylinder pressure. The introduction of 40% EGR delays combustion, and improves the fuel economy while substantially reducing the peak cylinder pressure. The research GDI engine with a top-entry/bowl-in-piston configuration was run at MBT with 40% EGR, and it was found that the point of 50% mass burned always occurs at about 15° ATDC on compression rather than at the typical 7° ATDC on compression for the conventional open-chamber PFI engine. At this condition the burn rates are similar for both the PFI and the GDI engines, although the GDI engine exhibits a mass-burn profile having a rapid initial rate and a slower rate near the end of combustion that is typical of stratified-charge combustion.

Ghandhi and Bracco [208] obtained measurements of the planar instantaneous fuel concentration near the spark gap just prior to ignition in a GDI engine operating at a light load, highly stratified condition. The distribution of the average equivalence ratio in a circle of 1.9 mm diameter centered on the spark plug showed that a large fraction of the cycles had an equivalence ratio below the lean limit, yet acceptable combustion was achieved in those cycles. In addition, a weak correlation was found between the local average equivalence ratio near the spark plug and the time required to achieve a 100 kPa pressure rise above the motoring pressure. The cause of this behavior is attributed to mixture motion during the spark discharge, which continually convects fresh mixture through the spark gap during breakdown.

Plackmann et al. [209] and Ghandhi [305] studied the effect of mixture stratification on GDI combustion rates in a constant-volume bomb. It was found that the highest combustion rate for an overall lean mixture is obtained when all of the fuel is contained in a stoichiometric mixture around the spark plug. Also it was observed that the total energy release of a stratified mixture with a richer mixture near the spark plug is limited by the mixing of the rich products with the available oxidizer before the mixture cools below the temperature required for oxidation. This indicates that, for a stratified GDI engine, the ideal mixture distribution is a homogeneous, stoichiometric mixture near the spark plug, with enhanced mixing during the expansion stroke being important to promote the oxidation of any rich combustion product.

Many investigations have verified that the spray cone angle is an important spray parameter that affects GDI combustion and emissions. Iriya et al. [210] observed a strong correlation of smoke emissions with the fuel film on the piston crown that is directly related to the spray cone angle in the Nissan GDI engine, and reported that larger spray cone angles can reduce the smoke emission significantly using the same fuel injection timing, as shown in Fig. 72. When the spray cone angle exceeds 70°, the effect becomes less significant. Karl et al. [193] conducted parametric tests of the effect of spray cone angle on the emissions of the Mercedes-Benz GDI engine. The experimental results, as shown in Fig. 73, indicate that the optimum spray cone for this system configuration is 90° for minimum ISFC, 105° for minimum UBHC emissions, and 75° for minimum NO_x emissions. This illustrates the inherent difficulty of spray-cone optimizations. Fig. 74 shows the effect of spray cone angle on the engine combustion stability, smoke emissions and engine torque for a GDI combustion system with a side-mounted injector. An optimal spray cone angle exists for a stable combustion process that produces the highest engine torque with minimum smoke emissions [101,211,342,350].

Finally, it should be noted that the GDI engine has an enhanced knock resistance when compared to the conventional PFI engine, with in-cylinder charge cooling being one of the main contributors. Retarding the fuel injection timing can further improve the engine knock resistance due to a slight stratification of the charge. However, such timings may not be desirable, as charge cooling that occurs after intake valve closure does not improve the volumetric efficiency, and charge stratification reduces the air utilization. The GDI engine

does not exhibit the transient knock that is frequently observed in the PFI engine during the first several cycles following the start of vehicle acceleration. Fig. 75 shows a comparison of the measured knock intensity during the acceleration of GDI and PFI engines [50,51]. Transient knock is generally caused by the selective transport of a lower boiling-point gasoline component that has a lower octane number. In the case of GDI engines, all of the gasoline components are transported into the cylinder and, as a result, transient knock is suppressed. This could permit the ignition timing to be advanced up to 10 s at the start of acceleration.

4.5. Injector deposit issues

Deposit formation is a significant concern with nearly all injector designs for GDI application, and should be accorded sufficient time and resources in any GDI development program. To neglect this important issue is to lengthen development time and decrease the required service interval in the field. The operating environment of the fuel injector is harsher for in-cylinder injection than for port injection, and the formation of deposits on the injector tip can be much more rapid than are experienced with PFI systems. Although the operating environment of diesel injectors is even more extreme, deposits tend to form much more gradually in the holes of diesel injection nozzles than on GDI injector tips. One important factor is the fuel, but another major influence is the 50–140 MPa injection pressure level. The corresponding pressure of 4–13 MPa in the GDI fuel system is not sufficient to mechanically affect the continued deposition of carbonaceous material on the injector tip. Thus, the design of the injector tip for inherent resistance to deposit formation is particularly critical for GDI applications. There are two general types of deposits; these include deposits generated from the soot and lubricating oil during the normal engine operation and those generated from the olefin or aromatic ingredient of gasoline during cycles of run and hot-soak.

The effects of injector deposits are manifested in two distinct areas. The first is a degradation in the spray quality delivered by the injector, and the second is a reduction in the static flow capacity of the injector, with less fuel mass per injection being delivered at the same fuel pulse width. In the case of direct cylinder injection, the temperatures and pressures encountered within the injector tip may be suitable for polymerization reactions to occur within gasoline. This leads to the formation of a waxy residue in the passages within the injector, which can change the flow calibration. If either the spray or the injector flow characteristics are altered, then the stratification process that has been carefully developed will be affected. It may be expected that any deviation from the optimized operating condition will have a negative impact on emissions compliance and driveability [173]. For most GDI injectors, the early stages of deposit formation do not result in significant flow reduction, but *can* result in substantial changes in spray skew, cone angle and spray symmetry, and in some changes in droplet-size distribution. The spray geometry, particularly the symmetry, is generally perturbed long before the cumulative deposit blockage reduces the flow by even 8% from the clean condition. As the operation of the GDI engine is much more sensitive to spray parameter variations than the PFI engine, the GDI engine, in general, exhibits a much greater sensitivity to low levels of deposits. For GDI engine designs that have a critical positioning of the spark gap relative to the spray periphery for light-load, stratified-charge operation, shifts in the spray geometry may be expected to result in a significant degradation of combustion in areas of the operating map. Combustion systems using controlled vaporization from fuel-impact surfaces, such as that in the Mitsubishi GDI engine, would be expected to exhibit less sensitivity to changes in spray characteristics, and thus be less sensitive to injector deposit formation. It should be emphasized that flow reductions due to deposits do not necessarily occur uniformly along a bank of cylinders, thus one effect of deposits is to cause cylinder-to-cylinder variations in the air–fuel ratio. All cylinders on the bank will receive the same fuel pulse width command in most control systems, but those injectors with more deposits will inject less fuel.

In comparison with the fuel spray from a clean injector, the spray from the injector with significant external deposits can exhibit a distorted, nonsymmetric spray envelope. The phase-Doppler data for this distorted spray shows that the distribution of droplet sizes (the droplet-size distribution curve) is affected very little, whereas the droplet velocity distribution is significantly changed. For one GDI injector with deposits the flow rate was found to be reduced 8% from that of the clean injector. However, the atomization level of the injector was not significantly degraded by deposit formation. The velocity distribution and spray shape were both significantly affected, with the spray cross-section changed from near circular to an elongated ellipse.

The observed deposits on the critical tip surfaces of GDI injectors generally fall into two categories. One is the thin, brittle-coating type that contains sulfur compounds, and the other is the softer carbonaceous type. The latter forms more rapidly, and is more easily removed with common solvents and cleaners. Deposits can form internally, externally, or in both locations, with internal deposits at or near the lapped seat of the needle or pintle being the most undesirable. The external deposits may form on the downstream face of an isolating director plate, or on the downstream face of the pintle. Internal deposits near the minimum metering area of the fuel flow path or in the swirl-channel exit area cause fuel flow rate reductions, whereas external deposits generally result in only a degradation in the spray geometry. The rate at which deposits form on the tip surfaces of a GDI injector depends upon both the inherent resistance of the injector design to deposit formation and the specific operating configuration in the combustion chamber. As with a port

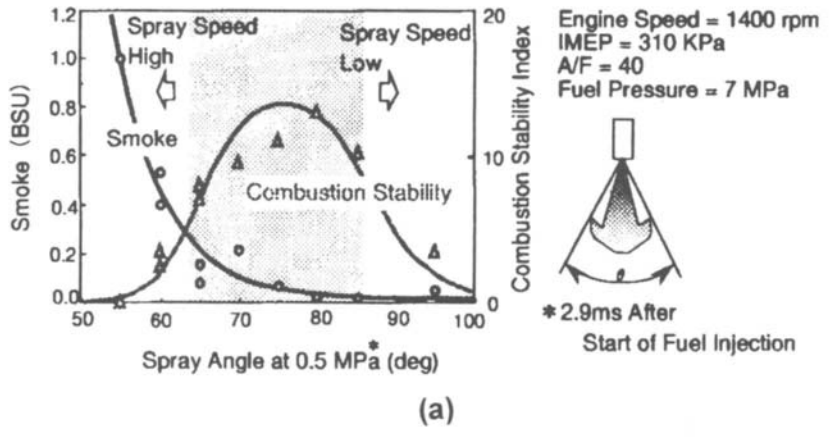

(a)

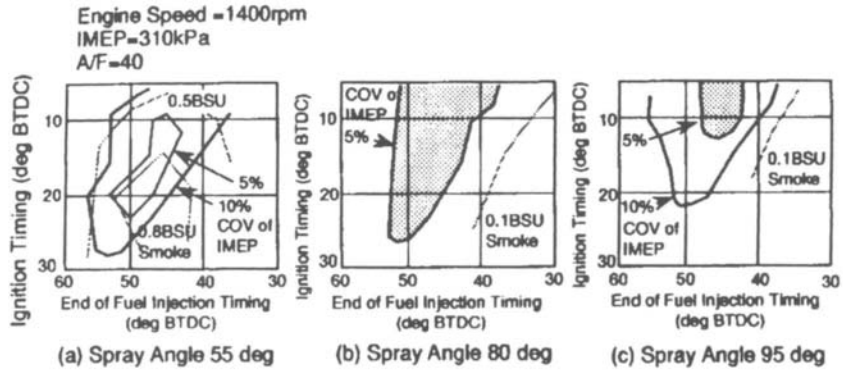

(b)

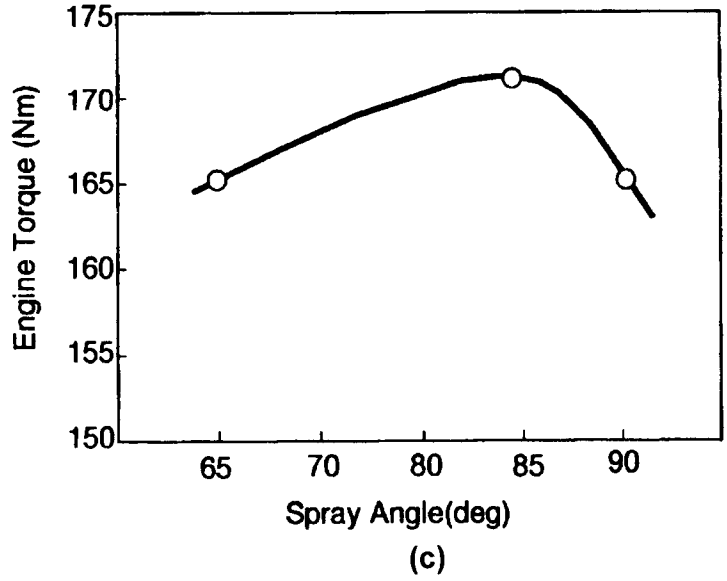

(c)

Fig. 74. Effect of the spray cone angle on combustion stability, engine performance and exhaust emissions [101].

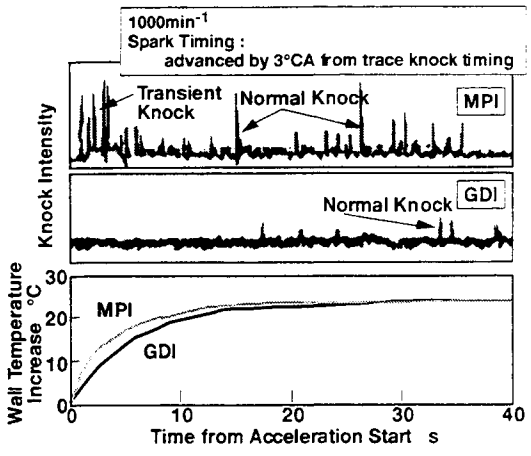

Fig. 75. Knock tendency of the Mitsubishi GDI engine during acceleration [50,51].

fuel injector, the inherent resistance of a GDI injector to deposit formation would ideally be determined by a standardized bench test using either an oven test or a dynamometer test in conjunction with a standard fuel, test configuration and test conditions. The lower the level of deposits that are formed in such a standard test, the higher the inherent resistance of the particular injector design. Examples of design parameters that would affect the inherent deposit resistance of an injector include a director plate for isolating the needle seat from direct contact with combustion gases, a more heat-conductive path from the tip to the injector threads or mounting boss, an increased fuel volume extending closer to the needle seat and special plating for the tip surfaces. Tip coatings were found to be quite effective in injector coking reduction, but this alone may not be sufficient to prevent the problem. Unfortunately, no proven, standardized test for deposit resistance has yet been adopted for GDI injectors, which is a situation that will have to be quickly resolved if rapid progress in direct-injection gasoline engines is to continue.

The standard deposit tests for pintle-type and director-plate-type port fuel injectors are discussed by Caracciolo and Stebar [212] and by Harrington et al. [213]. These tests were developed over a number of years, and were proven to correlate with field data from PFI engines; however, it is considered unlikely that the standard PFI tests can be effectively utilized for GDI injectors. It is well established that the hot soak time and tip temperature history are of critical importance for PFI deposit formation, and that deposit formation rates are very low for continuous operation. The initial indications for GDI applications, however, are that deposits *do* form under continuous operation, thus indicating that the formation mechanisms may differ from that of the PFI injector. The tip temperature is generally considered to be an important parameter for both the PFI and GDI injector, but the contribution of the temperature window and its cycle history is not known for

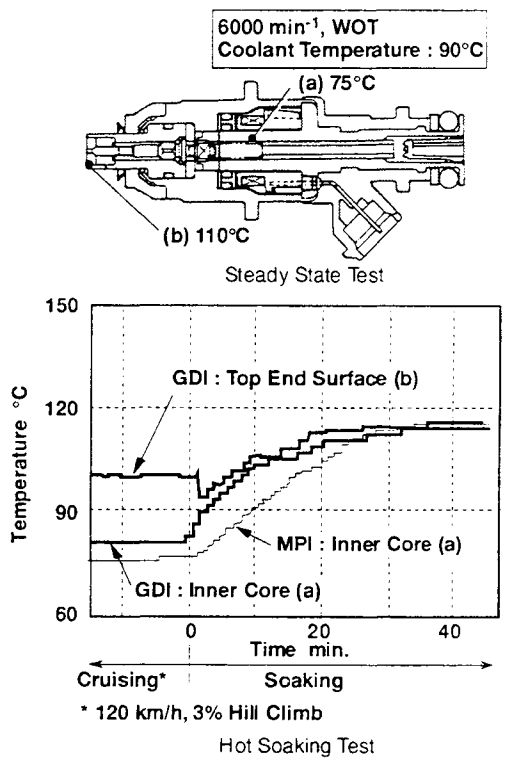

Fig. 76. Time history of the injector-tip temperature for the Mitsubishi GDI injector [50].

GDI applications. The role of the hot soak interval is not known in the current GDI literature, making this an important research topic. Dynamometer tests with on–off cycles can certainly be used to generate deposits, but extensive testing will be required to prove that a particular test correlates with GDI fleet data. Without an accepted industry test, the inherent resistance of a particular GDI design can only be evaluated by an ad hoc test within each company.

Knowledge of the inherent resistance of a GDI injector is necessary, but not sufficient, for interpreting the observed rate of deposit formation in a particular application. The inherent resistance or robustness of a specific injector design to deposit formation may be either enhanced or degraded by the configuration of the injector in the combustion chamber, and by the specific fuel that is being used. The tip temperature will be affected by the protrusion of the tip into the cylinder, the conductive path from the injector mounting boss to the coolant passage, and by the in-cylinder air velocity history at the tip location. It is recommended that the tip temperature be considered as an important variable, and that it be measured and logged during any development program. Micrographs from a scanning electron microscope should also be obtained for the orifice area of the injector tip during engine down periods.

The centrally mounted location for the injector is known to be subject to a higher thermal loading than is experienced

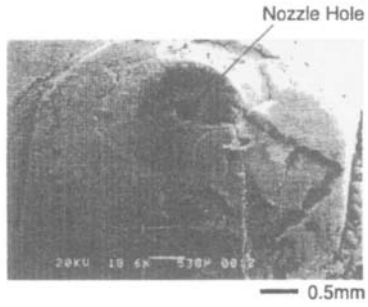

Fig. 77. Photograph of the appearance of a GDI injector with deposits after 30 h of engine operation [214].

at a location under the intake port. GDI combustion systems such as those of Mercedes-Benz, Isuzu and Ford that use a centrally mounted injector would be expected to yield 10–15°C higher injector tip temperatures than would be obtained with the Mitsubishi, Nissan, or Toyota system, in which the injector is located far from the exhaust valves and derive additional tip cooling from the intake air. Jackson et al. [195] reported that the upper limit for tip temperature of current GDI injectors is in the range of 150–200°C. Two-dimensional finite element analysis (FEA) and analytical calculations showed that the higher flame heat fluxes occur at the center of the combustion chamber. For a central injector the best location for minimum tip temperature is to be as close as possible to the intake valve seats. Fig. 76 shows the injector surface temperature as measured in the Mitsubishi GDI engine during the continuous high-speed full-load operation and a subsequent hot soak period [50]. It was reported that the injector tip temperature of the Mitsubishi GDI engine is not significantly different from that of the PFI injector. It was also claimed that no deposit problems were encountered with the tip temperature history shown in Fig. 76 during the durability test because the soot, lubricating oil or the deposit are washed away by the high-pressure gasoline jet. Some deposit formation has been noted for combustion systems that use a centrally mounted injector, where full-load tip temperatures of more than 150°C may be achieved. Engineers at Toyota [41] reported that the early injector deposit problem of the Toyota D-4 engine was alleviated by maintaining the injector tip temperature always below 150°C, and using a special organic material coating on the injector tip.

Kinoshita et al. [214] investigated the injector deposit formation mechanism using a Toyota D-4 engine. The injector deposit was classified into: soot deposited on the nozzle and needle surface; and fuel polymerized by thermal decomposition to form a gum-type deposit inside the nozzle. The outward appearance of an injector that contains significant deposits is shown in Fig. 77. An engine dynamometer test showed that the deposit effects were first evident after 2 h and that the flow rate continued to decrease during the first 8 h, after which no significant further decrease in the flow rate was observed. Fig. 78 shows a comparison of the nozzle

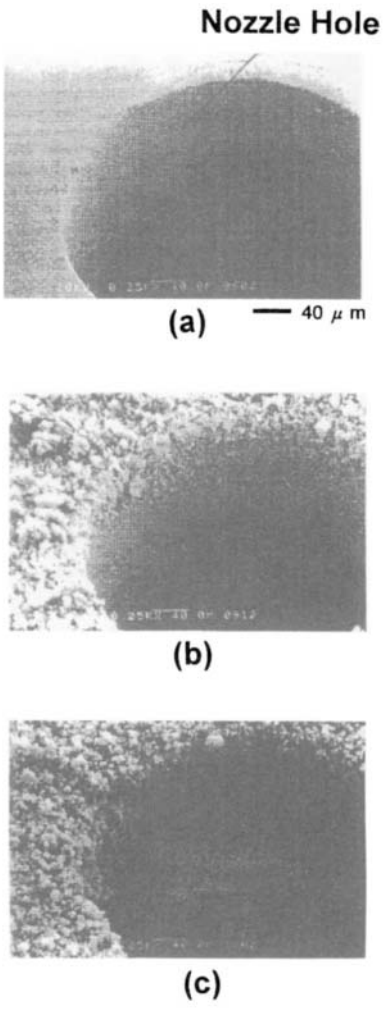

Fig. 78. Photographs of a GDI injector nozzle for different dynamometer test hours [214]: (a) new injector; (b) 4 h of dynamometer testing; and (c) 8 h of dynamometer testing.

hole appearance before and after the test. It was found that deposits were initially formed at the nozzle exit and progressed into the internal surfaces of the nozzle. The internal injector deposit occurred at the position where fuel resides after the end of each injection. Both the nozzle temperature and fuel distillation characteristics were found to significantly dominate the deposit buildup. Fig. 79 shows the effect of nozzle tip temperature on the injector flow rate reduction for a range of fuel types. As shown in Fig. 79(a), except for fuel E, all the other blended fuels have the same $T90$, which is the distillation temperature at which 90% of the fuel is vaporized. When comparing the blended fuels A and D in Fig. 79(b), it is evident that the flow rate is diminished significantly as the nozzle temperature exceeds $T90$. Even though the blended fuels A and E were tested at the same injector tip temperature, the flow rate reduction with fuel E is much less than that of fuel A, due to its high $T90$

Fuel Pressure	6 MPa
Injection Timing	180°BTDC
Spark Timing	25°BTDC
Engine Speed	1000 rpm

(a)

Test Fuels	Nozzle Tip Temperature (°C)	Air-Fuel Ratio	Smoke (B.S.U.)	T90 (°C)
A	165	12	0	150
B	100	12	0	150
C	154	10	1	150
D	155	15	0	150
E	165	12	0	168

(b)

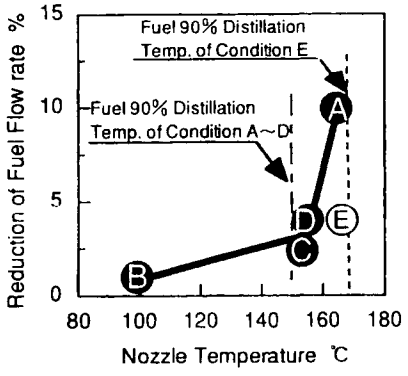

(c)

Fig. 79. Effects of the nozzle-tip temperature and fuel T90 point on injector deposit formation [214]: (a) engine operating conditions; (b) engine dynamometer testing conditions; and (c) effect of the nozzle-tip temperature on injector flow rate reduction.

point. A schematic explaining the mechanism of the injector deposit formation is illustrated in Fig. 80. When the injector tip is subjected to elevated temperatures, thermal decomposition of the fuel may occur inside the nozzle, where deposit precursors are formed. When the nozzle tip temperature is lower than T90, most of the fuel will stay as liquid even though some of the fuel may evaporate before the next injection event occurs. The continued presence of liquid fuel insures that the deposit precursors will be easily washed away during the next injection event. However, when the nozzle tip temperature exceeds the T90 of the tested fuel, most of the fuel will vaporize after the end of fuel injection. As a consequence, the deposit precursors are distributed on, and may attach to, the nozzle surface. This makes it more difficult to wash away all the deposit precursors during the next injection event. Eventually deposits may accumulate inside the nozzle. The theory suggests that it is important to retain some of the liquid fuel inside the nozzle between the injection events in order to prevent deposit buildup. Based upon this investigation, it was found that maintaining the injector tip temperature below the T90 point of the fuel being utilized is a critical factor in minimizing the formation and accumulation of deposits.

Mao [215] studied the carbon formation process inside a tube in order to understand the deposit formation process inside a gas turbine fuel injector. Some of the findings are also useful for understanding the deposit formation process in a GDI injector. It was found that the wall temperature appears to be the most significant parameter in determining the carbon deposit rate, with the fuel flow rate ranked second, and the fuel inlet temperature ranked third in importance. It was noted that the variation of deposit rate depends on whether the test apparatus provides a constant heat flux or a constant wall temperature in the test tube. It was found that the deposition rate remained approximately constant for wall temperatures below certain threshold values. As the wall temperature exceeded this value, the deposit rate increased sharply with increasing wall temperature. This suggests that the controlling mechanism for deposit formation changed, depending on the wall temperature. This agrees well with the investigation of injector deposit formation using the Toyota GDI engine [214]. It was also found that the deposit rate exhibits a maximum as a function of fuel flow velocity. The fuel inlet temperature was found to be not as significant as the wall temperature, but it had a noticeable effect on deposit rates when wall temperatures were high. Experimental results indicated that, initially, the deposit rate decreased with increasing fuel temperature. After reaching a minimum value, the rate of deposition begins to increase with a further increase in fuel temperature.

It is important to note that the interior wall material, the surface finish and surface coating all exhibit a significant influence on deposit formation. A fine micro-finish of the surface was found to significantly reduce the deposit rate, which, however, requires complex and time-consuming manufacturing operations. Surface coating was found to be able to delay the onset of deposition. But once a deposit layer is formed, the coated and uncoated surfaces exhibit very little difference in carbon deposition. It was also reported that the fuel sulfur content plays an important role during the initial process of deposit formation. The concentration of sulfur was relatively small in the case of heavy deposits when compared with those cases with moderate or small carbon deposits. It was speculated that the interfacial tension between the fuel deposit and the solid surface might be a key factor. Much remains to be learned with regard to the surface chemistry of GDI deposit precursors and deposit formation.

The following items represent important considerations in minimizing the formation of GDI injector deposits:

- injector tip temperature (maintained at less than 145°C);
- injector protrusion distance into chamber;
- heat path from injector body to engine coolant passages;
- air velocity variation at the injector tip during an engine cycle;

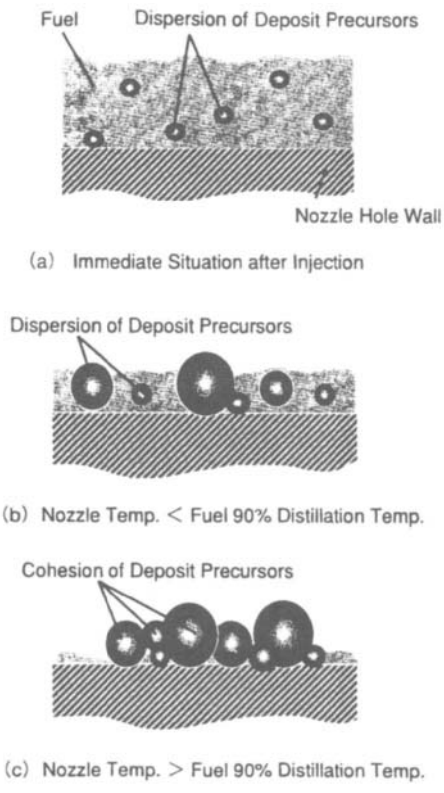

Fig. 80. Mechanism of injector deposit formation [214].

- proximity of bulk fuel inside injector to injector tip area;
- gasoline additives to inhibit cumulative deposit formation;
- special coating or plating of tip surfaces;
- internal and external surface finish of the nozzle tip;
- operating cycle, including hot-soak intervals (to be verified by future research).

The discussion above has dealt mainly with preventing or minimizing the formation of deposits, but there is another philosophy that can be invoked in parallel, although only by injector manufacturers. An injector can be designed with the important goal of minimizing the influence of deposits on the resulting flow rate and spray. This is known as an inherent tolerance or robustness to the presence of injector deposits. It is desirable, of course, to reduce the basic rate of deposition on the injector during the operation of the GDI engine. But, bearing in mind the inevitability of some deposition occurring with time, it is also desirable to have an injector flow-path design that exhibits a good tolerance to any deposits that *do* form. For example, 100 μg of deposits may form in 100 h of operation on two different injector designs, which is the same average rate of deposition. However, one injector design may exhibit a 3% flow reduction for this weight of deposits, while the flow in the second is reduced by only 1%. In this regard, some injector designs using swirl have proven to be quite sensitive to small amounts of deposits, particularly in terms of spray-symmetry degradation.

Finally, it is fair to note that a reasonable portion of the GDI deposit problem results from the lack of proven and effective GDI anti-deposit additives in the fuel supply [337]. The fuel qualities are, of course, different in Europe, Japan, and North America, and the gasoline sulfur content in North America may contribute to differing levels of deposit problems in those markets. The additives that are currently in the gasoline supply in North America were developed and improved mainly over the time period from 1984 to 1993 to minimize the rates of port-deposit and intake-valve-deposit formation. In the early development of PFI systems, injector deposits were a very significant problem that had to be alleviated [38,212], and this will have to be done for GDI systems [216,217]. The dilemma is that with no GDI vehicle currently in production in North America, there is no strong incentive to develop and blend new fuel additives for this application. Even if such GDI additives were proven and available for reducing GDI injector deposits, it will have to be carefully verified that adding them to the North American fuel supply would not adversely affect the formation of deposits in the 100 million PFI vehicles now in operation.

5. Fuel economy and emissions

5.1. Fuel economy potential

A current strategic objective for the automotive application of the four-stroke, gasoline engine is a substantial improvement in fuel consumption while meeting the required levels of pollutant emissions and engine durability. The improvement of passenger car fuel economy represents a very important goal that will determine the future use of SI engines instead of the small, high-speed, diesel engines [45,310,332,344–346,350,351,363]. The thermal efficiency of the GDI engine can be enhanced by increasing the compression ratio, or by using a lean mixture, thereby reducing the throttling losses and wall heat losses. As outlined conceptually by Karl et al. [193], the GDI engine using charge stratification offers the potential for reducing the part-loaded fuel consumption by 20–25% when the gas cycle, heat transfer and geometric configuration are optimized. Fig. 81(a) shows a computed balance of energy at 2000 rpm and 0.2 MPa BMEP. In this calculation the engine output and friction losses are maintained constant as the equivalence ratio is varied. In this study, the engine is operated in the homogeneous mixture mode at equivalence ratios of $\lambda = 1.0$–1.3, and in the stratified-charge mode at $\lambda =$ 1.6–3.4 with decreasing amounts of throttling. It is reported that the exhaust energy and the wall heat transfer are reduced by 10.8 and 12.5%, respectively, even though the air mass is increased. As a result, the predicted improvement in fuel consumption is 23%. This considerable increase in

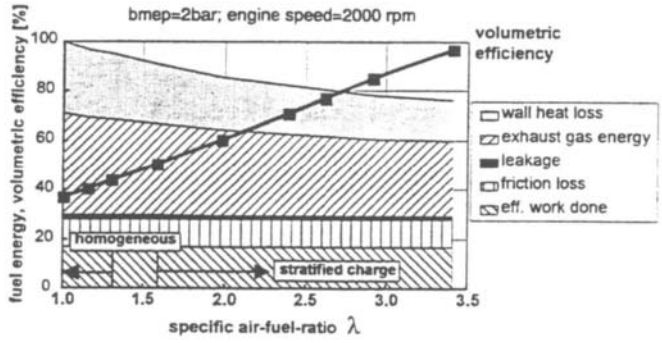

	Exhaust gas energy	Wall heat total	Wall heat gas exchange phase	Wall heat high pressure phase
λ = 1	Basis	Basis	Basis	Basis
λ = 1.3	-6%	-8%	-19%	-4%
λ = 3.4	-26%	-42%	-92%	-23%

	High pressure work	Gas exchange work	Total efficiency gain
λ = 1	Basis	Basis	Basis
λ = 1.3	-6%	-30%	5%
λ = 3.4	-20%	-95%	23%

(b)

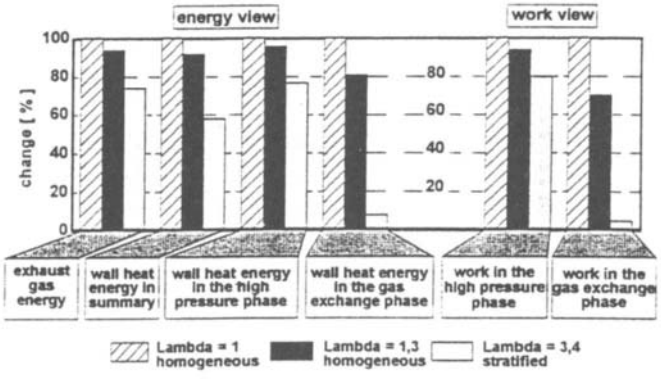

Fig. 81. Estimation of the energy balance for the GDI system under various degrees of charge stratification at 2000 rpm and 0.2 MPa BMEP [193]: (a) analyzed energy balance; (b) change of individual energies; and (c) change of individual energies.

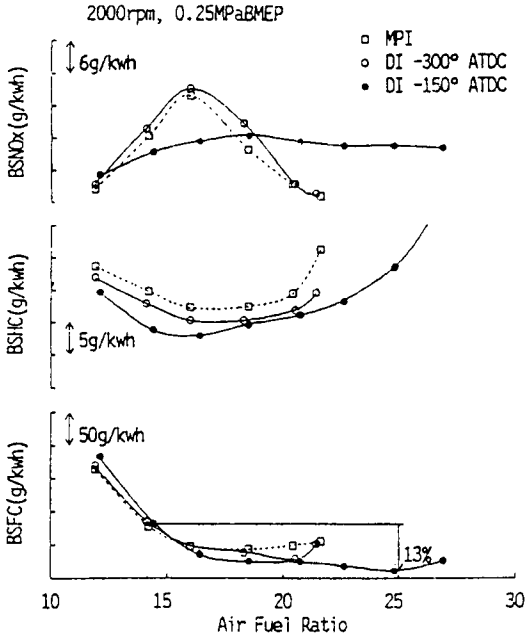

Fig. 82. Effect of the fuel injection timing and air–fuel ratio on the fuel consumption and emissions of the Isuzu prototype GDI engine [181].

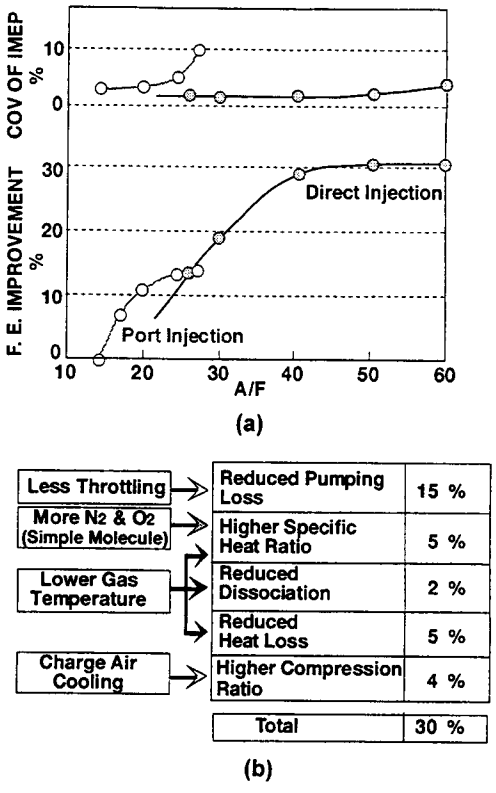

Fig. 83. Fuel economy improvement for the Mitsubishi GDI engine [20]: (a) comparison of the fuel economy improvement between the GDI and PFI engines; and (b) itemized contributions of the principal factors to the fuel economy improvement.

thermal efficiency cannot be explained by the unthrottling of the thermodynamic gas cycle alone. Fig. 81(b) and (c) shows the change of calculated individual energy balance at the same operating point. The thermodynamic benefits of the GDI technology at this operating point result from a reduction in the pumping loss of 95%, a reduction in heat losses of 42% and a reduction in exhaust energy of 26%. It can be seen that homogeneous lean operation at $\lambda = 1.3$ leads to an overall thermal efficiency gain of about 5%, which can be attributed to the reduction of pumping losses by 30%, the wall heat loss by 8% and a reduction in the exhaust energy by 6%. The potential for improvement in the fuel economy of PFI and GDI engines was also addressed by Seiffert [31] and it was concluded that a GDI engine that can achieve load control without throttling can exhibit significant improvements in fuel economy, resulting mainly from the decrease in pumping work and increases in the relative magnitude of the expansion stroke work. Indeed, thermodynamic analyses do indicate that the reduction of pumping work is the principal factor contributing to the improvement of the fuel economy of a GDI system that is able to achieve part-load operation by using an overall-lean, but stratified, mixture. Also contributing, but to a smaller degree, are reductions in the heat losses and in the specific heat ratio [20,218]. The gas near the cylinder wall is colder for part-load, stratified operation, thus there is a smaller heat differential between the wall and the burning gas, with less energy lost to the wall [203]. As discussed in the section on charge cooling, early injection can reduce the octane number requirement [40,69] and, as a result, the knock-limited engine compression ratio for the GDI engine can generally be increased to 11.5. As is well known, the effect of this higher compression ratio on fuel economy is significant. In summary, the major factors contributing to the improved BSFC of a GDI engine over that of a conventional PFI engine are:

- decreased pumping losses due to unthrottled part-load operation using overall lean mixtures;
- increased knock-limited compression ratio due to lower end-gas temperatures;
- increased cooling of the intake charge due to in-cylinder injection during induction;
- increased cycle efficiency to the incrementally higher specific heat ratio of lean mixtures;
- decreased cylinder wall and combustion chamber heat loss due to stratified combustion.

Shimotani et al. [181] compared the fuel consumption of a PFI engine with that of a GDI engine operated in the early injection homogeneous mode. As shown in Fig. 82, the lean limit achieved by the use of an injection timing of 60° ATDC on intake (−300° ATDC in the figure) on the GDI engine was basically the same as that obtained for the PFI

engine. However, retarding the fuel injection timing to 210° ATDC on intake (−150° ATDC in the figure) significantly extended the lean combustion limit for the GDI engine. It was found that the engine BSFC is generally improved when lean air–fuel ratios are used, although the effect becomes marginal for air–fuel ratios leaner than 20. The BSFC was improved about 13% at an air–fuel ratio of 25 over that obtained for a stoichiometric mixture. This air–fuel ratio yields the lowest BSFC for the engine operating condition tested. A significant improvement in fuel economy due to the use of a stratified charge in a GDI engine was also reported by Takagi [24]. It was found that stable combustion with a stratified-charge could be achieved for mixtures leaner than 40:1, with an acceptable COV of IMEP.

Wojik and Fraidl [204] noted that the GDI engine offers a fuel economy improvement potential of more than 25% when compared to current PFI engine technology. According to Fraidl et al. [57], the theoretical potential for improving the fuel economy by using direct gasoline injection is about 20% at part load, with an associated potential reduction of 35% in idle fuel consumption. Kume et al. [20] and Iwamoto et al. [50,51] reported that the BSFC may be improved by 30%, based upon tests of the Mitsubishi GDI engine. Fig. 83(a) shows the improvement in fuel economy that is obtained using late injection at an engine speed of 2000 rpm. The principal factors that contribute to the fuel economy improvement at 2000 rpm and an air–fuel ratio of 40, but without EGR, are shown in Fig. 83(b). It was claimed that a Mitsubishi "Galant", outfitted with the Mitsubishi GDI engine operating on the Japanese 10–15 mode cycle, achieved a fuel economy improvement of 35% over a conventional vehicle outfitted with a PFI engine. Idle fuel consumption was reduced by 40% due to a more stable combustion, which permitted a lower idle speed. It is very important to note in this review that some of the contributions to the 35% fuel economy improvement came from vehicle component improvements, such as a reduction in the vehicle weight. Ronald et al. [45] reported that an improvement of 25% in the fuel economy of the GDI engine as compared to the PFI engine is possible at an engine speed of 2000 rpm, and 30% may be achieved at 1200 rpm.

As is well known, many factors affect the net fuel economy improvement that may result from applying GDI technology to an engine–vehicle system. Without knowing the details of the baseline engine and/or vehicle, caution must be used in attributing the fraction of any reported fuel economy improvement that result from individual segments of the direct injection technology. Anderson et al. [40,69] reported that improvements in fuel consumption of up to 5% at part load and 10% at idle were obtained for the Ford GDI combustion system under stoichiometric operation. The best operation at part load was found to offer a fuel economy improvement of up to 12% as compared to the baseline PFI engine. The engine-out UBHC emissions, however, are comparable to those obtained with PFI operation using the same combustion system. It was also found that the NO_x emissions were less than those of the baseline PFI engine as a result of both charge cooling and the higher residual content of the charge; thus more than offsetting the effects of the maximum increase in compression ratio that could be used on the GDI engine.

Wirth et al. [144,219] reported that the ISFC of a stratified, unthrottled GDI with EGR exhibited a 22% improvement as compared to homogeneous stoichiometric PFI without EGR, while the improvement in BSFC was found to be 19%. This difference between ISFC and BSFC improvements results because the cylinder pressure level is higher in the stratified GDI case, leading to an incremental increase in engine friction (FMEP). Andriesse et al. [190] reported that a GDI engine that is operated in the homogeneous, stoichiometric mixture mode can provide a 7–10% reduction in fuel consumption without requiring a lean NO_x catalyst. This reduction was divided into:

- a higher compression ratio: 1.5–2% reduction;
- a higher EGR tolerance: 1.5–2% reduction;
- improved air–fuel control during warm up and transients: 1–2% reduction;
- downsizing of engine for same torque and power: 3–4% reduction.

It was claimed that a combined effect of improved volumetric efficiency (5%) and an increased compression ratio of 10.5–12 provide a BMEP gain of almost 10%.

Lake et al. [148] reported that the conventional PFI lean-burn engine can, when operated at an air–fuel ratio of 25, provide an overall fuel economy improvement of about 10–12% when compared to stoichiometric operation without EGR. A stratified GDI engine operating at an overall air–fuel ratio exceeding 40 was found to provide an overall fuel consumption improvement of up to 25% when compared to the same baseline. It was found that the fuel economy is improved slightly by adding uncooled EGR at light loads, even though the engine operates unthrottled. This was assumed to be due to the additional enhancement of mixing by hot EGR. The use of EGR, however, had little effect on fuel economy at intermediate loads, and ultimately degrades the obtainable fuel economy at high loads. It was reported by Jackson et al. [136,137,145,173,195,196] that for the best compromise between fuel consumption and emissions characteristics, the system should employ maximum EGR at part load, limiting the overall air–fuel ratio to be greater than 30. Combustion stability with a GDI engine system using a curved-crown piston was found to be better than that of a flat-crown system over the entire load range. Even with an air–fuel ratio of 50, a 17–20% reduction in the fuel consumption at 0.15 MPa BMEP is attainable. This was considered to be mainly due to the enhanced stratification that was achieved using the curved-crown piston. At a constant engine operating condition of 2000 rpm and a 0.2 MPa BMEP, a reduction in fuel consumption of 23%

was achieved for the unthrottled Mercedes-Benz GDI combustion system as compared to the homogeneous, stoichiometric, throttled operation of the same engine. It was noted that this was achieved not only due to the reduction in throttling losses, but also due to the decrease in the peak cycle temperature [193].

Wirth et al. [144,219] reported the results of a production vehicle that was fitted with a GDI engine optimized for both homogeneous and stratified operations. For the test schedule used, the engine operated in the stratified lean mode for only about 16% of the time. This illustrates the point that the improvement in the vehicle fuel economy of a GDI engine as compared to a PFI engine is very dependent on the engine–vehicle matching, driving cycle and GDI operating mode excursions. It was recommended by Fradil et al. [142] that the use of a sophisticated torque-based engine control system can provide significant benefits. By avoiding a close coupling to the driver, an extended operation of the engine within the stratified charge mode during transient conditions can be realized while maintaining vehicle driveability.

5.2. Emissions versus fuel economy compromise

The areas of significant potential of the direct-injection-gasoline, four-stroke SI engine are quite evident, and have been addressed extensively. The realization of a viable production engine, however, requires the successful implementation of emission control strategies, hardware, and control algorithms in order to achieve certifiable emission levels and acceptable driveability levels during load transients [220,221,291,292]. This is one of the barriers to the simple conversion of the current PFI engine to direct injection. Experience has shown that some fraction of the potential fuel economy gains will have to be compromised in order to achieve increasingly stringent emission standards such as the US ULEV and SULEV requirements. The key question for original equipment manufacturers (OEMs) in relation to GDI engines is whether the final margin in fuel economy for a particular engine system is sufficient to justify the additional hardware and complexity required. Another very important consideration is that the fuel economy margin should always be measured relative to the increasingly sophisticated PFI engine, which is, of course, a moving target. It is the specific details of the compromise between BSFC and test-cycle emissions, coupled with the increased system complexity, that will be the most important factors in determining the production feasibility of a GDI engine application. The current technologies for obtaining reductions in the emissions from GDI engines are summarized below and will be discussed in detail in this section.

- UBHC emissions during part-load and transients:
  - light throttling for part-load operation;
  - UBHC traps;
  - UBHC oxidation catalysts.
- NO_x emissions:
  - EGR;
  - three-way catalyst for stoichiometric operation;
  - lean-NO_x catalyst.
- Particulates:
  - optimize combustion system and combustion control strategies;
  - oxidation catalyst.

Even though the GDI engine offers a significant potential for fuel economy improvement, some mitigation in the potential fuel economy gain will occur when meeting strict emission limits [354]. For most automotive GDI applications, this is the dominating optimization criterion. The required emission-related compromises in operation will depend upon the combustion process, the EGR strategy, and the exhaust aftertreatment adopted. For example, it is difficult to realize ultra lean combustion while maintaining an effective catalyst operating temperature during steady, warm engine operation. As a result, extended periods of lean operation may be limited by the exhaust temperature. Kagawa et al. [222] investigated this phenomenon on a Wankel DISC engine and concluded that it is necessary to utilize some manifold vacuum in order to maintain the exhaust gas temperature above the effective operating temperature of the catalyst for extended periods of lean operation. With such a limitation, the stratified GDI engine can achieve a 10% improvement in fuel economy when compared with the conventional PFI combustion system. Although unthrottling the engine is a very effective way to improve the fuel economy of the GDI engine, slight throttling has been found to provide emission improvements at the expense of degrading some fuel economy [148]. Jackson et al. [145,173,195,196] reported that at 20% EGR, a 20% reduction in UBHC emissions can be achieved by throttling the engine slightly, with a 3% fuel consumption penalty. For a GDI concept with a five-speed, manual transmission, a 60% NO_x conversion efficiency is required to meet the EURO IV emissions standard with an engineering margin, which currently can only be provided by a NO_x storage device, together with a light throttling of the engine for UBHC control. This strategy yields a fuel consumption that is about 14% better than the conventional PFI engine. In contrast, a high-speed direct injection (HSDI) diesel with a five-speed manual transmission can be 14% better on fuel consumption but only about 3.6% better on CO_2 emissions than the best GDI concept.

Using a two-zone model, Iiyama and Muranaka [77] calculated the fuel consumption improvement of a GDI engine for a range of operating conditions. It was found that an improvement in fuel economy up to 20% could be achieved when compared with current PFI engines that use a three-way catalyst if the GDI engine were operated under stratified conditions over the entire operating range. The active operating temperature of the catalyst is a very

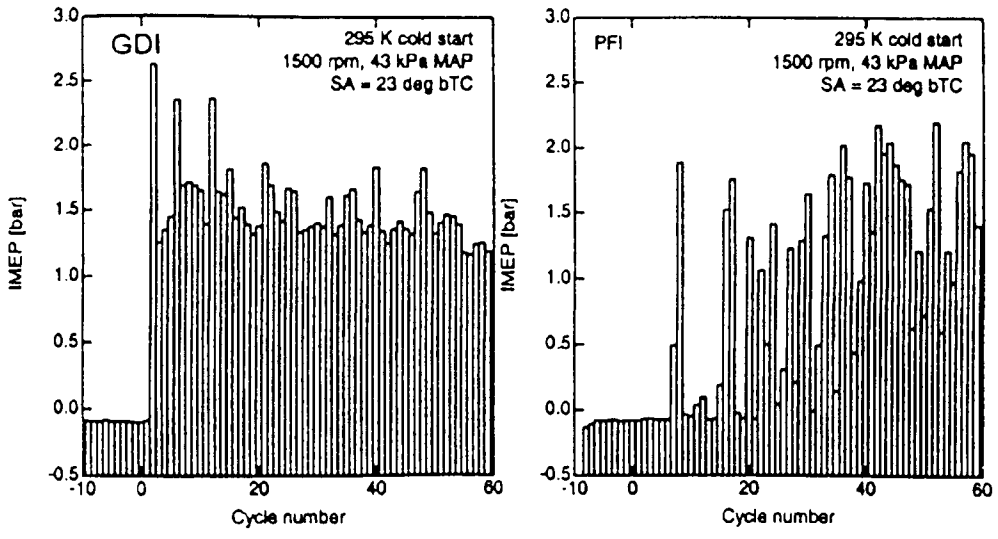

(a)

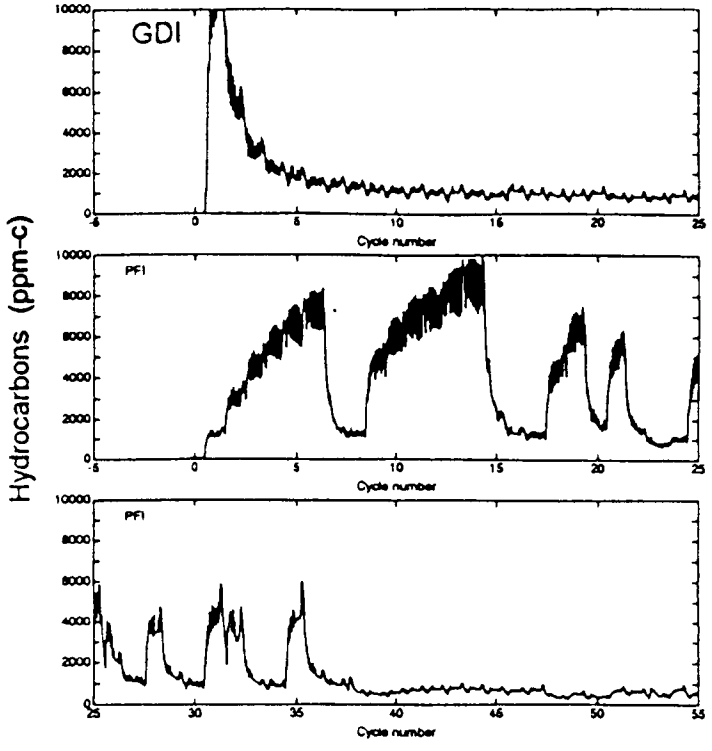

(b)

Fig. 84. Performance and emissions of the Ford prototype GDI engine [40]: (a) measured cold-start IMEP variations for a single-cylinder research engine operating with direct and port injections; and (b) measured cold-start UBHC variations for a single-cylinder research engine under the conditions of 295 K, 1500 rpm, 43 kPa MAP, and spark advance of 23° BTDC.

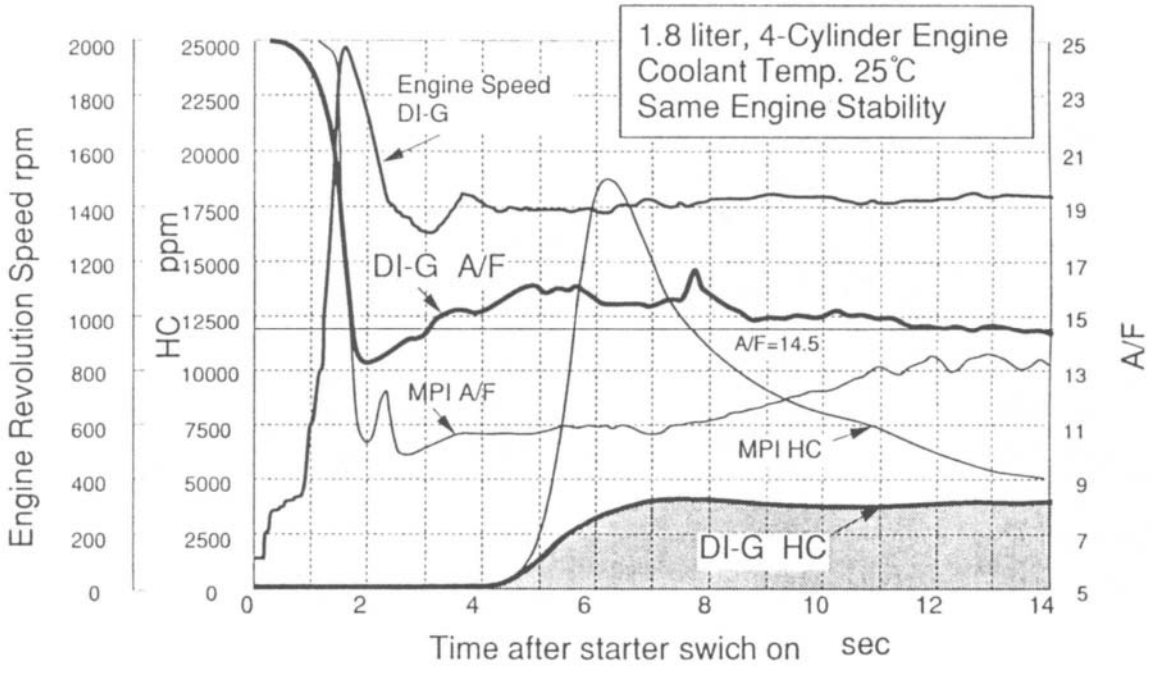

Fig. 85. Reduction of the UBHC emissions for the Nissan GDI engine at cold start [24].

important parameter, and the overall mixture cannot be ultra-lean if the catalyst inlet temperature is to be maintained above a critical threshold value. The analysis also indicates that the operating range of the stratified engine is narrowed somewhat when the emission constraints are applied, reducing the fuel economy improvement to 10%. It was noted that improvements in catalyst technology would be required in order to take full advantage of the benefits of highly stratified combustion.

5.2.1. UBHC emissions

One of the significant emission advantages of the four-stroke GDI engine is a potential reduction in UBHC emissions during an engine cold start and warm up. Direct in-cylinder injection of gasoline can completely eliminate the formation of a liquid fuel film on the intake port walls, which has the benefit of reducing the fuel metering errors and fuel transport delay that are associated with running from a liquid pool in the port of a PFI engine. Injection directly into the cylinder significantly improves the metering accuracy and the engine response under both cold start and transient conditions. As a result, it is very likely that both cold-enrichment compensation and acceleration-enrichment compensation can be substantially reduced in the engine calibration, reducing the total UBHC emissions. Experimental verification of this potential has been provided by a number of researchers, including Anderson et al. [40,69], Takagi [24], and Shimotani et al. [181,182].

The engine performance and emission levels of a GDI engine and a PFI engine under cold start conditions were compared by Shimotani et al. [181]. It was observed that the GDI engine exhibits a rapid rise in the IMEP following the first injection event, whereas the PFI engine requires about 10 cycles for the engine to attain stable combustion. This is attributed to the formation and growth of a fuel film on the intake valve and port wall of the PFI engine, wherein the fuel mass entering the cylinder on each cycle is not necessarily what is being metered by the injector on that cycle. As a result, misfires and partial burns occur and the UBHC emissions for the PFI engine are typically quite high during these cycles. To compensate for the fuel delay in reaching a steady-oscillatory state for the wall film, significant additional fuel must be added at cold start for the PFI engine. The GDI engine, however, has the potential of being started cold using a stoichiometric or even slightly lean mixture.

Anderson et al. [40] compared the cold start performance of GDI and PFI engines. The IMEP traces in Fig. 84(a) verify that the GDI engine did indeed fire on the second cycle, whereas the PFI engine failed to fire until the seventh cycle, after which misfire and partial-burn events continued. In comparison, the GDI engine exhibited relatively good combustion with little cycle-to-cycle variation following the first combusting cycle. The GDI engine might be expected to fire on the very first cycle if a slightly greater amount of fuel were injected to account for the fact that there might be no residual gas in the combustion chamber when the first fuel injection occurs. The high IMEP that is obtained for the second cycle is due to the fact that this is the first and only firing cycle in which combustion occurs without residual burned gases. In fact, the cylinder contains

residual unburned mixture from the first cycle instead of residual burned mixture. The IMEP produced is therefore greater than that obtained in any later cycle in spite of the fact that the combustion chamber surfaces are coldest on the first firing cycle. The lack of combustion on the first cycle with the GDI engine, however, does result in elevated UBHC emissions as shown by the fast FID measurements in Fig. 84(b). By the fifth cycle, the UBHC emissions attain a steady-state level, whereas the UBHC level builds steadily in the PFI engine until the first fire in the seventh cycle. The pattern of high UBHC emissions continues through as many as 35 cycles as misfire or partial burns continue for the PFI engine.

Takagi [24] reported results from a cold starting test of a 1.8L, four-cylinder GDI engine. As shown in Fig. 85, it was found that the engine exhibited improved transient response and a significant reduction in UBHC emissions when compared with a standard PFI engine. Four cycles were required for the GDI engine to attain a stable IMEP when operating at an air–fuel ratio of 14.5, whereas the PFI engine required 12 cycles to reach stable operation at an air–fuel ratio of 13. A comparison of the engine emission characteristics of GDI and PFI engines during a cold start was made by Shimotani et al. [182] for a coolant temperature range of 20–23°C, using both early intake fuel injection (30° ATDC on intake), and near bottom dead center injection (170° ATDC on intake). The UBHC emissions for the PFI and GDI engines for early injection were found to be higher than that obtained for the GDI engine using injection at the start of the compression stroke [367]. The effect of injection timing on the transient UBHC emissions during the first several seconds of a cold start was also conducted. The results of this study show that the UBHC emissions decreased and reached a minimum at 170° ATDC on intake, which is a 60% reduction when compared with that of early injection (30° ATDC on intake). The effect of coolant temperature on the part-load UBHC emissions and fuel consumption was a third investigation. The engine was operated at an engine speed of 1400 rpm with a BMEP of 150 kPa. The UBHC emissions were observed to decrease as the injection timing was retarded from early in the intake stroke to the middle of the intake stroke, and to increase for further later timings. At a coolant temperature of 20°C for the GDI engine, a 50% reduction in the steady-state UBHC emissions was obtained by retarding the injection timing from 30° ATDC to 110° ATDC on intake. For a coolant temperature of 80°C, the minimum BSFC occurred at an injection timing of 110° ATDC on intake. The data indicated that the injection timing must be optimally set at 110° ATDC on intake for cold operation in order to obtain low UBHC emissions, whereas a timing of 30° ATDC on intake is optimum for warm, steady-state operation. This timing schedule provides a good balance between UBHC emissions and fuel consumption. The effect of the operating air–fuel ratio on the cold start performance of GDI and PFI engines was also measured. Compared to the PFI engine, the GDI engine can operate two full ratios leaner at the same starting cycle number.

A vehicle test of an Isuzu prototype GDI engine was conducted by Shimotani et al. [182]. The injection timing was set at the end of the intake stroke for cranking, and at 110° ATDC on intake following the first firing. A stoichiometric air–fuel ratio was used. The UBHC and CO emissions upstream of the catalysts were measured for the first cycle in the LA-4 mode. The emissions data that were obtained during the first 60 s after the cold start are shown in Fig. 86(a). Through an optimized injection timing and the use of a leaner mixture, the GDI engine exhibits a clear reduction in both UBHC and CO. The catalyst temperature, UBHC conversion efficiency, and the integrated UBHC concentration after the catalyst are shown in Fig. 86(b), which is for the same engine operating condition as in Fig. 86(a). It was noted that the GDI engine provides a more rapid catalyst response, and that the UBHC emission level is lower than that obtained with the PFI engine. This is due to the rapid increase of the catalyst temperature after a cold start, resulting from the more rapid firing and improved A–F control capability afforded by direct injection. The time history of the air–fuel ratio from the 11th cycle of the LA-4 mode is shown in Fig. 86(c). For the conventional PFI engine, numerous calibration compensations are required to minimize the effect of fuel transport lag caused by the inherent fuel–wall wetting [327]. During speed and load transients the effectiveness of such compensation is limited, and tip-in and tip-out spikes of UBHC emissions occur. The more accurate control of the transient air–fuel ratio for the GDI engine is illustrated in Fig. 86(c), and the associated catalyst efficiency is shown in Fig. 86(d). It may be seen that the PFI engine shows a large fluctuation in the catalyst efficiency during engine transients, indicating a decrease in the UBHC conversion efficiency. This was not observed during the operation of the GDI engine, which implies that the more precise air–fuel control of the GDI engine can yield an associated improvement in the catalyst conversion efficiency. As a result, the UBHC emissions can be reduced, even during steady-state operation. Both the emissions and the BSFC are improved during the entire LA-4 mode for the GDI engine. The total reduction of the UBHC emissions can reach 45% for the entire LA-4 mode, showing the potential of the GDI engine for meeting the future emission standards for UBHC.

As opposed to UBHC emissions during a cold-start, the UBHC emissions for low-load operation represent a significant problem that is historically associated with gasoline DISC engines [223]. In the case of gasoline direct injection, the flame is eventually quenched in the extra-lean area at the outer boundary of the stratified region where the mixture is in transition from rich to lean [24]. As a result, a significant amount of UBHC remains in the total charge. The inability of the flame front to propagate from the rich mixture at the spark gap through all of the lean mixture in the outer portion of the combustion chamber is a key factor contributing to

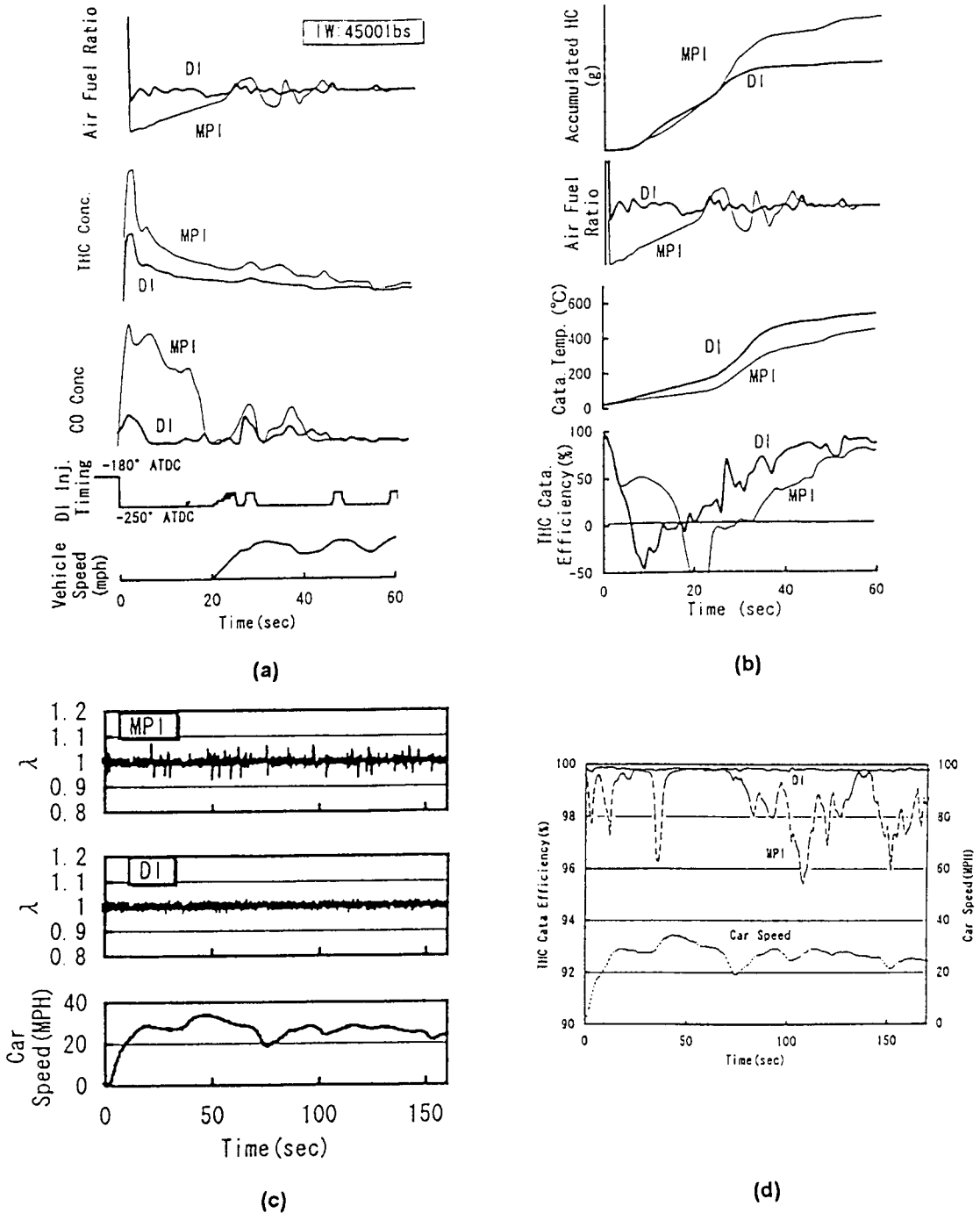

Fig. 86. Performance and emissions of the Isuzu GDI engine for the LA-4 mode vehicle test [182]: (a) engine-out UBHC emissions during the first cycle; (b) tailpipe UBHC emissions during the first cycle; (c) variation of the air–fuel ratio during the 11th cycle; and (d) catalyst efficiency during the 11th cycle.

the part-load UBHC emissions in GDI engines, and a substantial research effort is being directed towards the resolution of this problem. There can also be overly rich regions near the piston as a result of piston-crown and/or cylinder-wall wetting by the fuel spray. Unlike the diesel combustion in which UBHC emissions are very low with stratification at light loads, GDI engines operating in the stratified charge mode have a much lower compression

ratio, which greatly reduces the in-cylinder temperature. As a result HCs which do not participate in the combustion process have a much lower probability of post-combustion oxidation. The exhaust temperature is also low, making it more difficult for current three-way catalyst technology to operate at the high efficiencies necessary for satisfactory tailpipe emission levels. The low exhaust temperature also eliminates the possibility of any hydrocarbon oxidation in the exhaust port, as is observed with the PFI engine operating under a similar condition [199]. The key considerations regarding increased UBHC emissions from stratified-charge GDI engines are:

- flame extinction occurs for the very lean mixtures near the outer boundary of the stratified charge;
- poor combustion can occur in overly rich regions near the piston crown or cylinder wall due to spray–wall wetting;
- lower combustion temperature reduces the degree of post-flame oxidation of UBHC;
- lower exhaust gas temperature degrades the conversion efficiency of the catalyst system;
- lower exhaust gas temperatures significantly reduce the occurrence of UBHC oxidation in the exhaust port.

In general, it has been found that direct gasoline injection can yield a slight increase in UBHC emissions at idle, and can exhibit substantial increase at part load. For part-load operation at higher engine speeds, another source of UBHC is the decrease in the time available for mixture preparation, which is limited for direct injection. This can result in diffusion burning at the surface of liquid droplets. The application of EGR at low engine loads can also increase the UBHC emissions substantially, and, when coupled with the use of a higher compression ratio for the GDI application, can result in additional amounts of UBHC being forced into crevices, resulting in an incremental increase in the UBHC emissions [40,223–225].

A number of the very early observations that related to the UBHC emissions of DISC engines may still be applied directly to current GDI engines. A range of possible reasons for the increase in the UBHC emissions for DISC systems at low load were listed by Balles et al. [271], and by Frank and Heywood [227] for the TCCS combustion system. It was noted that at low load the mixture becomes too lean prior to ignition due to the mixing and diffusion of the injected fuel. As a result, the combustion efficiency was found to be low for many cycles, and the associated UBHC emissions were excessive. Generally, at low load an overall ultra-lean mixture was supplied in the TCCS engine that may have resulted in over-mixing. Due to the small quantity of fuel injected into the combustion chamber, the cyclic variation of the evaporation rate was found to be a significant factor. The UBHC emissions were traced mainly to cycles with the lowest combustion efficiency. Frank and Heywood [227–230] reported that the UBHC emissions exhibited little dependence on the piston crown temperature, which would indicate that the adherence of liquid fuel on the piston surface is not the main source of the UBHC emissions for the combustion system tested.

Any delay in the flame kernel development around the spark gap, or in the propagation rate of the flame through the mixture, is a contributing factor that increases the UBHC emissions. Frank and Heywood [228] pointed out that engine combustion events with large combustion delays yield a marked increase in the UBHC emissions. This indicates that, for the stratified combustion of lean mixtures, the resident time of the fuel inside the combustion chamber should be as short as possible. Thus, the spray characteristics at the end of the fuel injection event are important in determining the UBHC emissions. The fuel injected as the pintle is closing may not be well atomized, and has the least amount of time available to vaporize. With many pintle designs, the last fuel injected may have a trajectory that differs from that of the main jet [229], resulting in an increase in UBHC emissions.

Ronald et al. [45] studied the effect of air–fuel ratio on the UBHC emissions of a single-cylinder research GDI engine. The UBHC emissions were found to increase continuously with an enleanment of the air–fuel ratio for the stratified-charge mode. This was attributed to increasingly prevalent pockets of excessively lean mixture and, as a result, an incomplete combustion event. A further reason may be a reduced reaction rate along the exhaust pipe due to the decrease in the exhaust temperature. As the charge becomes more stratified, the amount of fuel compressed into the top land area of the piston decreases significantly, and less fuel is in contact with the cylinder wall. As a consequence, the UBHC emissions may be lower when compared with PFI operation. Although the PFI engine exhibits a marked decrease in the CO emissions for lean mixtures, the CO emissions of the GDI engine remain nearly constant.

Iiyama and Muranaka [77] concluded from calculations that pockets of mixture within the combustible range for air–fuel ratios richer than 30 are distributed randomly inside the flame. As a result, the flame does not propagate uniformly through these regions, yielding an increase in UBHC emissions. It was reported that high UBHC emissions at low load is an inherent feature of the stratified combustion concept itself. To reduce this type of UBHC emission, it is necessary to generate a highly stratified flow field. This tends to suppress the formation of rich pockets inside the combustion zone. One of the technologies for accomplishing this is the two-stage injection system proposed by Miyamoto et al. [201] and by Hattori et al. [202].

Anderson et al. [199] conducted a detailed computational analysis on the UBHC formation process of a stratified charge GDI engine using the KIVA code. It was found that there can be as much as 10% of the injected fuel remaining in liquid form at the time of ignition for late injection. This was true for both side-mounted and centrally-mounted injectors. The fuel on the piston crown was found to be the largest source of UBHC emissions. This impingement of

liquid fuel can result in incomplete combustion of the fuel-rich layer above the piston if it is insufficiently evaporated and mixed before the flame propagates beyond it. The total UBHC can be as much as 3.4% of the total fuel, with 0.6% resulting from the incomplete flame propagation, 2.7% from wall wetting, and 0.1% from the fuel injection system and the crevice. It was noted that for the late injection, stratified-charge mode, fuel vapor is present inside the spray very soon after the start of the injection, resulting in a 'solid cone' vapor distribution. The mixture is quite rich inside the spray and becomes increasingly leaner in the radial direction of the spray. A thin layer of lean mixture ($\phi <$ 0.5) exists at the outer edges of the spray region. The amount of fuel in this lean mixture region increases with time and crank angle due to continued mixing. This overly lean fraction can be as high as 20% of the total fuel injected by the time ignition occurs. These lean mixtures, if not completely burned, can be a very significant source of UBHC emissions. Any unburned lean mixtures outside the primary flame region would contribute to the engine-out UBHC emissions if the in-cylinder temperature is below 1000 K during the expansion stroke. For the leaner mixture, a slightly increased temperature does not promote further UBHC oxidation. Even though the equivalence ratio may be very high near the piston, oxidation of the UBHC in this region could be slowed significantly due to the low temperature. The calculations also indicated that isooctane can be oxidized if the in-cylinder temperature exceeds 1150 K. The flame can propagate into regions having an equivalence ratio of about 0.3. Oxidation of a mixture with an equivalence ratio of 0.2 is possible in about 1.5 ms if the in-cylinder temperature is at least 1150 K. A mixture having an equivalence ratio of less than 0.1 is only partially oxidized, with reaction ceasing after about 3 ms due to a rapid decrease of the cylinder pressure and temperature during expansion.

It is well known that the heat release of stratified-charge combustion occurs earlier than that of the homogeneous combustion. The addition of EGR will slow the combustion process due to the presence of the diluent and will shift the heat release to a later timing. When adding EGR to a stratified charge, the overall air–fuel ratio becomes richer. But, unlike throttling, adding EGR does not improve the flame propagation process since the lean regions are further diluted by the high exhaust gas concentration, which also results in flame quenching. The UBHC can be reduced in GDI engines by adding EGR, but the mechanism is complex, involving an increased burning period, later combustion phasing and increased post-flame oxidation, with the result that varying trends are reported in the literature. Jackson et al. [145,173,195,196] and Lake et al. [185] reported that the UBHC emissions increase in a manner similar to that in a PFI engine when the EGR percentage is increased at a constant air–fuel ratio. However, as there is no need to maintain a constant air–fuel ratio in the GDI engine, the UBHC reduction benefits can be obtained by adding EGR. The specific effect of EGR on UBHC reduction is combustion-system-dependent. It was reported that for a side-port engine with a central injector, UBHC emissions decrease as EGR is increased up to 20%. For the top-entry-port engine with a side-mounted injector, the UBHC emissions continue to decrease with an increase in EGR percentage up to the tolerance limit. An increased intake air temperature and the use of hot EGR are found to assist in reducing UBHC emissions.

Sasaki et al. [231] investigated the effect of EGR on combustion and emissions using a Toyota GDI engine, with the experimental results for a range of engine operating conditions shown in Fig. 87. It was found that a wide-cone, well-dispersed, fuel spray provides improved combustion stability. Both the UBHC and BSFC decrease initially as increasing percentages of EGR are added, with the trend being quite pronounced when the engine load is low. As the EGR percentage is further increased, both the BSFC and UBHC start to increase. The observed improvements in UBHC and BSFC are attributed to the increase in combustion temperature, which extends the air–fuel ratio limits of flame propagation. Lake et al. [148] reported that the use of EGR can reduce the UBHC emissions by between 30 and 39% over the load range of 0.15–0.4 MPa BMEP. This reduction was attributed to improvements in fuel mixing resulting from the heating effect of EGR and the local variations in the equivalence ratio and EGR distributions. However, Anderson et al. [199] warn that the UBHC emissions could actually increase because the addition of EGR could narrow the flammability limits even though the exhaust temperature is raised by adding high levels of EGR.

Although the GDI engine offers the potential for improving the BSFC by operating at part load without throttling, throttling is generally found to provide emission improvements at the expense of some fuel economy [148]. Theoretically, nonthrottling operation is possible at part load by using a stratified mixture; however, some throttle control is usually required in the production GDI engine [21]. This is because a GDI engine that is designed to operate in the stratified-charge mode must, of necessity, also operate for conditions such as cold starting and high load, which require a homogeneous charge. For such operating conditions it has been found that the use of some throttling is quite advantageous. However, as over half of the total GDI fuel economy benefit derives from the reduction of pumping losses [20], throttled operation may be expected to result in some degradation in fuel economy; and the use of the throttling in a GDI operating system should always be carefully evaluated [148]. The application of some throttling has been shown to be quite effective in achieving smoother transitions between engine operating modes and, at low load, is effective in elevating the very low exhaust temperatures that result from extended periods of stratified operation. This can significantly enhance the catalyst conversion efficiency. In addition, the flow of significant percentages of EGR for

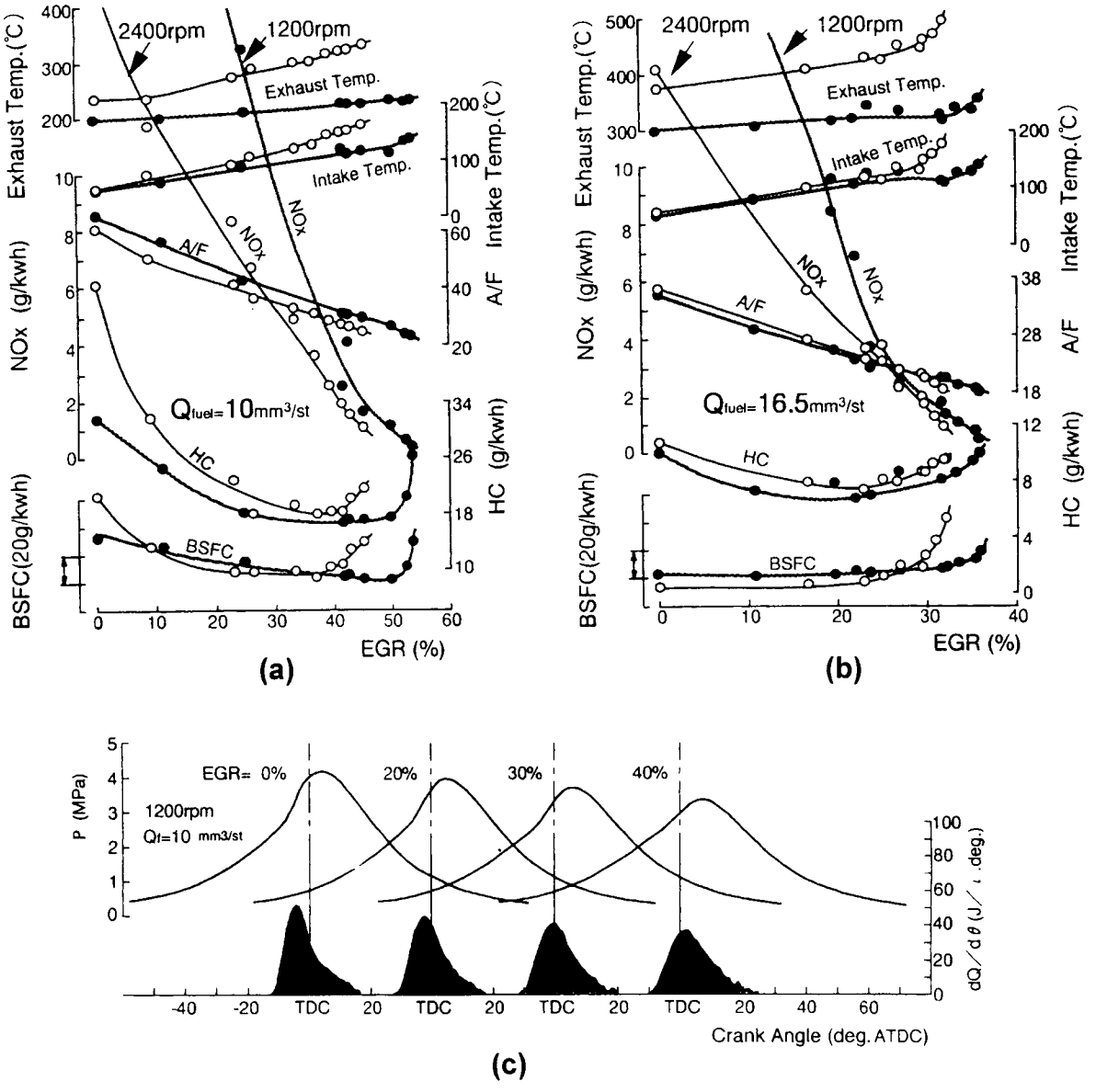

Fig. 87. Effect of EGR on engine performance and exhaust emissions [231]: (a) 1/8 load; (b) 3/8 load; and (c) combustion characteristics at various EGR rates, 1/8 engine load and an engine speed of 1200 rpm.

essential NO_x reduction may require an intake manifold vacuum that can be obtained most expeditiously by applying some throttling. A conventional vacuum-assisted power brake system also requires some vacuum that may be optionally provided by throttling rather than by an on-board vacuum pump. Also it is important to note that some GDI engines demonstrate an improvement in the compromise between emissions and fuel economy with the use of moderate amounts of throttling. An electronically controlled throttling system is generally used for GDI applications because of the improved control advantages over mechanically linked systems, and is effectively employed in the Toyota GDI engine system [21].

In general, it is possible to use moderate throttling of the engine at low load to reduce the UBHC emissions without significantly degrading the fuel economy. In addition, throttling may be successfully combined with the use of EGR to improve the overall compromise among fuel economy, NO_x and UBHC emissions. Lake et al. [148] investigated the effect of throttling on fuel economy and emissions as a function of EGR. It was reported that a 20% reduction in UBHC emissions could be obtained by the use of light

throttling at an EGR rate of 20%, with a fuel economy penalty of only 2.5%. Correspondingly, a 50% reduction in UBHC emissions by the use of some throttling results in a fuel economy penalty of approximately 8%, whereas throttling the engine without any EGR yields the lowest UBHC emissions at any air–fuel ratio level. Moreover, throttling does not cause any apparent change in NO_x emissions at a fixed EGR rate. If throttling is increased to enrich the mixture, NO_x decreases at a fixed EGR rate, but to the detriment of fuel economy. For most GDI designs, a 55% reduction in NO_x emissions can be achieved with a 2% loss of fuel economy by utilizing EGR with no throttling. An 80% reduction in NO_x emissions can be achieved by the use of throttling in conjunction with EGR, but with an associated 15% loss in fuel economy. Another approach for UBHC reduction is to limit the degree of low-load stratification and operate with a homogeneous throttled mode. This, however, would defeat one of the major reasons for creating a stratified charge engine, which is to improve fuel consumption by significantly reducing the light load pumping work.

It should be noted that the effect of throttling on engine-out UBHCs is very dependent on the specific combustion system. In general, throttling the engine will enrich the mixture, and will extend the flame further into the quenching zone. This comparatively richer combustion will also increase the burned gas temperature, which promotes the post-flame oxidation of UBHCs both inside the cylinder and in the exhaust port. As a result, throttling tends to reduce the UBHCs that result from quenching. However, the UBHCs that result from liquid fuel on the piston crown and cylinder wall may actually increase when throttling the engine, due to the locally over-rich combustion.

5.2.2. NO_x emissions

As the mixture becomes leaner, the conventional lean-burn PFI engine exhibits decreasing NO_x formation and engine-out NO_x emissions, which result from a reduction in the reaction zone temperature. However, in the case of the GDI engine that operates with a stratified charge, the temperature within the reaction zone remains high due to the presence of a stoichiometric or slightly rich mixture in the core region of the stratified charge. NO_x production is high in these areas even though the overall thermodynamic temperature is reduced due to the overall lean operation. The GDI engine can also achieve significant fuel economy benefits related to operation with a higher knock-limited compression ratio, but this also elevates the NO_x emission levels. Another factor is that the in-cylinder temperature is higher because of a larger compressed mass in the cylinder than exists for a comparable load for throttled operation. The net result is that the NO_x level of the GDI engine operating without EGR will generally be similar to that of the PFI engine, even though some GDI engines can operate at an air–fuel ratio leaner than 50 at low load. As reported by Ronald et al. [45], despite a leaning in the overall air–fuel ratio, a continuous *increase* of NO_x is observed for a GDI engine that is operating in the stratified-charge mode, whereas the NO_x emission level *decreases* for a PFI engine that is operating with an air–fuel ratio leaner than 16. GDI engines also exhibit significantly elevated NO_x emissions at idle as compared to PFI engines. This is the result of locally stoichiometric combustion and the associated high heat release rate at an elevated charge density, as compared to the slower homogeneous combustion of PFI engines at a lower temperature level.

As illustrated in Fig. 82 [181], the use of an early injection timing for a GDI engine produces NO_x at approximately the same level as that of the PFI engine. Retarding the GDI injection timing to 30° ATDC on intake (−150° ATDC in the figure) results in a significant decrease in the peak NO_x. However, for a mixture with an air–fuel ratio leaner than 20, the NO_x level is higher than is obtained with an earlier injection timing.

For an engine such as the GDI that is designed to operate with lean or even ultra-lean mixtures, it is unfortunately true that a conventional three-way catalyst cannot be used to remove NO_x, therefore other techniques for in-cylinder NO_x reduction or exhaust aftertreatment must be employed. There is a consensus in the literature that NO_x reduction aftertreatment for lean burn engines is a challenging task, especially in view of the lower exhaust gas temperatures. Further, part-load lean operation of the GDI engine is quite frequent, and contributes about half of the NO_x emissions for the total emission test cycle [51].

EGR is widely used for in-cylinder NO_x reduction, and it functions primarily as a diluent during the combustion of the fuel–air mixture [309,365]. The dilution of the mixture by EGR is a very straightforward method of reducing the peak combustion temperature; however, as compared to air dilution, dilution using exhaust gases decreases the polytropic index due to the presence of CO_2 and H_2O molecules, with the associated higher specific heat ratio. Therefore, the effect of EGR dilution on thermal efficiency has been determined to be inferior to that of air dilution. Further, the amount of EGR that can be introduced is limited because it tends to degrade the combustion stability. Consequently, it may be appropriate to use EGR in combination with other techniques [16]. In a conventional PFI engine, NO_x reduction using EGR fails near the lean combustion limit because the mixture in proximity to the spark gap is diluted by EGR, resulting in misfires or partial burns. For a GDI engine using charge stratification, the mixture near the spark gap is ideally either stoichiometric or slightly rich; therefore stable combustion is possible with a much higher level of EGR. However, there is an associated compromise between any NO_x reduction and a simultaneous degradation in both UBHC emissions and fuel consumption.

A comparison of the NO_x reduction performance as a function of EGR rate for PFI, GDI, and diesel engines is illustrated in Fig. 88 [134]. It is evident that a larger NO_x

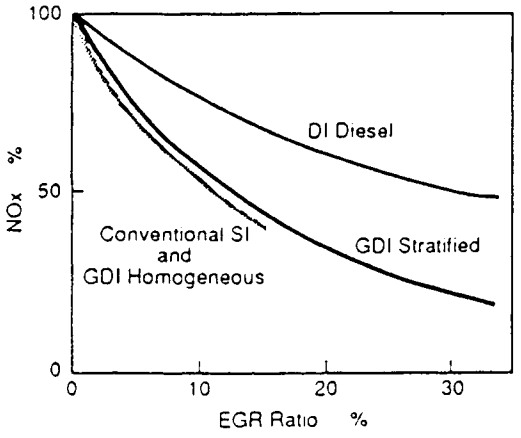

Fig. 88. Effect of EGR on NO_x reduction for different types of internal combustion engines [134].

reduction can be realized with EGR in the GDI engine than may be obtained in either the PFI engine or the diesel engine. For the GDI engine the fuel–air mixing time is comparatively longer than that of the diesel engine and, as a result, the NO_x emissions can be reduced significantly. Kume et al. [20] reported the effect of EGR rate on NO_x reduction, and these data are shown in Fig. 89. When compared with the engine-out NO_x of a PFI engine operating with a stoichiometric mixture, the NO_x reduction for the GDI engine with EGR can exceed 90% while maintaining improved fuel economy. It was noted that the flame temperature was found to be reduced by about 200 K with the use of 30% EGR. Meyer et al. [126] studied the effect of EGR on the in-cylinder fuel distribution by utilizing a separate EGR port and valve that introduced EGR directly into the cylinder. It was reported that the orientation of the EGR port and valve influences the in-cylinder fuel distribution significantly by producing an extra flow of recirculated

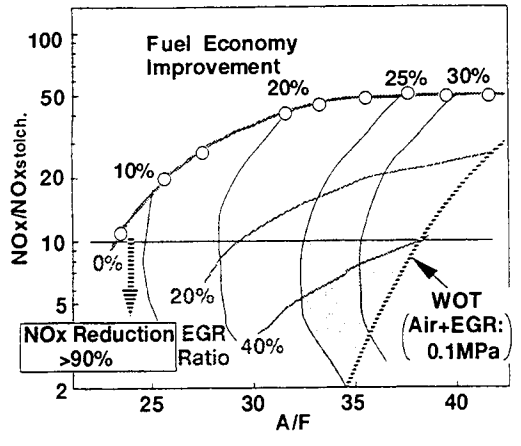

Fig. 89. Effect of EGR rate on the reduction of NO_x for the Mitsubishi GDI engine (2000 rpm, 15 mm^3 per injection) [20].

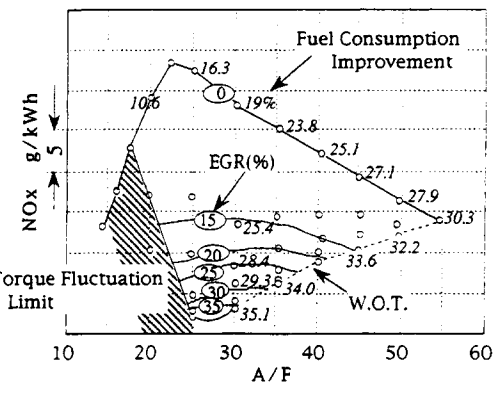

Fig. 90. Effect of EGR rate on the reduction of NO_x for the Toyota GDI engine (1200 rpm, 12 mm^3/s) [43].

exhaust gas within the combustion chamber. The EGR strategies used in their study created a fuel stratification inside the combustion chamber just prior to spark ignition, which was verified by in-cylinder fuel distribution measurements using the laser-induced fluorescence (LIF) technique.

Lake et al. [148] reported that stable combustion can be maintained in the Ricardo GDI engine operating in the early injection mode for EGR rates of up to 30%. An NO_x reduction of 88–95% was achieved for the stratified-charge, late-injection mode when EGR was applied. Both the ignition delay and the combustion period were found to be extended with EGR due to the decrease in the laminar flame speed. A high EGR tolerance was reported, which was attributed partly to the improvement in fuel–air mixing due to EGR heating effects. It was claimed that the high EGR tolerance yields an additional fuel economy benefit when compared to a PFI engine. A similar effect was also reported by Sasaki et al. [231]. The effects of EGR on the lean limit and NO_x emissions of a Toyota stratified-charge D-4 engine are shown in Fig. 90 [43]. It was reported that a stable combustion was obtained without throttling even when the air–fuel ratio was increased to 55. For this operating condition a 30% improvement in the fuel economy was achieved, but NO_x production was deemed to be a problem when compared to conventional homogeneous combustion. Without the use of EGR, the engine-out NO_x emissions for the Toyota D-4 engine increase as the mixture is enriched from an air–fuel ratio of 55, and reach a maximum at an air–fuel ratio of 22. Although the NO_x emissions decrease as the EGR rate increases, it was noted that misfires occur when the EGR rate is increased for the stratified-charge case. It was further reported that a stable combustion is obtained at an EGR rate of 40%, which yields both a 90% reduction in NO_x when compared with engine operation without EGR, and a 35% improvement in fuel economy, when compared with the conventional PFI engine.

It should be noted that providing the GDI engine with the required amount of EGR is a design challenge. Considerably higher EGR mass flow rates have to be metered and

distributed uniformly to individual cylinders at a much lower pressure differential than is typical with PFI engines. Such an increased EGR rate may result in a substantial temperature increase of the intake air, which may degrade the full load performance. It is also quite difficult to provide an appropriate amount of EGR during GDI mode transitions. Fraidl et al. [142] designed a variable EGR distributing system to circumvent the disadvantages of current EGR systems. A distribution plenum in close proximity to the cylinder is designed to be closed by means of a rotary disk valve. The opening of the cylinder feed lines is synchronized with the firing order, with the actual metering occurring within an electrically operated EGR valve. At part load, a large cross-section is opened to each individual cylinder, allowing a high EGR mass flow rate while maintaining an even distribution to all cylinders. At full load, or during engine transients, the EGR system close to the cylinder is shut off, improving the EGR dynamics. For the transition into part load operation, EGR is available close to the cylinder head by opening the distributing plenum. As only a small section of intake manifold is exposed to hot exhaust gas, the temperature increase of the induction air is less than with the conventional central feed design.

Even though EGR is widely employed for reducing the NO_x emissions in SI engines, there is a general view in the literature that the progress of GDI engines is strongly coupled to the development of lean-NO_x catalysts. This is because EGR cannot reduce the NO_x emissions over the entire engine speed-load map to meet the scheduled emission limits in North America, Europe and Japan. For example, within the US FTP emission test cycle the GDI engine operates for a significant fraction of the time with a lean homogeneous mixture at a stable lean limit. In such an operating condition, large amounts of EGR cannot be used, as the engine combustion stability would be significantly degraded. Also, the stratified-charge region in the operating map is narrowed when restricted to low NO_x levels, thus reducing the achievable fuel economy improvement. Therefore, a proven lean-NO_x-catalyst technology would definitely be a welcome tool in order to make optimum use of stratified combustion technology, as the conversion efficiencies and the durability of lean-NO_x catalysts are still lacking when compared with the current three-way catalyst. A significant research effort is currently being directed toward this desired technology [232]. A stoichiometric homogeneous mixture could be used in the GDI engine in combination with the three-way catalyst, but the achievable level of fuel economy would be theoretically lower for this class of GDI engine.

A number of technologies are currently being explored for NO_x reduction in lean-burn and stratified-charge engines. These, with the associated technical issues, are summarized as follows.

- Selective-reduction, lean NO_x catalysis:
  - reduces tailpipe NO_x emissions when engine is operated lean;
  - requires some UBHC to reduce NO_x;
  - lower conversion efficiency;
  - narrow working temperature range, depending on catalyst materials;
  - not as durable as conventional three-way catalysis;
  - high resistance against sulfur contamination.

- NO_x absorber:
  - stores NO_x while engine is operated lean;
  - converts stored NO_x during a rich excursion in air–fuel ratio;
  - no UBHC required to store NO_x;
  - can be installed downstream from other catalysts;
  - higher conversion efficiency over an operating window of 350–500°C;

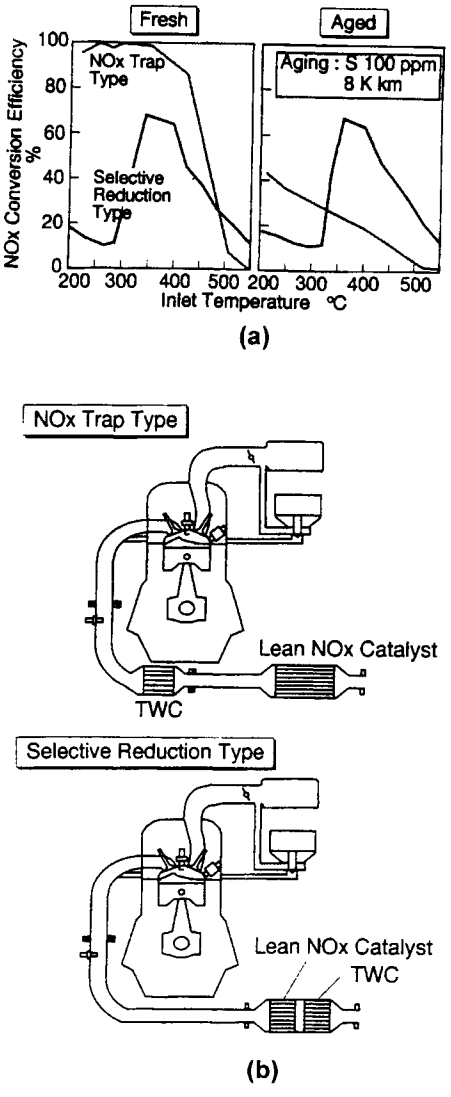

Fig. 91. Comparison of the selective-reduction-type and storage-type lean-NO_x catalysts [17].

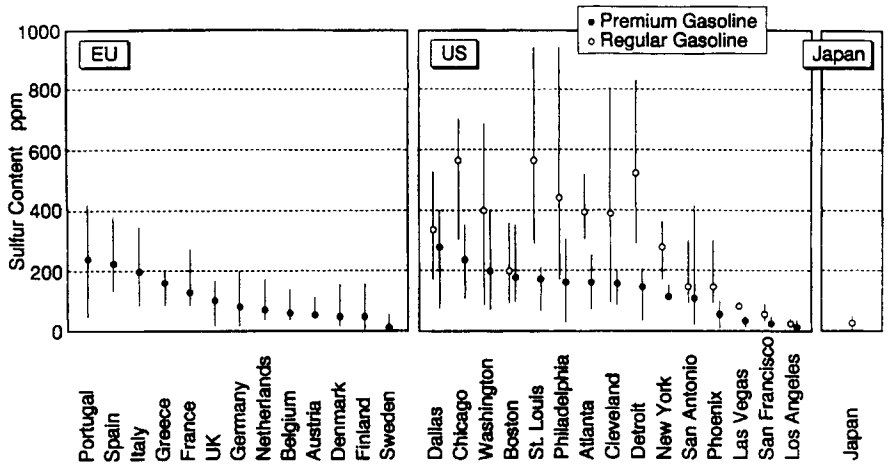

Fig. 92. Comparison of the gasoline sulfur levels in European, US and Japanese markets [17].

- rich mixture required for regeneration;
- complex control system required for regeneration;
- 2% fuel economy degradation due to regeneration;
- not as durable as conventional three-way catalysts;
- limited to low-sulfur gasoline.

- Plasma three-way catalyst:
  - expanded operating temperature range;
  - improving NO_x conversion efficiency while reducing the power consumption is a challenge.

The family of lean NO_x catalysts include NO_x reducing catalysts of zeolite and precious metal for oxygen-rich conditions, as well as an NO_x storage catalyst that is capable of trapping NO_x when the exhaust is oxygen-rich, then converting the stored NO_x during intermittent short periods of controlled over-fuelling. The NO_x storage catalyst has a high conversion efficiency; however, it is subject to sulfur poisoning and must be used with low-sulfur fuel. Fig. 91 shows a comparison of the selective reduction catalyst and NO_x trap catalyst [17]. This may be contrasted to the selective-reduction catalyst that incorporates the direct reduction reaction of NO_x by hydrocarbons, and exhibits a stable conversion capability even after lengthy operation with a high-sulfur fuel. However, the selective reduction catalyst has a much lower conversion efficiency and a narrower window of operating temperature.

One of the problems that complicates the application of NO_x storage-catalyst technology to stratified lean combustion is the generation of a precisely controlled rich excursion in the exhaust flow during extended periods of part-load operation. During lean operation, any brief increase in the fuel rate will result in a momentary increase in engine power, unless it is anticipated and controlled. During homogeneous lean mixture operation in the Toyota D-4 GDI system, fuel is injected during the intake stroke and the desired rich-mixture spike is obtained at 50 s intervals by the synchronized control of both fuel pulse width and simultaneous spark retard to maintain a constant output torque. For stratified-charge operation this spike is obtained by a complex control system command that not only provides a brief fuel pulse width and spark retard, but also by a simultaneous brief adjustment to the injection timing, throttle opening and the positions of the swirl control valve (SCV) and the EGR valve. It was reported that the NO_x emission level for this engine without either EGR or a NO_x storage catalyst is 1.85 g/km for the Japanese 10–15 mode test. With EGR control only, NO_x is reduced to 0.6 g/km, which is a 67% reduction. This can then be further reduced to 0.1 g/km with a stabilized NO_x storage catalyst. With the use of an NO_x storage-reduction catalyst, the periodic introduction of the required rich mixture results in a 2% loss of fuel economy potential [21]. Another possible strategy is to have a controlled secondary injection of fuel during the exhaust stroke. The use of a NO_x sensor is expected to contribute to an optimization of the regeneration process for the storage-type catalyst.

NO_x absorption catalysts show a high potential for NO_x removal under periodic lean–rich conditions. Engine and model bench tests have proven that significant NO_x reduction is feasible over a wide temperature range. A closely coupled interaction between the engine control system and the catalyst characteristics is required for best performance and lowest fuel consumption. However, as shown in Fig. 92, the high sulfur level in standard gasoline grades, particularly in North America, pose a major impediment to the wider application of this promising catalyst technology. Relatively small amounts of absorbed sulfur can cause a severe suppression of NO_x storage activity. Some evidence exists that SO_3 reacts preferentially with the NO_x absorbents, forming surface sulfate species that block the active sites from further NO_x absorption [232]. As the average sulfur levels of gasoline in the European and North American markets are substantially higher than that in the Japanese market, a significant challenge is presented to automotive engineers who are striving to introduce the GDI

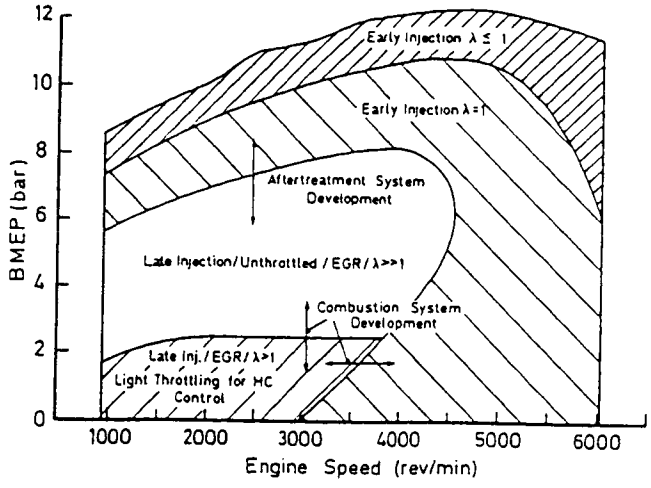

(a)

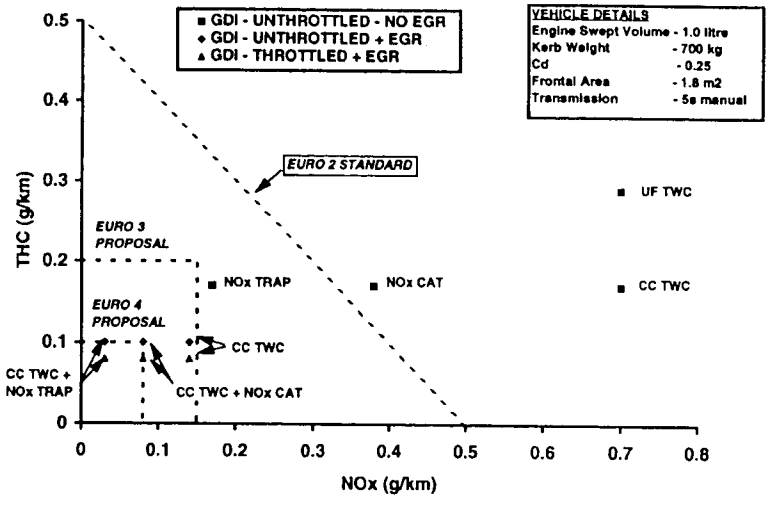

(b)

Fig. 93. Predicted emissions of different aftertreatment technologies for the ECE + EUDC cycle [136,137]: (a) control map for the Ricardo GDI engine; and (b) predicted results.

technology into those markets. In order to comply with the stringent NO_x emission regulations in Europe and North America, a more efficient NO_x catalyst that is more robust to sulfur-poisoning is required [41,338].

Iwamoto et al. [50,51] reported that the Mitsubishi GDI engine employs a selective-reduction catalyst to further reduce the NO_x emissions not only during the urban driving cycle, but also for the lean-burn condition associated with the highway driving cycle. This selective-reduction-type catalyst has three-way catalytic functions and a high inherent resistance against sulfur contamination; however, it currently has a relatively narrow working temperature range that limits its performance. It is claimed that the selective-reduction catalyst maintains a good efficiency in the mileage-accumulation durability test with high-sulfur gasoline. However, this type of catalyst may generate more N_2O and NO_2 emissions. Jackson et al. [145,173,195,196] subtracted emissions entering the catalyst from those measured at the catalyst outlet, with the results indicating that the catalyst increases N_2O and NO_2 emissions during the cycle. Another new technology that is being developed for potential application to GDI engines is a plasma system that provides for the simultaneous conversion of NO_x, UBHC and CO. The system features a surface plasma having low temperature, low pressure and low energy that could be packaged in a volume similar to a

conventional catalyst. The potential advantages of this system include a lower light-off temperature and an expanded range of operating temperature. Improving NO_x conversion efficiency while reducing the power consumption is a challenge of this emerging technology [311,369].

In order to assess the prospects of the GDI-powered vehicle for meeting the future emission regulations, Jackson et al. [136,137] predicted the vehicle emissions and fuel economy for various aftertreatment technologies using a driving-cycle simulation. The engine operating strategy was assumed to be as shown in Fig. 93(a). Multi-cylinder engine maps were constructed from steady-state emissions data that were obtained using a single-cylinder test engine. Adjustments were made in the cycle simulation for the effects of cold start and transient effects. The aftertreatment technologies considered in the simulation study and their conversion efficiencies (%) for the ECE/EUDC cycle are:

Aftertreatment technologies	Conversion efficiency (%)		
	UBHC	NO_x	CO
1. Underfloor three-way catalyst (UF TWC)	81/95	0/0	67/98
2. Close-coupled three-way catalyst (CC TWC)	90/95	0/0	85/98
3. Item 2 + NO_x catalyst (CC TWC + NO_x CAT)	90/95	40/50	85/98
4. Item 2 + NO_x trap (CC TWC + NO_x TRAP)	90/95	70/80	85/98.

The emission prediction results for the ECE + EUDC cycle are shown in Fig. 93(b). It was reported that with EGR and a close-coupled three-way catalyst the GDI vehicle has a reasonable engineering margin for meeting the EURO II (current) standard. To meet the EURO III (2000) standard with an engineering margin, however, would require EGR, a close-coupled three-way catalyst, and a 40–50% efficient $DeNO_x$ aftertreatment system. Meeting the EURO IV (2005) emissions standard would require EGR, a close-coupled three-way catalyst, and a 70–80% efficient $DeNO_x$ aftertreatment system. In addition, light throttling would be required to control engine-out UBHC emissions.

Andriesse et al. [190] reported that a GDI engine operating in the stoichiometric, homogeneous-charge mode is able to provide a fuel economy benefit of 7–10% while lowering NO_x emissions by at least 50%. This allows the EURO II emissions standard to be met with a conventional three-way catalyst system. The stratified GDI engine provides a 15–20% enhancement in fuel economy, but requires a lean NO_x catalyst with an efficiency of 80% to meet the EURO III standard, and an efficiency of 90% to meet the EURO IV standard.

In summary, it is apparent from the current literature that the attainment of regulatory levels of NO_x emissions is one of the major challenges facing GDI engine developers, particularly in the North American market [323].

5.2.3. Particulate emissions

In general, particulate matter (PM) is defined as all substances, other than unbound water, which are present in the exhaust gas in the solid (ash, carbon) or liquid phases. Engine particulates basically consist of combustion-generated, solid carbon particles, commonly referred to as soot, that result from agglomeration or cracking, and upon which some organic compounds have been absorbed. The carbon particles become coated with condensed and absorbed organic compounds, including unburned hydrocarbons and oxygenated hydrocarbons. The condensed matter can be comprised of inorganic compounds such as sulfur dioxide, nitrogen dioxide and sulfuric acid.

The size distribution of an exhaust aerosol from an engine is reported to be trimodal, with particle sizes ranging from several nanometers to several microns [233,234]. Both the peak magnitude and the shape of the size distribution curve change dramatically with engine type and operating condition. The complete size range is most effectively divided into three regions, or modes, that have physical significance. The three modes that are used in the literature to describe the particulate size distribution are the nuclei, accumulation and coarse modes. The nuclei mode is generally considered to be comprised of particles with equivalent diameters of less than 50 nm. The particles in this mode are primarily formed during combustion and dilution, usually by means of both homogenous and heterogeneous nucleation mechanisms. This mode normally contains the largest number of particles, thus dominating the number-weighted size distribution, but having an insignificant impact on the mass-weighted size distribution. The second region is denoted as the accumulation mode, and consists of particles having an equivalent diameter in the range from 50 to 1000 nm. These particulates are generally formed through the agglomeration of nuclei mode particles, and may contain a layer of condensed or absorbed volatile material. The particles in the accumulation mode normally contribute only a modest amount to the total number-weighted size distribution, but are generally the most significant in the mass-weighted size distribution. The third region, denoted as the coarse mode, is comprised of particulates having an equivalent diameter larger than 1000 nm. These particles are generally not a direct product of the combustion process, but are normally formed from the deposits on the valves and chamber walls that occasionally leave the solid surfaces and enter the exhaust system. The number density of the coarse mode particles is generally quite low, but can, under some conditions, influence the mass-weighted size distribution. The significance of each mode is, to some degree, dependent on the specific particulate emissions regulations. The US Environmental Protection Agency (EPA) has regulated PM emissions using mass-weighting, and its PM_{10} designation includes all particulate matters having equivalent

diameters of less than 10 μm. The new EPA "fine particle", or $PM_{2.5}$, standard includes all particles having equivalent diameters of less than 2.5 μm. This indicates the heightened interest in smaller particles that is reflected in the evolution of PM emissions standards. For particulates from diesel engines, only particles in the size range above 100 nm in diameter were found to have any significant effect on the mass-weighted PM_{10} and $PM_{2.5}$ mean values, and nuclei mode particles were found to have little or no effect on the mass-weighted distribution regardless of the number density [233].

Historically, gasoline engines have been exempt from the requirement to meet the particulate emissions standard for diesel engines. The justification for this has been that gasoline engines produced particulate emissions that were on the order of only 1% of those diesel engines. This was certainly the case prior to the advent of recent diesel particulate legislation [235]. Recent studies indicate that current gasoline SI engines often emit an increased fraction of nanoparticles even though steady-state particulate number emissions are generally several orders of magnitude lower than those from modern diesel engines [234,236]. Particulate number emissions from gasoline engines have also been shown to increase significantly when operated under high-load, transient and cold-start conditions. It was reported by Graskow et al. [236] that, unlike the PM emissions from diesel engines, the particulate emissions from PFI engines are quite unstable. Typically a stable baseline concentration of engine-out PM emissions is on the order of $\times 10^5$ particles/cm^3; however, a "spike" in the PM emissions is occasionally observed. These spikes are found to be composed of nearly 100% volatile particles of less than 30 nm in diameter, and can exhibit number densities exceeding 100 times that of the baseline concentration. An analysis of particulates from PFI engines by Andrews et al. [235] revealed that the bulk of the mass is ash, with the second largest fraction being unburned lubricating oil. Carbon emissions were found to be significant only at high load with mixture enrichment, whereas, at other operating conditions, carbon was reported to comprise less than 10% of the total PM mass. The large ash fraction of the gasoline PM emissions were found to include a large fraction of metal compounds, with calcium and sodium evident for operation at low load without EGR, and copper and magnesium predominant for operation with EGR.

Preliminary research indicate that GDI engines, as evolving powerplants for automotive applications, may emit a larger amount of particulates than do conventional PFI engines, especially during stratified-charge operation. Depending on the degree of combustion system optimization, smoke emissions from prototype GDI engines could be as high as 1.2 BSU [100,101,210]. A comparison of the particulate emissions for a current PFI SI engine, a current production GDI engine and a 1995 European IDI diesel engine for the US FTP cycle is illustrated in Fig. 94(a) These data represent mass measurements of particulate matter collected on filter media. It may be seen that the level of PM emissions for the GDI engine is between those of the diesel and PFI SI engines. As reported by Maricq et al. [237], the PM emissions from a vehicle powered by a GDI engine are on the order of 10 mg/mile. In comparison, the PM emissions from a comparable diesel-powered vehicle are on the order of 100 mg/mile. As compared to the 1–3 mg/mile PM emissions from a model PFI engine [235,237], the PM emissions from current production GDI engines are relatively high, even though they are well below the current US standard of 80 mg/mile as measured on the FTP test cycle. In interpreting this published comparison, it should be noted that both the PFI and GDI engines have been developed and mass-produced without major specific efforts being directed towards the minimization of particulate emissions.

Graskow et al. [238] measured the particulate emissions from a 1998 Mitsubishi GDI engine using a chassis-dynamometer test. It was reported that the average polydisperse number concentration was on the order of $\times 10^8$ particles/cm^3 and that the number-weighted, geometric mean particle diameter was from 68 to 88 nm. In contrast, modern PFI engines tested by the same authors [234,236] emit average particulate number concentrations ranging from 10^5 particles/cm^3 at light load to 10^7 particles/cm^3 at high load. Older PFI engines have been shown to emit number concentrations in excess of 10^8 particles/cm^3 for conditions corresponding to highway cruise operations. It was also reported that, for the operating conditions tested, the number-weighted, geometric mean diameters of the particulate matter emitted from the GDI engine are larger as compared to the PFI engines tested. This relatively large mean particle size is likely to increase the particulate mass emissions from the GDI engine, but could also lead to a decrease in the relative fraction of particles emitted in the nanoparticle size range.

Maricq et al. [237] investigated the PM emissions from a 1.83L, four-cylinder, four-valve production GDI engine for a range of operating conditions. As illustrated in Fig. 94(b), the particle number emissions are found to increase by a factor of 10–40 when the operating mode of the GDI engine is stratified-charge instead of homogenous-charge. The emissions of particulate matter exhibit a strong dependence on the GDI injection timing, and it was observed that the particle number and volume concentrations increase markedly as the injection timing is retarded. Advancing the spark timing generally yields an increase in both the particle number concentration and the mean particle size for both homogeneous and stratified-charge operation. An increase in the engine speed and load generally leads to an increase in PM emissions; however, this trend is dependent on the injection timing for stratified-charge operation. Based upon a chassis-dynamometer test that emulated the FTP test cycle, it was found that the PM emissions exhibit very substantial fluctuations, with a strong correlation existing between vehicle acceleration and the observed increases in PM emissions. These increases are theorized to occur

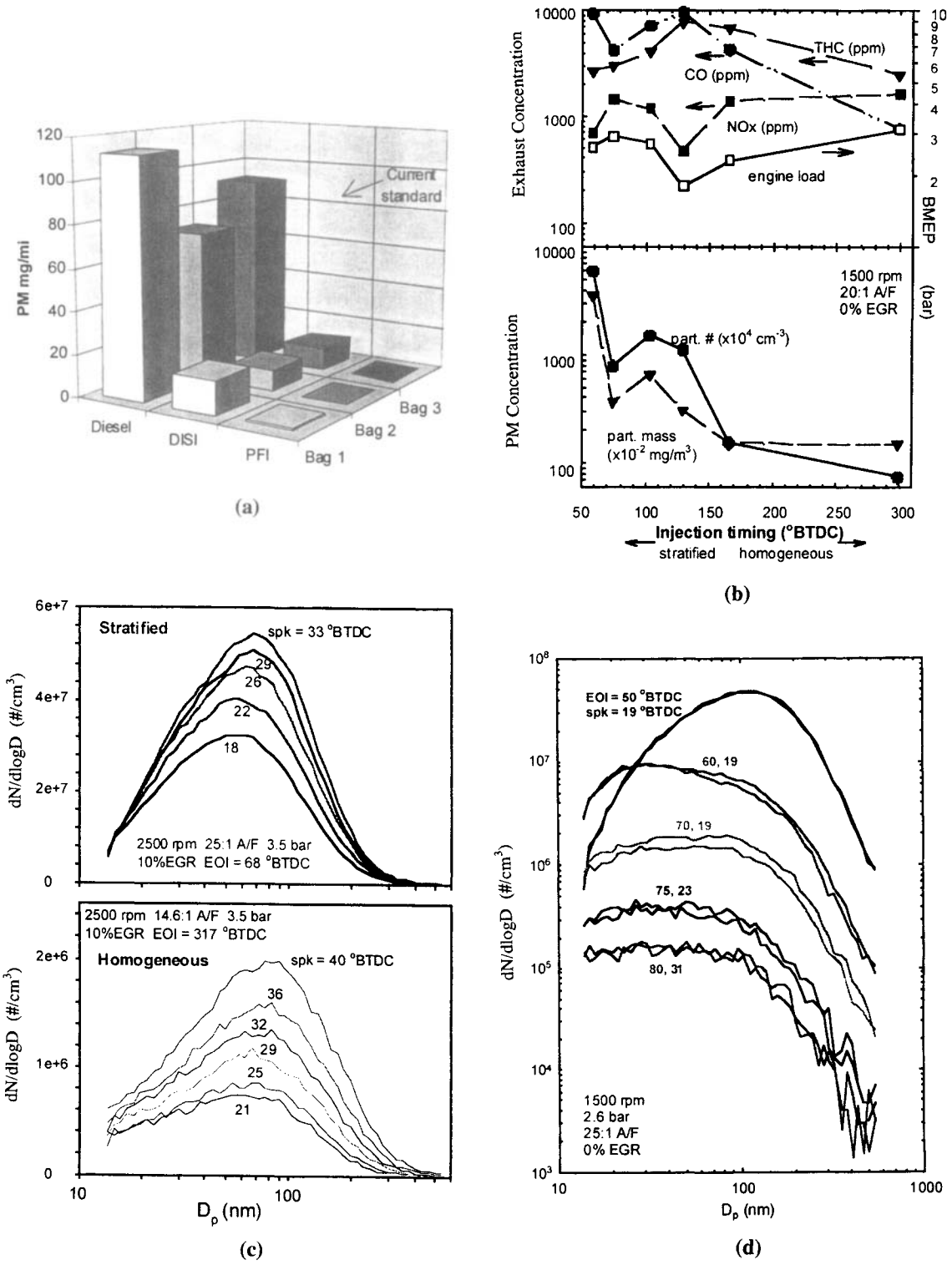

Fig. 94. PM emissions from GDI engines [237]: (a) comparison of FTP PM emission rates for a diesel, GDI and PFI vehicles; (b) PM, CO, UBHC, and NO_x emissions as a function of fuel injection timing (EOI); (c) particle size distributions as a function of fuel injection timing (EOI); and (d) particle size distribution as a function of spark timing.

because both the exhaust flow and the PM concentration in the exhaust gas increase with the added load needed to accelerate the vehicle. The observed PM concentration increases during the FTP test cycle were well correlated with changes from homogeneous-charge to stratified-charge operation. The particulates were in the size range from 15 to 600 nm, with the bulk of the particles being in the range of 50–100 nm. The measured number concentration was on the order of $\times 10^6$ particles/cm^3 for homogeneous operation, and $\times 10^7$ particles/cm^3 for stratified-charge operation.

As is evident from the experimental results illustrated in Fig. 94(b), operating a GDI engine in the stratified-charge mode has a significant effect on the overall particulate emissions. The PM emissions for this mode are found to vary significantly with small changes in the engine operating point. It was theorized that particulate matter can result from two types of rich combustion; that of a locally rich, gaseous air–fuel mixture and that of the diffusion burning of incompletely volatilized, liquid fuel droplets. The burning of liquid fuel droplets was reported to be an important source of PM emissions for late injection timing. For homogeneous-charge operation, the PM mass emissions remain quite independent of fuel injection timing, but the PM number concentration decreases monotonically as the injection timing is advanced. As illustrated in Fig. 94(c), the particle size distribution for homogeneous charge operation has an asymmetric shape. The peak in the distribution shifts slightly from about 70 nm for a spark timing of 21° BTDC to a value of 85 nm for a spark advance of 40° BTDC. These tends suggest that more nuclei mode particles are formed as the park is advanced, possibly due to faster nucleation and coagulation rates at the higher peak temperatures. Further, the post-flame oxidation rate will be slowed due to the decrease in the exhaust gas temperature as the spark timing is advanced. All of these factors contribute to the observed increase in peak particle number and mean particle size as the spark is advanced. For homogeneous-charge operation, the trend in particulate emissions with load was found to be quite similar to that measured for a PFI engine.

It is quite evident from the literature that the reduction of particulate emissions from GDI engines is an important research area. The specific processes of particulate generation for homogeneous-charge and stratified-charge operation need to be better understood, and more testes under carefully controlled conditions are required. The understanding that is gained will provide the ability to model, predict and control the processes that result in particulate matter, which will lead to significant reductions in the PM emissions of GDI engines.

6. Specific combustion systems and control strategies

6.1. Early research engines

Operating with a single, fixed ignition location imposes very stringent requirements on the mixture preparation process in GDI engines, as it is very difficult to provide a combustible mixture at the spark gap over the entire engine operating map. That is why most combustion control strategies are primarily directed towards the specifics of preparing and positioning the air–fuel mixture. A stratified-mixture region of repeatable location and charge distribution is important for achieving the fuel-economy potential of a GDI combustion system design. Stable stratification can be most easily achieved by using a divided chamber in which a subvolume and the main combustion chamber provide well-separated mixture regions. One of the better-known production applications of this technique is the combustion chamber geometry of the Honda compound vortex combustion chamber (CVCC) engine [378]. Although this is not a direct-injection engine, it is an early example of a production combustion system that operated with mixture stratification. For this combustion system, which is illustrated in Fig. 95, a secondary mixture preparation system feeds a fuel-rich mixture through an auxiliary intake valve into a pre-chamber containing the spark plug. A lean mixture is supplied to the main combustion chamber through the main fuelling system. After combustion is initiated in the pre-chamber, a rich burning mixture issues as a jet through an orifice into the main chamber, both entraining and igniting the lean main-chamber charge. This engine uses the flame-jet ignition technique, which can extend the operating limit of conventional SI engines to mixtures that are too lean to ignite with a spark. The disadvantage of flame-jet ignition is that increased wall heat losses and throttling losses between the pre-chamber and the main combustion chamber reduce the engine combustion efficiency. Additionally, such systems can only be operated at overall lean air–fuel ratios, thus limiting the maximum power output.

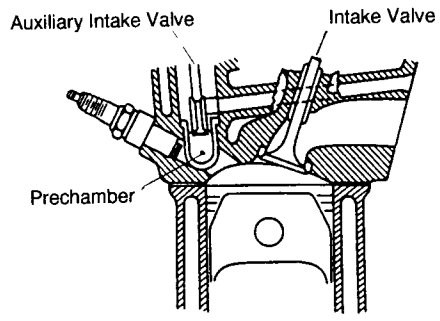

Fig. 95. Schematic of the Honda CVCC combustion system [378].

The concept of the direct-injection of gasoline in an SI engine is certainly not new. Early in 1954, the Benz 300SL [379] utilized the direct-injection system to solve a performance deficiency problem associated with the use of a carburetor. This is one of the first generation GDI engines as categorized by Iwamoto et al. [50] and is illustrated in Fig. 96. This GDI engine used early fuel injection to achieve a homogeneous air–fuel mixture.

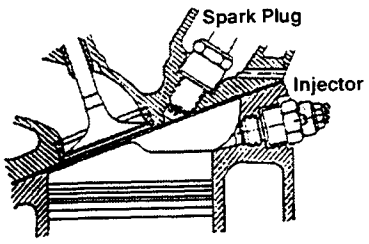

Fig. 96. The Benz 300SL GDI combustion system [379].

During the time frame from 1960 to 1978, numerous GDI systems were proposed to explore the potential of this type of engine. These are classified by Iwamoto et al. [50] as the second generation of GDI engines. A number of these engines utilized jet–wall interaction and film evaporation to achieve charge stratification by controlling the fuel distribution in an open chamber. An example of this type of combustion system is the MAN-FM system [10,11], which is shown schematically in Fig. 97. Extensive testing led to the conclusion that the MAN-FM system has the disadvantages of the increased wall heat losses, as well as increased UBHC and soot emissions. Also as is the case for the CVCC divided chamber, only stratified-charge operation is possible. Even if the elevated compression ratio of the MAN-FM engine is taken into consideration, the engine specific power is still limited when compared to homogeneous, stoichiometric operation of the conventional PFI engine.

Other GDI engines using a close proximity between the fuel injector and the spark gap were developed in the period from 1970 to 1979. The well-known systems that place the ignition source directly in the periphery of the fuel spray are the Ford PROCO [14] and the Texaco TCCS [9] systems.

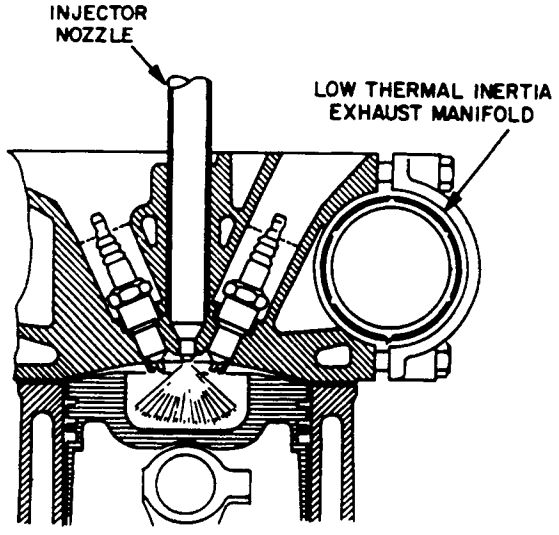

Fig. 98. The Ford PROCO combustion system [14].

The combustion concepts of these two systems are illustrated in Figs. 98 and 99. The centrally located injector provides a hollow-cone fuel spray that is stabilized by a strong air swirl (Ford PROCO), or provides a narrow jet tangentially into a piston bowl with air swirl motion (TCCS). In both cases ignition stability is achieved primarily by the close spatial and temporal spacing of injection and ignition. The PROCO system with a swirl-stabilized central plume allows slightly longer ignition delays than does the TCCS system; however, unfavorable mixture ignition conditions occur when crossflow velocities are high. The Texaco TCCS system may be regarded as a classic

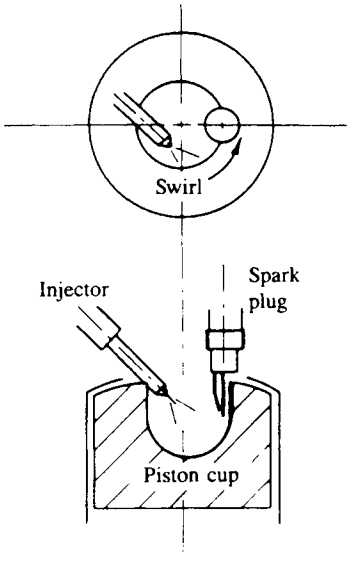

Fig. 97. The MAN-FM combustion system [10].

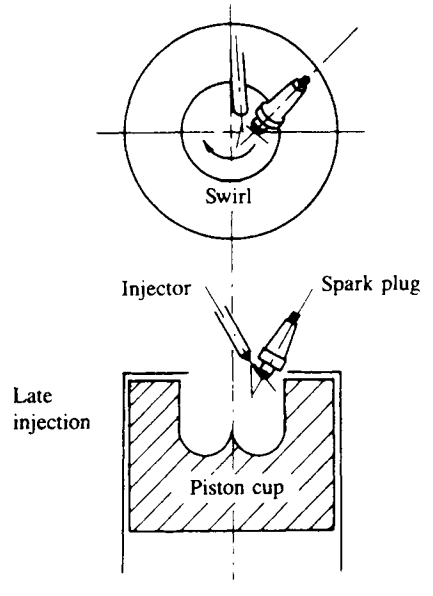

Fig. 99. The TCCS combustion system [9].

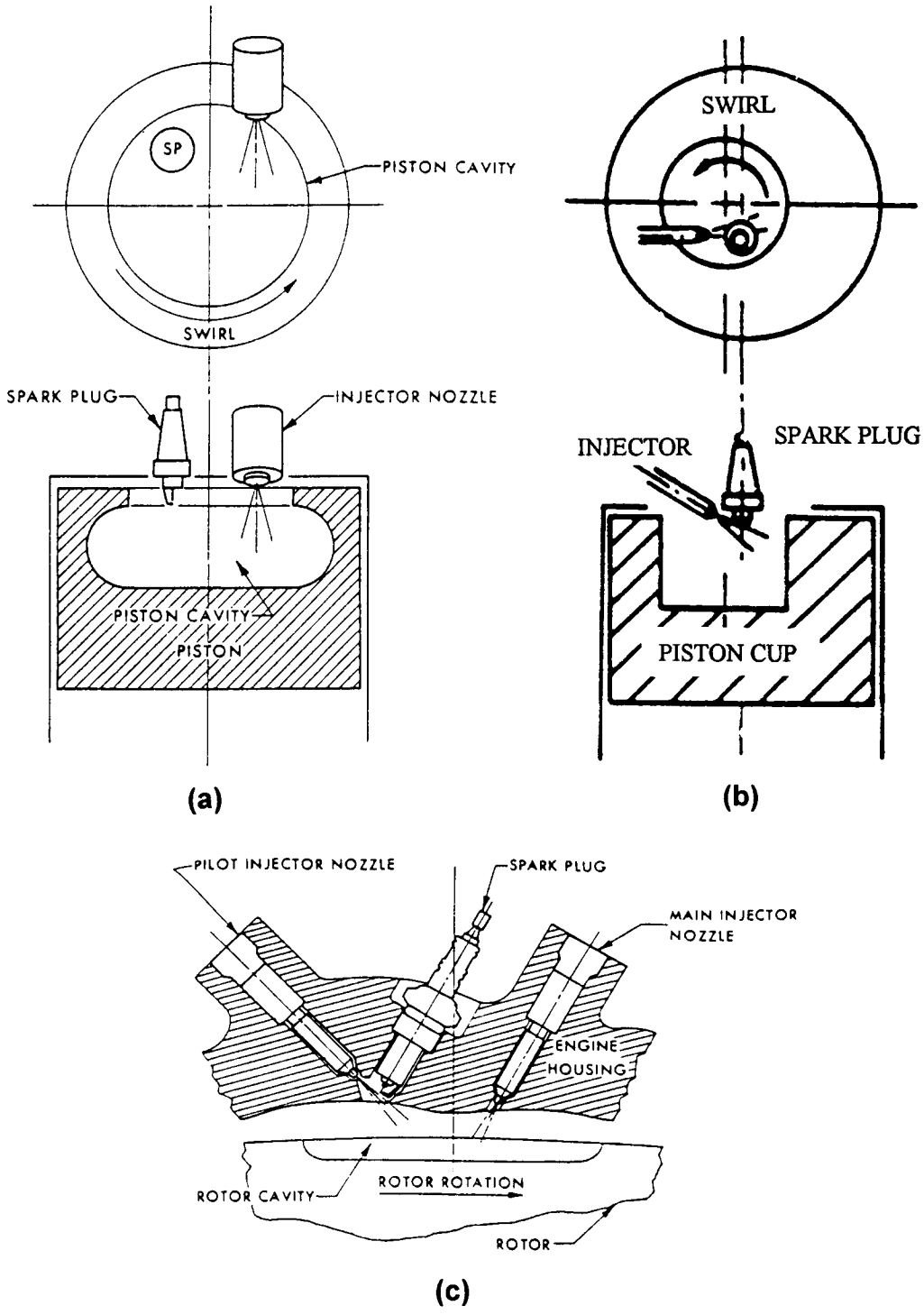

Fig. 100. Other DISC combustion systems: (a) MCP [239]; (b) International Harvest–White [240]; and (c) SCRC [241].

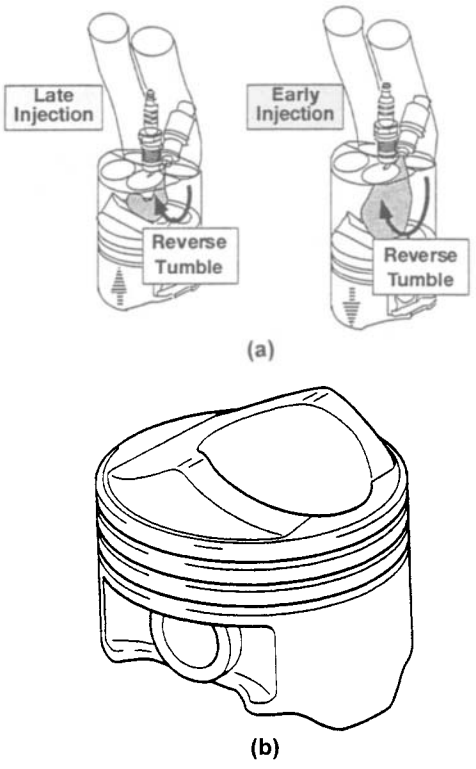

Fig. 101. Schematic of the Mitsubishi GDI combustion system [20]: (a) fuel injection strategies; and (b) piston geometry.

representative of a fully stratified combustion system, whereas the Ford PROCO combustion system was purposely designed with the objective of matching the specific output of the pre-mixed-charge engine using high EGR rates. The PROCO stratified-charge engines employed an injection system with an operating fuel pressure of 2 MPa, with injection occurring early in the compression stroke, while the TCCS engines utilized a high-pressure, diesel-type injection system. Although the minimum BSFC values of both of these engines were quite good, the control of UBHC emissions was extremely difficult for light-load operation. NO_x emissions were controlled using EGR rates of up to 50%. Even with this level of EGR, the NO_x emissions for both the PROCO and TCCS systems significantly exceeded the current emission standards, thus the use of a lean-NO_x catalyst would be required if these combustion strategies were to be implemented today. The power output of the late-injection TCCS system was also soot-limited. Further studies of stratified-charge engines have shown that high air swirl is desirable for obtaining the required level of fuel–air mixing, and that high-energy ignition sources enhance the multi-fuel capability. In spite of significant measures to reduce autoignition and maximize air utilization, these engines were not able to achieve the specific power output of then-current PFI engines. Additional GDI engine concepts from the 1970s that are based upon different geometric combinations of fuel spray plume and spark gap, such as the Mitsubihsi combustion process (MCP) [239], International Harvester and White Motors (IH–White) [240], and Curtiss–Wright stratified charge rotary combustion (SCRC) [241] are shown in Fig. 100(a)–(c), respectively.

A direct-injection combustion system for both GDI and DI diesel engines that operates by injecting fuel onto a central pedestal in a piston cavity was developed by Kato et al. [242,243]. In this combustion system, fuel is injected by a single-hole nozzle against the flat surface of the pedestal. The fuel deflects orthogonally and symmetrically in a disk shape and forms the air–fuel mixture. As the result of having a comparatively rich mixture present in the vicinity of the pedestal, and of initiating ignition at the center of the rich mixture, stable combustion is achieved. As the air–fuel mixture is always formed near the pedestal, there is little fuel in the squish area. Therefore, it is possible to prevent end-gas detonation in GDI applications and it is claimed that this type of engine can be operated at compression ratios of up to 14.5 on gasoline. With this combustion system, however, the UBHC emissions are found to be very high, which represents a significant development problem [244].

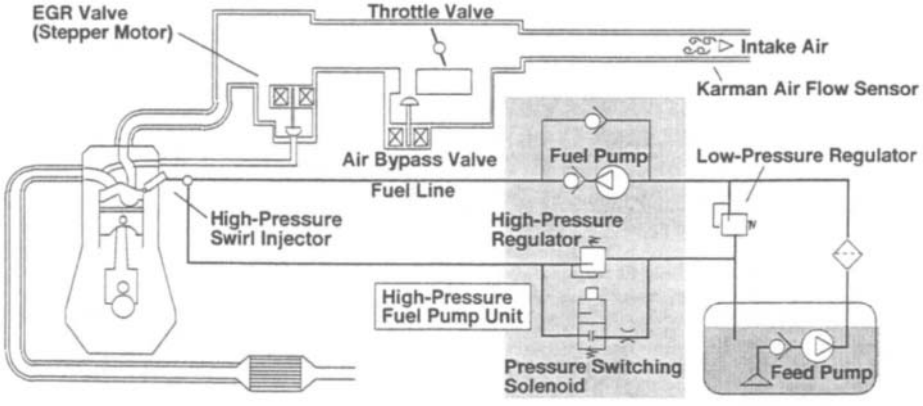

Fig. 102. The Mitsubishi GDI engine system layout [50,51].

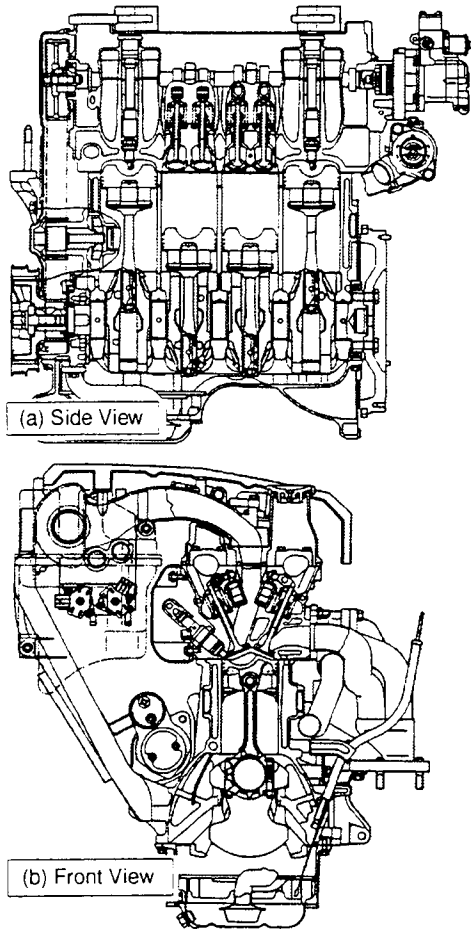

Fig. 103. The cutaway of the Mitsubishi I4 GDI engine [194].

Many new mixture-preparation and combustion-control strategies for direct-gasoline-injection, four-stroke, spark-ignition engines have been proposed and developed since 1990 by automotive companies, fuel system manufacturers and research institutions. Currently, five automotive companies have already put this engine technology into production in both the Japanese and European markets. These types of engines are classified as third-generation GDI engines [50]. Based on the information available in the literature, the key features of these specific GDI engines that have been developed during this recent time period are briefly summarized in Table 2 and the details of some of these combustion systems are given below.

6.2. Mitsubishi combustion system

The Mitsubishi GDI combustion system was discussed in detail by Kume et al. [20], Ando et al. [15–19], Kuwahara et al. [49,134,207,245,246], Kamura and Takada [194], Iwamoto et al. [50,51], Yamamoto et al. [247], Yamaguchi [248–251,370], McCann [46], Auer [252], Schreffler

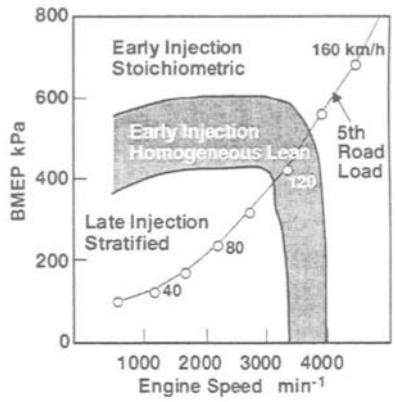

Fig. 104. The Mitsubishi GDI control map [50,51].

[253,352,353], Demmler [254], Lewis [328], Ward [364] and Treece [362]. The schematic of the engine layout, the engine cutaway, and the piston geometry are shown in Figs. 101–103. The combustion mode calibration is illustrated in Fig. 104. An early injection strategy is utilized for engine operation at high loads. In most of this zone, the engine uses a stoichiometric mixture and is operated at a slightly rich condition at full load. For the lowest-load conditions in this zone, the engine operates with a homogeneous, lean mixture for further improvement of fuel economy. The air–fuel mixture is in the range of 20–25. The first GDI engine that was launched in Japan in 1996 is based on the production 4G93 SI engine, using dual overhead camshafts, four valves per cylinder, in an inline four-cylinder configuration. The main differences from the 4G93 are the cylinder head and piston design, and a high-pressure fuel pump and injectors. In the Mitsubishi dual-catalyst system, the first catalyst uses pure iridium, which works during the lean period. A normal platinum catalyst is mounted downstream to catalyze the gases during non-lean periods. Mitsubishi's Galant and Legnum, the station wagon variant, are powered by this GDI engine. The fuel economy provided by the Mitsubishi 4G93 GDI engine was reported to show a significant improvement when compared to the comparable displacement, conventional PFI engine on the Japanese urban test cycle, while the 0–100 km/h acceleration time is enhanced by 5%. Due to the inherent in-cylinder charge cooling and improved intake port design, the volumetric efficient of the Mitsubishi GDI engine is increased by 5% over the entire engine operating range. In combination with an increased compression ratio of 12, the total power output is increased by 10% [50,51], which is shown in Fig. 105. The principal features of Mitsubishi 1.8L four-cylinder GDI system are:

- four cylinders;
- four-valve DOHC pentroof combustion chamber;
- bore × stroke : 81 × 89 mm;
- displacement—1864 cm^3;
- compression ratio—12:1;

Table 2
Key features of production, prototype and research GDI engines

Manufacturer	Displacement (cm^3)	Bore × stroke (mm)	No. of cylinders	Valves per cylinder	Compression ratio	Piston geometry	Charge motion	Injector location	Spark plug location	Fuel pressure (MPa)	Comments
Audi	1196		3	5		Bowl	Tumble	Intake side	Central	10	Prototype
Fiat	1995		4	4	12		Tumble, swirl	Central	Central		Prototype, homogeneous only
Ford	575	90.2 × 90.0	1	4	11.5	Flat	Tumble	Central	Central	5	Homogeneous only
Honda	1000		3	4		Bowl	Swirl	Central	Central		Prototype for hybrid application
Isuzu	528	93.4 × 77.0	1	4	10.7	Flat	Tumble, swirl	Central, intake side	Central	5	Homogeneous only
Isuzu	3168	93.4 × 77.0	V6	4	10.7	Flat	Tumble, swirl	Central, intake side	Central	5	Prototype, homogeneous only
Mazda	1992	83 × 92	4	4	11	Bowl	Tumble, swirl	Intake side	Central	7	Prototype
Mercedes	538.5	89 × 86.6	1	4	10.5	Bowl		Central	Central	Variable: 4–12	
Mitsubishi	1864	81 × 89	4	4	12	Bowl	Tumble	Intake side	Central	5	Production in Japan
Mitsubishi	1468	75.5 × 82	4	4	11	Bowl	Tumble	Intake side	Central	5	Production in Japan
Mitsubishi	3496	93 × 85.8	V6	4	10.4	Bowl	Tumble	Intake side	Central	5	Production in Japan
Mitsubishi	1864	81 × 89	4	4	12.5	Bowl	Tumble	Intake side	Central	5	Production in Europe
Mitsubishi	4500		V8	4		Bowl	Tumble	Intake side	Central		Prototype
Nissan	1838	82.5 × 86	4	4	10.5	Bowl	Swirl	Intake side	Central	10	Prototype
Nissan	1769	80 × 88	4	4	10.5	Bowl	Swirl	Intake side	Central	7	Production in Japan
Nissan	2987	93 × 73.3	V6	4	11	Bowl	Swirl	Intake side	Central	Variable: 7–9	Production in Japan
Nissan	2500		V6								Prototype for hybrid application
Orbital	1796	80.6 × 88	4		10.4					Fuel: 0.72; air: 0.65	Prototype, air-assisted
Renault	2000		4	4		Bowl	Tumble	Central	Production in Europe, homogenous only	5–10	Production in Europe, homogenous only
Subaru	554	97 × 75	1	4	9.7	Bowl	Tumble	Central	Intake side	7	
Toyota	1998	86 × 86	4	4	10	Bowl	Swirl	Intake side	Central	8–13	Production in Japan

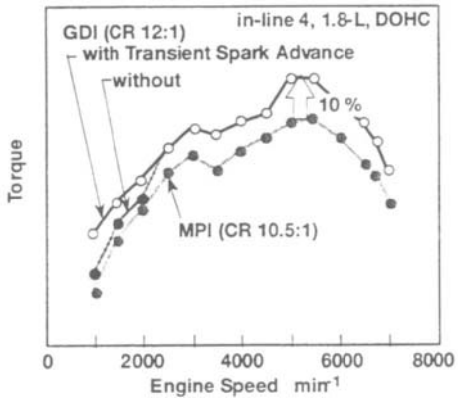

Fig. 105. Full load performance of the Mitsubishi GDI engine [50,51].

- central spark plug;
- a spherical compact piston cavity to redirect the mixture plume to maintain charge stratification;
- intake port—up-right straight intake ports to generate an intense tumble with a direction of rotation opposite to that of the conventional horizontal intake ports of PFI engines;
- intake tumble ratio—1.8;
- injector located underneath intake port and between two intake valves;
- high-pressure, swirl injector with a tangential slot-type swirler;
- common-rail fuel system using a fuel rail pressure of 5 MPa;

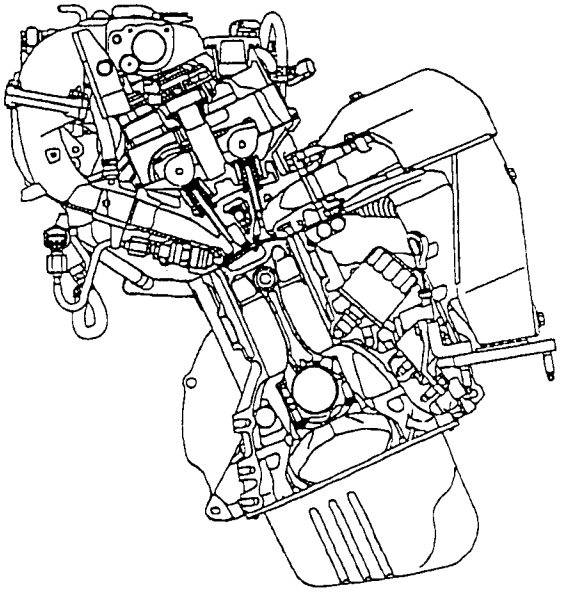

Fig. 106. Cutaway view of the Toyota GDI D-4 engine [41].

- air control—throttle valve with electronic air-by-pass valve for smooth transition between different operating modes;
- ignition system—60 mJ in energy and narrow-gap platinum plug;
- part-load mode—late injection at the air-fuel ratio of up to 40:1;
- high-load mode—early injection;
- NO_x reduction—electric EGR system at a maximum rate of 30% and selective-reduction lean-NO_x catalyst;
- EGR control—achieved by an EGR valve actuated by a stepping motor;
- octane requirement—92 RON;
- engine idle speed—600 rpm;
- power—112 kW JIS net at 6500 rpm;
- torque—128 N m at 5000 rpm.

The main specifications of the Mitsubishi 1.5L four-cylinder combustion system are:

- four cylinders;
- four-valve DOHC pentroof combustion chamber;
- bore × stroke—75.5 × 82 mm;
- displacement—1468 cm^3;
- compression ratio—11:1;
- common-rail fuel system;
- design fuel pressure—5 MPa;
- octane requirement—unleaded regular gasoline.

The main specifications of the Mitsubishi 3.5L V6 combustion system are:

- six cylinder V engine;
- bore × stroke—93 × 85.8 mm;
- displacement—3496 cm^3;
- compression ratio—104:1 to allow the use of regular grade, unleaded gasoline (premium grade recommended);
- fuel rail design pressure—5 MPa;
- spark plug—a large protrusion into the chamber;
- intake system—a variable length induction system for improving low- and middle-speed torque;
- power—180.2 kW JIS at 5500 rpm;
- torque—343.1 N m at 2500 rpm.

Mitsubishi introduced the 1.8L inline four-cylinder GDI engine into European market in 1997. The major differences of this European version from that of the Japanese version are:

- The compression ratio was increased from 12:1 to 12.5:1.
- The injector mounting is more vertical in order to target the spray towards the center of the bowl in the piston. This reduces the variation in spray targeting with injection timing, promoting a stable, combustible mixture over a wider operating window.
- The Japanese GDI engine was tuned to give the best fuel savings at idle speeds while the European version is tuned to optimize the highway fuel economy.

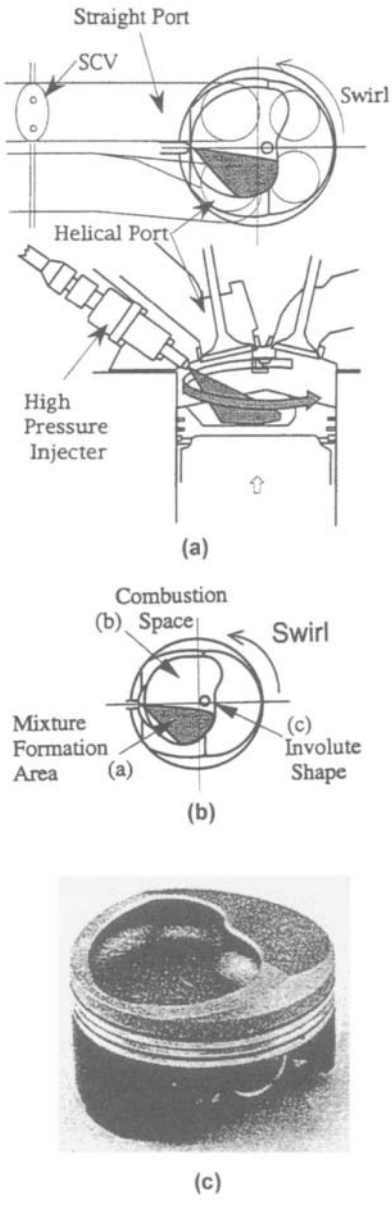

Fig. 107. Combustion chamber configuration of the Toyota GDI engine [41].

- The crossover point of the European version from lean (40) to normal (14.5) air–fuel ratio was increased from 2000 to 3000 rpm. The lean range vehicle speed is extended to highway cruise at 120–130 km/h.
- The intake manifold was extended from 265 to 400 mm to enhance the low-speed torque characteristics.
- A two-stage injection strategy, called two-stage mixing, was added to improve low-speed torque and suppress knock by injecting part of the fuel during intake stroke and the remaining portion during compression.
- A second two-stage injection strategy, called two-stage combustion, was employed during cold start for a more rapid catalyst light off by injecting a fraction of the fuel during the intake stroke and the remaining portion during expansion stroke.

The largest GDI engine so far developed by Mitsubishi is a 4.5L, 90°, V8 engine using 32 valves and four camshafts. The piston bowl is reported to be a slightly shallower than that in the original I4 and V6 GDI engines. Two high-pressure, single-plunger, injection pumps are utilized, one for each cylinder bank.

6.3. Toyota combustion system

The Toyota direct-injection combustion system has been described in several recent publications [21,22,41,43,60, 139,170,203,226,255–261,273,319,356,358,359,361,371]. The principal components and stratification concepts that are used in the GDI engine, which is designated as the D-4, are illustrated in Figs. 106–108. As shown in Fig. 107, a uniquely shaped cavity in the piston is employed. Zone (A) of the cavity is designed to be the mixture formation area, and is positioned upstream of the spark plug. The wider zone (B) is designed to be combustion space and is effective in promoting rapid mixing. The increased width in the swirl flow direction was reported to enhance the flame propagation after the stratified mixture is ignited. The involute shape (C) is designed to direct the vaporized fuel towards the spark plug. The intake system consists of both a helical port and a straight port, which are fully independent. An electronically activated SCV of the butterfly-type is located upstream of the straight port. When the SCV is closed, the resulting swirl ratio is reported to be 2.1. The helical intake port utilizes a variable-valve-timing-intelligent (VVT-i) cam-phasing system on the intake camshaft. These valves are driven by a DC motor so that the desired valve opening angle can be controlled according to the engine operating conditions. Fig. 109 shows the detailed SCV operating map. For light-load operation the SCV is closed, which forces the induction air to enter through the helical port, thus creating a swirling flow. Highly atomized fuel is injected into the swirling flow near the end of the compression stroke. The flow moves the rich mixture to the center of the chamber around the spark plug, while part of the fuel disperses into the air in the combustion chamber, forming a stratified air–fuel mixture. For heavy-load operation the SCV is opened, and the intake air is inducted into the cylinder with a lower pressure loss. The fuel is injected during the intake stroke, resulting in a homogeneous mixture. The main features of this GDI system are summarized as follows:

- four cylinders;
- four-valve pentroof combustion chamber;
- bore × stroke—86 × 86 mm;
- displacement—1998 cm^3;
- compression ratio—10:1;

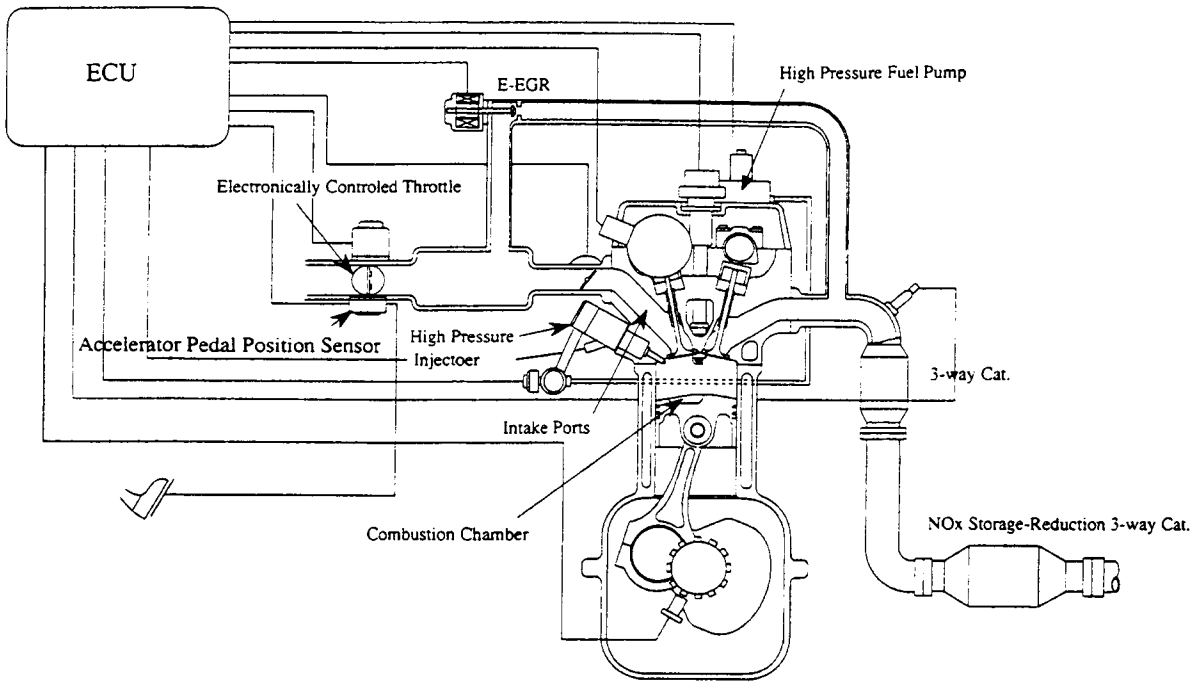

Fig. 108. Toyota GDI engine system [21].

- spark plug located slightly away from the center of the combustion chamber;
- piston and bowl—deep-bowl-in-asymmetrical-crown;
- intake port—one helical port with VVT-i system and SCV;
- injector located under the straight intake port;
- fuel injector—high-pressure swirl; two-stage injection; solid-cone spray;
- common-rail fuel system using a variable fuel rail pressure from 8 to 13 MPa;
- four-mode operation: stratified, semi-stratified, lean, and stoichiometric;
- part-load mode—late injection at the air–fuel ratio of up to 50;
- high-load mode—early injection;
- torque transition between stratified-charge and homogeneous-charge operations controlled by two-stage injection and an electronic throttle control system;
- NO_x reduction—electronically controlled EGR, NO_x storage-reduction catalyst, and standard three-way catalyst;
- NO_x storage catalyst regeneration frequency: once ever 50 s during lean operation;
- octane requirement—91 RON;
- power—107 kW at 6000 rpm;
- torque—196 N m at 4400 rpm.

As illustrated in Fig. 62, a special two-stage injection process is used for the transition between light-load and heavy-load operation. This process creates a weakly stratified mixture in order to achieve a smooth transition of torque from ultra-lean operation to either lean or stoichiometric operation. The Toyota D-4 GDI engine operates using four operating regimes having distinctively different mixture strategies and/or distributions. The first is stratified-charge operation using an air–fuel ratio range of 25–50. The vehicle operates in this ultra-lean zone under steady light-load, for road-loads of up to 100 km/h. The second operating regime is a transitional, semi-stratified zone with

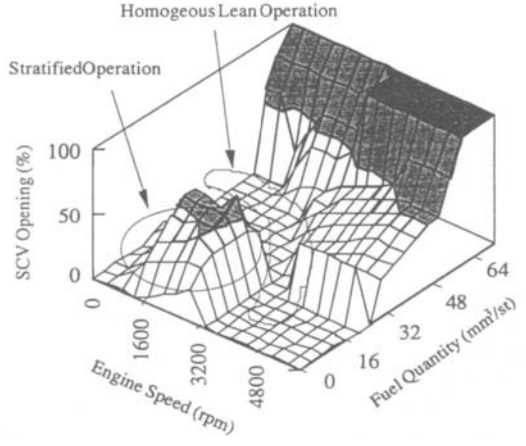

Fig. 109. Detailed SCV operating map of the Toyota GDI engine [21].

the air–fuel ratio ranging from 20 to 30. Within this zone, fuel is injected twice within each engine cycle, once during the intake stroke and once during the compression stroke. The third operating regime utilizes injection during the intake stroke to operate the engine in the homogeneous combustion mode using a lean air–fuel ratio of 15–23. The fourth regime is denoted as the stoichiometric power zone, and is similar to the third, except that the air–fuel ratio range is from 12 to 15. The common-rail fuel pressure is adjusted by the control system from 8 to 13 MPa in order to optimize the injection rate for short fuel pulse widths. It is also reported that another low-pressure fuel injector is employed in an auxiliary throttle body in order to enhance cold startability.

The Toyota D-4 GDI engine also incorporates an electronic-throttle-control system that was reported to reduce the harshness of torque transitions, thus improving the driveability. The VVT-i technology is used to maximize torque in the low to mid-speed ranges, and to maximize power at high speed. The VVT-i varies intake valve opening and closing by 20°. At low engine loads the intake valves are opened earlier, increasing the overlap between the intake and exhaust valves. This results in internal EGR, which was reported to increase the total EGR ratio while requiring less EGR from the external system. As a result, the VVT-i system also contributes to NO_x emissions reduction. With the VVT-i system and an increase in the compression ratio to 10:1, about 10% more torque is obtained from the D-4 engine in the low to mid-rpm ranges than is obtainable with the conventional PFI engine. With the electrically controlled throttle valve, the manifold vacuum pressure at the throttle valve is halved from 67 kPa for a conventional PFI engine to 39 kPa at idle. At a steady 40 km/h speed, it is only 11 kPa, which is very close to a wide-open throttle manifold vacuum.

The D-4 GDI engine, which is officially designated as the 3S-FSE, shares the basic dimensions of the conventional 3S-FE, dual-overhead-camshaft, four valves per cylinder, inline, four-cylinder engine that was first installed in the Japanese Corona Premio compact sedan. Two small converters, each with 0.5 L volume, are situated immediately downstream from the exhaust manifold. These catalysts have the function of keeping the exhaust temperature high enough for efficient operation of the 1.3 L underfloor catalytic converter. A lean-NO_x catalyst that is designed for NO_x storage and cleaning is used with the D-4 engine. This catalyst contains rhodium for storage and release, and platinum for cleaning, both on an alumina bed, and stores NO_x during periods of lean-burn operation. The stored NO_x is converted at intervals of 50 s during lean operation by utilizing very brief periods of stoichiometric operation. These required cleaning periods are less than one second, and degrade fuel economy by an estimated 2%. It is claimed that the emission levels of oxides of nitrogen are reduced by as much as 95% on the Japanese test cycle. The fuel economy of the D-4 engine, when utilized with a four-speed automatic transmission, is reported to be about 30% better than that of the conventional PFI engine. For operation on the Japanese urban 10/15-mode cycle, a fuel consumption of 17.4 km/l was achieved, as compared to 13 km/l for the conventional PFI engine. The vehicle acceleration was also reported to be improved by approximately 10%, reaching 100 km/h from a standstill in less than 10 s.

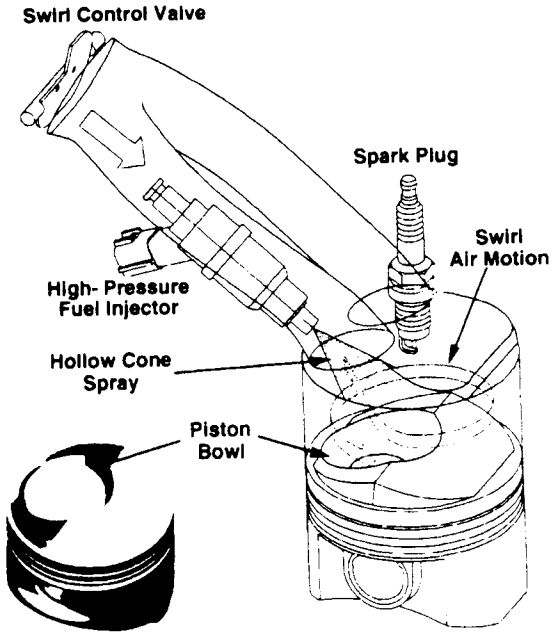

Fig. 110. The Nissan GDI combustion system [99].

6.4. Nissan combustion system

The Nissan GDI engine, NEODi (Nissan Ecology Oriented performance and Direct Injection), is designed with a centrally mounted spark plug; and with the injector located underneath the intake port and between the two intake valves [23–27,66,99,100,138,191,192,210,262–266,339,340,377]. The combustion chamber layout, engine and SCV control maps and system diagram are shown in Figs. 110–112. The engine can operate in both the stratified-charge mode and the homogeneous-charge mode, and a 30% reduction in cold-start UBHC emissions relative to the baseline PFI engine was reported. The engine could be operated with stable combustion using a mixture leaner than an air–fuel ratio of 40, resulting in a 20% improvement in fuel economy when compared with a baseline PFI engine that operates with a stoichiometric mixture. The principal features of the Nissan prototype I4 GDI combustion system are summarized as follows:

- four cylinders;
- four-valve pentroof combustion chamber;
- bore × stroke—82.5 × 86.0 mm;

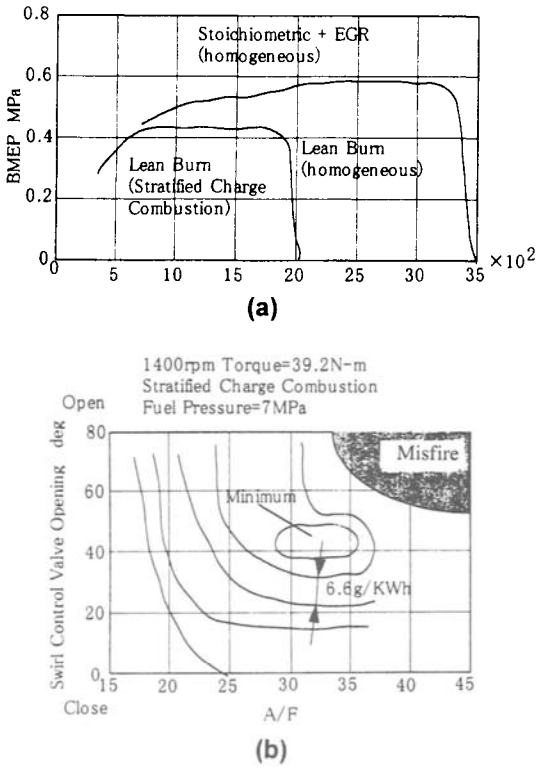

Fig. 111. The control map of the Nissan 1.8L Inline4 GDI engine and the detailed SCV operating map [191].

- displacement—1838 cm^3;
- compression ratio—10.5:1;
- centrally mounted spark plug;
- curved piston crown;
- conventional intake port design;
- reverse tumble obtained by masking the upper side of the intake valve;
- injector located between the intake valves and beneath the intake port, at an angle of 36° down from the horizontal plane;
- common-rail fuel system and swirl injector operating at a design pressure of 10.0 MPa;
- hollow-cone fuel spray with a cone angle of 70° and an SMD of 20 μm;
- part-load mode—late injection for stratified operation at an air–fuel ratio of up to 40:1;
- high-load mode—early injection for homogeneous operation.

The major features of the Nissan 3L, V6 production GDI engine that is installed in the Nissan Leopard for the Japanese market are as follows:

- six cylinder V engine;
- displacement—2987 cm^3;
- bore × stroke—93 × 73.3 mm;
- compression ratio—11:1;
- shallow dish-in piston crown;
- injector mounted between the intake valves and beneath the intake port;
- fuel injector—CASTING NET injector with an inclined injector mounting;
- common-rail fuel system using a design fuel rail pressure from 7 to 9 MPa;
- intake port deactivation for generating variable in-cylinder swirl;
- two-stage camshafts;
- power—171.5 kW JIS at 6400 rpm;
- torque—294 N m at 4000 rpm.

The piston crown incorporated a shallow dish that is designed to have minimum effect on the in-cylinder airflow field. This bowl design is intended to provide efficient combustion during homogeneous mode operation, as contrasted with piston crowns using deep bowls. However,

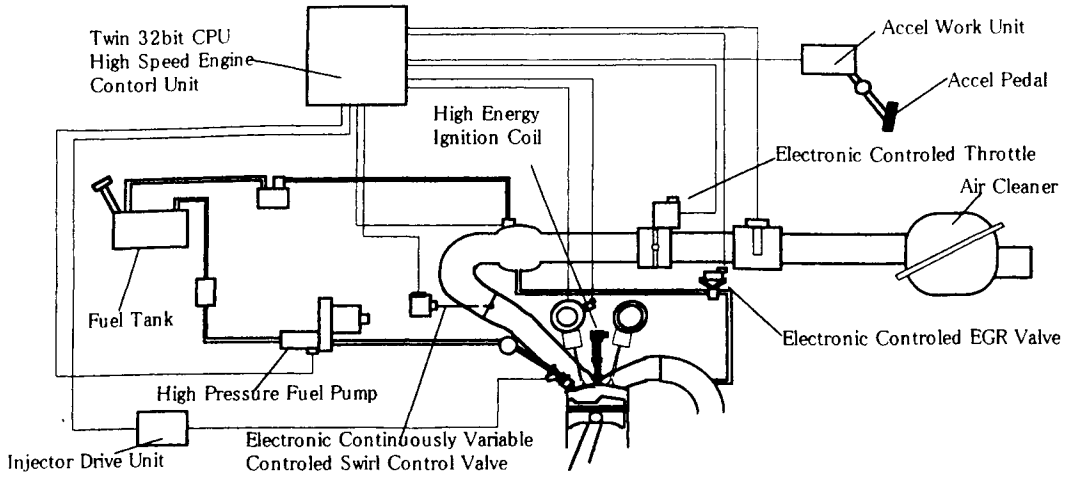

Fig. 112. The Nissan 1.8L Inline4 GDI engine system [191].

some difficult is encountered in controlling the air–fuel mixture for an ultra-lean combustion. It is confirmed that the CASTING NET injector has the capability of uniformly distributing fuel within the shallow dish in the piston crown.

The major features of the Nissan 1.8L, I4 production GDI engine are as follows:

- four cylinders;
- four-valve pentroof combustion chamber;
- displacement—1769 cm^3;
- bore × stroke—80 × 88 mm;
- compression ratio—10.5:1;
- shallow dish-in piston crown;
- injector mounted between the intake valves and beneath the intake port;
- fuel injector—CASTING NET injector;
- fuel injection pressure—0.3–7.0 MPa;
- intake port deactivation for generating variable in-cylinder swirl;
- engine used with CVT.

6.5. Ford combustion system

The prototype Ford GDI engine is designed to operate in the homogeneous, stoichiometric mode, and utlilizes a centrally located fuel injector and spark plug [40,48,69]. The schematic of the combustion chamber has been illustrated previously in Fig. 47. The intake ports of the four-valve, single-cylinder head were designed to yield the volumetric efficiency that would normally be expected with the smaller intake valve flow area. The main features of the Ford GDI combustion system are summarized as follows:

- single cylinder engine;
- four-valve, DOHC, pentroof combustion chamber;
- bore × stroke—90.2 × 90.0 mm;
- displacement—575 cm^3;
- exhaust/intake valve area ratio—0.77;
- compression ratio—11.5:1;
- in-cylinder flow: no net swirl, but small tumble component;
- near-centrally mounted spark plug;
- vertical, near-centrally mounted injector;
- high-pressure swirl injector;
- fuel pressure—5.0 MPa;
- homogeneous, early injection mode only;
- octane requirement—91 RON.

Fuel consumption improvements of up to 5% at part load and 10% at idle with stoichiometric operation were reported for steady-state operation of the Ford GDI engine. Optimum lean operation at part load provided a fuel consumption improvement of up to 12% when compared to Ford baseline PFI engine, whereas emissions were found to be comparable. An observed increase in UBHC emissions was attributed to the increased compression ratio. NO_x emissions were found to be lower than those of the PFI engine, which was attributed to the enhanced charge cooling and a higher residual gas content for the GDI engine.

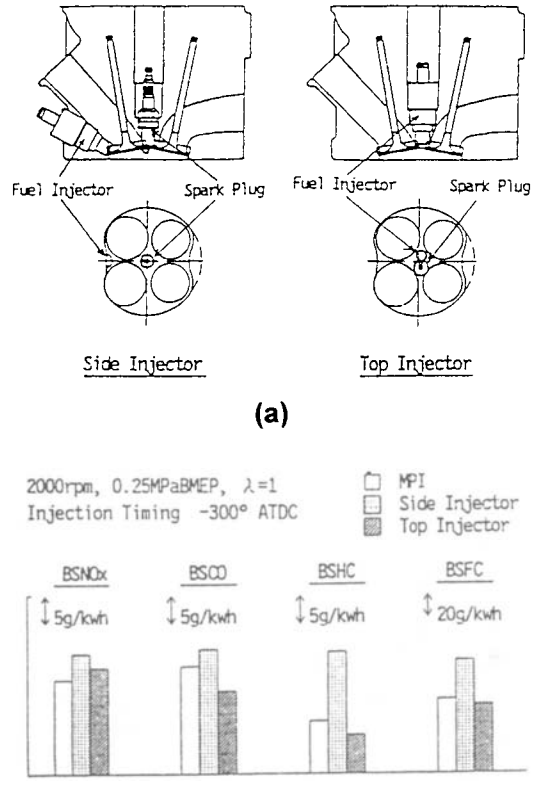

Fig. 113. The Isuzu GDI combustion system [181]: (a) configuration of combustion chamber; and (b) effect of the injector location on engine emissions.

6.6. Isuzu combustion system

A single-cylinder pentroof four-valve SI engine was converted to operate as a direct-injection gasoline engine [181]. This prototype/research engine has the provision for either a centrally mounted or a side-mounted fuel injector. Fig. 113(a) shows the combustion chamber geometry and the injector locations. A comparison of the engine performance variation with injector location was made between the center mounting and the side mounting positions. Fig. 113(b) shows the effect of injector location on the engine performance and emissions at part load. The center-mounted location exhibits a level of exhaust emissions (UBHC and NO_x) that is identical to that of the equivalent PFI engine when injection is completed by 60° ATDC on intake at an engine speed of 2000 rpm and an air–fuel ratio of 14.7. The side-mounting location exhibits an apparent increase in the UBHC emissions and fuel consumption as compared to the baseline PFI engine. This is considered to be the result of fuel impingement on the cylinder linear near the exhaust

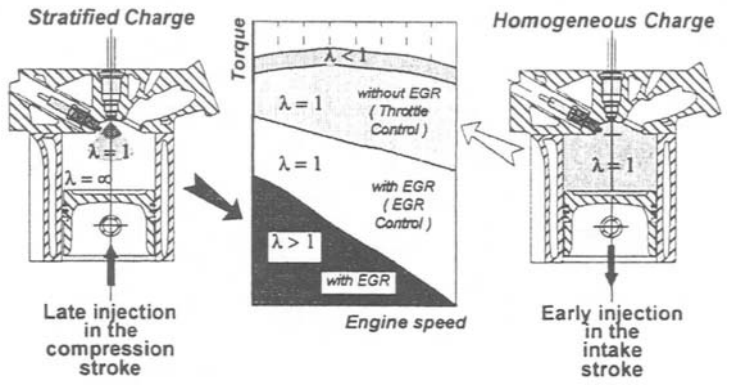

Fig. 114. The Mercedes-Benz GDI combustion system [193].

valve, with some of the fuel being absorbed in the oil film. For the center-mounting location the emissions and engine performance are quite similar to that of the PFI engine when the fuel is injected during the early portion of the intake stroke. Based upon this evaluation, the centrally mounted injector location was selected for the Isuzu V6 prototype GDI engine. Vehicle tests using this engine under cold-start condition were also conducted [182]. The principal features of the Isuzu GDI combustion system are summarized as follows:

- single cylinder and V6 engines;
- four-valve, DOHC, pentroof combustion chamber;
- bore × stroke—93.4 × 77.0 mm;
- displacement—528 cm^3 per cylinder;
- compression ratio—10.7:1;
- near-centrally mounted spark plug;
- flat piston crown;
- standard intake port: at a tumble ratio of 0.63 and a swirl ratio of 0.0;
- vertical, near-centrally mounted injector;
- high-pressure swirl injector to produce a spray with a cone angle of 40–60°;
- common-rail fuel system with a design rail pressure of 5 MPa;
- homogeneous, early injection mode *only*;
- intake valve opening—12° BTDC;
- intake valve closing—54° ABDC.

6.7. Mercedes-Benz combustion system

The Mercedes-Benz GDI combustion system has a vertical, centrally mounted, fuel injector [193]. The schematic of the combustion chamber and the control map are illustrated in Fig. 114. Dynamometer tests of the Mercedes-Benz GDI combustion system for a range of injection pressures from 4 to 12 MPa indicate that the fuel consumption, UBHC emissions and COV of IMEP are minimized at 8 MPa; however, the NO_x emission level was found to be maximized there. The data reveal that the combustion duration is the shortest at a fuel injection pressure of 8 MPa and that the corresponding 50% heat release point occurs before TDC on compression. In addition to the fuel economy improvement, engine-out NO_x emissions are reduced by approximately 35% as compared to a conventional PFI engine; however, the engine-out UBHC emissions are significantly higher. For the load range of 0.2–0.5 MPa IMEP, the minimum ISFC is obtained at an engine speed of 2000 rpm. It was claimed that at lower or higher engine speeds, the fuel consumption increases as a result of degradation in the mixture homogeneity. The specifications of the Mercedes-Benz prototype GDI combustion system are summarized as follows:

- single-cylinder, four-valve, pentroof engine;
- major portion of combustion chamber is formed by a bowl in the piston;
- bore × stroke : 89 × 86.6 mm;
- stroke to bore ratio—0.973;
- displacement—538.5 cm^3;
- compression ratio—10.5:1;
- intake valve inclination to deck—19.5°;
- spark plug located between the intake valves and in the immediate vicinity of the injector tip;
- axisymmetric-reentrant-bowl-in-piston centered on cylinder axis;
- vertical, centrally mounted injector;
- high-pressure common rail fuel system;
- variable fuel pressure from 4 to 12 MPa;
- cone spray with a geometric cone angle between 75 and 105°;
- part-load mode—late injection for stratified operation;
- high-load mode—early injection for homogeneous operation.

6.8. Mazda combustion system

The combustion system layout of the Mazda prototype GDI engine [141] is shown in Fig. 115. The major features of the engine are:

- four cylinder;

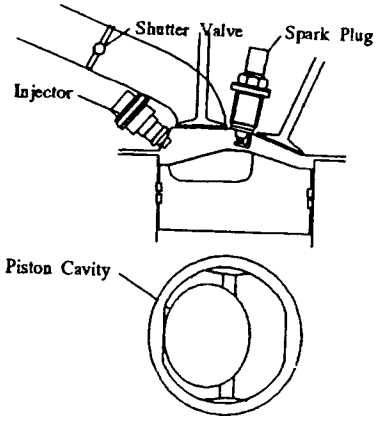

Fig. 115. The Mazda GDI combustion system [141].

- four-valve, DOHC pentroof combustion chamber with a smaller intake-side valve inclination angle;
- displacement—1992 cm^3;
- bore × stroke—83 × 92 mm;
- compression ratio—11:1;
- independent intake port with shutter valve for swirl generation;
- injector—intake side mounted, with an inclination angle of 36°;
- fuel pressure—7 MPa;
- fuel injector static flow rate—17 cm^3/s;
- spray characteristics—hollow-cone spray with a cone angle of 60° and an SMD of 20 μm.

6.9. Audi combustion system

The combustion chamber layout of the Audi 1.2L, three-cylinder prototype GDI engine [267,268] is shown in Fig. 116. The main features of this GDI system are:

- three cylinder, all-aluminum engine;
- five valves (three intake valves and two exhaust valves), pentroof combustion chamber;
- vertical straight intake port;
- centrally mounted spark plug;
- injector mounted between the intake valves and beneath the intake port;
- fuel injection pressure—10 MPa;
- spherical compact piston bowl;
- power—55 kW at 5500 rpm;
- torque—115 N m at 3000 rpm.

6.10. Honda combustion system

A schematic of the Honda 1.0L prototype GDI engine [183] is shown in Fig. 117. The engine specifications are:

- three-cylinder engine;
- 1.0 L total displacement;
- four-valve pentroof combustion chamber;

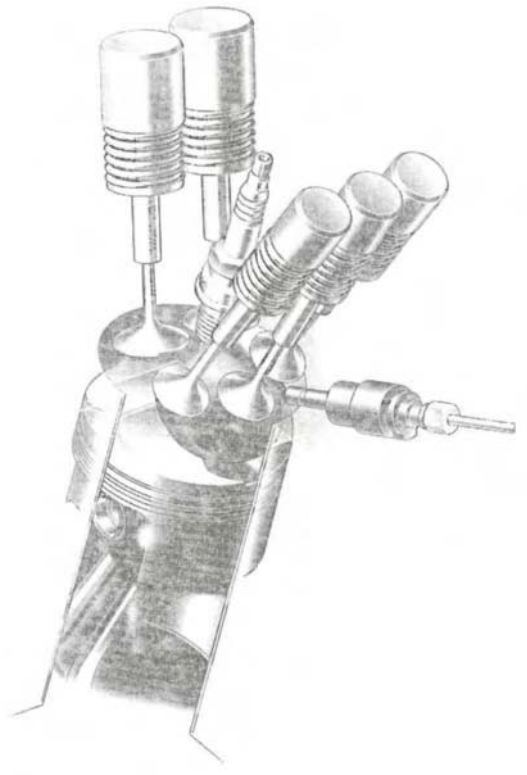

Fig. 116. The Audi GDI combustion system [268].

- centrally mounted fuel injector;
- inclined spark plug in close proximity to the injector;
- shallow bowl in piston crown;
- in-cylinder air swirl utilized.

This engine was designed for a hybrid-vehicle application.

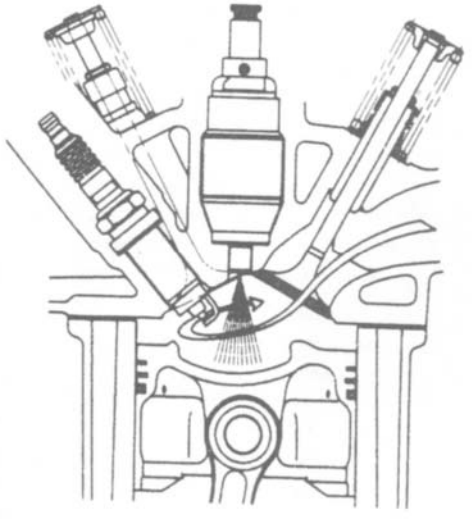

Fig. 117. The Honda GDI combustion system [183].

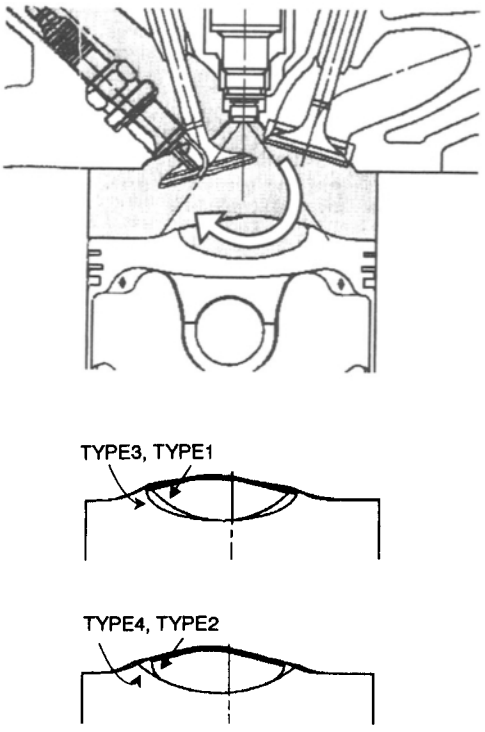

Fig. 118. The Subaru GDI combustion system [87].

A motor/generator is attached to the engine and serves as an additional source of power when accelerating. It is claimed that this configuration provides vehicle performance exceeding that provided by a 1.5 L conventional PFI engine.

6.11. Subaru combustion system

A schematic of the combustion chamber layout for the Subaru research GDI engine [87] is illustrated in Fig. 118. A high-pressure swirl injector is located at the center of the chamber and the fuel is injected vertically into the cylinder. An inclined spark plug is located between the intake valves on the intake side of the engine. With this configuration, the fuel spray does not impinge onto the electrode of the spark plug. Four types of piston cavity as shown in the figure were tested both numerically and experimentally. The type 2 design was found to demonstrate the highest combustion efficiency. The main features are summarized as follows:

- single cylinder engine;
- four-valve, DOHC pentroof combustion chamber;
- displacement—554 cm^3;
- bore × stroke : 97 × 75 mm;
- compression ratio—9.7:1;
- conventional straight tumble port at a tumble ratio of 0.7;
- curved piston crown;
- spark plug located between the intake valves;
- centrally mounted fuel injector;
- single-fluid, high-pressure, swirl injector;
- fuel injection pressure—7.0 MPa.

6.12. Fiat combustion system

The Fiat prototype GDI engine was reported by Andriesse et al. [189,190]. The main features of the Fiat GDI combustion system are summarized as follows:

- inline four-cylinder engine;
- four-valve, DOHC pentroof combustion chamber;
- displacement—1995 cm^3;
- compression ratio—12:1;
- moderate tumble with port deactivation possible;
- centrally mounted fuel injector and spark plug;
- homogeneous mode *only*.

It was reported by Andriesse et al. [189] that the optimal start of injection (SOI) timing for volumetric efficiency may not be the same as that for the maximum torque due to the limited time for achieving charge homogenization. For the Fiat GDI combustion system, the maximum torque is obtained at an injection timing that is about 20–30 crank angle degrees earlier than that for the maximum volumetric efficiency. In comparing the homogeneous, stoichiometric combustion systems with centrally mounted and side-mounted injectors, it was pointed out by Andriesse et al. [190] that charge homogenization is optimum for the configuration having a centrally mounted injector, resulting in lower smoke emissions as well as a higher torque. Conversely, the configuration incorporating a side-mounted injector yields the best high-speed volumetric efficiency. Part-load results show a slight benefit in UBHC emissions for the centrally mounted injector configuration, even though the difference is small. It was concluded that the overall difference between these two injector positions is limited for a

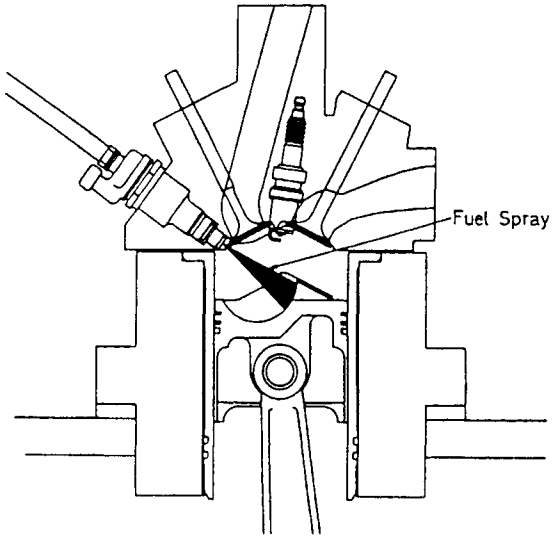

Fig. 119. The Ricardo GDI combustion system [136,137].

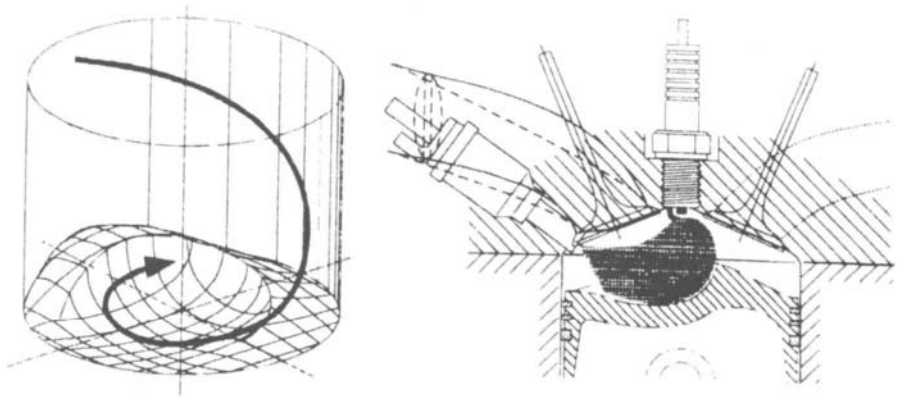

(a)

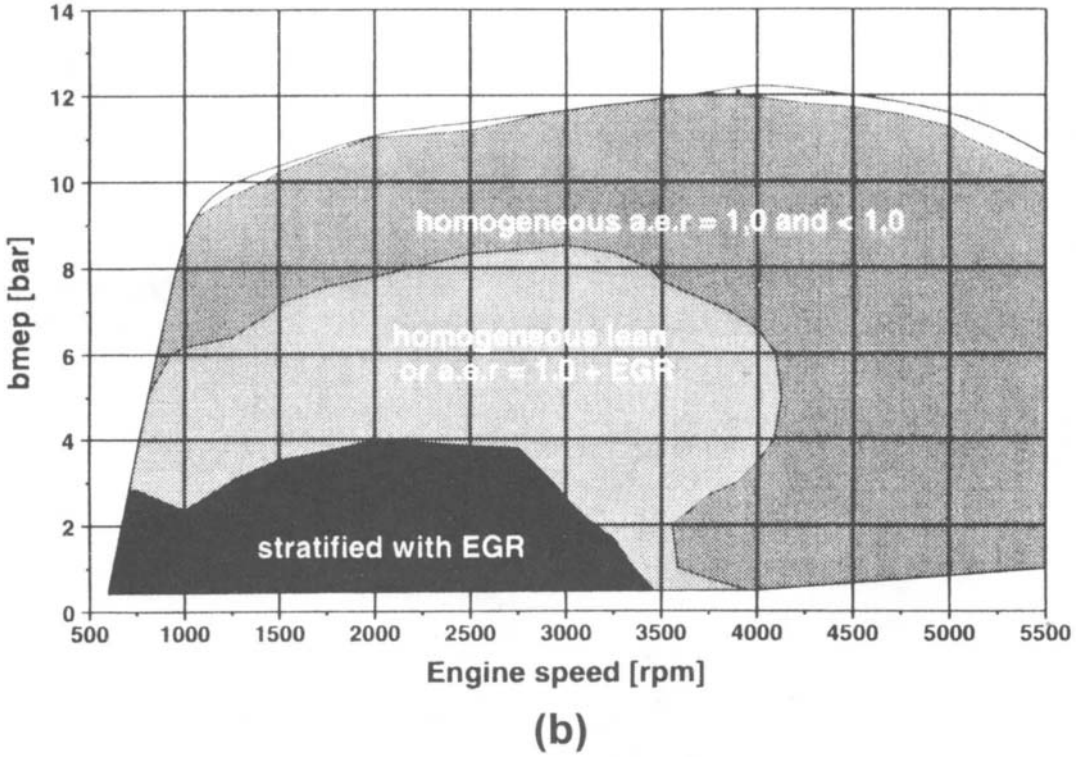

(b)

Fig. 120. The AVL swirl-based GDI combustion system and the proposed GDI control map [144,219].

homogeneous, stoichiometric GDI operation. Therefore, it was recommended that the selection of the combustion system configuration should be made with significant weight attached to manufacturing issues.

6.13. Renault combustion system

The Renault production GDI engine for the European market was reported by Scott [380] and Birch [381]. The main features of the Renault GDI combustion system are as follows:

- inline four-cylinder engine;
- four-valve, DOHC pentroof combustion chamber;
- displacement—2000 cm^3;
- air motion–tumble;

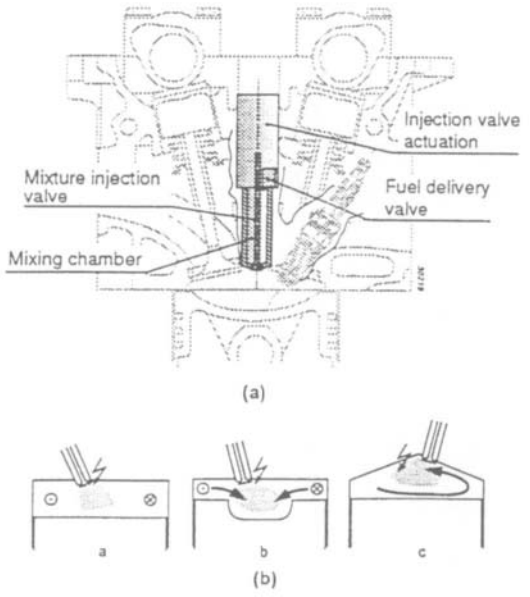

Fig. 121. The AVL direct mixture injection (DMI) concept [57]: (a) layout of the combustion chamber for direct mixture injection; and (b) mixture preparation strategies.

- vertical, near-centrally mounted injector;
- near-centrally-mounted spark plug;
- deep bowl in piston crown;
- Siemens single-fluid, high-pressure, swirl injector;
- common-rail fuel system using a design fuel rail pressure from 5 to 10 MPa;
- EGR (up to 25%) is used whenever the engine load is between 0 and 50–60%;
- homogeneous, stoichiometric operation *only*;
- standard three-way catalyst;
- power—103 kW at 5500 rpm;
- maximum torque—200 Nm.

6.14. Ricardo combustion system

Engineers at Ricardo [187] investigated the combustion and charge motion requirements of a GDI engine that is based on a strategy of early injection to achieve a homogeneous mixture. The project goal was to achieve improvements in the cold-start emissions and transient response of a GDI engine system that could utilize a three-way catalyst, and to document the performance parameters of a GDI engine for homogeneous, stoichiometric combustion. The resulting Ricardo GDI engine was found to produce UBHC levels that are nearly equivalent to those from the PFI baseline engine for part-load operation using a stoichiometric mixture. The NO_x emission levels were also found to be identical, indicating a similar air–fuel ratio at the spark gap for these two engines. However, the Ricardo GDI engine exhibited an exceptional EGR tolerance when compared with the baseline PFI engines. This was attributed to the increased turbulence intensity that results from the direct injection of fuel into the cylinder. The experimental results also confirmed that the GDI engine was clearly superior in engine transient response and cold-start UBHC emissions. The fuel economy for stoichiometric operation was found to be 6% better than for the comparable PFI engine.

Jackson et al. [136,137,145,173] reported results obtained using a later version of the Ricardo GDI system that incorporates a top-entry port head in combination with a curved piston, as depicted in Fig. 119. This engine was designed to operate using both the early and late injection modes. In the stratified-charge operating mode, the minimum values of UBHC and COV of IMEP were obtained with a narrow cone fuel spray having a relatively low injection rate for such a top-entry configuration. It is important to note that the combustion characteristics were found to be more sensitive to the fuel injection rate than to the spray cone angle. For a given fuel rail pressure, the use of an injector with a reduced fuel injection rate generally yields a lower spray penetration rate. This, in turn, reduces the spray impingement on the piston crown and cylinder walls, which is a primary source of UBHC emissions. It was noted, however, that the injector flow capacity must accommodate with rated power operation, which requires an acceptable injection pulse width at maximum speed and load. From the engine speed-load map that is shown in Fig. 93, it may be seen that this GDI engine operates in the homogeneous-charge mode above 50% rate load. Above 70% load, the early injection mode, with either a stoichiometric or a slightly rich mixture, is used. Stratified-charge operation is thus restricted to the lower load and speed where fuel consumption is critical. The engine runs fully unthrottled from 70 to 20% of full-load, and with light throttling below 20% load to control UBHC emissions. The typical features of this research GDI engine are:

- single cylinder engine;
- four-valve pentroof combustion chamber;
- bore × stroke—74 × 75.5 mm;
- displacement—325 cm^3;
- compression ratio—12.7:1;
- centrally mounted spark plug;
- curved piston crown;
- hydra head with a top-entry port to generate reverse tumble;
- fuel injection pressure range—5–10 MPa;
- part-load mode: late injection for stratified operation;
- high-load mode: early injection for homogeneous operation;
- intake valve opening: 16° BTDC on intake;
- intake valve closing: 48° ABDC on intake.

6.15. AVL combustion system

Engineers at AVL [57,82,97,142–144,219] developed a

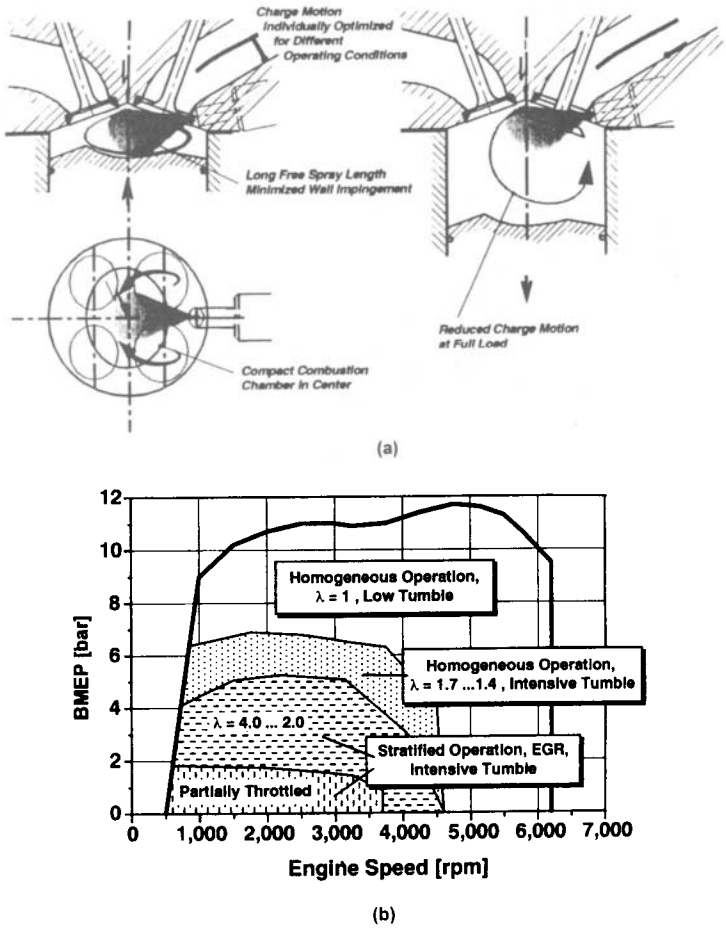

Fig. 122. The FEV flow-guided combustion system and the proposed GDI control map [269,270].

number of GDI combustion systems based upon swirl, tumble and a swirl/tumble combination. An example of their swirl-based GDI combustion system [144] and the proposed combustion control map [219] is shown in Fig. 120. GDI combustion systems generally exhibit a compromise between the requirement of a minimum mixture formation time and the maximum time interval between injection and combustion if stratification is to be maintained. A separation of these two opposing requirements is considered to provide the highest flexibility for a GDI system. Based upon this consideration, Fraidl et al. [57] proposed the direct-mixture-injection (DMI) concept. The objective of this injection strategy is to combine the advantages of air-assisted injection and pre-vaporization of the fuel, without the need for an external pressurized air supply.

Fig. 121(a) shows the schematic of the DMI system. The DMI valve incorporating a standard poppet-valve geometry with electrically controlled actuation provides for the injection of the mixture and the recharging of the pre-chamber. The DMI valve recovers the gas pressure required for injection by withdrawing a small amount of the compressed charge from the cylinder in the preceding engine cycle. To avoid combustion in the pre-chamber, the DMI valve is closed at the time of the spark; however, the mixture can be injected into the main chamber at any time prior to ignition. After the DMI valve is closed, liquid fuel is injected into the pre-chamber and is vaporized in preparation for injection during the next engine cycle. The mixture preparation quality is substantially enhanced by the pre-vaporization of the fuel. The DMI system effectively decreases the engine crank angle interval that is required for fuel vaporization as compared to the conventional GDI injection. It is claimed that the processes of fuel metering and injection into the pre-chamber can be achieved by means of a constant displacement method using a low fuel pressure. The required fuel pressure exceeds the maximum pre-chamber pressure only slightly, as a high degree of fuel atomization is not required. Further claims include additional advantages regarding mixture stratification strategies, such as a reduced mixture penetration velocity that results from the comparably low pressure difference between the

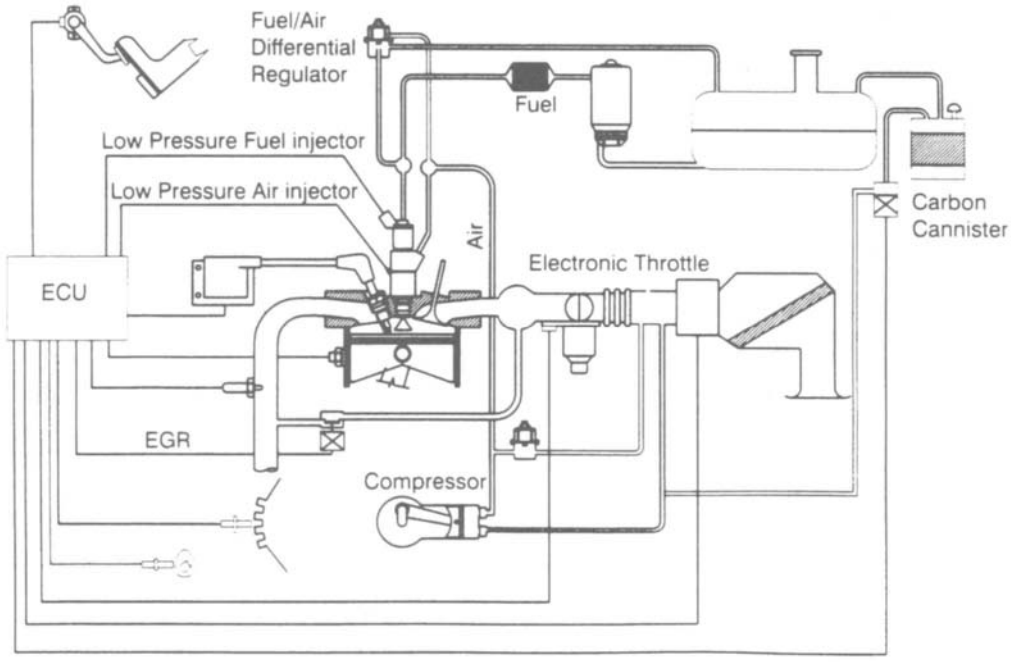

Fig. 123. The Orbital air-assisted GDI engine system [72].

pre-chamber and the combustion chamber, as well as from the low momentum associated with the fuel vapor as compared to fuel droplets. Several DMI-based mixture preparation strategies are illustrated in Fig. 121(b).

The DMI system was found to have some problem areas that will require further development. As the mixture is injected into the main chamber by the small pressure difference between the pre-chamber and the main chamber, all of the evaporated fuel may not be injected. This fuel metering error is commonly referred to as the fuel hang-up, and commonly occurs with injection from intermediate cavities. At high engine speeds or under cold-start conditions, the fuel inside the pre-chamber may not evaporate completely, and wall wetting is likely to occur. These conditions result in fuel metering errors. Moreover, during engine transients the pressure inside the pre-chamber, as sampled from the previous cycle may not be appropriate for metering the current cycle. This results in UBHC spikes during engine transient operation.

6.16. FEV combustion system

The FEV charge-motion-controlled GDI concept was described in detail by Hupperich et al. [269] and Grigo et al. [270]. In this combustion system, a strong tumble flow is generated by means of a movable control gate. This tumble airflow field is, in turn, utilized to establish a stratified charge. Fig. 122 shows a schematic of this GDI concept and the corresponding engine control map. It was found that the combustion characteristics are significantly influenced by the tumble ratio, which was optimized for a number of engine-operating conditions. It was determined that a simple two-stage, tumble system utilizing a simple control gate is adequate. A system providing a continuously variable tumble ratio is not required. The study showed that for a spray-guided combustion system, the heat release is quite high in the early stages of combustion, but is reduced significantly after half of the injected fuel mass is consumed. Similar combustion characteristics were also observed for the wall-guided system. The flow-guided system yields the higher combustion efficiency when compared with the spray-guided and wall-guided alternatives, and also exhibits the latest timing of the 50% mass

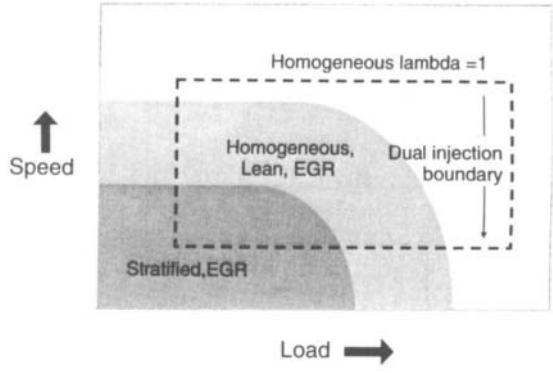

Fig. 124. The proposed air-assisted GDI engine control map [73].

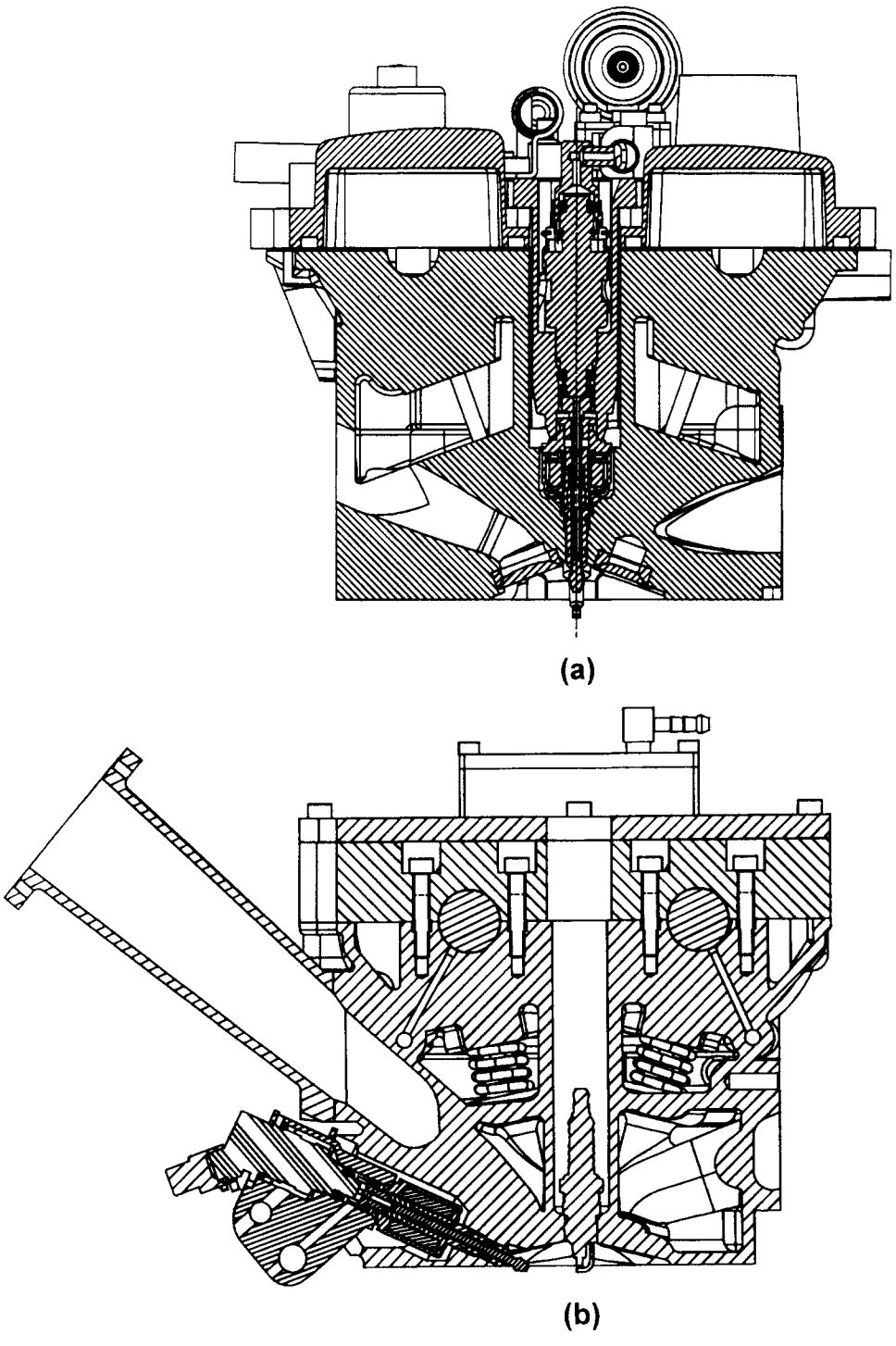

Fig. 125. Proposed packaging solutions of air-assisted GDI engines for both centrally and side-mounted injectors [73].

burn fraction. The major geometric features of the FEV GDI combustion system are summarized as follows:

- four-valve pentroof combustion chamber;
- side-entry port;
- side-mounted injector positioned beneath the intake port;
- variable tumble flow;
- shallow bowl in the piston crown.

6.17. Orbital combustion system

The application of the air-assisted fuel system that has been developed for two-stroke engines to automotive four-stroke GDI engines has been reported by Houston et al. [72] and Krebs et al. [73]. It was reported that the inherent qualities of the air-assisted fuel system in combination with careful design of the combustion chamber could enable high charge stratification with late injection timings and very stable combustion over a wide range of operating conditions. The schematic of the Orbital GDI system using an air-assisted fuel injection system is illustrated in Fig. 123 [72]. Figs. 124 and 125 illustrate the examples of a proposed control map for the air-assisted GDI as well as the possible packaging solutions for centrally mounted and side-mounted fuel injectors [73]. The main features of the Orbital GDI combustion system are summarized as follows:

- four-cylinder, 1.8 l DOHC engine;
- bore × stroke—80.6 × 88 mm;
- displacement—1796 cm^3;
- compression ratio—10.4:1;
- low tumble and zero swirl for the in-cylinder flow field;
- combined spark plug and injector, near-centrally mounted;
- air-assisted fuel system with a fuel pressure of 0.72 MPa and air pressure of 0.65 MPa.

7. Conclusion

The key areas of the theoretical potential and the current research and development status of the spark-ignition, four-stroke, direct-gasoline-injection engine have been discussed in detail in each of the sections of this treatise. It is quite evident from the technical literature worldwide that significant incremental gains in engine performance and emission parameters are indeed indicated and, to some degree, have been achieved. Specific technical issues related to BSFC, UBHC, NO_x, particulate matter and fuel sprays in GDI combustion systems have been addressed and discussed, which has clearly accentuated the numerous practical considerations that will have to be addressed if the GDI engine is to realize its full potential and become a major future automotive powerplant. These key considerations are:

- Can a sufficient enhancement in operating BSFC be achieved in a stratified-charge GDI to offset the increased system complexity as compared to a PFI engine?
- Can the applicable US, European and Japanese emission standards that are applicable in the 2000–2012 time frame be achieved and maintained for the required durability intervals?
- Can a production-feasible compromise be obtained between the required system complexity and overall system reliability, considering that the required GDI hardware may incorporate multi-stage injection, variable swirl-and-tumble control hardware and variable fuel pressure?
- Can injector fouling due to deposit formation be minimized for the wide range of fuel quality and composition in the field such that reasonable service intervals can be achieved?
- Can control-system strategies and algorithms be developed and implemented such that sufficiently smooth transitions from stratified-charge, late-injection operation to mid-range to homogeneous-charge, early-injection operation may be obtained, thus yielding driveability levels that are comparable to current sequential PFI systems?

In determining which GDI system configuration delivers the most advantages, much work remains to be done. The field experiences of the production Mitsubishi, Toyota, Nissan and Renault GDI systems are being accumulated, and will be analyzed and discussed by engineers in the GDI field. The delivered emission indices and brake specific fuel consumption are being critically evaluated for each mode of the operating map, and are being compared to those obtained with other GDI configurations and strategies. In addition, the relative merits of spray-wall and spray-flow control strategies using both tumble and swirl are being determined. This will permit a more knowledgeable evaluation of the relative merits of each system. Even when the merits of each of these production and prototype GDI engines are fairly well established, much research and development will still be required for system optimization in order to develop production configurations.

For very nearly the same reasons that port fuel injection gradually replaced the carburetor and the throttle-body injector, and that sequential PFI gradually displaced simultaneous-fire PFI, a GDI combustion configuration that is an enhancement of one of the systems discussed in this treatise will emerge as the GDI system of choice, and will gradually displace the sequential PFI applications.

References

[1] Mitchell E, Alperstein M, Cobb JM, Faist CH. A stratified charge multifuel military engine—a progress report. SAE Technical Paper, No. 720051, 1972.
[2] Lewis JM. UPS multifuel stratified charge engine development program—field test. SAE Technical Paper, No. 860067, 1986.
[3] Kim C, Foster DE. Aldehyde and unburned fuel emission measurements from a methanol-fueled Texaco stratified charge engine. SAE Technical Paper, No. 852120, 1985.
[4] Baranescu GS. Some characteristics of spark assisted direct injection engine. SAE Technical Paper, No. 830589, 1983.
[5] Duggal VK, Kuo TW, Lux FB. Review of multi-fuel engine concepts and numerical modeling of in-cylinder flow processes in direct injection engines. SAE Technical Paper, No. 840005, 1984.
[6] Enright B, Borman G, Myers PP. A Critical review of spark

ignited diesel combustion. SAE Technical Paper, No. 881317, 1988.
[7] Iida Y. The current status and future trend of DISC engines. Preprint of JSME Seminar (in Japanese), No. 920-48, 1992. p. 72–6.
[8] Wood CD. Unthrottled open-chamber stratified charge engines. SAE Technical Paper, No. 780341, 1978.
[9] Alperstein M, Schafer GH, Villforth FJ, III. Texaco's stratified charge engine—multifuel, efficient, clean, and practical. SAE Technical Paper, No. 740563, 1974.
[10] Meurer S, Urlaub A. Development and operational results of the MAN FM combustion system. SAE Technical Paper, No. 690255, 1969.
[11] Urlaub AG, Chmela FG. High-speed, multifuel engine: L9204 FMV. SAE Technical Paper, No. 740122, 1974.
[12] Haslett RA, Monaghan ML, McFadden. Stratified charge engines. SAE Technical Paper, No. 76075, 1976.
[13] Simko A, Choma MA, Repko LL. Exhaust emissions control by the Ford Programmed Combustion process—PROCO. SAE Technical Paper, No. 720052, 1972.
[14] Scussei AJ, Simko AO, Wade WR. The Ford PROCO engine update. SAE Technical Paper, No. 780699, 1978.
[15] Ando H. Combustion control technologies for direct-injection gasoline engines. Proceedings of the 73rd JSME Annual Meeting (V) (in Japanese), No. WS 11-(4), 1996. p. 319–20.
[16] Ando H. Combustion control technologies for gasoline engines. IMechE Seminar of Lean Burn Combustion Engines. S433, 3–4 December 1996.
[17] Ando H. Mitsubishi GDI engine strategies to meet the European requirements. Proceedings of AVL Conference on Engine and Environment, vol. 2, 1997. p. 55–77.
[18] Ando H et al. Combustion control for Mitsubishi GDI engine. Proceedings of the Second International Workshop on Advanced Spray Combustion, Hiroshima, Japan, 24–26 November, Paper No. IWASC9820, 1998. p. 225–35.
[19] Ando H et al. Mixture preparation in gasoline direct injection engine. 1998 FISITA Technical Paper, No. F98T050, 1998.
[20] Kume T, Iwamoto Y, Iida K, Murakami M, Akishino K, Ando H. Combustion control technologies for direct injection SI engine. SAE Technical Paper, No. 960600, 1996.
[21] Harada J, Tomita T, Mizuno H, Mashiki, Ito Y. Development of a direct injection gasoline engine. SAE Technical Paper, No. 974054, 1997.
[22] Sawada O. Automotive gasoline direct injection. JSME Seminar (in Japanese), No. 97-88, 1997. p. 57–64.
[23] Takagi Y. The role of mixture formation in improving fuel economy and reducing emissions of automotive S.I. engines. FISITA Technical Paper, No. P0109, 1996.
[24] Takagi Y. Combustion characteristics and research topics of in-cylinder direct-injection gasoline engines. Proceedings of the 73rd JSME Annual Meeting (V) (in Japanese), No. WS 11-(3), 1996. p. 317–8.
[25] Takagi Y. Simultaneous attainment of improved fuel consumption, output power and emissions with direct injection SI engines. Japan Automobile Technology 1998;52(1):64–71.
[26] Takagi Y. Challenges to overcome limitations in S.I. engines by featuring high pressure direct injection. Proceedings of the Second International Workshop on Advanced Spray Combustion, 24–26 November 1998, Hiroshima, Japan, Paper No. IWASC9819, 1998. p. 214–24.
[27] Takagi Y, Itoh T, Muranaka S, Iiyama A, Iwakiri Y, Urushihara T, Naitoh, K. Simultaneous attainment of low fuel consumption, high power output and low exhaust emissions in direct injection S.I. engines. SAE Technical Paper, No. 980149, 1998.
[28] Buchheim R, Quissek F. Ecological and economical aspects of future passenger car powertrains. FISITA Technical Paper, No. P1404, 1996.
[29] Douaud A. Tomorrow's efficient and clean engines and fuels. FISITA Technical Paper, No. K0006.
[30] Fansler TD, French DT, Drake MC. Fuel distribution in a firing direct-injection spark-ignition engine using laser-induced fluorescence imaging. SAE Technical Paper, No. 950110, 1995.
[31] Seiffert U. The automobile in the next century. FISITA Technical Paper, No. K0011, 1996.
[32] Jewett D. Direct injection boosts mileage, maintains muscle. Automotive News 1997;March:21.
[33] Jewett D. Engines run leaner and burn fuel more completely. Automotive News 1997;March:21.
[34] Buchholz K. Chrysler updates two-stroke engine progress. Automotive Engineering 1997;1:84.
[35] Ader B, Bohland M, Doring C, Heine B, Schlerfer J, Wahl S. Simulation of mixture preparation. Proceedings of the Third International FIRE User Meeting, 16–17 June 1997.
[36] Fry M et al. Direct injection of gasoline—practical considerations. SAE Technical Paper, No. 1999-01-0171, 1999.
[37] Kakuhou A et al. LIF visualization of in-cylinder mixture formation in a direct-injection SI engine. Proceedings of the Fourth International Symposium COMODIA 98, 1998. p. 305–10.
[38] Zhao F, Lai MC, Harrington DL. The spray characteristics of automotive port fuel injection—a critical review. SAE Technical Paper, No. 950506, 1995.
[39] Cheng WK, Hamrin D, Heywood JB, Hochgreb S, Min K, Norris M. An overview of hydrocarbon emissions mechanisms in spark-ignition engines. SAE Technical Paper, No. 9332708, 1993.
[40] Anderson RW, Brehob DD, Yang J, Vallance JK, Whiteaker RM. A new direct injection spark ignition (DISI) combustion system for low emissions. FISITA-96, No. P0201, 1996.
[41] Nohira H et al. Development of Toyota's direct injection gasoline engine. Proceedings of AVL Engine and Environment Conference, 1997. p. 239–49.
[42] Zhao F, Lai MC, Harrington DL. A review of mixture preparation and combustion control strategies for spark-ignited direct-injection gasoline engines. SAE Technical Paper, No. 970627, 1997.
[43] Matsushita S, Nakanishi K, Gohno T, Sawada D. Mixture formation process and combustion process of direct injection S.I. engine. Proceedings of JSAE (in Japanese), No. 965, 10 October 1996. p. 101–4.
[44] Pischinger F, Walzer P. Future trends in automotive engine technology. FISITA Technical Paper, No. P1303, 1996.
[45] Ronald B, Helmut T, Hans K. Direct fuel injection—a necessary step of development of the SI engine. FISITA Technical Paper, No. P1613, 1996.
[46] Mccann KA. MMC ready with first DI gasoline engine.

WARD's Engine and Vehicle Technology Update 1995;21(11):1–2.

[47] Pontoppidan M et al. Experimental and numerical approach to injection and ignition optimization of lean GDI-combustion behavior. SAE Technical Paper, No. 1999-01-0173, 1999.

[48] Yang J, Anderson R. Use of split fuel injection to increase full-load torque output of a direct-injection SI engine. SAE Technical Paper, No. 980495, 1998.

[49] Kuwahara K et al. Two-stage combustion for quick catalyst warm-up in gasoline direct injection engine. Proceedings of the Fourth International Symposium COMODIA 98, 1998. p. 293–8.

[50] Iwamoto Y, Noma K, Yamauchi T, Ando H. Development of gasoline direct injection engine. SAE Technical Paper, No. 970541, 1997.

[51] Iwamoto Y, Noma K, Nakayama O, Yamauchi T. Development of gasoline direct injection engine. Proceedings of JSAE Spring Convention (in Japanese), No. 971, 1997. p. 297–300.

[52] Shelby M et al. Early spray development in gasoline direct-injected spark ignition engines. SAE Technical Paper, No. 980160, 1998.

[53] Zhao F, Yoo J-H, Lai M-C. In-cylinder spray/wall interactions of a gasoline direct-injection engine. Proceedings of ILASS-America, 1997.

[54] Dodge LG. Fuel preparation requirements for direct-injected spark ignition engines. Proceedings of ILASS-America, 1996. p. 120–4.

[55] Dodge LG. Fuel preparation requirements for direct-injected spark ignition engines. SAE Technical Paper, No. 962015, 1996.

[56] Fujieda M, Siraisi T, Oosuga M. Influence of the spray pattern on combustion characteristics of the direct injection SI engine. Proceedings of ILASS-Japan (in Japanese), 1995, p. 173–7.

[57] Fraidl GK, Piock WF, Wirth M. Gasoline direct injection: actual trends and future strategies for injection and combustion systems. SAE Technical Paper, No. 960465, 1996.

[58] Xu M, Markle LE. CFD-aided development of spray for an outwardly opening direct injection gasoline engine. SAE Technical Paper, No. 980493, 1998.

[59] Xu M et al. Recent Advances in direct injection gasoline injector technology and fuel preparation strategy. Proceedings of the Second International Workshop on Advanced Spray Combustion, 24–26 November 1998, Hiroshima, Japan, Paper No. IWASC9818, 1998. p. 201–13.

[60] Tomoda T, Sasaki S, Sawada D, Saito A, Sami H. Development of direct injection gasoline engine—study of stratified mixture formation. SAE Technical Paper, No. 970539, 1997.

[61] Lefebvre AH. Atomization and sprays, Washington, DC: Hemisphere, 1989.

[62] Varble D et al. Design, modeling and development of a unique gasoline direct injection fuel system. ISATA 98VR028, Dusseldorf, Germany, 1998.

[63] Varble D et al. Development of a unique outwardly-opening direct injection gasoline injector for stratified-charge combustion. Aachen Colloquium Automobile & Engine Technology, 5–7 October 1998.

[64] Pontoppidan M, Gaviani G, Marelli M. Direct fuel-injection—a study of injector requirements for different mixture preparation concepts. SAE Technical Paper, No. 970628, 1997.

[65] Schapertons H, Emmenthal KD, Grabe HJ, Oppermann W. VW's gasoline direct injection (GDI) research engine. SAE Technical Paper, No. 910054, 1991.

[66] Okada Y et al. Development of high-pressure fueling system for a direct-injection gasoline engine. SAE Technical Paper, No. 981458, 1998.

[67] Tatschl R. PDF modeling of stratified-charge SI engine combustion. SAE Technical Paper, No. 981464, 1998.

[68] Hiroyas H. Experimental and theoretical studies on the structure of fuel sprays in diesel engines. Proceedings of ICLASS-91, Keynote Lecture, 1991. p. 17–32.

[69] Anderson RW, Yang J, Brehob DD, Vallance JK, Whiteaker RM. Understanding the thermodynamics of direct injection spark ignition (DISI) combustion systems: an analytical and experimental investigation. SAE Technical Paper, No. 962018, 1996.

[70] Schmidt D et al. Pressure-swirl atomization in the near field. SAE Technical Paper, No. 1999-01-0496, 1999.

[71] Miyamoto T, Kobayashi T, Matsumoto Y. Structure of sprays from an air-assist hollow-cone injector. SAE Technical Paper, No. 960771, 1996.

[72] Houston RA, Cathcart GP. Combustion and emissions characteristics of Orbital's combustion process applied to a multicylinder automotive direct injected 4 stroke engine. SAE Techhnical Paper, No. 980153, 1998.

[73] Krebs S et al. A cooperative approach to air-assisted direct gasoline injection. Proceedings of GPC'98, Advanced Engine Design and Performance, 1998. p. 89–102.

[74] Stocker H et al. Application of air-assisted direct injection to automotive 4-stroke engines—the total system approach. Aachen Colloquium Automobile & Engine Technology, 5–7 October 1998. p. 711–29.

[75] Zhao F, Taketomi M, Nishida K, Hiroyasu H. Quantitative imaging of the fuel concentration in a SI engine with laser Rayleigh scattering. SAE Technical Paper, No. 932641, 1993.

[76] Zhao F, Taketomi M, Nishida K, Hiroyasu H. PLIF measurements of the cyclic variation of mixture concentration in a SI engine. SAE Technical Paper, No. 940988, 1994.

[77] Iiyama A, Muranaka S. Current status and future respective of DISC engine. Proceedings of JSAE (in Japanese), No. 9431030, 1994. p. 23–9.

[78] Zhao F, Yoo J-H, Liu Y, Lai M-C, Zhang L, Yoshida Y. Characteristics of gasoline direct-injection sprays. Proceedings of ILASS-America, 1997.

[79] Zhao F, Yoo J-H, Liu Y, Lai M-C. Characterization of direct-injection gasoline sprays under different ambient and fuel injection conditions. Proceedings of ICLASS-97, 1997.

[80] Yoo J-H et al. Visualization of direct-injection gasoline spray structure inside a motoring engine. Proceedings of ILASS-America'98, 1998. p. 101–5.

[81] Yoo JH, Kim SK, Zhao F, Lai MC. Visualization of direct-injection gasoline spray and wall-impingement inside a motoring engine. SAE Technical Paper, No. 982702, 1998.

[82] Fraidl GK, Winklhofer E, Piock W, Schoeggl P, Wirth M. Gasoline DI engines: the complete system approach by interaction of advanced development tool. SAE Technical Paper, No. 980492, 1998.

[83] Evers LW. Characterization of the transient spray from a high pressure swirl injector. SAE Technical Paper, No. 940188, 1994.

[84] Zhao F, Lai M-C, Liu Y, Yoo J-H, Zhang L, Yoshida Y. Spray characteristics of direct-injection gasoline engines. Proceedings of ILASS-America, 1996. p. 150–4.

[85] Zhao F, Yoo JH, Liu Y, Lai MC. Spray dynamics of high pressure fuel injectors for DI gasoline engines. SAE Technical Paper, No. 961925, 1996.

[86] Yamauchi T, Wakisaka T. Computation of the hollow-cone sprays from high-pressure swirl injector from a gasoline direct-injection SI engine. SAE Technical Paper, No. 962016, 1996.

[87] Yamauchi T et al. Numerical analysis of stratified mixture formation in direct injection gasoline engines. Proceedings of Direkteinspritzung im Ottomotor, 1998. p. 166–85.

[88] Naitoh K, Takagi Y. Synthesized spheroid particle (SSP) method for calculating spray phenomena in direct-injection SI engines. SAE Technical Paper, No. 962017, 1996.

[89] Han Z, et al. Modeling atomization processes of pressure-swirl hollow-cone fuel sprays. Atomization and Sprays 1997;7:663–84.

[90] Lippert A et al. Modeling of multicomponent fuels using continuous distributions with application to droplet evaporation and sprays. SAE Technical Paper, No. 972882, 1997.

[91] Hoffman J, Martin JK, Coates SW. Spray photographs and preliminary spray mass flux distribution measurements of a pulsed pressure atomizer. Proceedings of ILASS-America, 1996. p. 288–91.

[92] Ren WM, Nally S. Computation of the hollow cone spray from a pressure-swirl injector. Proceedings of ILASS-America'98, 1998. p. 115–9.

[93] Ren WM, Shen J, Nally JF. Geometrical effects on flow characteristics of a gasoline high pressure swirl injector. SAE Technical Paper, No. 971641, 1997.

[94] Ren WM et al. Computations of hollow-cone sprays from a pressure swirl injector. SAE Technical Paper, No. 982610, 1998.

[95] Preussner C, Doring C, Fehler S, Kampmann S. GDI: interaction between mixture preparation, combustion system and injector performance. SAE Technical Paper, No. 980498, 1998.

[96] Parrish S, Farrell PV. Transient spray characteristics of a direct-injection spark-ignited fuel injector. SAE Technical Paper, No. 970629, 1997.

[97] Wirth M, Piock WF, Fraidl GK. Actual trends and future strategies for gasoline direct injection. IMechE Seminar of Lean Burn Combustion Engines, S433, 3–4 December 1996.

[98] Salters D, Williams P, Greig A. Fuel spray characterization within an optically accessed gasoline direct injection engine using a CCD imaging system. SAE Technical Paper, No. 961149, 1996.

[99] Iiyama A et al. Attainment of high power with low fuel consumption and exhaust emissions in a direct-injection gasoline engine. FISITA Technical Paper, No. F98T048, 1998.

100] Iiyama A et al. Realization of high power and low fuel consumption with low exhaust emissions in a direct-injection gasoline engine. Proceedings of GPC'98, Advanced Engine Design & Performance, 1998. p. 76–88.

[101] Nogi T et al. Stability improvement of direct fuel injection engine under lean combustion operation. SAE Technical Paper, No. 982703, 1998.

[102] Das S, Dent JC. A study of air-assisted fuel injection into a cylinder. SAE Technical Paper, No. 941876, 1994.

[103] Diwakar R, Fansler TD, French DT, Ghandhi JB, Dasch CJ, Heffelfinger. Liquid and vapor fuel distributions from an air-assist injector—an experimental and computational study. SAE Technical Paper, No. 920422, 1992.

[104] Emerson J, Felton PG, Bracco FV. Structure of sprays from fuel injectors part III: the Ford air-assisted fuel injector. SAE Technical Paper, No. 900478, 1990.

[105] Schechter MM, Levin MB. Air-forced fuel injection system for 2-stroke D.I. gasoline engine. SAE Technical Paper, No. 910664, 1991.

[106] Ikeda Y, Nakajima T, Kurihara N. Spray formation of air-assist injection for two-stroke engine. SAE Technical Paper, No. 950271, 1995.

[107] Ikeda Y, Nakajima T, Kurihara N. Size-classified droplet dynamics and its slip velocity variation of air-assist injector spray. SAE Technical Paper, No. 970632, 1977.

[108] Ikeda Y, Hosokawa S, Sekihara F, Nakajima T. Cycle-resolved PDA measurement of size-classified spray structure of air-assist injector. SAE Technical Paper, No. 970631, 1997.

[109] Kim KS, Kim SS. Spray characteristics of an air-assisted fuel injector for two-stroke direct-injection gasoline engines. Atomization and Sprays 1994;4:501–21.

[110] Lee CF, Bracco FV. Initial comparisons of computed and measured hollow-cone sprays in an engine. SAE Technical Paper, No. 940398, 1994.

[111] Laforgia D, Chehroudi B, Bracco FV. Structure of sprays from fuel injectors-part II, the Ford DFI-3 fuel injector. SAE Technical Paper, No. 890313, 1989.

[112] MacInnes JM, Bracco FV. Computation of the spray from an air-assisted fuel injector. SAE Technical Paper, No. 902079, 1990.

[113] Gentili R, Marini A. Pro-jet air-assisted fuel injection system for two-stroke S.I. engines. SAE Technical Paper, No. 960360, 1996.

[114] Wang WB, Peng YY. Spray measurement and visualization of gasoline injection for 2-stroke engine. SAE Technical Paper, No. 930496, 1993.

[115] Wang JH, Huang HH, Peng YY, Horng PF, Wang WB. Application of low-pressure air-assisted fuel injection system on two-stroke motorcycle. SAE Technical Paper, No. 911253, 1991.

[116] Kenny RG, Kee RJ, Carson CE, Blair GP. Application of direct air-assisted fuel injection to a SI cross-scavenged two-stroke engine. SAE Technical Paper, No. 932396, 1993.

[117] Gentili R, Frigo S, Tognotti L. Development of a pumpless air assisted injection system for two-cycle, S.I. engines. SAE Technical Paper, No. 940397, 1994.

[118] Ghandhi JB, Felton PG, Gajdeczko BF, Bracco FV. Investigation of the fuel distribution in a two-stroke engine with an air-assisted injector. SAE Technical Paper, No. 940394, 1994.

[119] Duret P, Ecomard A, Audinet M. A new two-stroke engine with compressed-air assisted fuel injection for high efficiency low emissions applications. SAE Technical Paper, No. 881076, 1988.

[120] Duret P. The fields of application of IAPAC compressed air assisted DI fuel injection. Modern Injection Systems for Direct Injection in Spark-Plug and Diesel Engines, ESSEN-HAUS DER TECHNIK, 23–24 September 1997.

[121] Iwata M, Furuhashi M, Ujihashi M. The spray characteristics and engine performance of EFI injector. Proceedings of the Technical Conference of JSAE (in Japanese), No. 861, 1986. p. 29–32.

[122] Saito A, Kawamura K, Tanasawa Y. Improvement of fuel atomization electronic fuel injector by air flow. Proceedings of ICLASS-88, 1988. p. 263–70.

[123] Sugimoto T, Takeda K, Yoshizaki H. Toyota air-mix type two-hole injector for 4-valve engines. SAE Technical Paper, No. 912351, 1991.

[124] Zhao F, Yoo J-H, Lai M-C. The spray structure of air-shrouded dual-stream port fuel injectors with different air mixing mechanisms. Proceedings of the 1996 Spring Technical Conference of the ASME Internal Combustion Engine Division, ICE-Vol. 26-2, 1996. p. 21–9.

[125] Casarella MV. Emission formation mechanisms in a two-stroke direct-injection engine. SAE Technical Paper, No. 982697, 1998.

[126] Meyer J, Kiefer K, Von Issendorff F, Thiemann J, Haug M, Schreiber M, Klein R. Spray visualization of air-assisted fuel injection nozzles for direct injection SI-engines. SAE Technical Paper, No. 970623, 1997.

[127] Meyer J, Graul W, Kiefer K, Thiemann J, Landry M. Study and visualization of the fuel distribution in a stratified spark ignition engine with EGR using laser-induced fluorescence. SAE Technical Paper, No. 970868, 1997.

[128] Newmann R. Being direct. Engine Technology International 1997;November:66–70.

[129] Houston R, Newmann R. Application of Orbital's low pressure, air-assisted fuel system to automotive direct injection 4-stroke engines. Modern Injection Systems for Direct Injection in Spark-Plug and Diesel Engines, Essen-Haus der Technik, 23–24 September 1997.

[130] Hoffman J, Eberhardt E, Martin JK. Comparison between air-assisted and single-fluid pressure atomizers for direct-injection SI engines via spatial and temporal mass flux measurements. SAE Technical Paper, No. 970630, 1997.

[131] Kono S. Study of the stratified charge and stable combustion in DI gasoline engines. SAE Technical Paper, No. 950688, 1995.

[132] Moriyoshi Y, Muroki T. Proposition of a stratified charge system by using in-cylinder gas motion. SAE Technical Paper, No. 962425, 1996.

[133] Fansler TD, French DT. Swirl, squish and turbulence in stratified-charge engines: laser-velocimetry measurements and implications for combustion. SAE Technical Paper, No. 870371, 1987.

[134] Kuwahara K, Watanabe T, Shudo T, Ando H. A study of combustion characteristics in a direct injection gasoline engine by high-speed spectroscopic measurement. Proceedings of the Internal Combustion Engine Symposium—Japan (in Japanese), 1996. p. 145–50.

[135] Baby X, Floch A. Investigation of the in-cylinder tumble motion in a multi-valve engine: effect of the piston shape. SAE Technical Paper, No. 971643, 1997.

[136] Jackson NS, Stokes J, Whitaker PA, Lake TH. A direct injection stratified charge gasoline combustion system for future European passenger cars. IMechE Seminar of Lean Burn Combustion Engines, S433, 3–4 December 1996.

[137] Jackson N et al. Gasoline combustion and gas exchange technologies for the 3 litre/100 km car—competition for the diesel engine. International Symposium on Powertrain Technologies for a 3-Litre-Car, 1996. p. 45–56.

[138] Iiyama A. Direct injection gasoline engines. Technical Seminar at Wayne State University, 26 February 1996.

[139] Yamada T. Trends of S.I. engine technologies in Japan. FISITA-96 Technical Paper, No. P0204, 1996.

[140] Furuno S et al. The effects of inclination angle of swirl axis on turbulence characteristics in a 4-valve lean burn engine with SCV. SAE Technical Paper, No. 902139, 1990.

[141] Yamashita H et al. Mixture formation of direct gasoline injection engine—in cylinder gas sampling using fast response ionization detector. Proceedings of JASE Fall Convention (in Japanese), No. 976, 1997. p. 5–8.

[142] Fraidl G et al. Gasoline direct injection—an integrated systems approach. Proceedings of AVL Engine and Environment Conference, 1997. p. 255–78.

[143] Fraidl GK, Piock W, Wirth M. Straight to the point. Engine Technology International 1997;November:30–34.

[144] Wirth M et al. Gasoline DI engines: the complete system approach by interaction of advanced development tools. SAE Technical Paper, No. 980492, 1998.

[145] Jackson NS, Stokes J, Lake TH. Stratified and homogeneous charge operation for the direct injection gasoline engine—high power with low fuel consumption and emissions. SAE Technical Paper, No. 970543, 1997.

[146] Choi K et al. A research on fuel spray and air flow fields for spark-ignited direct injection engine using laser image technology. SAE Technical Paper, No. 1999-01-0503, 1999.

[147] Han Z, Reitz RD, Yang J, Anderson RW. Effects of injection timing on air/fuel mixing in a direct-injection spark-ignition engine. SAE Technical Paper, No. 970625, 1997.

[148] Lake TH, Sapsford SM, Stokes J, Jackson NS. Simulation and development experience of a stratified charge gasoline direct injection engine. SAE Technical Paper, No. 962014, 1996.

[149] Stanglmaier RH, Hall MJ, Matthews RD. Fuel-spray/charge motion interaction within the cylinder of a direct-injection, 4-valve, SI engine. SAE Technical Paper, No. 980155, 1998.

[150] Hall M et al. In-cylinder flow and fuel transport in a 4-valve GDI engine: diagnostics and measurements. Proceedings of Direkteinspritzung im Ottomotor, 1998. p. 132–46.

[151] Alger TF et al. Fuel-spray dynamics and fuel vapor concentration near the spark plug in a direct-injected 4-valve SI engine. SAE Technical Paper, No. 1999-01-0497, 1999.

[152] Moriyoshi Y, Nomura H, Saisyu Y. Evaluation of a concept for DI combustion using enhanced gas motion. SAE Technical Paper, No. 980152, 1998.

[153] Moriyoshi Y et al. Analysis of stratified charge combustion in an idealized chamber. Proceedings of the 1998 JSAE Spring Convention, No. 984, Paper No. 9831018, 1998. p. 31–4.

[154] Moriyoshi Y et al. Combustion control of gasoline DI engine using enhanced gas motion. Proceedings of the Fourth International Symposium COMODIA 98, 1998. p. 299–304.

[155] Martin JK. Fuel/air mixture preparation in SI engines.

Proceedings of 1995 KSEA International Technical Conference, Part I: Automotive Technology, 1995. p. 155–61.
[156] Han Z, Reitz RD, Claybaker P.J. Rutland C, Yang J, Anderson RW. Modeling the effects of intake flow structures on *fuel/air* mixing in a direct-injected spark ignition engine. SAE Technical Paper, No. 961112, 1996.
[157] Spiegel L, Spicher U. Mixture Formation and combustion in a spark ignition engine with direct fuel injection. SAE Technical Paper, No. 920521, 1992.
[158] Han Z, Fan L, Reitz RD. Multi-dimensional modeling of spray atomization and air/fuel mixing in a direct-injection spark-ignition engine characteristics. SAE Technical Paper, No. 970625, 1997.
[159] Ohsuga M, Shiraishi T, Nogi T, Nakayama Y, Sukegawa Y. Mixture preparation for direct-injection SI engines. SAE Technical Paper, No. 970542, 1997.
[160] Duclos J-M et al. 3D modeling of intake, injection and combustion in a DI-SI engine under homogeneous and stratified operating conditions. Proceedings of the Fourth International Symposium COMODIA 98, 1998. p. 335–40.
[161] Kono S, Kudo H, Terashita. A study of spray direction against swirl in D.I. engines. Proceedings of COMODIA-90, 1990. p. 269–74.
[162] Stanglmaier RH et al. The effect of in-cylinder wall wetting location on the HC emissions from SI engines. SAE Technical Paper, No. 1999-01-0502, 1999.
[163] Harrington DL. Interactions of direct injection fuel sprays with in-cylinder air motions. SAE Transition 1984:93.
[164] Harrington DL. Analysis of spray penetration and velocity dissipation for non-steady fuel injection. ASME Technical Paper 04-DGP, 1984.
[165] Whitaker PA et al. Comparison of top-entry and side-entry direct injection gasoline combustion systems. International Conference Combustion Engines and Hybrid Vehicles, IMechE, London, 28–30 April 1998.
[166] VanDerWage B, Hochgreb S. The effect of fuel volatility on sprays from high-pressure swirl injectors. Paper for the 27th Symposium (International) on Combustion, No. 2E08, University of Colorado at Boulder, 2–7 August 1998.
[167] VanDerWege BA et al. The effect of fuel volatility on sprays from high-pressure swirl injectors. Proceedings of the Fourth International Symposium COMODIA 98, 1998. p. 505–10.
[168] Hochgreb S, VanDerWege B. The effect of fuel volatility on early spray development from high-pressure swirl injectors. Proceedings of Direkteinspritzung im Ottomotor, 1998. p. 107–16.
[169] Koike M, Nomura Y, Saito A, Tomoda T, Sawada D. Vaporization of high pressure gasoline spray. Proceedings of JSAE Spring Convention (in Japanese), No. 971, 1997. p. 325–8.
[170] Sugiyama M, Sato M, Isaka K, Saito K, Imatake N. Oil dilution reduction study with direct injection S.I. engine. Proceedings of JSAE Spring Convention (in Japanese), No. 972, 1997. p. 173–6.
[171] Fujimoto H et al. Study on the oil dilution of a DI gasoline engine—1st report: dilution on the cylinder wall. Proceedings of the JSAE Spring Convention (in Japanese), May 1999.
[172] Sagawa T et al. Study on the oil dilution of a DI gasoline engine—2nd report: dilution in the oil pan. Proceedings of the JSAE Spring Convention (in Japanese), May 1999.
[173] Jackson NS, Stokes J, Whitaker PA. A gasoline direct injection (GDI) powered vehicle concept with 3 litre/100 km fuel economy and EC stage 4 emission capability. Proceedings of the EAEC 6th European Congress, Italy, 2–4 July 1997.
[174] Stocker H et al. Gasoline direct injection and engine management—challenge and implementation. Proceedings of AVL Engine and Environment Conference, 1997. p. 111–33.
[175] Felton PG. Laser diagnostics for direct-injection gasoline engines. IMechE Seminar of Lean Burn Combustion Engines, S433, 3–4 December 1996.
[176] Weimar H et al. Optical investigations on a Mitsubishi GDI-engine in the driving mode. SAE Technical Paper, No. 1999-01-0504, 1999.
[177] Miok J, Huh KY, Noh SH. Numerical prediction of charge distribution in a lean burn direct-injection spark-ignition engine. SAE Technical Paper, No. 970626, 1997.
[178] Selim MYE, Dent JC, Das S. Application of CFD to the matching of in-cylinder fuel injection and air motion in a four stroke gasoline engine. SAE Technical Paper, No. 971601, 1997.
[179] Joh M et al. Numerical prediction of stratified charge distribution in a gasoline direct-injection engine—parametric studies. SAE Technical Paper, No. 1999-01-0178, 1999.
[180] Li G et al. Modeling fuel preparation and stratified combustion in a gasoline direct injection engine. SAE Technical Paper, No. 1999-01-0175, 1999.
[181] Shimotani K, Oikawa K, Horada O, Kagawa Y. Characteristics of gasoline in-cylinder direct injection engine. Proceedings of the Internal Combustion Engine Symposium—Japan (in Japanese), 1995. p. 289–94.
[182] Shimotani K, Oikawa K, Tashiro Y, Horada O. Characteristics of exhaust emission on gasoline in-cylinder direct injection engine. Proceedings of the Internal Combustion Engine Symposium—Japan (in Japanese), 1996. p. 115–20.
[183] Yamaguchi J. Honda integrated motor assist to attain the world's top fuel efficiency. Automotive Engineering 1997;12:49–50.
[184] Mundorff F, Carstensen H, Bierbaumer J. Direct injection—development trends for gasoline and diesel engines. Proceedings of JSAE Spring Convention, No. 971, 1997. p. 301–4.
[185] Lake TH. Comparison of direct injection gasoline combustion systems. SAE Technical Paper, No. 980154, 1998.
[186] Leduc P et al. Gasoline direct injection: a suitable standard for the (very) near future. Proceedings of Direkteinspritzung im Ottomotor, 1998. p. 38–51.
[187] Lake TH, Christie MJ, Stokes J, Horada O, Shimotani K. Preliminary investigation of solenoid activated in-cylinder injection in stoichiometric S.I. engine. SAE Technical Paper, No. 940483, 1994.
[188] Lee S et al. A comparison of fuel distribution and combustion during engine cold start for direct and port fuel injection systems. SAE Technical Paper, No. 1999-01-1490, 1999.
[189] Andriesse D, Ferrari A, Imarisio R. Experimental investigation on fuel injection systems for gasoline DI engines. Direkteinspritung im Ottomotor, Haus Der Technik E.V., 45117 Essen, 12–13 March 1997.
[190] Andriesse D et al. Assessment of stoichiometric GDI engine technology. Proceedings of AVL Engine and Environment Conference, 1997. p. 93–109.
[191] Ashizawa T et al. Development of a new in-line 4-cylinder direct-injection gasoline engine. Proceedings of the JSAE

Fall Convention, No. 71-98, Paper No. 9838237, p. 5–8, 1988.

[192] Noda T et al. Effects of fuel and air mixing on WOT output in direct injection gasoline engine. Proceedings of JSAE Fall Convention (in Japanese), No. 976, 1997. p. 1–4.

[193] Karl G, Kemmler R, Bargende M. Analysis of a direct injected gasoline engine. SAE Technical Paper, No. 970624, 1997.

[194] Kamura H, Takada K. Development of in-cylinder gasoline direct injection engine. Automobile Technology (in Japanese) 1996;50(12):90–5.

[195] Jackson NS, Stokes J, Lake TH, Whitaker PA. Research and development of advanced direct injection gasoline engines. Proceedings of the 18th Vienna Motor Symposium, 24–25 April 1997.

[196] Jackson NS et al. A gasoline direct injection (GDI) powered vehicle concept with 3 l/100 km fuel economy and EC stage 4 emission capability. Paper presented at the EAEC Sixth European Congress Lightweight & Small Cars—the Answer to Future Needs, Italy, 2–4 July 1997.

[197] Ghandhi JB, Bracco FV. Fuel distribution effects on the combustion of a direct-injection stratified-charge engine. SAE Technical Paper, No. 950460, 1995.

[198] Edward R et al. Influence of fuel injection timing over the performances of a direct injection spark ignition engine. SAE Technical Paper, No. 1999-01-0174, 1999.

[199] Anderson R, Yang J, Brehob D, Yi J, Han Z, Reitz R. Challenges of stratified charge combustion. Direkteinspritung im Ottomotor, Haus Der Technik E.V., 45117 Essen, 12–13 March, 1997.

[200] Moser W, Mentgen D, Rembold H. Gasoline direct injection—a new challenge for future engine management systems. MTZ Worldwide 1997;58(9):1–5.

[201] Miyamoto N, Ogawa H, Shudo T, Takeyama F. Combustion and emissions in a new concept DI stratified charge engine with two-stage fuel injection. SAE Technical Paper, No. 940675, 1994.

[202] Hattori H, Ota M, Sato E, Kadota T. Fundamental study on DISC engine with two-stage fuel injection. JSME Int J 1995;B38(1):129–35.

[203] TOYOTA. Direct-injection 4-stroke gasoline engine. TOYOTA Press Information'96, August 1996.

[204] Wojik K, Fraidl GK, Engine and vehicle concepts for low consumption and low-emission passenger cars. FISITA Technical Paper, No. P1302, 1996.

[205] Arcoumanis C, Gold MR, Whitelaw JH, Xu HM. Local charge stratification in spark-ignition engines. I.MechE Seminar of Lean Burn Combustion Engines, S433, 3–4 December 1996.

[206] Kano M et al. Analysis of mixture formation of direct injection gasoline engine. Proceedings of JSAE Fall Convention (in Japanese), No. 976, 1997. p. 9–12.

[207] Kuwahara K et al. Mixture preparation and flame propagation in gasoline direct-injection engine. Proceedings of the 14th Japan Internal Combustion Engine Symposium (in Japanese), 1997. p. 115–20.

[208] Ghandhi JB, Bracco FV. Mixture preparation effects on ignition and combustion in a direct-injection spark-ignition engine. SAE Technical Paper, No. 962013, 1996.

[209] Plackmann J et al. The effects of mixture stratification on combustion in a constant-volume combustion vessel. SAE Technical Paper, No. 980159, 1998.

[210] Iriya Y, Noda T, Iiyama A, Fujii H. Engine performance and the effects of fuel spray characteristics on direct injection S.I. engines. Proceedings of JSAE Fall Convention (in Japanese), Paper No. 9638031, 1996.

[211] Noma K, Iwamoto Y. Optimized gasoline direct injection engine for the European market. SAE Technical Paper, No. 980150, 1998.

[212] Caracciolo F, Stebar RF. An engine dynamometer test for evaluating port fuel injector plugging. SAE Technical Paper, No. 872111, 1987.

[213] Harrington DL, Stebar RF, Caracciolo F. Deposit-induced fuel flow reduction in multiport fuel injectors. SAE Technical Paper, No. 892123, 1989.

[214] Kinoshita M et al. Study of nozzle deposit formation mechanism for direct injection gasoline engines. Proceedings of JSAE Fall Convention (in Japanese), No. 976, 1997. p. 21–4.

[215] Mao C-P. Investigation of carbon formation inside fuel injector systems. Proceedings of ILASS-America'98, 1998. p. 344–8.

[216] Arters DC et al. A comparison of gasoline direct injection and port fuel injection vehicle; Part I—fuel system deposits and vehicle performance. SAE Technical Paper, No. 1999-01-1498, 1999.

[217] Arters DC et al. A comparison of gasoline direct injection and port fuel injection vehicles; Part II—lubricant oil performance and engine wear. SAE Technical Paper, No. 1999-01-1498, 1999.

[218] Brehob D et al. Stratified-charge engine fuel economy and emission characteristics. SAE Technical Paper, No. 982704, 1998.

[219] Wirth M et al. Direct gasoline injection engine concepts for future emission regulations. Proceedings of GPC'98, Advanced Engine Design and Performance, 1998. p. 103–12.

[220] Lake T et al. Development of the control and aftertreatment system for a Euro IV G-Di vehicle. SAE Technical Paper, No. 1999-01-1281, 1999.

[221] Kusell M et al. Motronic MED7 for gasoline direct injection engines: control strategies and calibration procedures. SAE Technical Paper, No. 1999-01-1284, 1999.

[222] Kagawa L, Okazaki S, Somyo N, Akagi Y. A study of a direct-injection stratified charge rotary engine for motor vehicle application. SAE Technical Paper, No. 930677, 1993.

[223] Giovanetti AJ, Ekchian JA, Heywood JB. Analysis of hydrocarbon emission mechanisms in a direct injection spark-ignition engine. SAE Technical Paper, No. 830587, 1983.

[224] Drake MC, Fansler TD, French DT. Crevice flow and combustion visualization in a direct-injection spark-ignition engine using laser imaging techniques. SAE Technical Paper, No. 952454, 1995.

[225] Kaiser W et al. Engine out emissions from a direct-injection spark-ignition (DISI) engine. SAE Technical Paper, No. 1999-01-1529, 1999.

[226] Matthews R et al. Effects of load on emissions and NOx trap/catalyst efficiency for a direct injection spark ignition engine. SAE Technical Paper, No. 1999-01-1528, 1999.

[227] Frank RM, Heywood JB. The effect of piston temperature on

hydrocarbon emissions from a spark-ignited direct-injection engine. SAE Technical Paper, No. 910558, 1991.
[228] Frank RM, Heywood JB. Combustion characterization in a direct-injection stratified-charge engine and implications on hydrocarbon emissions. SAE Technical Paper, No. 892058, 1989.
[229] Frank RM, Heywood JB. The importance of injection system characteristics on hydrocarbon emissions from a direct-injection stratified-charge engine. SAE Technical Paper, No. 900609, 1990.
[230] Frank RM, Heywood JB. The effect of fuel characteristics on combustion in a spark-ignited direct-injection engine. SAE Technical Paper, No. 902063, 1990.
[231] Sasaki S, Wawada D, Ueda T, Sami H. Effects of EGR on direct injection gasoline combustion. Proceedings of JSAE Spring Convention (in Japanese), No. 971, 1997. p. 333–6.
[232] Strehlau W, Leyrer J, Lox ES, Kreuzer T, Hori M, Hoffmann M. Lean NO_x catalysis for gasoline fueled European cars. Automotive Engineering 1997;2(2):133–5.
[233] Kittleson DB. Engines and nanoparticles: a review. J Aerosol Sci 1998;29(5/6):575–88.
[234] Graskow B et al. Particle emissions from two PFI spark ignition engines. SAE Technical Paper, No. 1999-01-1144, 1999.
[235] Andrews G et al. The composition of spark ignition engine steady state particulate emissions. SAE Technical Paper, No. 1999-01-1143, 1999.
[236] Graskow BR. Characterization of exhaust particulate emissions from a spark ignition engine. SAE Technical Paper, No. 980528, 1988.
[237] Maricq M et al. Particulate emissions from a direct-injection spark-ignition (DISI) engine. SAE Technical Paper, No. 1999-01-1530, 1999.
[238] Graskow B et al. Particle emissions from a DI spark ignition engine. SAE Technical Paper, No. 1999-01-1145. 1999.
[239] Miyake M. Developing a new stratified-charge combustion system with fuel injection for reducing exhaust emissions in small farm and industrial engines. SAE Technical Paper, No. 720196, 1972.
[240] Bechtold RL. Performance, emissions, and fuel consumption of the White L-163-S stratified-charge engine using various fuels. SAE Technical Paper, No. 780641, 1978.
[241] Jones C. A progress report on Curtiss–Wright's rotary stratified charge engine development. SAE Technical Paper, No. 740126, 1974.
[242] Kato S, Onishi S. New mixture formation technology of direct fuel injection stratified combustion SI engine (OSKA). SAE Technical Paper, No. 871689, 1987.
[243] Kato S, Onishi S. Direct fuel injection stratified charge engine by impingement of fuel jet (OSKA)—performance and combustion characteristics. SAE Technical Paper, No. 900608, 1990.
[244] Kato S. DISC engine technologies. JSME Seminar (in Japanese), No. 890-65, 1989. p. 71–81.
[245] Kuwahara K, Ueda K, Ando H. Mixing control strategy for engine performance improvement in a gasoline direct injection engine. SAE Technical Paper, No. 980158, 1998.
[246] Kuwahara K et al. Control of mixing and combustion for Mitsubishi GDI engine. Proceedings of the 1998 JSAE Spring Convention, No. 984, Paper No. 9833791, 1998. p. 35–8.
[247] Yamamoto S, Tanada H, Hirako O, Ando H. Analysis of the characteristics of the spray for GDI engine. Proceedings of JSAE Spring Convention (in Japanese), No. 971, 1997. p. 329–32.
[248] Yamaguchi J. Mitsubishi DI gasoline engine protype. Automotive Engineering 1995;September:25–9.
[249] Yamaguchi J. Mitsubishi Galant sedan and Legnum wagon. Automotive Engineering 1996;November:26–9.
[250] Yamaguchi J. Mitsubishi extends gasoline direct-injection to V6. Automotive Engineering 1997;8:77–81.
[251] Yamaguchi J. Mitsubishi prototype GDI V8. Automotive Engineering 1998;1:93–4.
[252] Auer G. Mitsubishi re-engineers GDI engine for Europe. Automotive News Europe 1997;May:12.
[253] Schreffler R. Mitsubishi seeks help in expanding GDI range. Ward's Engine Update 1999;March 1:5.
[254] Demmler A. Smallest GDI engine. Automotive Engineering 1999;3:40.
[255] Yamaguchi J. Toyota readies direct-injection gasoline engine for production. Automotive Engineering 1996;November:74–6.
[256] Gualtieri J, Sawyer CA. Toyota, Mitsubishi DI gas engines debut. Automotive Industries 1995;August:30.
[257] Yamaguchi J. Direct-injection gasoline engine for Toyota. Automotive Engineering 1997;5:29–31.
[258] Yamaguchi J. Direct-injection gasoline engine for Toyota. Automotive Engineering 1997;May:29–31.
[259] Visnic B. Toyota moving cautiously with D-4 engine. Ward's Engine and Vehicle Technology Update 1997;June 1:12.
[260] Ozasa T et al. Schlieren observations of in-cylinder phenomena concerning a direct-injection gasoline engine. SAE Technical Paper, No. 982696, 1998.
[261] Kano M et al. Analysis of mixture formation of direct injection gasoline engine. SAE Technical Paper, No. 980157, 1998.
[262] Itoh T, Takagi Y, Iiyama A, Muranaka S. Combustion characteristics of a direct injection stratified S.I. engine. Proceedings of JSAE Spring Convention (in Japanese), No. 971, 1997, p. 337–40.
[263] Tatsuta H et al. Mixture formation and combustion performance in a new direct-injection SI V-6 engine. SAE Technical Paper, No. 981435, 1998.
[264] Ito Y et al. Study on improvement of torque response by direct injection gasoline engine and its application. Proceedings of the JSAE Fall Convention, No. 71-98, Paper No. 9838246, 1998, p. 9–12.
[265] Yamaguchi J. Nissan direct-injection gasoline V6. Automotive Engineering 1998;1:91–3.
[266] Kakuhou A. Characteristics of mixture formation in a direct-injection SI engine with optimized in-cylinder swirl air motion. SAE Technical Paper, No. 1999-01-0505, 1999.
[267] AUDI. Audi Frankfurt Autoshow, September 1997.
[268] Birch S. Advances at Audi. Automotive Engineering 1997;11:30.
[269] Hupperich P et al. Direct injection gasoline engines—combustion and design. SAE Technical Paper, No. 1999-01-0170, 1999.
[270] Grigo M et al. Charge motion controlled combustion system

for direct injection SI engines. Proceedings of Global Powertrain Conference on Advanced Engine Design and Performance, 1998. p. 66–75.

[271] Balles EN, Ekchian JA, Heywood JB. Fuel injection characteristics and combustion behavior of a direct-injection stratified-charge engine. SAE Technical Paper, No. 841379, 1984.

[272] Abraham J. Entrainment characteristics of sprays for diesel and DISI applications. SAE Technical Paper, No. 981934, 1998.

[273] Alain F. et al. In-cylinder flow investigation in a gasoline direct injection four valve engine: bowl shape piston effects on swirl and tumble motions. 1998 FISITA Technical Paper, No. F98T049, 1998.

[274] Arcoumanis C, et al. Optimizing local charge stratification in a lean-burn spark ignition engine. IMechE 1997;D211:145–54.

[275] Arcoumanis C et al. Modeling of pressure-swirl atomizer for gasoline direct-injection engines. SAE Technical Paper, No. 1999-01-0500, 1999.

[276] Automotive Engineer. Healthy future of GDI predicted by Mitsubishi. Automotive Engineer 1997;12:6.

[277] Automotive Engineer. Toyota's D4 direct injection gasoline engine. Automotive Engineer 1997;12:60.

[278] Automotive Engineer. Nissan develops new direct injection engines. Automotive Engineer 1997;22(9):6.

[279] Automotive Engineer. Getting more direct. Automotive Engineer 1997;12(9):81.

[280] Bartolini CM et al. Experimental analysis of a new water hammer gasoline direct injection system. SAE Technical Paper, No. 981936, 1998.

[281] Birch S. Gasoline direct-injection developments. Automotive Engineering 1988:88.

[282] Bladon S. Carisma GDI vs. Rover 420 DI, Diesel Car & 4×4, No. 1, 1998, p. 36–42.

[283] Brooks B. Nissan to direct-inject VQ engines. Ward's Engine and Vehicle Technology Update 1997;August 15:15.

[284] Brooks B. DI gasoline engine problems outlined. Ward's Engine Update 1998;February 1:2.

[285] Brooks B. Daimler-Benz may use Orbital/Siemens DI. Ward's Engine Update 1998;July 15:3.

[286] Burk P et al. Future aftertreatment strategies for gasoline lean burn engines. Proceedings of AVL Engine and Environment Conference, 1997. p. 219–31.

[287] Carnevale C. Cylinder to cylinder AFR control with an asymmetrical exhaust manifold in a GDI system. SAE Technical Paper, No. 981064, 1998.

[288] Chaouche A et al. NSDI-3: a small bore GDI engine. SAE Technical Paper, No. 1999-01-0172. 1999.

[289] Chinn J, Yule A. Computational analysis of swirl atomizer internal flow. Proceedings of ICLASS-97, 1997.

[290] Choi N et al. Effect of in-cylinder air motion on fuel spray characteristics in a gasoline direct injection engines. SAE Technical Paper, No. 1999-01-0177, 1999.

[291] Cole R. Exhaust emissions of a vehicle with a gasoline direct-injection engine. SAE Technical Paper, No. 982605, 1998.

[292] Cole R. Gaseous and particulate emissions from a vehicle with a spark-ignition direct-injection engine. SAE Technical Paper, No. 1999-01-1282, 1999.

[293] Cousin J, Ren W, Nally S. Transient flows in high pressure swirl injectors. SAE Technical Paper, No. 980499, 1998.

[294] Daisho Y, Shimizu A, Saito, T, Choi KH. A fundamental study on charge stratification. Proceedings of COMODIA-85, 1985. pp. 423–32.

[295] Davy MH. Effects of injection timing on liquid-phase fuel distributions in a centrally-injected four-valve direct-injection spark-ignition engine. SAE Technical Paper, No. 982699, 1998.

[296] El-Emams SH et al. Performance of a stratified charge spark-ignition engine with an injection of different fuels. Proceedings of the Fourth International Symposium COMODIA 98, 1998. p. 329–34.

[297] Ellzey J. Simulation of stratified charge combustion. SAE Technical Paper, No. 981454, 1998.

[298] Fan L et al. Comparison of computed spray in a direct-injection spark-ignited engine with planar images. SAE Technical Paper, No. 972883, 1997.

[299] Fan L et al. Intake flow simulation and comparison with PTV measurements. SAE Technical Paper, No. 1999-01-0176, 1999.

[300] Farrell P et al. Intake air velocity measurements for a motored direct injection spark ignited engine. SAE Technical Paper, No. 1999-01-0499, 1999.

[301] Faure MA et al. Application of LDA and PIV techniques to the validation of a CFD Model of a direct injection gasoline engine. SAE Technical Paper, No. 982705, 1988.

[302] Fujikawa T et al. Quantitative 2-D fuel distribution measurements in a direct-injection gasoline engine using laser-induced fluorescence technique. Proceedings of the Fourth International Symposium COMODIA 98, 1998. p. 317–22.

[303] Fukushima C. Mitsubishi clears California NO_x requirement with new version of GDI engine, plans U.S. launch. The Japan Automotive Digest 1997;III:37.

[304] Gajdeczko B et al. Application of two-color particle image velocimetry to a firing production direct-injection stratified-charge engine. SAE Technical Paper, No. 1999-01-1111, 1999.

[305] Ghandhi J. Observations of stratified combustion in an engine and constant volume bomb. Proceedings of Direkteinspritzung im Ottomotor, 1998. p. 147–65.

[306] Glaspie CR, Jaye J, Lawrence TG, Lounsberry TH, Mann LB, Opra JJ, Roth DR, Zhao F-Q. Application of design and development techniques for direct injection spark ignition engines. SAE Technical Paper, No. 1999-01-0506, 1999.

[307] Han Z et al. Multidimensional modeling DI gasoline engine sprays. Proceedings of ILASS-America, 1997. p. 75–9.

[308] Han Z et al. Internal structure of vaporizing pressure-swirl fuel sprays. Proceedings of ICLASS-97, 1997. p. 474–81.

[309] Heisler H. Advanced engine technology. SAE, 1995.

[310] Heitland H et al. Can the best fuel economy of today's engines still be improved? SAE Technical Paper, No. 981912, 1998.

[311] Hepburn J et al. Engine and aftertreatment modeling for gasoline direct injection, SAE 982596, 1998.

[312] Hoffman J, Khatri F, Martin J. Mass-related properties of various atomizers for direct-injection SI engines. SAE Technical Paper, No. 980500, 1998.

[313] Ikeda Y et al. Development of NO_x storage-reduction 3-way catalyst for D-4 engines. Proceedings of the 1998 JSAE Fall

Meeting (in Japanese), No. 101-98, Paper No. 9839597, 1998. p. 9–12.
[314] Ikeda Y et al. Development of NO_x storage-reduction 3-way catalyst for D-4 engines. SAE Technical Paper, No. 1999-01-1279, 1999.
[315] Ismailov M et al. Laser-based techniques employed on gasoline swirl injector. Proceedings of the Fourth International Symposium COMODIA 98, 1998. p. 499–504.
[316] Jeong K et al. Initial flame development under fuel stratified conditions. SAE Technical Paper, No. 981429, 1998.
[317] Johnson D et al. Electronic direct fuel injection system applied to an 1100cc two-stroke personal watercraft engine. SAE Technical Paper, No. 980756, 1998.
[318] Jost K. Direct injection for SI engines. Automotive Engineering 1997;May:60–1.
[319] Kano M, Saito K, Basaki M, Matsushita S, Gohno T. Analysis of mixture formation of direct injection gasoline engine. SAE Technical Paper, No. 980157, 1998.
[320] Kato S et al. Quantitative measurement of air–fuel mixture distribution in a cylinder using LIF. Proceedings of SAE-Japan (in Japanese), No. 9738823, October 1997.
[321] Kawamura K et al. Development of instrument for measurement of air-fuel ratio in vicinity of spark plug—applications to DI gasoline engine. Proceedings of the 14th Japan Internal Combustion Engine Symposium (in Japanese), 1997. p. 133–8.
[322] Kech JM et al. Analyses of the combustion process in a direct injection gasoline engine. Proceedings of the 4th International Symposium COMODIA 98, 1998. p. 287–92.
[323] Kobayashi T et al. Development of NO_x trap type catalyst for direct injection gasoline engine. SAE Technical Paper, No. 1999-01-1468, 1999.
[324] Koike M et al. Influences of fuel vaporization on mixture preparation of a DI gasoline engine. Proceedings of the 1998 JSAE Spring Convention (in Japanese), No. 982, Paper No. 9832378, 1998, p. 103–6.
[325] Lacher S et al. In-cylinder mixing rate measurements. SAE Technical Paper, No. 1999-01-1110, 1999.
[326] Lai M-C et al. Characteristics of direct injection gasoline spray wall impingement at elevated temperature conditions. Proceedings of the 12th Annual Conference on Liquid Atomization and Spray Systems, May 1999.
[327] Lenz U et al. Air–fuel ratio control for direct injecting combustion engines using neutral networks. SAE Technical Paper, No. 981060, 1998.
[328] Lewis A. Mitsubishi GDI, Diesel Car and 4×4, No. 12, 1997. p. 20–1.
[329] Li J, Chae J, Jeong Y, Lee S, Zeng K, Cho M, Noh J. Preliminary investigation of a diffusing oriented spray stratified combustion system for DI gasoline engines. SAE Technical Paper, No. 980150, 1998.
[330] Li SC, Gebert K. Spray characterization of high pressure gasoline fuel injectors with swirl and non-swirl nozzles. SAE Technical Paper, No. 981935, 1998.
[331] Lykowski J. Spark plug technology for gasoline direct injection GDI engines. SAE Technical Paper, No. 980497, 1998.
[332] Morello L et al. Global approach to the fuel economy improvement in passenger cars. International Symposium on Powertrain Technologies for a 3-Litre-Car, 1996. p. 33–43.
[333] Moriyoshi Y, Takagi M. Control of flow field during compression stroke by that of intake flow. Proceedings of the Japan 13th Internal Combustion Engine Symposium (in Japanese), 1997. p. 299–304.
[334] Moriyoshi Y, Nomura H. Combustion characteristics of a direct injection gasoline engine with enhanced gas motion. Proceedings of JSAE Spring Convention (in Japanese), No. 971, 1997. p. 341–4.
[335] Moriyoshi Y et al. Analysis of flame propagation phenomenon in simplified stratified charge conditions. Proceedings of JSAE Fall Convention (in Japanese), No. 976, 1997. p. 17–20.
[336] Moriyoshi Y et al. Combustion analysis of a direct injection gasoline engine from theoretical and experimental viewpoints. Proceedings of the 14th Japan Internal Combustion Engine Symposium (in Japanese), 1997. p. 127–32.
[337] Morris SW. The evaluation of performance enhancing fluids and the development of measurement and evaluation techniques in the Mitsubishi GDI engine. SAE Technical Paper, No. 1999-01-1496, 1999.
[338] Muller W et al. Durability aspects of NO_x absorption catalysts for direct injection gasoline vehicles with regard to European application. SAE Technical Paper, No. 1999-01-1285, 1999.
[339] Naitoh K et al. Numerical simulation of the fuel mixing process in a direct-injection gasoline engine. Proceedings of the 14th Japan Internal Combustion Engine Symposium (in Japanese), 1997. p. 139–43.
[340] Naitoh K et al. Numerical simulation of the fuel mixing process in a direct-injection gasoline engine. SAE Technical Paper, No. 981440, 1998.
[341] Ohm I et al. Initial flame development under fuel stratified conditions. SAE Technical Paper, No. 981429, 1998.
[342] Ohyama Y et al. Mixture formation in gasoline direct injection engine. Proceedings of Direkteinspritzung im Ottomotor, 1998, p. 79–106.
[343] Parrish SE et al. Intake flow effects on fuel sprays for direct-injection spark-ignited engines. Proceedings of the Fourth International Symposium COMODIA 98, 1998. p. 311–6.
[344] Piccone A et al. Strategies for fuel economy improvement of gasoline powertrains. International Symposium on Powertrain Technologies for a 3-Litre-Car, 1996. p. 77–93.
[345] Piock WF et al. Future gasoline engine concepts based on direct injection technology. Proceedings of the 1998 JSAE Spring Convention, No. 984, Paper No. 9831009, 1998. p. 27–30.
[346] Plapp G et al. The role of future engine control systems for gasoline engines fuel economy improvement. International Symposium on Powertrain Technologies for a 3-Litre-Car, 1996. p. 57–66.
[347] Pontoppidan M, Gaviani G, Marelli M, Bella G, Rocco V. Improvements of GDI-injector optimization tools for enhanced SI-engine combustion chamber layout. SAE Technical Paper, No. 980494, 1998.
[348] Risi AD et al. A study of H_2, CH_4, C_2H_6 mixing and combustion in a direct-injection stratified-charge engine. SAE Technical Paper, No. 971710, 1997.
[349] Robeck CM et al. Simulation of stratified charge combustion. SAE Technical Paper, No. 981454, 1998.
[350] Sandquist H et al. Influence of fuel volatility on emissions and combustion in a direct injection spark ignition engine. SAE Technical Paper, No. 982701, 1998.

[351] Schdidt G et al. Comparison of direct injection petrol and diesel engines with regard to fuel efficiency. 1998 FISITA Technical Paper, No. F98T053, 1998.
[352] Schreffler R. MMC, Japanese work to expand gasoline DI tech. Ward's Engine Update 1998;February 1:2–3.
[353] Schreffler R. Mitsubishi says GDI is LEV-ready. Ward's Engine Update 1998;February 15:2.
[354] Scott D. Euro gasoline engines follow DI trend. Ward's Engine Update 1998;24(7):1–2.
[355] Sendyka B. A description of the shape of an air-fuel mixture and determination of the injection advance angels related to the spark discharges in a gasoline direct-injection engine. SAE Technical Paper, No. 980496, 1998.
[356] Shiraishi T, Nakayama Y, Nogi T, Ohsuga M. Effect of spray characteristics on combustion of a direct injection spark ignition engine. SAE Technical Paper, No. 980156, 1998.
[357] Stan C et al. Fluid dynamic modeling of gasoline direct injection for compact combustion chambers. SAE Technical Paper, No. 980755, 1998.
[358] Stovell C et al. Emissions and fuel economy of 1988 Toyota with a direct injection spark ignition engine. Paper submitted to the 1999 SAE Fuels & Lubricants Meeting, 1999.
[359] Stovell C et al. Emissions and fuel economy of 1998 Toyota with a direct injection spark ignition engine. SAE Technical Paper, No. 1999-01-1527, 1999.
[360] Su J et al. Towards quantitative characterization of transient fuel sprays using planar laser induced fluorescence imaging. Proceedings of ILASS-America'98, 1998. p. 106–10.
[361] TOYOTA. Toyota's D-4 direct-injection gasoline engine. Frankfurt Autoshow, September 1997.
[362] Treece J. Mitsubishi develops cleaner-burning engine—gasoline direct-injection unit slated for U.S. in '99 1998;February 23.
[363] Warburton A. GDI head-to-head interview. Automotive Engineer 1998;3:18–9.
[364] WARD. Mitsubishi to go all-out with GDI engines. Ward's engine and Vehicle Technology Update, 19 August 1997.
[365] WARD. EEGR valve may help reduce NO_x. Ward's Engine Update, 15 February 1998. p. 8.
[366] Wensing M et al. Spray formation of high pressure gasoline injectors investigated by two-dimensional Mie and LIEF techniques. SAE Technical Paper, No. 1999-01-0498, 1999.
[367] Williams PA. Effects of injection timing on the exhaust emissions of a centrally-injected four-valve direct-injection spark-ignition engine. SAE Technical Paper, No. 982700, 1988.
[368] Williams P et al. Observations on the in-cylinder sprays in a firing single-cylinder direct-injection gasoline engine. Proceedings of Direkteinspritzung im Ottomotor, 1998. p. 117–31.
[369] Winkler K et al. The development of an emission aftertreatment system for gasoline direct injection passenger cars. 1998 FISITA Technical Paper, No. F98T218, 1998.
[370] Yamaguchi J. Mitsubishi extends gasoline direct-injection to V6. Automotive Engineering 1997;August:77–81.
[371] Yamaguchi J. Toyota's new engine technology—the D4 direct-injection gasoline engine and the inline-four 1ZZFE engine. Automotive Engineering 1998;11:66–8.
[372] Yang J et al. Simulation of the effect of wakes behind fuel droplets on fuel vapor diffusion in direct-injection SI engines. Proceedings of the Fourth International Symposium COMODIA 98, 1998. p. 323–8.
[373] Stutzenberger H, Preussner C, Gerhardt J. Gasoline direct injection for SI engines-development status and outlook. VDI, the 17th International Vienna Engine Symposium, 25–26 April 1997.
[374] Zhao F, Yoo JH, Lai MC. The spray characteristics of dual-stream port fuel injectors for applications to 4-valve gasoline engines. SAE Technical Paper, No. 952487, 1995.
[375] Ohyama Y, Nogi T, Ohsuga M. Effects of fuel/air mixture preparation on fuel consumption and exhaust emission in a spark ignition engine. IMechE Paper, No. 925023, C389/232, 1992. p. 59–64.
[376] Preussner C, Kampmann S. Gasoline direct injection, a new challenge for future gasoline control systems—part 2: injector and mixture formation, MTZ, vol. 58, 1997.
[377] Yasuoka M et al. A study of a torque control algorithm for direct injection gasoline engine. Proceedings of the 14th Japan Internal Combustion Engine Symposium (in Japanese), 1997. p. 121–5.
[378] Date T, Yagi S. Research and development of the Honda CVCC engine. SAE Technical Paper, No. 740605, 1974.
[379] Scherenberg H. Ruckbliik uber 25 Jahre Benzin—Einspritzung in Deutschland. MTZ, 16, 1955.
[380] Scott D. Renault first Euro automaker with gasoline direct injection. Ward's Auto World 1999;3:138.
[381] Birch S. Direct gasoline injection from Renault. Automotive Engineering International 1999;7:28–9.